TECHNICAL REPORT NO. 1-813

THE STABILITY DURING CONSTRUCTION OF THREE LARGE UNDERGROUND OPENINGS IN ROCK

by

E. J. Cording

January 1968

Sponsored by

Defense Atomic Support Agency

Conducted by

U. S. Army Engineer Waterways Experiment Station
CORPS OF ENGINEERS
Vicksburg, Mississippi

TECHNICAL REPORT NO. 1-813

THE STABILITY DURING CONSTRUCTION OF THREE LARGE UNDERGROUND OPENINGS IN ROCK

by

E. J. Cording

January 1968

Sponsored by

Defense Atomic Support Agency
NWER Subtask 13.191

Conducted by

U. S. Army Engineer Waterways Experiment Station
CORPS OF ENGINEERS
Vicksburg, Mississippi

THE CONTENTS OF THIS REPORT ARE NOT TO BE USED FOR ADVERTISING, PUBLICATION, OR PROMOTIONAL PURPOSES. CITATION OF TRADE NAMES DOES NOT CONSTITUTE AN OFFICIAL ENDORSEMENT OR APPROVAL OF THE USE OF SUCH COMMERCIAL PRODUCTS.

FOREWORD

This report was prepared in the Nuclear Weapons Effects Division, U. S. Army Engineer Waterways Experiment Station, under the sponsorship of the Defense Atomic Support Agency as part of Nuclear Weapons Effects Research Subtask 13.191, "Rock Mechanics Research Related to Deep Underground Protective Construction." The work was accomplished during the period October 1965 through July 1966. During this time, Mr. G. L. Arbuthnot, Jr., was Chief of the Nuclear Weapons Effects Division, and Mr. L. F. Ingram was Chief of the Physical Sciences Branch.

This report was prepared by 1LT Edward J. Cording, CE, and is essentially a thesis submitted in partial fulfillment of the requirements for the degree of Doctor of Philosophy in Civil Engineering to the University of Illinois, Urbana, Illinois.

Director of the Waterways Experiment Station during the preparation of this report was COL John R. Oswalt, Jr., CE. Technical Director was Mr. J. B. Tiffany.

THE STABILITY DURING CONSTRUCTION OF THREE LARGE UNDERGROUND OPENINGS IN ROCK

Edward James Cording, Ph. D.
Department of Civil Engineering
University of Illinois, 1967

ABSTRACT

Three large rock-bolted underground cavities were constructed at the Nevada Test Site. Two of the cavities, approximately 100 feet in diameter and 140 feet high, were constructed at a depth of 1300 feet in a very weak tuff of excellent rock mass quality. The third cavity, approximately 60 feet in diameter and 80 feet high, was constructed at a depth of 350 feet in a jointed granite of high intact strength and fair to good rock mass quality.

The stability of the cavities was monitored throughout construction by measuring rock displacements, observing fractures in near-surface rock, and observing the behavior of the rock-bolt support system. Supporting field and laboratory tests were performed in order to evaluate intact and in-situ properties of the rock mass.

Radial movement of the cavities was measured using extensometers anchored at various depths in holes drilled from the cavity surface. Displacement versus depth profiles were used to determine the depth at which rock movement was concentrated. By comparing rock movement with excavation and support progress, a continual estimate of the cavity stability was obtained. Large displacements, or large rates of displacement, were indicative of potentially unstable behavior. Displacements were compared with displacements predicted from elastic theory, using a finite element

solution and simple closed solutions.

Initial measured displacements in all cavities approximated the displacements predicted from elastic theory (0.02 inch in the granite and 0.5 inch in the tuff), although there generally was a greater concentration of movement in the shallow, destressed zones. In some cases, continued movements occurred which were related to opening and displacement along shallow discontinuities. In the granite, shallow movements of approximately 0.1 to 0.2 inch occurred along preexisting joint surfaces. In the tuff, shallow movements of 1.0 to 2.0 inches occurred along new extension fractures which formed through the intact portion of the rock mass. The fractures formed as soon as an area was excavated and were oriented parallel to the cavity surface, giving the tuff cavities an onionskin appearance. The opening of shallow fractures and joints was minimized by prompt placement of tensioned rock bolts.

Large, deep movements occurred along joint and bedding planes intersecting the plane surface of Tuff Cavity II. Displacements of 1.0 to 2.0 inches occurred at depths between 10 and 30 feet within a period of one week. At the same time, bolts broke, bearing plates dished, and shear fractures formed. The area was stabilized by placing additional long rock bolts.

From a study of underground openings reported in the literature, as well as from observations in the three cavities, it was found that a deformation modulus can be used to estimate stable displacements in the rock surrounding openings. (Relationships were established between rock mass quality and the deformation modulus of the rock mass.) However, a deformation modulus has no significance for large discontinuous movements,

which often occur when stresses are reduced by excavation of a rock mass. Displacements of the underground openings were often 3 to 10 times the displacements predicted using a deformation modulus.

The orientation of extension fractures parallel to the surface of an opening suggests the applicability of an extension strain failure theory, where the limiting strain is reached when the bond between particles breaks. This implies that the cohesive or tensile characteristics of the rock govern extension failure phenomena.

Rock-bolt support restrains the rock mass and prevents large discontinuous movements which result in loosening and loss of strength in the rock mass. One of the major unknowns in designing a support system is the amount of support pressure to be applied to the rock surface.

THE STABILITY DURING CONSTRUCTION OF THREE LARGE UNDERGROUND OPENINGS IN ROCK

by

EDWARD JAMES CORDING
B.S., Wheaton College, 1960
M.S., University of Illinois, 1963

THESIS

Submitted in partial fulfillment of the requirements
for the degree of Doctor of Philosophy in Civil Engineering
in the Graduate College of the
University of Illinois, 1967

Urbana, Illinois

BLANK PAGE

ACKNOWLEDGMENTS

The cooperation and interest of many individuals and agencies made this study possible. The writer is particularly indebted to his advisor, Dr. D. U. Deere, Professor of Civil Engineering and Geology, University of Illinois, for his guidance, valuable suggestions, and active interest throughout the project. Many of the ideas presented in this thesis originated with Dr. Deere. The contributions by the members of the writer's committee--their encouragement and constructive criticism--are also appreciated.

The thesis is based on projects sponsored by the Department of Defense at the Nevada Test Site; Dr, Mel Merritt of Sandia Corp. was project monitor. The field rock mechanics investigation was carried out under the Fenix and Scisson, Inc., Mining Department; Mr. Donald Waltman was chief engineer, and Mr. Jerry Dowling was project engineer. The following civil and mining engineers performed much of the field testing and construction control: Mr. Owen Cecil, Mr. Sheldon Murphy, Dr. F. D. Patton, and Mr. Robert Rommel. Their contribution to the observations and interpretations of rock behavior was greatly appreciated. Reynolds Electrical Engineering Co. field supervisors and mining crews cooperated in performing tests and making observations on this nonroutine project.

Many individuals of the U. S. Geological Survey contributed to the study. Messrs. John Ege and W. Emerick, geologists, provided much useful information on the geology of Rainier Mesa and the Climax Stock. Mr. James Scott, geophysicist, was in charge of the seismic testing program and

performed the analysis of test results. Mr. Dave Cunningham, field engineer, was in charge of the seismic crew. The seismic program was very capably performed by this experienced group.

The laboratory testing program was performed in the Civil Engineering Department Rock Mechanics Laboratory at the University of Illinois by Messrs. Richard Coon, James Coulson, and Andrew Merritt, graduate students.

Dr. Salvador Reyes, Professor of Soil Mechanics, University of the Phillipines, developed the finite element program and contributed his valuable time in adapting it to the specific requirements of the problem. Mr. James Coulson, graduate student in Civil Engineering at the University of Illinois, ably performed the program checking and program production.

The writer also wishes to thank Mr. C. J. Monahan, Chief of the Geology Section of the U. S. Army Engineer District, Walla Walla, Corps of Engineers; and the personnel of Shannon and Wilson, Inc., for making the field test results on Dworshak Dam available.

Funds for the interpretation of results and the final report were provided under the Nuclear Weapons Effects Research Program by the Defense Atomic Support Agency to the U. S. Army Engineer Waterways Experiment Station. The writer wishes to express his appreciation to the Director and the personnel of the Waterways Experiment Station for their contributions to the project. The Nuclear Weapons Effects Division provided direct support for the analysis and interpretation of results. The drafting, editing, and printing of the final report were performed by the Reproduction and Reports Branch.

TABLE OF CONTENTS

TABLE OF CONTENTS (CONT'D)

LIST OF TABLES

LIST OF FIGURES

SYMBOLS

a	Radius at surface of an opening
c	Cohesion intercept, Mohr envelope
d	Displacement
E	Young's modulus
E_{df}	Young's modulus determined from field seismic velocities
E_{dl}	Young's modulus determined from laboratory sonic velocity
E_r	Rock deformation modulus, in-situ
E_t	Young's modulus, tangent at one-half unconfined compressive strength, intact specimen
E_t/σ_{ult}	Modulus ratio, from unconfined compression test on intact specimen
g	Acceleration of gravity, 32.2 ft/sec^2
i	Angle of inclination of joint plane
p	External hydrostatic pressure
p_i	Internal hydrostatic pressure
q	Pressure on plane surface
r	Radial component of polar coordinate system
R	Radial distance to elastic-plastic boundary
t	Tan $(45 + \phi/2)$
V_p	Compressional velocity
V_{pf}	Compressional velocity, field
$V_{pl(0)}$	Compressional velocity, laboratory, at zero axial stress
$V_{pl(5000)}$	Compressional velocity, laboratory, at 5000-psi axial stress (static)

	V_s	Shear velocity
	V_{sf}	Shear velocity, field
	w	Water content, % by weight of solids
Subscripts	d	Dynamic
	f	Field
	l	Laboratory
	p	Compressional
	s	Shear
Greek	γ	Unit weight
	ϵ	Strain
	ϵ_f	Strain at failure
	θ	Angular component of polar coordinate system
	μ	Poisson's ratio
	μ_{df}	Poisson's ratio, field seismic
	σ	Stress
	σ_h	Natural horizontal stress
	σ_r	Radial stress
	σ_t	Ultimate tensile strength
	σ_v	Natural vertical stress
	σ_{ult}	Ultimate compressive strength
	σ_θ	Tangential stress
	ϕ	Angle of internal friction
	ϕ_j	Residual strength of joint surface

BLANK PAGE

THE STABILITY DURING CONSTRUCTION OF THREE LARGE UNDERGROUND OPENINGS IN ROCK

CHAPTER 1

INTRODUCTION

1.1 GENERAL

Three large, rock-bolted underground cavities were constructed in 1965 at the Nevada Test Site as part of the Nuclear Weapons Effects Test Program of the Department of Defense. The engineering design and inspection of the cavity construction were the responsibility of Fenix and Scisson, Inc. The construction was carried out by Reynolds Electrical Engineering Company. Professor D. U. Deere, University of Illinois, was consultant to Fenix and Scisson, Inc., for recommendations on the design and construction of the three cavities. During the first six months of construction, the writer was employed by Fenix and Scisson, Inc., as a field engineer, responsible to Professor Deere, to monitor the behavior of the cavities.

Two of the cavities, approximately 140 feet high and 100 feet wide, were constructed at a depth of 1300 feet in a mesa composed of a relatively unjointed tuffaceous rock of very low strength. A third, smaller cavity was constructed at a depth of 350 feet in a granitic stock. The rock in this location had high intact strength and was moderately jointed.

1.2 MONITORING PROGRAM IN THE CAVITIES

Monitoring of the cavity behavior was considered an essential element in the design and construction of the cavities. It provided a means of checking the design assumptions concerning the character and behavior of the rock mass surrounding the cavities, and a means whereby the construction

of the cavities could be controlled and modified as necessary. It was particularly important that the cavities in tuff be closely monitored, because of the large size of the openings and the very low strength of the rock (the tangential stresses at the surface of the cavities exceeded the intact, unconfined strength of the tuff specimens). On the basis of the observed behavior, modifications to the construction program were made. The modifications included the placement of large amounts of cement grout at low pressures in open joint systems, and also included the installation of extra bolts in slabby areas, across joint zones, and in zones where excessive movements were observed. Gunite was placed as required in areas of slabby rock.

Rock behavior was monitored continuously so that potentially unstable conditions could be detected in enough time to permit the application of corrective measures. The types of in-situ behavior which could be observed, and therefore monitored, were rock-bolt loads, rock fracturing, and rock displacement. Rock-bolt loads were measured with load cells or were estimated by observing the bending of bearing plates and the failure of rock-bolt assemblies. Rock fracturing was observed at the cavity surface and in the first few feet of open boreholes. Seismic refraction surveys also provided information on the depth and nature of the fractured rock surrounding the opening. Rock displacements were measured with multiple-position extensometers placed in boreholes which extended radially from the cavity surface. Excessive displacements were almost invariably associated with rock fracturing. The displacement measurements provided an estimate of the depth and areal extent of zones where fracturing (or discontinuous movement) was occurring. Because the displacement measurements were sensitive to discontinuous behavior, they were relied upon to provide an early warning of unstable conditions.

1.3 USE OF DISPLACEMENT MEASUREMENTS TO ESTIMATE STABILITY

Displacement measurements have been used increasingly in the past decade by both civil and mining engineers for estimating the stability of underground openings. Both the magnitude and the rate of movement have been useful in estimating stability. Lang (1964)* describes "unstable" deformations, i.e. "deformations that will inevitably lead to overall failure or collapse," as deformations which have an accelerating rate with respect to load or with respect to time (load held constant) (Fig. 1). Isaacson (1958) states: "It seems possible, then, that in measurements of underground closure any significant departure from progressive flattening in the curve obtained by plotting strain against time may be a valuable indication that the rock is not approaching a state of stable equilibrium and that there is danger of eventual failure." Another means of estimating unstable displacements is to compare the magnitude of the displacement with the theoretical displacement for a continuum: large displacements with respect to the predicted displacement are often indicative of discontinuous--and possibly unstable--behavior.

This section summarizes some of the available information on the deformation of underground openings. The displacements observed in these openings may be divided into two major types: continuous and discontinuous. Continuum behavior may include elastic, plastic, or creep characteristics; the criterion is that continuity between elements be maintained. Minor displacements occurring in the vicinity of joints and fractures may be considered part of the continuum displacement of the rock mass, as long as

---

* Authors and dates refer to list of references at end of text.

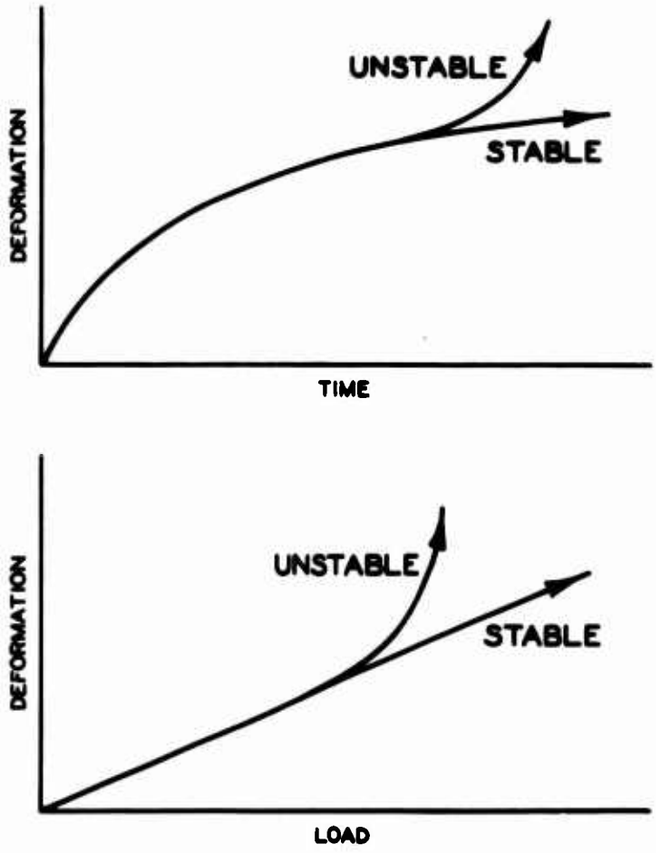

Fig. 1. Stable and unstable deformations

they do not become large and unpredictable in the area of interest. For many rock types. the continuum displacements may also be considered to be elastic, where the displacements are proportional to the changed stress conditions which occur as the restraining rock is excavated from the vicinity of the opening. Elastic. continuum theories may be used to predict these displacements. Even though the behavior is not perfectly elastic, the theory provides a reasonable answer if the proper deformation modulus, at the stress level of interest, is assumed.

Elastic, continuum displacements are stable, and there is no necessity for restraining this movement; in fact, the elastic movements occurring upon excavation are usually due to such large stress changes, and the rock has such a high modulus that the movements could not be restrained by any normal type of rock support system. In most cases, supports are placed after a portion of the elastic movement has occurred. If the supports are placed prior to the elastic movement, they must be capable of deforming with the rock mass.

The second type of displacements common in a rock mass is the discontinuous movement which occurs along joints and newly formed fractures. It is this type of displacement which is indicative of unstable conditions. Discontinuous displacements are not proportional to stress but occur when some yield or failure stress is exceeded along a discontinuity. They often take place with time, as deterioration and progressive failure of the rock occur. It is therefore important that discontinuous movements be restrained as soon as possible to prevent continued failure and the buildup of large thicknesses of failed rock which must be artificially supported.

The concept of strain loses its significance for discontinuous

behavior. Large movements occur across very small distances, making it impossible to determine an average displacement per unit length. Thus, continuum theories are not adequate for estimating large discontinuous movements.

Discontinuous behavior is most pronounced for unloading conditions, such as occur during the excavation of openings, as stresses are relieved at the rock face allowing loosening and opening along fractures. The amount of discontinuous movement depends to a large extent on the nature of the rock support. The support pressures required to maintain the stability of the rock mass are usually quite small with respect to the stress changes caused by excavation of the opening, particularly if the supports are installed before large discontinuous movements begin to occur. However, if the rock is improperly restrained, the rate of movement becomes unstable--and has an increasing rate with respect to time or load--until failure occurs by the falling out of slabs, failure of the support, or closure of the opening.

Rooms in Bedded Deposits: Jonathan Mine, Zanesville, Ohio

Some of the earlier displacement measurements reported in the literature were made in unsupported test rooms in bedded deposits by the U. S. Bureau of Mines (Merrill, 1954, 1957, 1958). At the Jonathan Mine, Zanesville, Ohio, the rock consists of bedded shale and limestone of excellent quality, having very few joints perpendicular to the bedding capable of forming detached blocks of rock. In one series of tests, the sag of the roof was measured as the size of the room was enlarged. In another series, compressed air was introduced into a bedding plane separation above a 20-inch limestone roof layer in a 50- by 100-foot room. The sag of the roof

layer and the surface strains were measured as the air pressure was increased. Changes in air pressure produced almost immediate changes in the roof strain and sag. As failure was approached, the rate of deflection and strain in the roof layer increased with respect to the applied pressure (Fig. 2). Although an increase in fractures was not visually observed, the increased roof deflection was accompanied by a corresponding increase in the microseismic noise rate which indicated that new fractures had formed. At failure, rock spalls occurred in the roof along the boundaries of the room, and pieces 1 to 6 inches thick and 1 to 5 feet square fell from the center of the room.

In the first series of tests, roof sag was measured using convergence extensometer measuring rods attached to fixed points in the floor and roof of the opening. Stratascopes were used in boreholes to visually observe the amount of bedding plane separation.

Remote reading instruments were required for the 20-inch roof layer which was tested to failure. To measure roof sag, rotary potentiometers were used. Wires attached to rods fixed in the roof and floor were wrapped around the potentiometer pulleys. Constant tension in the wires was maintained by a deadweight system. The strains in the roof layer were determined using a telescoping rod attached to fixed points on the roof surface. A differential transformer attached to the rod provided an electrical readout of the rod displacement.

The 20-inch roof layer was analyzed using the theory for a gravity loaded beam with ends clamped. The extreme fiber stress computed at failure agreed closely with the modulus of rupture determined from laboratory tests. The in-situ modulus determined from the pressure-deflection

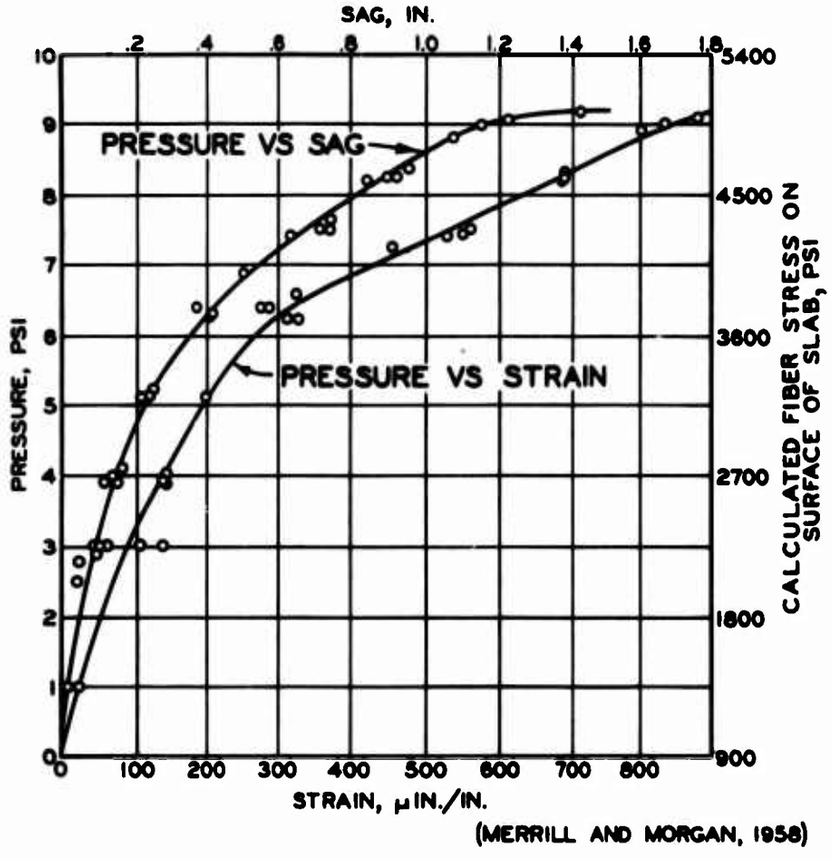

Fig. 2. Sag and strain versus pressure, bedded limestone roof slab, Jonathan Mine

measurements was initially 11×10^6 psi, agreeing closely with the laboratory modulus of 10.4×10^6 psi. Although the laboratory stress-strain behavior was approximately linear to failure, the calculated in-situ modulus decreased from 11×10^6 psi to 2×10^6 psi as failure approached (Fig. 2). This is an example of the unstable deformation criteria described by Lang (1964)--increasing deformation rate with respect to load. It is apparent that, as failure approached, increased inelastic behavior consisting of discontinuous movements along new and previously formed fractures occurred in the roof layer.

The movements due to the changes in the stress field surrounding the opening formed a relatively insignificant part of the measured deflections and were not analyzed. In other examples to be presented in this section, the deflections due to the changed stress field around the openings are of much greater importance, and the analysis must consider these effects. Beam theory is not applicable to these cases; it should be limited to situations as described above, where the roof layers can be analyzed as distinct beams which separate from the overlying beds.

Room and Pillar Mines: White Pines Mine, Michigan

Displacement measurements were made in a room and pillar test stope at the White Pines Mine to determine the feasibility of mining at depths greater than 2000 feet (Scott and Parker, 1964). Movement occurred in both the roof and floor of the stope in response to the stress changes around the openings as they were excavated. (Approximately 40% of the total convergence consisted of floor heave.) In contrast to the observed movement in the Jonathan Mine, only a slight portion of the total convergence was attributable to gravity forces in the immediate roof slabs.

The test stope covered an area 250 by 350 feet at a depth of 2200 feet in a bedded sandstone, siltstone, and shale. Within this area, 20-foot-wide by 15-foot-high drifts and crosscuts were mined, leaving 30- by 40-foot pillars. The stope was mined in two passes. During the first pass the drifts and alternate crossdrifts were mined. In the second-pass mining, the remaining crossdrifts were excavated, increasing the total extraction from 56 to 66%. Roof support consisted of 4- and 7-foot bolts on 4-foot centers.

Movements were measured by leveling, using a Wild NIII precision level and an invar leveling rod. The invar rod was attached to fixed points anchored at depths from 6 inches to 20 feet in the floor or roof. Measuring stations were placed during the first-pass mining.

The results of the measuring program showed that a general roof subsidence of approximately 3 to 4 mm and a floor heave of at least 2 mm occurred in the center portions of the stoped area, due to mining of the stope. (The total convergence, or pillar shortening, was therefore 5 to 6 mm.) Roof subsidence was smaller near the edge of the stoped area. Superposed on the general roof subsidence of 3 to 4 mm was an additional roof sag of approximately 1 mm which occurred between pillars. This was most pronounced at intersections, where the minimum clear span was approximately 30 feet. It is possible that additional floor heave also occurred between pillars, but measurements were not made at these locations. Increased roof displacement occurred in the vicinity of fault zones.

A large increase in roof displacement occurred during second-pass mining: 2.5 mm of the total 4 mm displacement occurred during the initial pass when 56% of the ore was extracted; an additional 1.5 mm occurred

during the second-pass mining when the extraction was increased from 56 to 66%. It was observed that the amount of pillar spall (extension type fractures) also increased during the second-pass mining. Even though the total stress on the pillars was probably less than one-fourth their crushing strength, it seems apparent that the increased load applied to the pillars caused a significant increase in the amount of inelastic behavior of the pillars--in this case exhibited as shallow spalling of the pillars.

The relative displacements between the rock surface and the 20-foot depth were quite small, indicating that significant shallow roof sag and bed separation were not occurring. Measurable rock movement to a depth of approximately 250 feet from the opening would be expected for a stope of this size.

After the stope was completed, small additional movements occurred. The rate of movement decreased with time, indicating a stable condition. However, in one instance during mining, a significant increase in the rate of movement occurred at one of the roof stations. The increased movement occurred only in the shallow roof zone; no increase was observed at the 20-foot depth. The area was roped off and a small roof fall occurred.

Most of the displacements which occurred in the stope can be analyzed using elastic theory. Young's modulus determined from laboratory tests on intact specimens was 6×10^6 to 7×10^6 psi. The in-situ deformation modulus, determined from pillar shortening, is approximately 4×10^6 psi for first-pass mining, and 3×10^6 psi for first- and second-pass mining combined. The presence of in-situ discontinuities is undoubtedly responsible for the low in-situ modulus. The lower modulus is a result of a certain amount of inelastic behavior due to local spalls and movement along joints

and fractures. The decrease in in-situ modulus with increased extraction indicates that further extraction might cause large inelastic movements and possible failure of the pillars. However, most of the observed movements were fairly uniform and reasonably predictable. Gross, discontinuous movements did not commonly occur. Thus, the movements indicated that the overall stability of the stope was maintained.

Multiple Openings

In the previous examples the movements occurring during excavation of an opening were described. This section describes the behavior of openings already excavated which fall within the zone of influence of nearby mining operations. The situation commonly occurs when a large area, such as a stope or block-caved mine, is excavated in the vicinity of an access drift. The stresses previously existing around the drift are changed by the nearby excavation, in some cases to such an extent that distortion and failure of the drift occur. In other instances the change in stress is so small that the movements in the drift can be predicted from elastic theory.

Climax and San Manuel Mines. Merrill and Johnson (1964) observed the movement in unlined and concrete-lined drifts located 15 to 45 feet below block-caving areas of the Climax Molybdenum Mine, Colorado, and the San Manuel Copper Mine, Arizona. The openings were subjected to abrupt and large changes in stress during caving. These changes frequently produced minor failures that damaged the lining of the openings. In some cases, major failures occurred which required the use of additional support.

As the block-caved region approached the drift, vertical stresses built up in the abutment rock ahead of the caved region and caused

distortion of the drift. The vertical diameter decreased and the horizontal diameter of the drift increased under these changed stress conditions. Local failures often occurred around the drift due to the increased vertical stress: tension cracks up to 0.5 inch wide occurred in the roof; local crushing and spalls occurred in the side walls. As the caved region passed over the drift, the vertical stresses were relieved and the horizontal stresses increased, causing an increase in the vertical diameter and decrease in the horizontal diameter of the drift. Local failures also occurred; in this case the tension cracks were in the side walls and the splintered and spalled rock in the roof and floor.

Instrumentation in the drifts consisted of electrical resistance strain gages embedded in the concrete, Whittemore extensometers to measure surface displacements between points 10 inches apart, convergence extensometers to measure the change in diameter of the drifts, and Carlson strain meters (extensometers) grouted in boreholes extending 5 to 10 feet radially from the drift surface.

Much of the observed movement was small and elastic; the strains were on the order of 0.1 to 0.3%. However, the local failures and continued closure which occurred around some of the drifts are indicative of unstable behavior.

Julin (1964) also reports the results of measurements made at the Climax Molybdenum Mine. Measurements were made in order to better understand the conditions contributing to crushing of the access drifts during caving. Severe damage to the drifts (located below the caved area) would often occur immediately ahead of the caved area, in the highly stressed, uncaved abutments. Convergence measurements in the drifts showed that the

maximum stresses were occurring in the drifts which were approximately 70 feet ahead of the uncaved ore. Once the caved areas were exhausted and filled with the broken country rock they were again capable of supporting a portion of the overburden stresses, thus distributing the loads more uniformly throughout the area and decreasing the large areas of high stress concentration around the actively caved area. Therefore, by keeping the actively caved area as small as possible, extreme abutment loads causing failure of the drifts were minimized.

Star Mine, Burke, Idaho. Waddell (1964) reports on measurements made in access drifts during stoping of a vertical vein at a depth of 6000 feet at the Star Mine, Burke, Idaho. The vein was mined from the bottom to the top in 200-foot vertical sections. Mill tailings were used to replace the ore in the mined out portion of the vein. The access drifts were parallel to and 50 feet from the vein and were located every 200 vertical feet. The access drifts were 8 by 8 feet in cross section and were rock-bolted.

The behavior of the drifts was similar to that observed at the Climax Mine; however, because the vein was vertical, the maximum change in stress occurred in the horizontal direction. The horizontal stresses that built up in front of the upward-advancing vertical stope caused large horizontal closure of the access drifts. Horizontal closure of the drifts ranged from 1/2 to 1 inch in stable areas to 1 foot in areas where rock failure occurred. Approximately 2/3 of the rock movement occurred within 6 feet of the wall of the drift. In almost all cases the vertical closure in the drift was less than the horizontal; it rarely exceeded 1 inch.

Most of the movement in the drifts took place as the vein was mined,

over a period of one to two years. The rate of closure was fairly constant as the stope approached the drift. As the stoping was completed the rate of closure decreased. Large decreases in the horizontal stress (and increases in the horizontal diameter) were not observed as the stopes passed the opening as they were at the Climax and San Manuel Mines. It is probable that the horizontal stresses were transmitted through the tailings which replaced the mined ore; thus the mined out stope did not completely behave as a hollow slit.

A variety of instruments were used to measure rock movement. These included strain-gaged, tensioned rock bolts (these were not too reliable), clusters of single-position borehole extensometers anchored at varying depths, transit and survey levels, tapes to measure changes in the diameter of drifts, and multiple-position borehole extensometers. The multiple-position extensometers were placed to depths up to 70 feet. Anchorage was obtained using six explosive anchors placed at various depths in the borehole. The wires running from the anchor to the surface were tensioned by a deadweight system. Readout at the surface was provided by a mechanical dial-pulley assembly to which the wires were attached.

South African Gold Fields. Much of the movement described in the preceding paragraphs was inelastic and associated with closure and failure of the drifts. Ortlepp and Cook (1964) have measured movements in the rock surrounding advancing stopes at depths of approximately 5000 and 8000 feet in the South African gold fields and found close correlation with elastic theory. This indicated to the authors the validity of using elastic strain-energy concepts in the prediction and analysis of rockbursts. Much of the rock failure observed in these mines is by rockbursting.

The rock is typically a hard, massive quartzite with an intact strength of 36,000 psi and a Young's modulus of 12×10^6 psi; the stress-strain curve is linear to failure.

Rock movement was measured by precise leveling of rods anchored 8 feet above the access drifts; the drifts were located 50 feet below the advancing horizontal stopes. Some measurements were also made using borehole extensometers.

By measuring the absolute displacement of the rock 8 feet above the drift, the general displacement of the rock toward the advancing stope could be measured. (These measurements were far enough from the drift that they were not strongly affected by its closure.) As the stope passed over the access drifts, upward displacements on the order of 2 to 7 inches occurred toward the stope. The observed displacements correlated quite closely with the theoretical displacements around a slit in an elastic medium, using the elastic constants determined from tests on intact specimens (Ortlepp and Cook, 1964).

This would indicate that the rock mass was relatively unjointed and had the same properties as the intact specimen: the movements were measured far enough from the immediate vicinity of both the access drift and the stope that the effect of loosening and fracturing around the openings did not affect the measurements. Thus, the behavior was elastic.

In one instance, measurements were made with a vertical borehole extensometer which extended upward from the drift across the path of the advancing stope. Movements of the rock both above and below the stope were toward the stope. Because of the large size of the stope, much of the

displacement occurred at depth, reflecting a general movement of a large volume of rock surrounding the stope. When the stope intersected the borehole, anchors in the immediate vicinity of the floor moved up more than elastic theory would predict, thus indicating a lower deformation modulus near the stope, undoubtedly a result of near-surface loosening of the rock mass.

Rockbursts

Rock movements have been measured in deep mines in order to predict the occurrence of rockbursts. Moruzi and Pasieka (1964) have compared the closure of drifts with the occurrence of rockbursts in the Falconbridge Mine, at a depth of 4000 feet in a hard, elastic jasperoid and norite. They found a slight increase in closure prior to a rockburst and a decreased rate of closure after the burst. Isaacson (1958) states that increases in closure rate indicate that the excavation is tending toward a state of violent collapse.

However, because rockbursts are brittle and rapid failures, it is not always possible to observe a gradual increase in displacement leading toward failure. In some cases, a cessation of movement may also be indicative of rockburst conditions (Spalding, 1949). A hard zone of rock may be encountered which allows stresses to build up with very little deformation until the rock mass reaches its ultimate strength and fails. Spalding suggests that any extreme variation from a normal condition be suspect. The prediction of rockbursts from displacement measurements is difficult, and if at all successful, requires continued observations and experience at a specific site.

The results of measurements in deep mines in the McIntyre gold deposit,

Ontario (Cochrane, Carter, and Barron, 1964), serve to illustrate the difficulty involved in using displacement measurements to predict rockbursts.

Stress and deformation measurements were made during the mining of two remnant stopes bounded by compressible waste areas. One stope was in a weak lava, the other stope was in a high-strength, brittle porphyritic rock susceptible to rockbursts. In the lava remnant the stress buildup was small, but the deformation was large (0.68 inch when the face came within 20 feet of the 10-foot borehole extensometer located in the hanging wall). In the porphyritic rock, a large buildup of stress occurred, but very little deformation took place. The extensometer registered no flow or crushing tendencies of the rock, even when the stope face was within 10 feet of the unit. A small rockburst occurred in the face of the stope at this time.

Civil Works: Tunnels

Displacement measurements have been used to determine the stability during the construction of civil works structures, such as tunnels and large underground openings. The emphasis in civil works construction is on permanent support and long term stability. In many cases, rock failures which are allowed to occur in a temporary mining situation cannot be tolerated for a permanent structure.

Measurements have been made in tunnels not only to determine stability, but also in an attempt to estimate the loads that will be applied to the support system as the rock continues to creep into the opening.

When analyzing tunnel movements, it should be noted that much of the initial elastic (continuum) displacement occurs prior to the installation of the measuring system. The recorded displacements, therefore, are a

result of the continued excavation of the tunnel, as the stress conditions change from a three-dimensional distribution near the face to the two-dimensional distribution of a long tunnel. In addition, discontinuous movements begin to occur, as the rock loosens around the opening. The loosening of the rock is not directly related to excavation progress but is quite dependent on the ability of the support system to restrain the rock mass. For a highly jointed or bedded rock mass, much of the discontinuous movement is in the crown, due to the gravity load of the near-surface rock. The discontinuous movements are often time-dependent, so that the rock mass surrounding the opening is described as having creep characteristics.

Finally, movement of the rock around the opening is affected by the interaction of a continuous support system (such as steel sets) with the rock wall, as the support takes load and distributes it around the perimeter of opening.

Tunnels of the Hydro-Electric Power Commission, Ontario. Displacements were measured during the construction of pressure tunnels in the Niagara area in order to estimate the rock load which would act on the permanent concrete lining (Hogg, 1958). The tunnels were 50 feet in diameter, located 300 feet beneath the ground surface in bedded sandstones, limestones, and shales (Fig. 3a). Construction was by the heading and bench method. Steel ribs for temporary support of the crown were placed approximately 25 feet behind the heading face. Chord movements of the tunnels were measured during construction using invar tapes and fixed reference pins anchored 3 feet into the walls of the tunnel. Reference pins were installed immediately after excavation of the heading so that initial readings could be obtained prior to excavation of the bench.

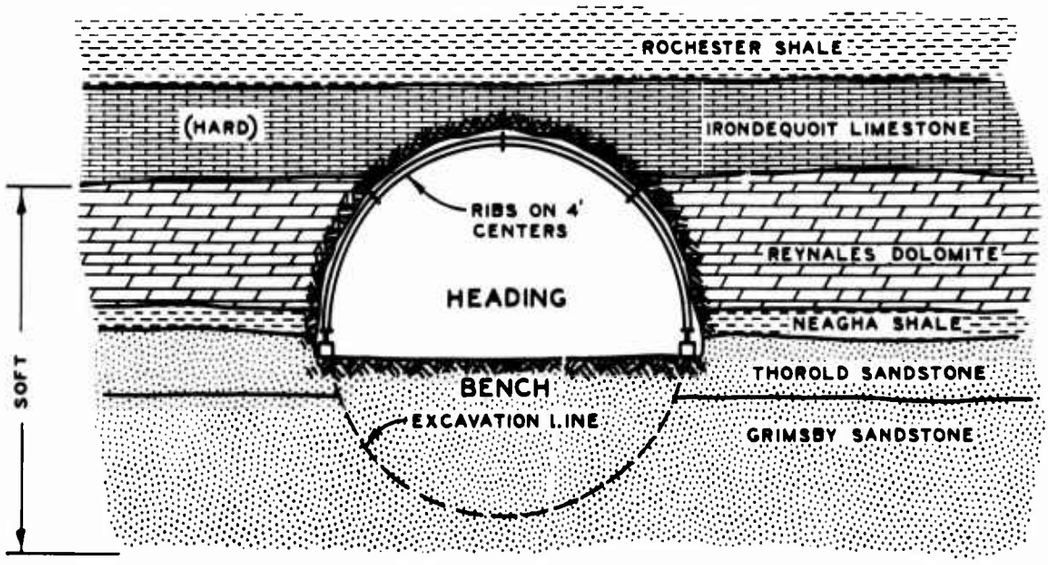

a. TYPICAL TUNNEL CROSS SECTION

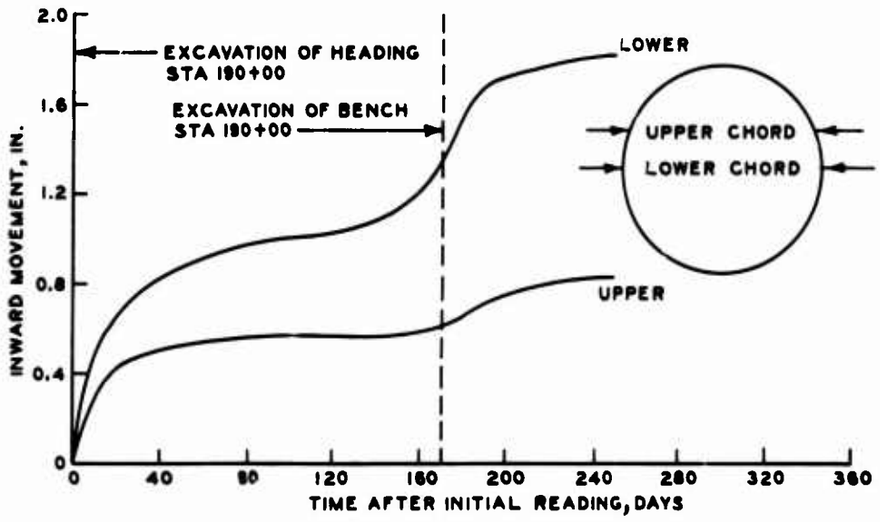

b. TYPICAL ROCK MOVEMENT VS TIME, STA 190+00, TUNNEL NO.1

(HOGG, 1958)

Fig. 3. Horizontal chord movement of tunnel wall, bedded sedimentary rocks, Ontario

Fig. 3b shows the typical horizontal movements observed in Tunnel 1. An inward horizontal movement of 1 inch occurred due to excavation of the heading; a further 0.8 inch movement was due to excavation of the bench. The rate of movement decreased logarithmically with time. Heaving and cracking of the sandstone in the invert would often occur as the bench was excavated. However, vertical movements in the hard limestone crown were very small--approximately 0.050 inch.

A second tunnel was driven parallel to and 250 feet from the first tunnel. The horizontal movements in the second tunnel were approximately 1/4 to 1/3 the movements observed in the first tunnel. In one instance, vertical movement of the invert was measured using a rod anchored in the floor. Bench removal caused an upward movement of the invert of 0.5 inch. Shearing displacements along bedding planes were also observed in shallow vertical drill holes in the bench of Tunnel 2. The upper layer of the bench was displaced toward Tunnel 1 with respect to the lower layers. The excavation of Tunnel 2 had very little effect on the rock movement in Tunnel 1.

The horizontal movements in the tunnels plotted as a straight line on a logarithmic time plot. The extension of this line was used to predict the movement which would affect the permanent concrete lining. The actual rock loads applied to the lining were much smaller than predicted, because of contraction of the concrete as it cooled (Hogg, 1958).

The intact (laboratory) modulus of the bedded deposits ranged from less than 1×10^6 psi to 10×10^6 psi. The inward wall movement determined from elastic theory is 0.1 inch, assuming a hydrostatic stress distribution and a rock modulus of 1×10^6 psi. The vertical displacement in the crown

approximated the predicted elastic displacement. However, the horizontal displacements of the walls were an order of magnitude greater than predicted. It is apparent that inelastic and discontinuous movements were occurring in the rock around the tunnels. Much of the observed movement--the large horizontal displacements, the shearing displacements along bedding planes, and the small movements in the crown--is a result of anisotropy and extreme variations in modulus and strength of the bedded deposits.

Wyoming and Colorado Highway Tunnels. In 1964 and 1965, rock movement was measured during construction of 30-foot-diameter twin highway tunnels near Green River, Wyoming, in bedded marlstones, siltstones, sandstones, and shales (Dutro, 1966). Rock movement was also measured in the Straight Creek test tunnel in Colorado, driven full face in a granite (Hartmann, 1966). Both tunnels were supported by steel sets. The purpose of the measurement program was to "determine the actual tunnel support requirements."

Rock displacement was measured with multiple-position extensometers placed in holes drilled radially at the tunnel surface. The extensometers consisted of 8 anchors placed at varying depths in a single borehole, with wires running from the anchors to strain-gaged cantilever steel strips at the surface. The changes in electrical resistance were calibrated to give the displacement of the anchors. (Problems are involved with this type of measuring system because of the changing tension on the anchor wires for large displacements of the anchors.) Load cells were placed on the steel ribs to measure the loads applied to the steel sets.

With the multiple anchors, the depth of the loosened zone in the crown, where movement into the cavity was occurring, was defined. From the load cell measurements it was observed that loads on the steel sets

were initially high and decreased to a residual value as the sets yielded and redistributed their load.

It appears from the figures presented by Dutro and Hartmann that the near-surface rock in the crown of the tunnels moved into the opening while the rock in the side walls moved away from the opening. The magnitude of these movements could not be determined from the figures presented. The extensometers were probably installed after much of the initial elastic movement had occurred so that the observed movements were a result of loosening of the near-surface rock and interaction of the steel sets with the walls of the opening. It is possible that as the steel sets were loaded by the loose rock in the crown, they applied lateral force to the rock on the side walls, causing it to displace away from the opening. Rock movements observed in a pattern-bolted tunnel would, in all probability, differ significantly from those observed with the steel sets.

Civil Works: Large Openings

In recent years, many large underground openings have been built for civil works projects, primarily underground powerhouses and defense installations. Moye (1959) reports that over 300 underground powerhouses have been built throughout the world at depths up to 1450 feet beneath the surface. These openings differ from large mine openings, such as block caving systems, because their stability must be maintained throughout construction. The openings are usually constructed in increments from the top down, and the upper portions of the opening are stabilized before excavation proceeds further. Because the openings are excavated gradually (unlike tunnel construction), it is relatively easy to measure the rock movement caused by excavation. Thus it is possible to make corrections to

the excavation and support program on the basis of the observed movements.

Snowy Mountain Hydroelectric Authority. The powerhouses of the Snowy Mountain Hydroelectric Authority, Australia, are perhaps the most completely documented of any large underground construction reported in the literature. (Lang, 1957, 1959; Moye, 1959; Alexander, Worotnicki, and Aubrey, 1964; and others.) Two underground powerhouse machine halls, Tumut I and Tumut II approximately 300 feet long, 110 feet deep, and 60 and 50 feet wide, were constructed in a moderately jointed granite and granite gneiss at depths of 750 and 1000 feet beneath the surface, respectively. In-situ stress measurements at Tumut II by the flat jack method (corrected for the stress concentration at the opening) revealed the presence of high natural horizontal stresses of approximately 1800 psi. The natural vertical stress was approximately 1500 psi. The natural stresses at Tumut I were similar.

The rock mass characteristics in Tumut I are described by Lang (1959). "The joint spacing in the granite gneiss was usually between 6 inches and 2 feet. The joint surfaces were usually smooth and slickensided and dark green in color due to thin coatings of chlorite.... Most joints were tightly closed. Because of the nature of the joint surfaces it was common in the excavations for the granite gneiss to break to the natural joint planes rather than break across the rock resulting in angular surfaces and local small overbreak in many places." The granite gneiss would probably be termed a rock of fair to good rock mass quality (Appendix A).

"The joint spacing in the granite was variable but was generally in the range of 1 to 5 feet. The more closely jointed zones occurred irregularly, and slickensided joints were not so common as in the gneiss. Most joints were tightly closed, and because of this it was found that breakage

of the granite often occurred along new fracture surfaces rather than along natural joints." The granite would be termed a rock of excellent rock mass quality (Appendix A).

"It was judged that the (Tumut I) powerhouse could be constructed in either rock type, but because of the difference in jointing it was considered that large openings would be easier to construct in the granite and would require less permanent support. For this reason the greater part of the station was located in the thickest granite sheet." The intact elastic modulus of the granite was approximately 8×10^6 psi.

The instrumentation in Tumut II (more extensive than that in Tumut I) consisted of Carlson strain meters (embedded, unbonded resistance strain meters) and stress meters (mercury-filled cells) embedded in the concrete ribs, located in the crown of the chambers. Rock strain was measured with Huggenberger deformeters of 20-inch base length, and rock displacement by precise levels using a geodetic theodolite. Rock dilation was measured with restrained rock-bolt deformeters anchored at depths from 4 to 14 feet. Angular deflections at the spring line and on the walls were measured with a Galileo clinometer.

The crown of Tumut I machine hall was initially excavated its full width and rock-bolted. However, the excavation procedure was changed when the workmen became apprehensive, working under such a large rock-bolted span. Parallel slots were then cut across the crown and rock bolts and temporary steel ribs were placed in the slots where the surface of the crown was exposed. The rock between the slots was excavated after the steel ribs had been installed. The steel ribs were later removed with no detectable movement of the crown. Permanent concrete ribs were installed

in the crown, and the main body of the machine hall was excavated by quarrying methods.

Rock bolts consisted of mild steel bars, 1 inch in diameter and 10 to 15 feet long, and were spaced on 4- to 5-foot centers throughout the chamber. The bolts had mechanical slot and wedge anchors and were tensioned to a nominal load of 15,000 pounds. Bolts in the walls of the chamber were later grouted for permanency.

Strain measurements were made in the concrete rib of Tumut I throughout construction. As excavation proceeded downward, cracking occurred in the concrete where the ribs joined the rock abutment (at the spring line). This was consistent with the measured rotation of the abutments. The rotation created stresses in the rib near the abutment which were several times greater than the average stress throughout the rib.

Horizontal displacements of the machine hall walls were measured near the end of construction using a precise survey method. The excavation of approximately 30 feet of rock from the lower portion of the machine hall caused an inward displacement at the abutment (spring line) of approximately 0.4 inch, in the vicinity of a high angle fault located behind the wall; and 0.15 inch inward displacement at other portions of the abutment, not in the vicinity of the fault. Loosening of granite joint blocks was also observed in the vicinity of the closely jointed rock associated with the steeply dipping faults. Much of the rock movement associated with the fault was inelastic and discontinuous and occurred after construction had been completed.

Moye (1959) describes the rock fracturing which occurred in the Tumut I machine hall. A pillar isolated by the excavation began to fail by spalling

parallel to its surface. Spalling parallel to the free surface was also observed around the penstock tubes after their construction, as the excavation of the nearby machine hall increased the stresses around the penstocks. Tension cracks were also formed across the concreted draft tubes and penstock tubes as the machine hall was excavated. The cracks paralleled the machine hall surface, and dipped steeply toward the bottom of the machine hall. Some of the cracks were open 1/2 inch. These failures are similar to the extension type (relief) fracturing observed in the cavities constructed at the Nevada Test Site, discussed in Chapter 5.

In Tumut II machine hall, the design and construction of the concrete ribs were modified to reduce the cracking which occurred at Tumut I. To reduce the strains which would occur in the ribs, the ribs were placed after 20 feet had been excavated from beneath the abutment level.

Wall displacements were measured throughout construction; the average displacements along the walls are illustrated in Fig. 4. The inward displacement of the walls occurred during construction and can be correlated with excavation progress. The wall displacements correspond to a deformation modulus of approximately 2.2×10^6 psi, based on photoelastic model studies and in-situ stress determinations. The modulus determined from the strain in the concrete ribs was approximately 7.3×10^6 psi. Alexander (1964) attributes the lower modulus on the side walls to decompression of the jointed rock--"a pseudo-elastic expansion of jointed rock"--whereas the rock in the crown was subjected to increased compression, and therefore did not open along joint planes. The large, plane surface of the walls also contributed to loosening. Joints subparallel to the walls aggravated this condition. Small rock falls and opening of joints on the surface of the

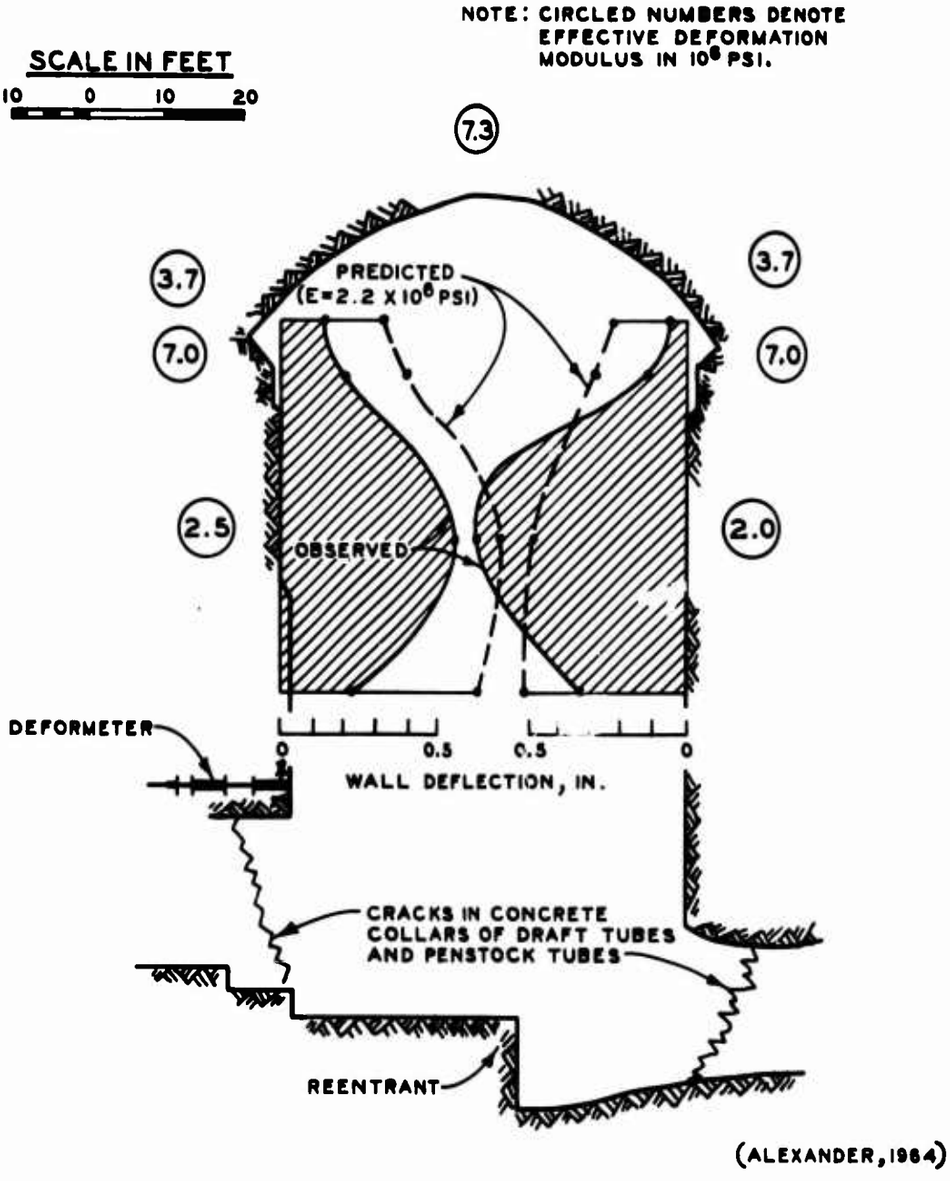

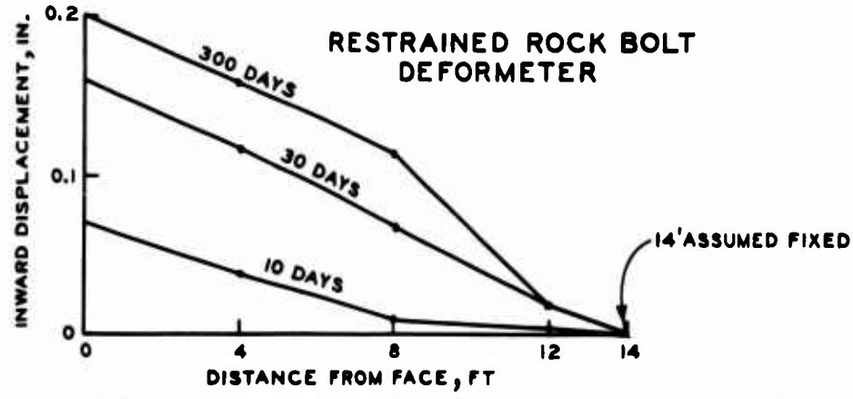

Fig. 4. Wall displacement and observed deformation modulus in Tumut II machine hall, Australia

walls were observed. In one instance continued freshening was visible in the dust along joints in the walls, and was culminated in a small rock fall (1/2 cubic yard). Alexander concludes that "the high wall dilation observed in Tumut II showed that rock bolting did not fully prevent active general decompaction in the large flat wall surfaces."

"Evidence of the general dilation of the machine hall walls was also obtained in the eight penstock and draft tube tunnels which enter the machine hall through the walls. These tunnels were excavated 8 months prior to the machine hall and were lined with concrete to prevent rock spalling due to concentration of rock stress as the machine hall was excavated over the face of the tubes. Cracks in the 10-foot-long concrete collars were observed in the eight tubes after the machine hall was excavated over the face of the tubes. These cracks had a characteristic dip of 50 to 80 degrees downward toward the machine hall" (Fig. 4). In one draft tube a crack width of 0.2 inch was observed. Four rock-bolt deformeters located near the draft tube also showed this dilation (Fig. 4). The surface moved inward 0.2 inch with respect to the 14-foot anchor; and much of this movement was concentrated between 8 and 12 feet, indicating the possibility of a crack.

Photoelastic studies showed that the reentrant blocks located in the invert of the machine hall were subjected to radial tension. Stapeldon (1961) considered this to be the main factor in the observed deterioration of the reentrant rock.

The cracking observed in the penstock tubes and draft tubes in Tumut II was quite similar to that observed in Tumut I.

The values of the deformation modulus for the rock at Tumut I and II are compared as follows (Alexander, 1964):

Method of Test	Mean Modulus psi × 10^6 Tumut I	Tumut II
1. Unconfined compression test (intact specimens)	8	8
2. Dynamic test (intact specimen)	8	8
3. Flat jack test, rock in place	5	6
4. From strains in machine hall roof	2	5
5. Expansion of pressure shafts during filling	2	(3)
6. Deflection of machine hall walls	(very low)	2
7. Plate bearing tests on rock in place	--	1
8. Dilation of machine hall walls (deformeters)	--	0.8 to 7.0

The rock at Tumut II was more tightly jointed than at Tumut I. This, together with the two faults at Tumut I (one located above the crown, the other dipping at a steep angle behind one of the walls), was probably the major reason that the effective modulus determined from the strains in the machine hall ribs was higher at Tumut II than at Tumut I (Alexander, 1964).

Kariba Underground Works, Zambezi River, Federation of Rhodesia and Nyasaland. The machine hall at the Kariba damsite is 468 feet long, 75 feet wide, and 132 feet high. It is located at a depth of 200 feet in a foliated biotite gneiss (Lane and Roff, 1961). Rock in the upper portions of the underground works was described as "a broken and altered gneiss with seams of decomposed gneiss and slickensides." The lower portions of the underground works are in a sound gneiss which is "compact and jointed with

few fissures." Most of the machine hall was located in the sound gneiss, although a portion of the crown was in the heavily jointed gneiss, and the northwest corner of the machine hall was intersected by a fault zone.

The crown of the hall was supported by a concrete arch, bearing on rock abutments at the spring line. Large portions of the wall were supported by concrete linings arched vertically and anchored to the rock top and bottom. The lower portions of the walls were supported by buttresses tied into the machine foundations. Grout was pumped into fractures in the rock and into gaps between the rock and concrete lining to prevent excessive seepage and to provide a monolithic concrete-rock structure. The concrete linings and the grout were designed for water pressure as well as rock pressure. Some drainage was provided in the walls of the machine hall.

Rock bolts were placed during excavation to secure potentially weak areas of the rock face. Timbering was also used to support some heavily jointed portions of the crown. Excavation and concreting of the crown were carried out full face. The main hall was then excavated in lifts.

Horizontal movement of the walls was generally less than 0.5 inch, except in the vicinity of the heavily jointed fault zone at the northwest end, where 1.5 inches of movement were recorded. The jointed zone was reinforced with tensioned cables placed between the machine hall wall and a construction gallery. Subsequent movements were small.

One of the concrete buttresses located near the fault zone was highly stressed and developed shear cracks. However, the low strains recorded by the embedded acoustic strain meters indicate that most of the buttresses, as well as the concrete linings in the wall and crown, have not been highly stressed (Lane and Roff, 1961).

The observed movement of the walls of the machine hall is larger than would be predicted from elastic theory. If a modulus of 4×10^6 psi is assumed for the sound gneiss and a horizontal pressure of 400 psi is assumed for the natural rock stress, then the predicted movement would be approximately 0.15 inch. The movement in the fault zone was an order of magnitude larger than this, indicating discontinuous rock movement.

NORAD Combat Operations Center. Large, intersecting chambers were constructed in Cheyenne Mountain, Colorado, to provide protection against nuclear weapons for the NORAD Combat Operations Center. The underground complex consists of three parallel chambers, 45 feet wide, 60 feet high, and 600 feet long, separated by rock pillars 100 feet wide and connected by three intersecting chambers 32 feet wide and 56 feet high. (Underwood and Distefano, 1964.) Chambers were constructed by the heading and bench method; the benches were excavated in two lifts. Rock bolts were typically 8 and 10 feet long on 4-foot centers in the crown of the chambers and 10 feet long on 5-foot centers on the walls of the chambers. The bolts were mechanically anchored. The bolts were tensioned and, at a later date, completely grouted.

The rock-bolt support placed in the chambers was designed for dynamic stability as well as the static construction stability. Initially it was planned to install safety bolting and delay the pattern bolting until the excavations were complete. Underwood and Distefano state that "Some experts believed that pattern bolting should be delayed for several weeks until all potentially slabby rock had worked loose and been scaled down, but the majority of experts believed that pattern bolting should be installed as close to the headings as possible after scaling." They conclude

that "An...important factor in any rock strengthening program is prompt and adequate support of the rock immediately following excavation. Contract specifications must be specific in this regard as words such as 'soon as possible' may not be soon enough."

The site was located in a moderately jointed, coarse-grained granite having an intact strength ranging from 10,000 to 20,000 psi. Much of the jointing was along two major high angle systems oriented at right angles to each other. A few shear zones paralleled one of these systems.

The chambers were oriented so that the predominant joint systems would cut the chamber walls at an angle, rather than paralleling the walls. However, a minor high angle joint set was present which was subparallel to the walls of the large chambers and caused slabbiness on the south walls of the large chambers.

Some problems with opening of joints and loosening of rock blocks were encountered at chamber intersections, where the major joint systems cut across the corners of the pillars. At two of the intersections (A-2 and B-3) fractures were open as much as 1 to 1-1/2 inches at the surface, along joints which dipped 30 to 50 degrees toward the corners and daylighted a few feet above the invert. Stratascope observations revealed open joints as far as 13 feet from the face at one of the corners. In order to strengthen the corners to resist dynamic loads, it was decided to reduce the mass of rock located forward of the joint planes by 75 to 100 cubic yards. The remaining rock would be supported with high-strength, grouted bolts placed normal to the joint system. The rock was removed from the top down in small rounds (up to 35 cubic yards) and 1-inch-diameter, 24- to 30-foot rock bolts were immediately installed. At one intersection, 0.2 inch

movement occurred at a 24-foot-long extensometer located 24 feet above the invert, due to blasting at the toe. After the movement occurred, additional bolts were placed and excavation was temporarily suspended. At the other intersection, a maximum outward movement of 0.13 inch was recorded. A number of 12- to 28-foot-long restrained rock-bolt deformeters were installed in the corners after construction had been completed in order to monitor future rock movement. Only insignificant (0.035 inch) movements were recorded following their installation.

Major support problems were encountered at another intersection (B-2) where one of the high angle shear zones intersected the opening. In order for the intersection to be stable under dynamic loads, it was decided that a reinforced concrete lining (eggshell shaped) would be required, extending through both the invert and the crown. Underwood and Distefano summarize the monitoring program at the B-2 intersection: "In the B-2 intersection, where it was necessary to greatly enlarge the opening in already unstable ground in order to provide space for the concrete structures, numerous gages were installed and read after every blast to make sure no serious movement had occurred. The size and magnitude of each successive round was governed by these readings. It is significant to note that movements much larger than those recorded at the A-2 intersection were recorded at this intersection. It is also significant to note that movements were always quickly brought under control by the application of a few rock bolts in the affected area."

It is apparent that the movements observed in the corners of the intersections were inelastic and related to movement along discontinuities. The NORAD experience reinforces the observations made at Tumut, that large

discontinuous movements and stability problems are often associated with reentrant corners and with joint and wall geometrics which tend to isolate thin wedges of rock near the surface of the opening.

Morrow Point Powerplant. An underground powerhouse is presently nearing completion at Morrow Point Dam in the Black Canyon of the Gunnison River, west-central Colorado (Seery, 1966). The machine hall is 206 feet long, 57 feet wide, and 134.5 feet high, located at a depth of 400 feet in a schist with some quartzite and some pegmatite intrusions. A system of stress relief joints parallels the canyon walls. Faults and foliated weakness planes in the schist are present at the site. Two shear zones were also present in the vicinity of the chamber which caused support problems.

To construct the chamber, a pilot, exploratory tunnel was driven near the crown of the machine hall. The crown was then excavated and bolted. The lower portion of the chamber was excavated by benching. Rock bolts were 12 to 20 feet long, placed on 4-foot centers, and tensioned and grouted. Additional bolts were placed, as necessary, in shear zones. No unsupported rock was permitted more than 4 or 5 feet from the headings for a period longer than 12 hours after blasting.

Instrumentation during construction consisted of eight multiple-position borehole extensometers (the type described for the Colorado and Wyoming Tunnels), precision level surveys, and tape convergence measurements.

Three extensometers were installed in the pilot tunnel prior to excavation of the crown. As the heading passed the extensometer locations, the extensometers experienced their maximum displacements. Two units showed

0.35 inch displacement between the surface and the 50-foot depth. The movement was essentially complete within 200 hours after the heading passed the instruments. One unit displaced 0.02 inch. The multiple-position units showed that the movements in the crown were concentrated near the opening, and dropped off rapidly with depth.

On one of the side walls of the chamber, the extensometer and precise survey measurements indicated an inward movement of approximately 2 inches in a period of two months. Upon completion of blasting operations, the wall apparently stabilized. However, additional treatment to the wall was considered necessary to provide for its permanent stability. Long (up to 78-foot) rock bolts and stressed tendon anchorages are to be installed. Drainage will also be provided behind the wall for the full length of the chamber. The drainage tunnel will provide access to the tendon anchorages. Additional support of the lower portion of the chamber will be provided by post-stressing the reinforced concrete structures supporting the generator units (Seery, 1966).

Predicted inward elastic displacements in the crown of the chamber, for a deformation modulus of 4×10^6 psi, should be on the order of 0.05 inch. The observed displacements of 0.35 inch indicate that possible near-surface loosening occurred in the crown, decreasing the deformation modulus. Examination of the extensometer displacement-depth records may confirm this conclusion. The 0.02 inch movement observed at one of the extensometer locations in the crown is probably quite close to a predicted elastic, unjointed movement.

The predicted elastic displacement for the side walls is on the order of 0.2 inch. The observed 2 inch inward displacement of the wall was

therefore definitely inelastic and discontinuous, and, from the nature of the remedial support program outlined by Seery, was probably deep-seated and associated with weakness planes behind the wall of the chamber.

Picote Powerplant. Information on rock displacement can be obtained from Serafim's (1961) report on stress measurements at Picote Powerplant. The powerplant is approximately 53 feet wide and 115 feet high, and is located at a depth of 260 feet in a jointed granite. A fault is located 15 feet behind and parallel to the upstream wall of the powerplant.

The first stage of construction consisted of excavating the crown and abutments and placing concrete in the crown of the powerplant. Following this, the lower portion of the powerplant was excavated. Extensive use was made of rock bolts throughout construction.

Strains were measured in the concrete arch during excavation of the lower portion of the powerplant. Compressive strains were highest in the portion of the arch nearest the fault. A survey of the crane rails (at the spring line) showed that horizontal, inward displacements occurred during excavation of the lower portion of the powerplant. The largest movements were on the upstream wall and were attributed to the presence of the fault.

Serafim estimated the natural stress in the rock surrounding the opening on the basis of the observed displacements of the crane rails on the downstream wall. A value of 600 psi was obtained for the natural stress, using an elastic equation for the deformation around a cylindrical opening, and substituting a laboratory modulus for the deformation modulus of the rock mass. This value, Serafim concluded, correlated closely with the natural stress determined by strain relief measurements

(overcoring of strain rosettes) at the surface of the opening, and was indicative of high horizontal stresses in the rock mass.

Although displacement measurements may be used to obtain a rough estimate of in-situ stress conditions, it is not a recommended practice to determine the natural stresses in a rock mass solely on the basis of the long-term displacements at the wall of an opening. As has been shown previously, large discontinuous movements commonly occur in the near-surface rock, particularly over extended periods of time; and it is often not possible to relate these displacements to a laboratory modulus, or even a deformation modulus for the rock mass. However, Serafim's calculations show that the displacements of the downstream walls, although perhaps not perfectly elastic, can be approximated with a reduced deformation modulus. The magnitudes of the displacement and the assumed elastic modulus were not given in the paper, but it is possible to obtain a rough estimate of the deformation modulus of the rock mass by comparing the natural in-situ stresses calculated by Serafim (approximately 600 psi) with those estimated from the height of overburden above the powerplant: for a depth of 260 feet, the natural vertical stress should be on the order of 300 psi, and the natural horizontal stress should fall in the range of 200 to 600 psi. The deformation modulus based on the deflection of the downstream wall would therefore range from 1/3 to 1 times the laboratory modulus. Thus, the movement of the downstream wall was approximately elastic, while the movement of the upstream wall, affected by the presence of the fault, was larger and was possibly discontinuous.

Extension type failures were also observed at Picote Station. Rock

spalls (popping rock) formed parallel to the walls of the drifts leading to the main powerplant as the powerplant was excavated. Serafim considered this another indication of the presence of high horizontal stresses in the rock mass.

The combined stress concentrations formed by the excavation of the powerplant and the presence of the drifts were sufficient to cause failure of the relatively high-strength granite. Granite is almost invariably found at shallow depths as a blocky, jointed rock, but it is interesting to note that the granite at Picote was sufficiently competent that stress relief occurred by the formation of fresh fractures, rather than by opening and movement along existing joint surfaces. Similar failures were also observed by Moye (1959) in the drifts around the Tumut I chamber, in granite.

Other Powerhouses. Other underground powerhouses where measurement of rock movement has been made include the Poatina Underground Powerplant, Tasmania (Endersbee and Hofto, 1963), Boundary Dam Undergound Powerplant. (Strandberg, 1966, Schilling, 1966) and the powerhouse at Oroville damsite, California. The Oroville powerhouse was recently completed and the results are not available in the literature.

1.4 SCOPE OF THESIS

It is apparent that the stability of underground openings is of concern in both mining and civil works construction. More and more emphasis is being placed upon observing the behavior of openings and understanding the factors affecting stability. As our knowledge of rock behavior improves, it will be possible to realize more economy and safety in the construction of underground openings. Openings formerly considered technically or practically infeasible will be built.

In recent years in the civil works field, an emphasis has been placed on large openings. The question has been asked, "Are there limiting sizes and depths for such openings?" In some instances, limits have been defined based on assumed governing theoretical relations. However, the limits are not so much a matter of theory as a matter of practicality and engineering experience. Some of the limitation is involved with the present construction methods--the ability to rapidly excavate and support a large opening. Improved techniques for rock-bolting and rock excavation will be needed.

Further understanding of the behavior of rock around an opening--in particular, the strengthening of the rock mass by the artificial support--is needed in order to be able to economically construct both large and small underground openings. One of the major problems is determining the amount of rock-bolt support required to maintain a stable opening in a rock mass of a given rock quality. This problem can be broken down into other related problems: defining the quality of the rock mass in engineering terms, determining the modes of rock failure around openings and the effect of bolting upon rock failure, delineating the strength and deformation characteristics along an irregular joint surface, and determining the restraint required to prevent a jointed rock mass from becoming discontinuous and unstable. These are some of the problems which were apparent during the construction of the cavities at the Nevada Test Site. This thesis summarizes the behavior observed during the construction of the cavities--particularly the behavior related to the stability of the openings--and attempts to define the problems and, where possible, provide answers to the questions concerning the support and stability of underground openings.

A description of the rock displacement and rock fracturing observed

during construction of the cavities in tuff is presented in Chapter 4. In Chapter 5, the observed behavior is discussed and compared with elastic and elastic-plastic theories for stress and displacement around openings. The boundary conditions and material properties which must be considered in the analysis of the cavity behavior are outlined in Chapter 2, Construction of the Cavities, and Chapter 3, Rock Characteristics. In Chapter 6, the behavior in the granite (a high-strength, jointed rock) is compared with the behavior in the tuff (a very low-strength, relatively unjointed rock). Chapter 7 summarizes the information presented in the thesis and presents the conclusions. Appendix A summarizes the rock classification methods used to aid in defining the rock mass characteristics (strength and deformation properties) on the basis of exploratory information. Most of this effort was concentrated in the exploration for the granite cavity, where the in-situ properties differed quite significantly from the intact rock properties. In Appendix B, displacement-depth relations are presented for 32 of the extensometer units installed in Cavities I and II.

CHAPTER 2

CONSTRUCTION OF THE CAVITIES

2.1 CONSTRUCTION OF THE CAVITIES IN TUFF

Cavities I and II were located at a depth of 1300 feet (floor elevation, 6160 feet) in Rainier Mesa. Access to the cavities was obtained through a 4700-foot tunnel which entered the side of the mesa (Fig. 5). The cavities were approximately hemispherical in shape, with the plane surface of the hemisphere inclined 68 degrees from the horizontal (Fig. 6). The radius of the hemisphere varied from 60 to 75 feet, and the height of the cavities was 138 feet. The top was domed to prevent undesirable stress conditions and excessive slabbing during the initial stages of excavation.

Rock Bolts

The upper portion of the cavities was supported with 32-foot-long rock bolts on 3-foot centers, the middle portion with 24-foot bolts on 3-foot centers, and the lower portion with 16-foot bolts on 6-foot centers. The plane face of the cavities was bolted with 24-foot bolts on 6-foot centers. The proposed bolting pattern on the plane face was less conservative than the bolting pattern used in other portions of the cavity. (This was a requirement of the cavity users.) For this reason, emphasis was placed on monitoring the movements of the plane face. Extra bolts were spotted on the cavity surfaces as required, particularly where slabs or joint sets were present. In Cavity II, movement of the plane face occurred which necessitated extensive additional support. Over large areas of the face, 48-foot bolts were placed on 3-foot centers.

Bolts were predominantly 1-1/8-inch-diameter, A431 steel reinforcing

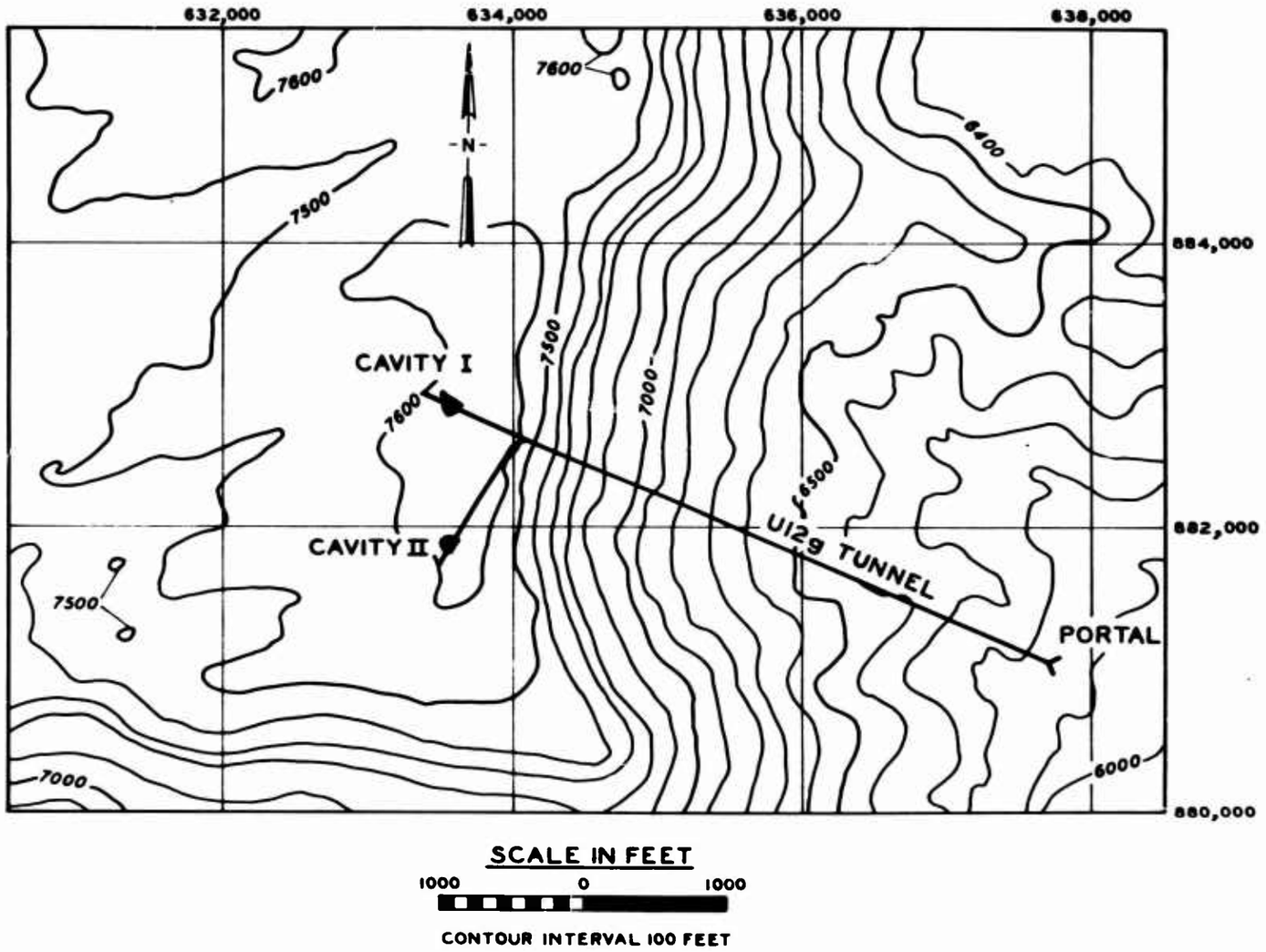

Fig. 5. Location of Cavities I and II, Rainier Mesa, Nevada Test Site

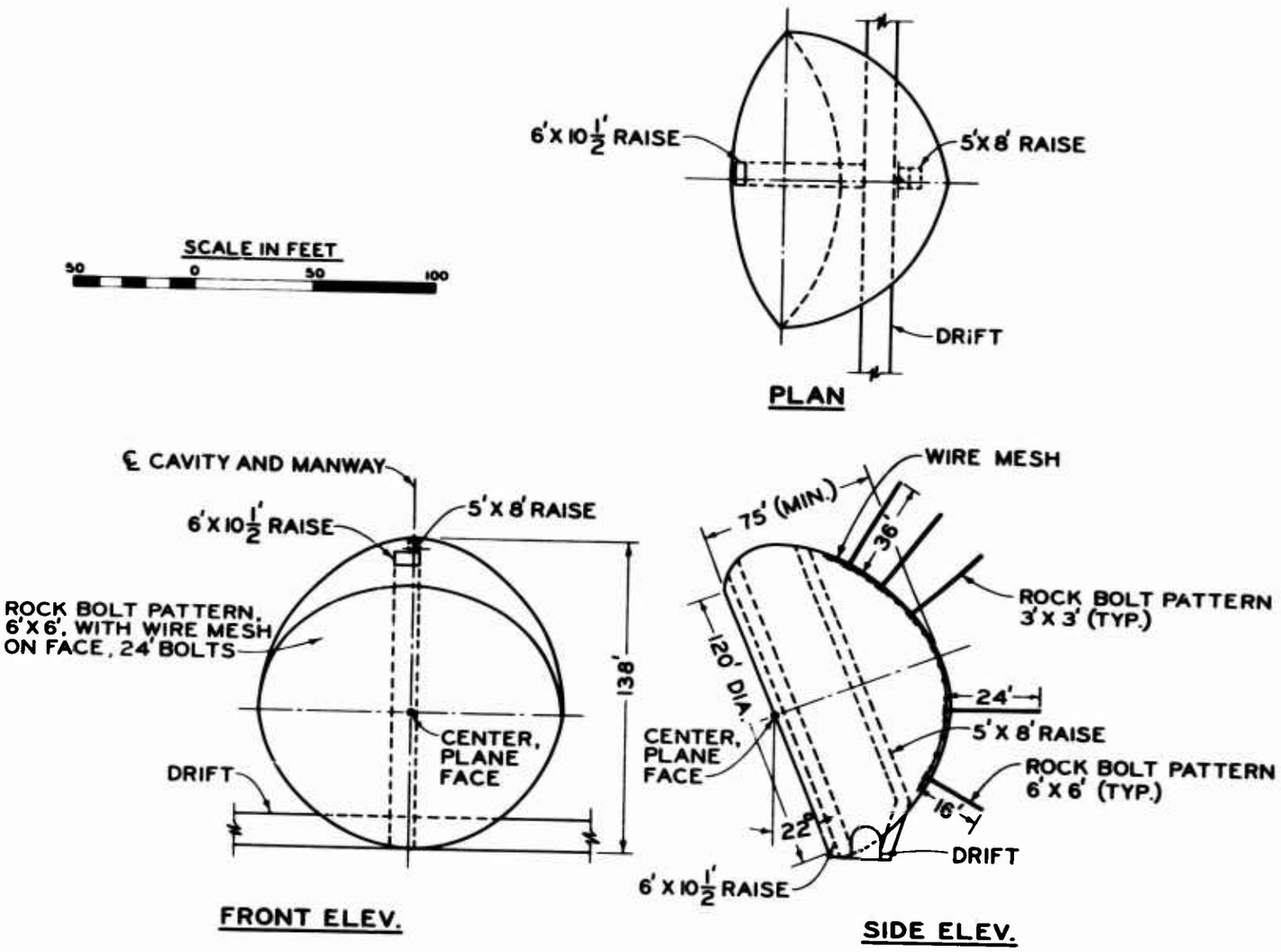

Fig. 6. Configuration of Cavities I and II

bars and had an ultimate strength of 85,000 pounds. The bolts were anchored with a fast-setting gypsum grout (RANCO F-81 Sulfaset) which was pumped to the rear 9 feet of the hole. (The tuff was incapable of supporting standard expansion shell anchors.)

Bearing plates (8 by 8 by 1/2 inch thick) were used beneath the nut and washer of the bolt assembly to distribute the bolt load to the rock surface. Cement mortar was placed beneath the plates to fill irregularities in the rock surface.

Each bolt was tensioned to 30,000-pound load using torque wrenches, after the grout anchor and bearing plate mortar had set. Loads on the rock bolts installed in the cavities were checked by two methods. One method consisted of retorqueing the bolt assembly after its initial torque. All bolts installed in the tuff cavities were torqued twice (the second torque was at least 24 hours after the first). If the bolt failed to hold its tension during this period it was replaced. Following their initial two torques, selected bolts were periodically checked by retorqueing to determine if they had maintained their initial tension.

The other method consisted of placing Horstman Bolt-Tension Meters between the nut and the bearing plate of selected bolts. The meters were steel cylinders with calibrated photoelastic elements attached to one side. The photoelastic patterns were read with a polarizing lens. The number of fringes viewed on the elastic element was directly proportional to the load on the rock bolt. A decrease in the number of fringes would therefore indicate reduced tension in the bolt. Approximately 30 of these meters were installed in the cavities.

These two methods showed that in most instances the bolt loads held

fairly constant, with some slight load increases due to movement of the rock into the cavity. In other instances the bolt loads were observed to decrease. Results of torque-checking of 100 bolts showed that approximately 15% lost more than half their initial torque over a period of 2 to 6 months. This decrease can be attributed to creep or a loss of support in either the anchorage or in the mortar behind the bearing plate. It is probable that much of this loss of bolt tension can be attributed to creep of the Sulfaset anchorage. The Sulfaset grout anchorage may be undesirable for use in permanent rock-bolt installations, particularly if the grout must be pumped, thus necessitating a thin, weak Sulfaset-water mix.

Construction Procedure

The cavities were excavated by driving two 68-degree raises from the main tunnel to the proposed dome of the cavity. The dome was then opened and rock-bolted. Excavation proceeded downward with the bolting following closely behind the blasting. (Bolting was usually kept within 10 feet of the bottom.) No blasting was permitted adjacent to areas where the bolts were untorqued.

The construction cycle in the cavities was as follows: shot holes were drilled approximately 4 to 6 feet into the cavity walls or down into the bottom of the cavity. (Fig. 7 shows charges being loaded prior to blasting the wall in the upper portion of Cavity I. A 3.6-foot horizontal cut is to be made.) After blasting, the slabby rock was barred down. In the upper portion of the cavities, 6-foot-long bolts with Perfo sleeve anchors were immediately placed (on approximately 6-foot centers) and a 2-by 2-inch number 6 wire mesh was attached to the bolts. This provided temporary support and prevented continued slabbing of the cavity walls.

Fig. 7. Blasting in dome of Cavity I. Bolts 8 ft above floor have been tensioned. Miners are loading charges prior to blasting approximately 4 ft into the wall

Fig. 8. Rock bolts on curved surface of Cavity I. The 32-ft bolts are ready for placement of mortar beneath bearing plate and application of tension. Note the friable white tuff bed above the harder red tuff. Slabbing is not prominent

(The 6-foot bolts were only occasionally used in the middle and lower portions of the cavity.) The 2-inch-diameter bolt holes were then drilled and the long, 1-1/8-inch-diameter bolts were grouted in place and tensioned (Fig. 8). Shot holes and bolt holes were drilled with pneumatic percussion drills (jacklegs and stopers) and air-operated augers mounted on jumbos. The augers operated very satisfactorily in the tuff--they were capable of drilling more rapidly and to greater depths than the percussion drills.

Muck was removed from the cavities through the two raises. In the dome of the cavities, two-drum slushers (cable-operated buckets) were used to move the muck into the raises. Eimco excavators (air-operated, track-mounted end loaders) were used to remove the muck when the cavity size was large enough to accommodate them.

Construction History

Cavity I was excavated in 6 months with very little delay once the dome of the cavity was excavated. The excavation and support in the dome were difficult because the techniques used were unfamiliar to the mining crews. For this reason, many uneven surfaces and rock protrusions were present. After construction had been completed, a 2-inch sand-cement layer was pneumatically placed (gunited) over the upper 30 feet of the cavity to support rock slabs which were beginning to break and crack between the rock bolts.

Cavity II was excavated in 7-1/2 months. Excavation and support in the dome of the cavity were not as difficult because of the experience gained from Cavity I. Most of the construction difficulties in Cavity II were associated with the joint systems which intersected the cavity surface. Low-pressure cement grouting was used throughout construction to fill the open joint systems which intersected the dome and the plane face of the

cavity. Approximately 1100 bags of cement were pumped into the fault zones.

A 2-month strike occurred near the end of construction of Cavity II. During this period very little rock was excavated. At the end of the strike, a thin, friable tuff bed was exposed on the plane face. At this time, large movements occurred along bedding and joint planes intersecting the face, and remedial bolting was required. Two months after completion of the cavity, approximately 2 inches of gunite were placed over slabby areas on the dome and the plane face.

Wire safety nets (1/2-inch mesh) were placed across Cavities I and II, 30 feet below the dome, after construction had proceeded approximately 20 feet below that elevation. The net prevented rock and broken bolts from falling on the men working below. It also proved to be a useful means of gaining access to the dome of the cavity (refer to Fig. 9). From the net, the condition of the rock surface could be checked, extensometers read, bolts replaced, and gunite placed.

2.2 CONSTRUCTION OF THE CAVITY IN GRANITE

The granite cavity (Cavity III) was similar in shape to the tuff cavities, but was much smaller in size. It had a total height of 76 feet, with a hemispherical radius of 35 feet. The plane face of the cavity had an orientation which was chosen to coincide with the predominant joint orientation (strike: N43^{o}E, dip: 74^{o}SE).

Rock Bolts

The upper portion of the cavity was supported with 24-foot-long rock bolts on 3-foot centers, the middle portion with 16-foot bolts on 3-foot centers, and the lower portion with 8- to 16-foot bolts on 6-foot centers. The plane face of the cavity was bolted with 16-foot bolts on 6-foot

Fig. 9. Safety net below dome of Cavity I

centers. Extra bolts were placed normal to the predominant joints and fault zones, as required. Bolts consisted of 1- and 1-1/8-inch reinforcing bars, anchored with standard expansion shells and tensioned to a minimum of 20,000 pounds by torqueing. The bolts were completely grouted after torqueing, using a fast-setting gypsum grout (RANCO F-81 Sulfaset) which was pumped into the hole. Because the bolts were grouted after torqueing, loss of bolt tension was not a problem as it was in the cavities in tuff.

Construction Procedure

The cavity location was reached from the surface by excavating a 400-foot shaft, then driving a 200-foot drift from the shaft to the proposed cavity location. From the drift, a raise was driven to the proposed dome of the cavity, where excavation was commenced. During the driving of the drift and raise, the faults and major joint systems were mapped (Fig. 10). The final location and orientation of the cavity were chosen from this information.

The construction cycle in the cavity was similar to that described for the tuff cavities. The cavity was excavated in 3 months. Very little difficulty was encountered in excavation and support of the cavity.

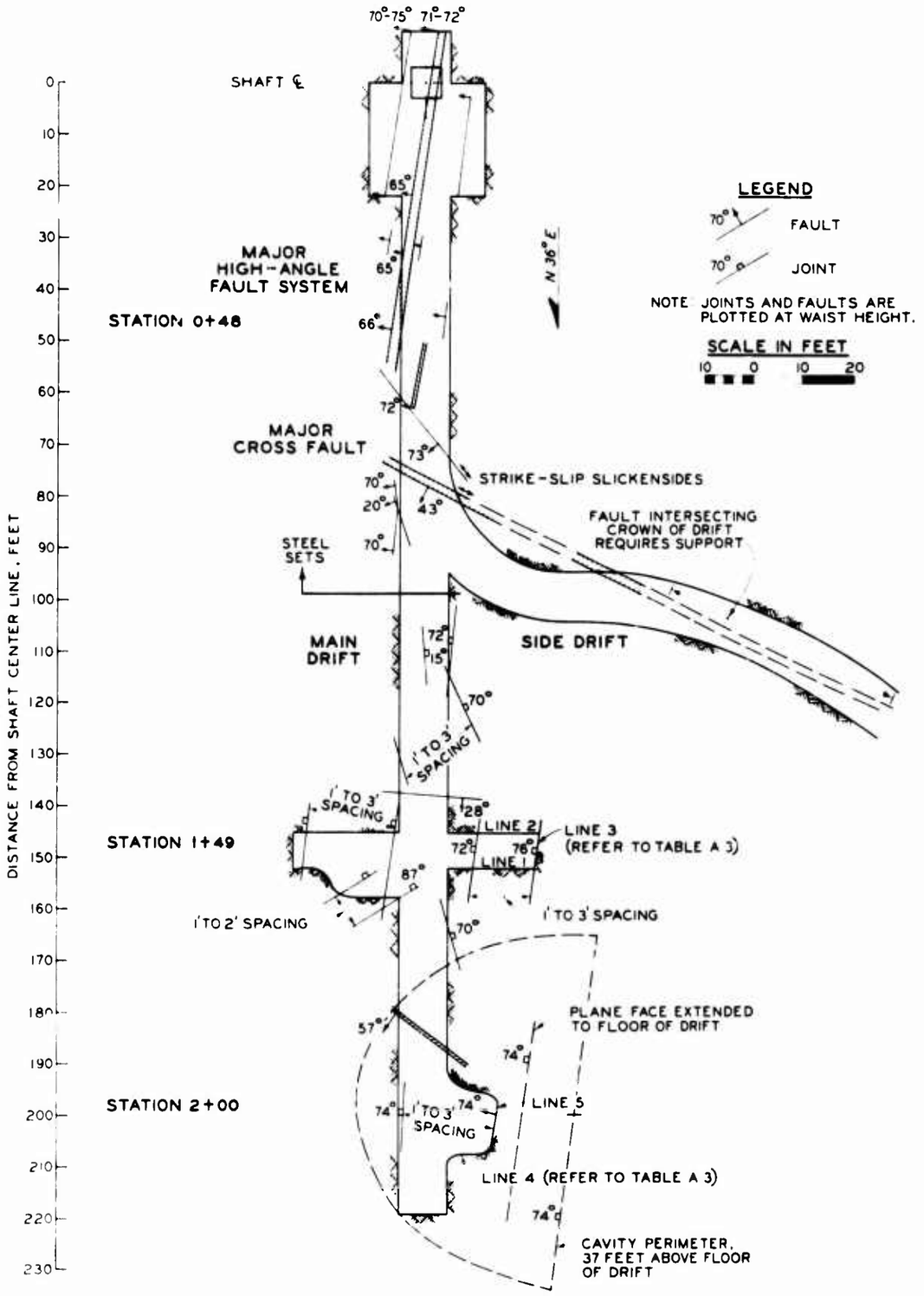

Fig. 10. Plan of Cavity III and access drift, showing major joint and fault systems

CHAPTER 3

ROCK CHARACTERISTICS

3.1 CHARACTERISTICS OF THE TUFF

Introduction

Rainier Mesa consists of ash-fall and ash-flow tuffs, capped by a relatively hard, welded tuff. The rock in the vicinity of the cavities consists of alternating layers of red to yellow-white porous tuffs of very low intact strength (Fig. 11). The tuff is predominantly thick-bedded and massive, except for occasional thin beds (3 to 18 inches) of soft, friable, white tuff (Fig. 8). The bedding planes dip 8 to 15 degrees. In general, the tuff in the vicinity of the cavities was not heavily jointed, and would be classified on the basis of its in-situ properties as a good to excellent quality rock.

Natural Discontinuities

In the first 2400 feet of the tunnel leading to the cavities, a series of high angle faults was present. One fault, at station 14+00, had a hard, polished slickensided surface containing striations which indicated a predominant dip-slip movement. Many high angle joints were also present in the first 2400 feet of the tunnel. One prominent series was vertical and had a strike of 45 degrees across the tunnel. In the last 2400 feet of the tunnel, some high angle joints were present, but there was very little evidence of faulting (Emerick, 1963).

In Cavity I, the tuff had very few natural joints. Some tight vertical joints were present, but did not cause overbreak during construction. Bedding plane weaknesses caused some preferred orientation of the cavity surface (Fig. 11).

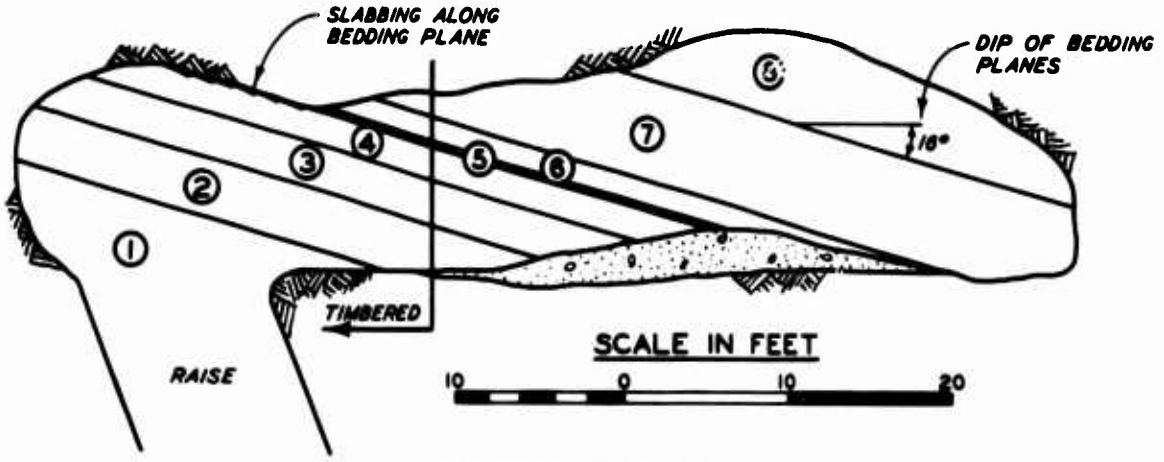

VERTICAL SECTION

LEGEND

① WHITE TUFF, WITH RED TUFF INCLUSIONS, RELATIVELY HARD

② RED TUFF, HARD

③* WHITE TUFF, MEDIUM HARDNESS

④* WHITE TUFF, RELATIVELY SOFT

⑤* THIN RED TUFF, HARD

⑥* WHITE TUFF, MEDIUM HARDNESS

⑦ MASSIVE RED TUFF, HARD

⑧ WHITE TUFF, HARD

* DISTINCT BEDDING PLANES; TENDENCY TO BREAK ALONG BEDDING PLANES.

Fig. 11. Bedding in tuff, dome of Cavity I

In Cavity II, high angle joint systems were present which, in combination with the friable white tuff beds, caused overbreak and deep-seated movements on the plane face. Their location is shown in Fig. 12. Joint set 2 (a set of natural shear fractures) was open (1 to 3 inches) and took large quantities of cement grout. The set was present in some portions of the cavity as a 5- to 10-foot-wide zone of vertical fractures, spaced a few inches apart. Faulting, with approximately 1 inch of vertical offset, was observed on this set.

In both cavities, natural fractures were more prevalent in the harder, brittle tuffs. Vertical fractures could often be traced in a more brittle rock, but when a soft bed was encountered, the fractures tended to be smaller and less distinct, or missing altogether. The same fracture zone could often be picked up again beneath the soft zone. Alteration and weathering along the joints were not apparent. The cavities were above the water table, and drips along joint planes were not observed in either cavity.

Intact Properties

The intact properties of the tuff were determined from standard tests (described by Miller and Deere, 1967) on NX core specimens taken from the vicinity of the cavities. The tests were performed in the Rock Mechanics Laboratory of the Civil Engineering Department at the University of Illinois.

Fig. 13 shows the typical behavior in unconfined compression of a relatively uncracked specimen. The stress-strain curve, as well as Poisson's ratio and the sonic pulse velocity, is plotted as a function of the axial stress. Two cycles are shown: the first cycle was run to

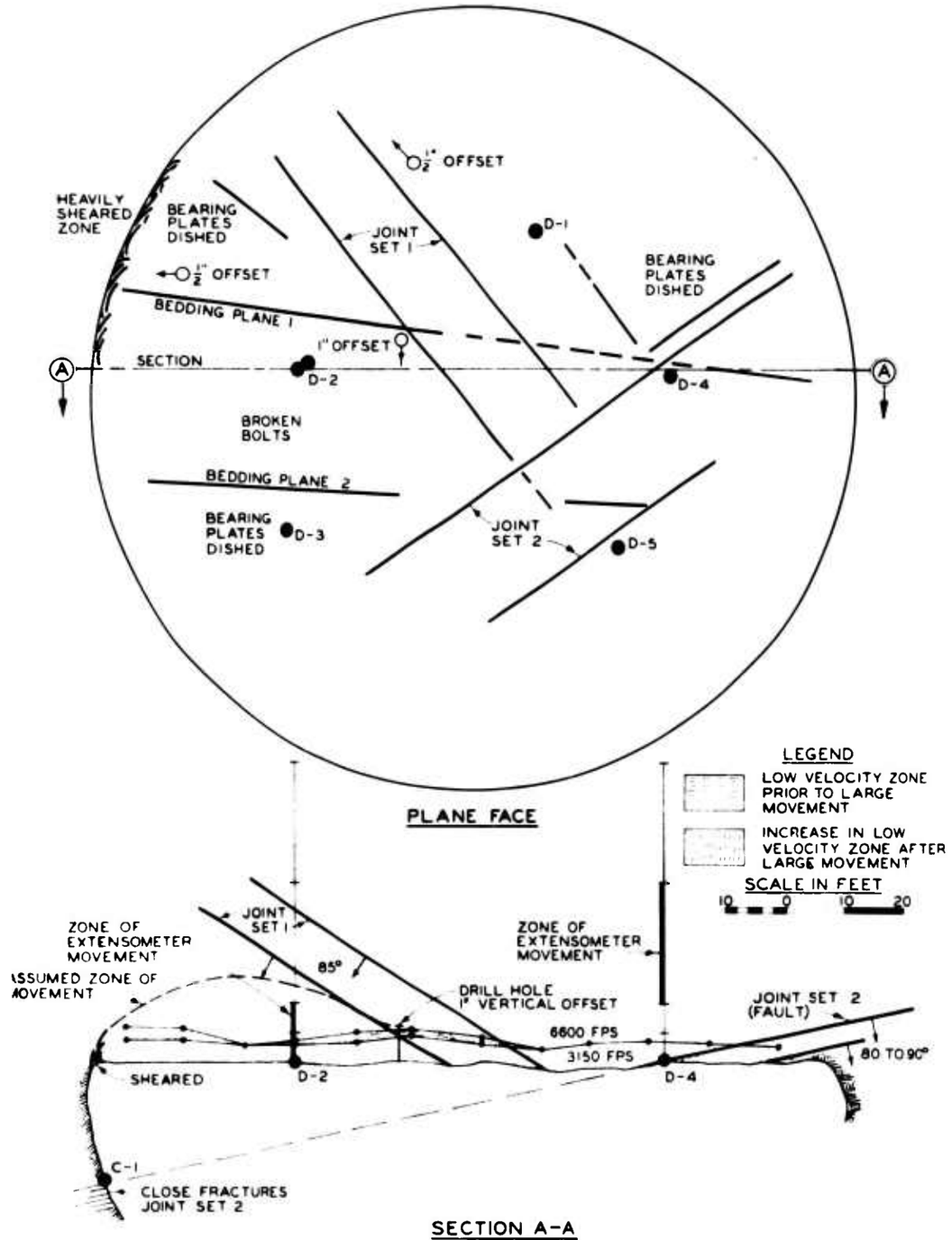

Fig. 12. Plane face, Cavity II

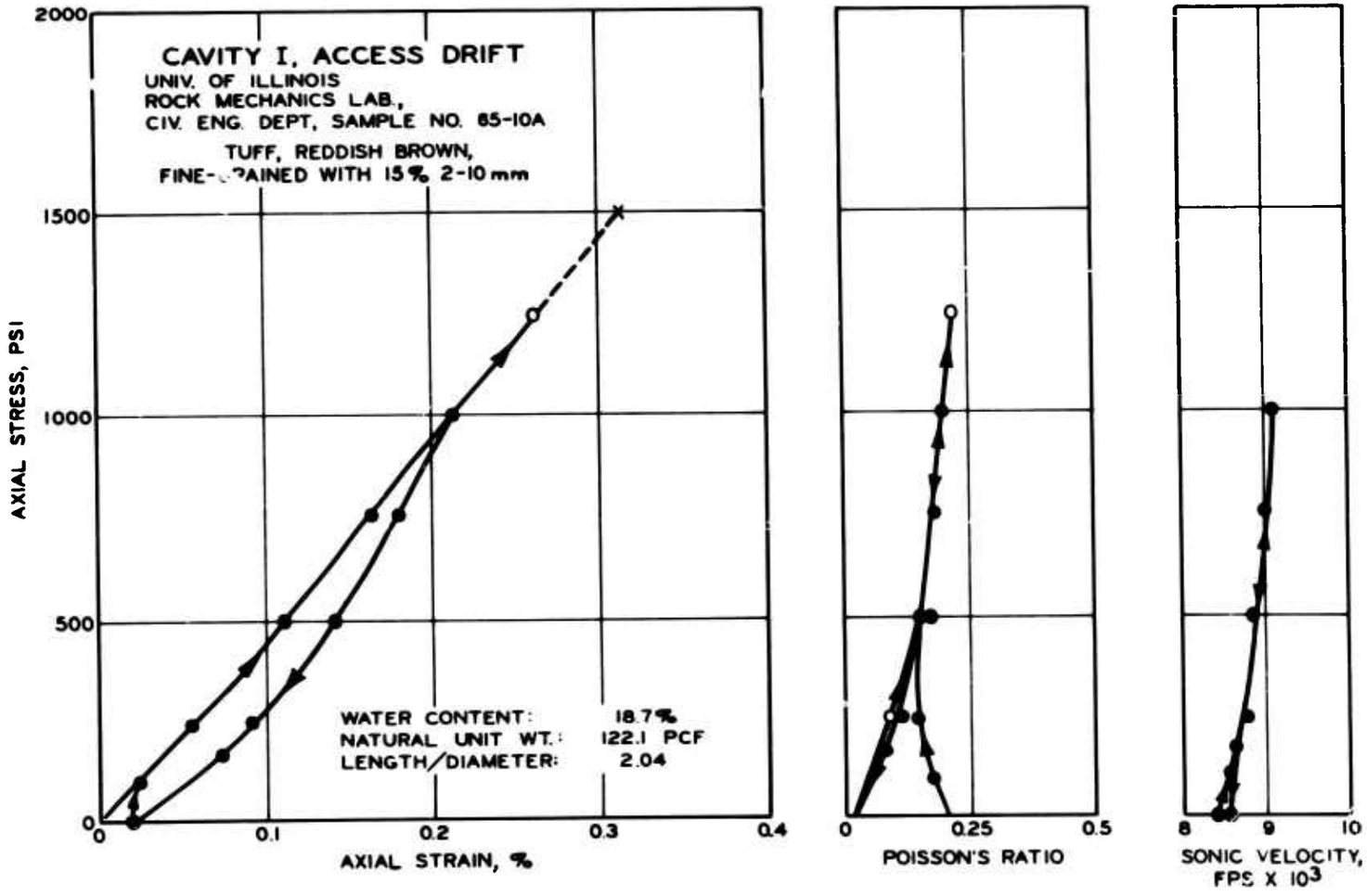

Fig. 13. Typical unconfined stress-strain behavior, intact tuff specimen

1000 psi in 250-psi increments. Each increment was placed in a few seconds time but was allowed to remain approximately 2 minutes while the vertical and lateral strains were read and recorded (SR-4 gages and strain indicator) and the sonic velocity obtained. The load was decreased in decrements to zero. The second loading was then initiated and continued to failure. The stress at failure is correctly plotted but the strain is only estimated beyond the point of the last reading (shown therefore as dashed line).

The stress-strain curves for the tuff samples were approximately linear. In many instances there was a slight increase in modulus at higher stress levels which was probably a result of crack closing. Poisson's ratio and the sonic velocity also increased as the samples were compressed and cracks were closed. Much of the change in properties at the low stress levels was a result of sample disturbance. For this reason, the stress-strain properties recorded in Table I were determined at the higher stress levels. The table summarizes the results of tests on 39 natural water content specimens and six air-dry specimens. Although measured strengths for the natural water content specimens ranged as high as 5200 and as low as 640 psi, most of the tuff in the cavities, and 75% of the samples tested, fell in the strength range of 1000 to 1800 psi. According to the engineering classification for intact rock (Miller and Deere, 1967), the tuff is a very low-strength rock of average modulus ratio.

Laboratory uniaxial and triaxial tests performed on samples from Rainier Mesa are reported by Obert (1964). The samples are believed to have been tested dry. There was considerable scatter in strengths throughout the mesa, but for samples taken from the cavity access drifts, the

TABLE I

SUMMARY OF INTACT PROPERTIES OF THE TUFF

Location	Rock Type	w %	γ pcf	σ_{ult} psi	E_t psi	Poisson's Ratio μ	V_p(lab) fps
			Natural Water Content				
Cavity I, access drift (6 samples)	Red tuff	23.0	115	1450	0.45 x 10^6	0.38	8,170
Cavity I, access drift (10 samples)	Red tuff	19.2	121	1650	0.50 x 10^6	0.22	8,340
Cavity II, inclined core hole from access drift (10 samples)	Red and yellow tuff	18.1	121	1350	0.52 x 10^6	0.22	9,090
Avg (39 samples)		19.3	120	1400	0.50 x 10^6	0.24	8,750
			Maximum Strength				
Cavity I, core hole U-4 at center of plane face (1 sample)	Yellow tuff	17.5	125	5125	2.26 x 10^6	0.09	12,050
			Air Dry				
Cavity I, inclined core hole from access drift (6 samples)	Red and yellow tuff	4.6	100	3240	0.92 x 10^6	0.15	8,150

Note: All samples approximately 2-1/8 inches in diameter by 4-1/4 inches long.

w , water content in percent of dry weight.

γ , natural unit weight (unless air-dried as noted).

σ_{ult} , ultimate unconfined compressive strength.

Elastic constants E_t (modulus of elasticity) and μ (Poisson's ratio) are tangent values at stress equal to one-half of compressive strength.

V_p(lab) , sonic pulse velocity (dilatational) under axial stress of 1000 psi.

uniaxial strengths averaged 2700 psi, and the triaxial properties (from tests at confining pressures of 500 and 1000 psi) were ϕ = 36 degrees and c = 500 psi .

Drying of the Tuff

When exposed to air, the tuff will dry out and become more brittle. The test results for samples allowed to air-dry in the laboratory are shown in Table I. The water content of the air-dried samples averaged 4.6%. The strength and modulus of the samples were almost twice the strength and modulus for natural water content samples.

Drying of the tuff occurred at the surface of both the tunnel and cavity walls. Water contents were determined from samples taken from the surface slabs in Cavity I in August, 1-1/2 months after completion of the cavity:

Description	Water Content, %
Air-dry sample (lab)	4.6
Dome (surface slab)	13.2
Curved surface (surface slab)	17.2
(1-foot depth)	22.6
Plane face, center of cavity (surface slab)	24.9

These results show that drying in the dome was much more advanced than in the lower portions of the cavity, where only slight drying of the rock had occurred. Drying was also more advanced at the surface than at a depth of 1 foot.

Very little drying could occur when the tuff was freshly excavated; therefore, drying was not the cause of the initial fracturing and slabbing observed throughout the cavities. However, some of the deterioration and

breakup of surface slabs which occurred after the cavities were completed was a result of drying. This condition was most pronounced in the dome of the cavities.

Rock Mass Quality

The NX core was recovered in pieces approximately 1 foot long, indicating that the natural joints were widely spaced. Based on the fracture frequency, the in-situ character of the rock (Rock Mass Quality, Appendix A) is excellent. The shallow fractured rock and jointed rock zones have a higher joint frequency and, therefore, a much lower quality (poor to fair).

Another measure of rock mass quality is the ratio of field seismic compressional velocity to the laboratory sonic compressional velocity (V_{pf}/V_{pl}). Onodera (1962) used a "soundness ratio" $(V_{pf}/V_{pl})^2$ to estimate the quality of a rock mass. His correlation was as follows:

	Rock Mass Quality	Soundness Ratio (V_{pf}/V_{pl})	Velocity Ratio (V_{pf}/V_{pl})
I	Excellent	0.75-1.00	0.88-1.00
II	Good	0.50-0.75	0.70-0.88
III	Fair	0.35-0.50	0.60-0.70
IV	Poor	0.20-0.35	0.45-0.60
V	Very poor	0-0.20	0-0.45

A ratio of one is indicative of an excellent quality rock, where the rock mass has few natural discontinuities, and the in-situ properties are therefore similar to the properties of an intact specimen. A similar correlation was obtained by Deere, Hendron, Patton, and Cording (1967). They related the velocity ratio to the "Rock Quality Designation," a quantitative estimate of rock mass quality described in Appendix A.

In Cavity I the velocity ratio for the undisturbed tuff was 0.89;

in Cavity II it was 0.79. In the shallow fractured zones in the cavities, the velocity ratio averaged 0.33. According to the above correlations between rock mass quality and velocity ratio, a velocity ratio of 0.89 denotes an excellent rock, 0.79 a good rock, and 0.33 a very poor rock.

Because the tuff is not heavily jointed, its in-situ deformation characteristics would be expected to be similar to those of the intact specimen. Displacements in the cavities were predicted on the basis of the average intact modulus of the tuff (0.5×10^6 psi) determined from samples tested at their natural water content.

Natural State of Stress

The natural state of stress in the tuff mesa was reported by Obert (1964). Lucius Pitkin, Inc., performed the tests using the U. S.

Bureau of Mines deformation-overcoring method for determining in-situ stresses. The holes were overcored to a depth of approximately [illegible] feet in the sides of 10- to 16-foot-wide tunnels. The maximum stress concentration usually occurred at the most shallow measurement, which was 20 inches from the tunnel. Stresses near the surface were approximately 1.5 to 2.0 times the natural stress away from the opening. The stresses decreased gradually from the surface to a depth of [illegible] inches (1.5 to 2.0 radii) from the edge of the opening.

Fig. 14 compares the stresses determined at the end of the overcored holes (at a sufficient distance from the tunnel surface to be relatively unaffected by the stress concentration around the tunnel) with the height of overburden. Although there was considerable scatter, the natural vertical stress was found to be approximately equal to the stress due to the weight of overburden (1000 psi at the cavity location). Horizontal stresses were approximately one-half the vertical. These values were used in the elastic equations for displacement prediction.

3.2 CHARACTERISTICS OF THE GRANITE

Cavity III was located at a depth of 3[illegible]0 feet in the Climax stock, a granitic intrusion at the Nevada Test Site. In the vicinity of the cavity the rock is a porphyritic quartz monzonite of high intact strength. The average in-situ quality of the rock (Rock Mass Quality, Appendix A) was fair to good. Jointing in the vicinity of the cavity cut the rock into blocks approximately 6 inches to 2 feet in width.

Geologic Setting

The geologic setting of the Climax stock was described by Houser and Poole (1961):

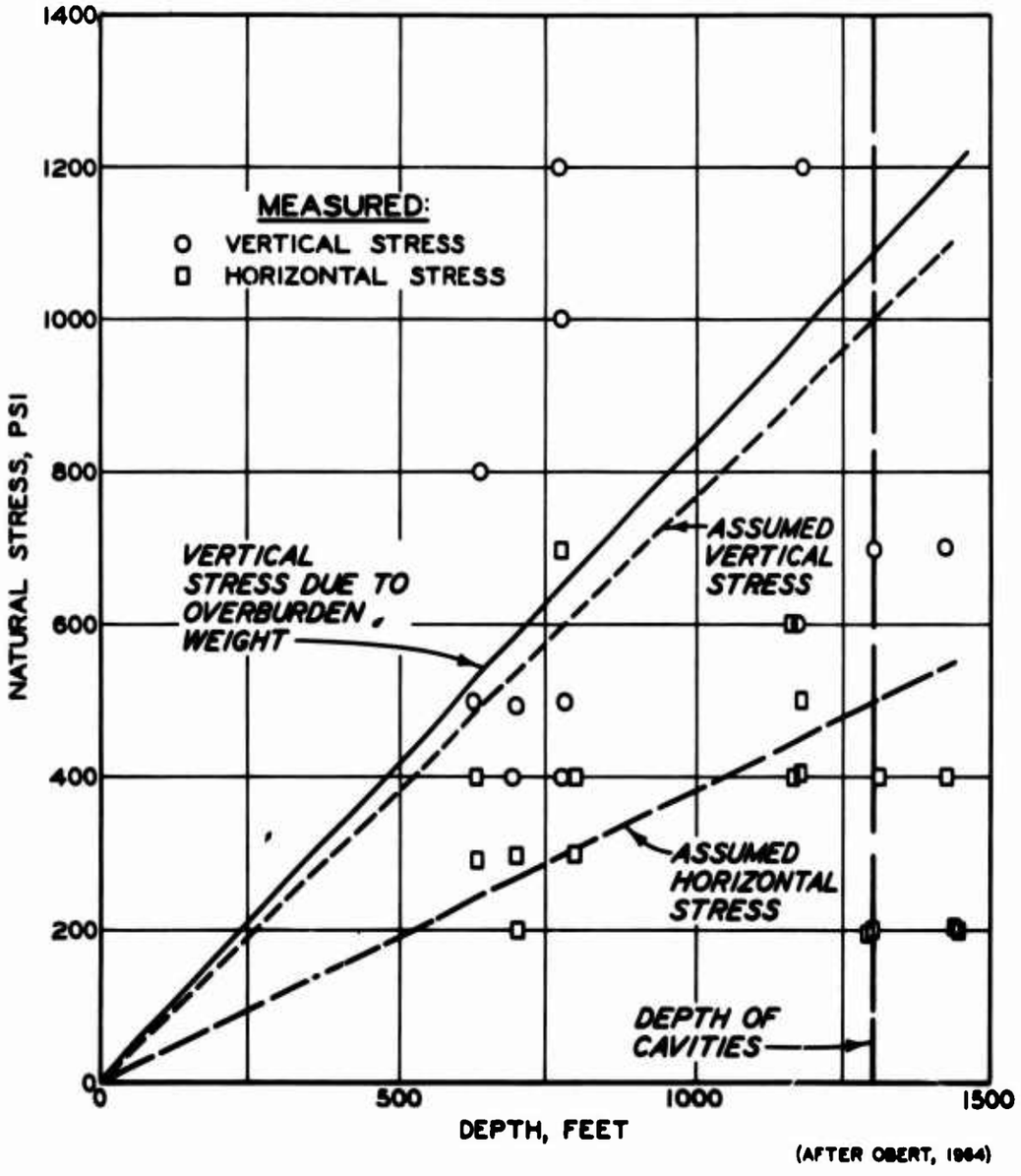

Fig. 14. Natural stresses in Rainier Mesa

"The Climax composite stock is exposed over an area of about 1.5 square miles and consists predominantly of granodiorite and porphyritic quartz monzonite. Spilite and pegmatite dikes are common locally. Pervasive hydrothermal alteration of the granodiorite quartz monzonite has formed clays, sericite, albite, orthoclase, pyrite and quartz. Post-intrusion faults are common in the granitic rocks, and in the adjacent metamorphosed carbonate rocks, where vertical displacements of as much as 500 feet occur. Three prominent joint sets with average attitudes of N32°W, dip 22°NE, N64°W, dip vertical, and N35°E, dip vertical are present in the stock."

Natural Discontinuities

Fig. 10 shows the orientation of the major joint and fault systems encountered in the drifts. The predominant set consists of joints and faults which strike approximately 7 degrees off the line of the main drift and dip from 65 to 75 degrees. This set was encountered as a major fault in the first 100 feet of the main drift. The fault varied from 1 to 7 feet in width and consisted of closely sheared and weathered (very poor quality) rock with a red and yellow soft clay gouge, 1 to 3 inches thick. A sketch of the fault at station 0+48 is shown in Fig. 15.

Also present in the drift was a low angle joint system which dipped in the direction of the drift. Both the fault and the low angle joint system tended to create a loose and slabby rock condition when intersecting the crown of the drift. Light steel sets were placed on 6- to 8-foot centers for the first 100 feet of the drift in order to support the loosened rock. Fig. 16 shows the support being placed in the fault zone at station 0+48.

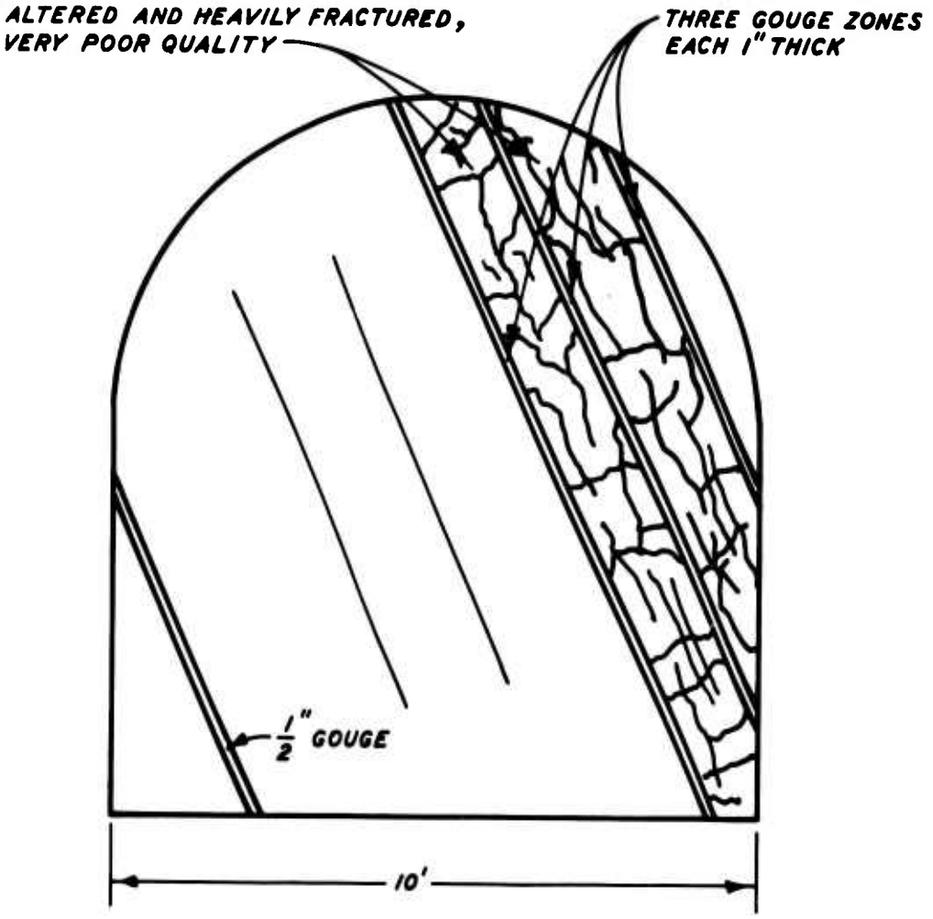

Fig. 15. Fault zone, station 0+48, Cavity III access drift

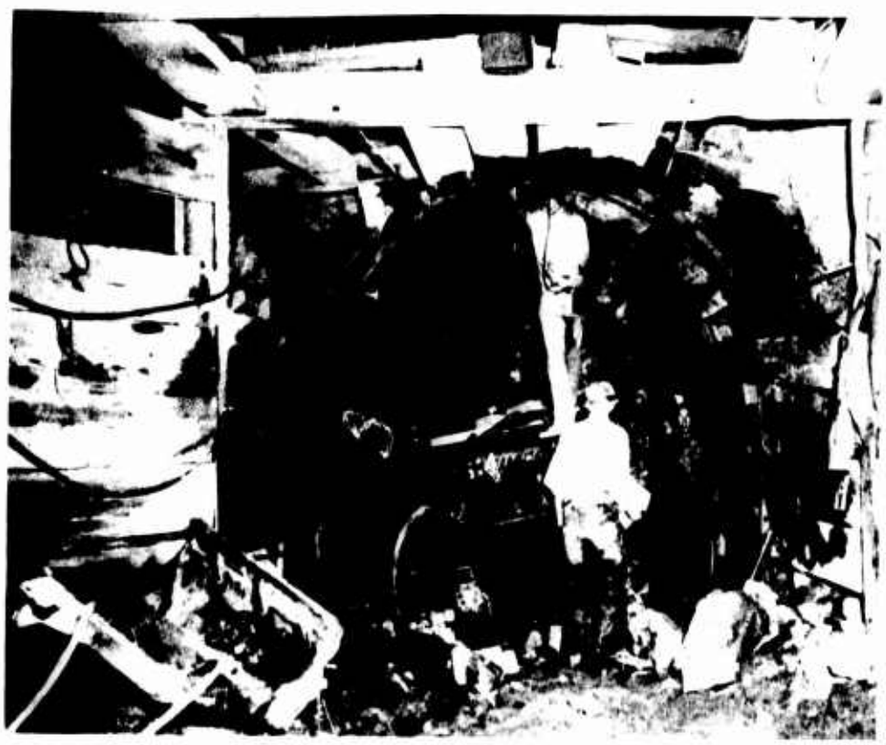

a. Overall view

b. Close-up view

Fig. 16. Placing lagging in fault zone, station +40', Cavity III access drift

Faults were also encountered which struck across the main drift. One of these was a major fault which dipped at 45 degrees and crossed the drift at station 0+80. It contained a 6-inch gouge zone of soft red and yellow clay and a 1/2- to 1-inch-thick, hard clayey slickensided material. (The direction of the slickensides indicated that strike-slip movement had occurred.) The fault created some support difficulties in a side drift which was driven from the main drift at this location. Initially, the fault was in the lower portion of the side drift, but when approximately 50 feet had been driven, the fault began to intersect the crown of the drift (striking parallel to the drift). This resulted in a loose and slabby rock condition overhead. Steel sets were placed in this area to support the slabs.

In zones where several faults intersected each other it was commonly observed that the faults were distorted and the thickness of the fault zone was increased. Gouge and altered rock were more evident in these locations. Major faults intersecting in the vicinity of station 0+80 exhibited these characteristics. The condition also existed in the cavity.

The Rock Mass Quality in the last 100 feet of the main drift was good to excellent; there were no critically oriented faults; and the only support required was a few 6-foot rock bolts to hold loose slabs. The major high angle joint set was present in this portion of the drift as a series of tight joints spaced on 1- to 3-foot centers (Fig. 17a). Fig. 17b shows the rock being barred down, 12 feet above the main drift at station 2+00, after blasting the first round for the raise. This is excellent rock.

The rock in the cavity was of good to fair quality, with some poor rock in the fault zones. (Fig. 18 is a photograph of the rock surface in

a. View along drift center line

b. 12 ft above floor of drift in raise

Fig. 17. Good to excellent rock, station 2+00 (raise station), Cavity III access drift

Fig. 18. Placing mortar behind bearing plate in dome of Cavity III

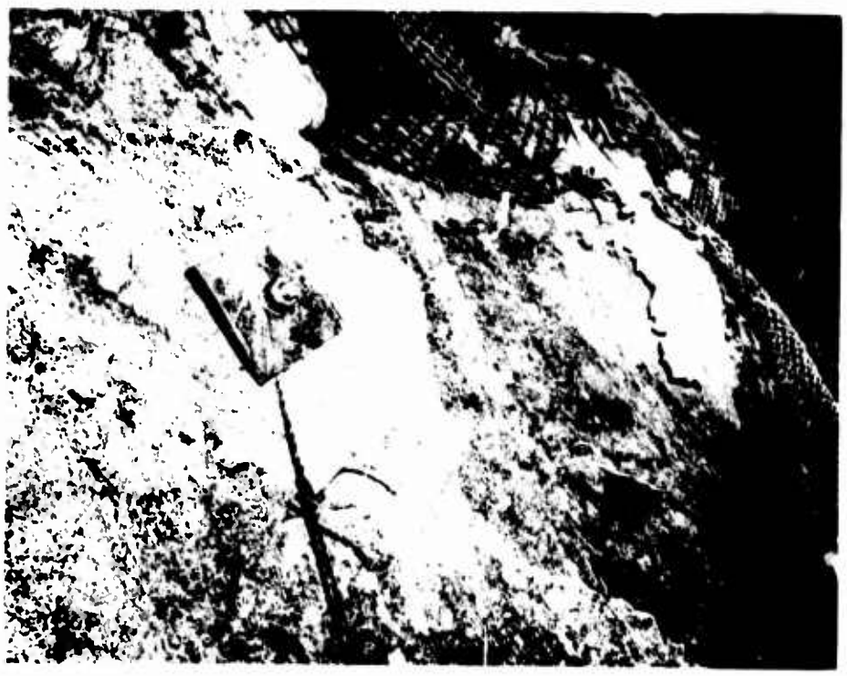

Fig. 19. Plane face of Cavity III

the dome.) Many of the irregularities of the cavity surface were caused by the major high angle fault system and the low angle joint system which were first encountered in the main drift. Weathering and alteration were observed on many of the faults and some of the joints which intersected the cavity. Limonite stains, sericite, and pyrite were present in addition to the products of shear and crushing (mylonites and gouge), which formed along fault planes.

The plane face of the cavity was oriented parallel to the main joint system in order to obtain a relatively smooth, plane surface without resorting to smooth-wall or presplit blasting techniques (Fig. 19). Most of the right side of the plane face fell on a smooth joint surface, as desired. However, the joint surface was not smooth and continuous over the entire face. Directly to the left of the center of the cavity, a high angle fault intersected the plane face at a 5- to 15-degree angle. This distorted the joint system which formed the plane face, and caused overbroken and tight areas on the face.

The cavity was located above the natural water table. Dripping water was observed in only one location where one of the high angle fault systems intersected the dome of the cavity. The dripping was assumed to be due to vadose water percolating downward through the joint system.

Intact Properties

Laboratory tests performed on quartz monzonite samples from the Climax stock are discussed in detail in Appendix A, Rock Mass Properties. Two unweathered, intact NX core specimens taken from Cavity III had the following average properties:

Unconfined compressive strength	26,600 psi
E_t (Young's tangent modulus at one-half unconfined compressive strength)	10.4×10^6 psi
Sonic compressional velocity, zero axial stress	21,000 fps
Sonic compressional velocity, 5000-psi axial stress	21,600 fps
Unit weight (air-dry)	167 pcf

For the unweathered samples, the stress-strain curve was linear to failure. According to the Engineering Classification for Intact Rock (Miller and Deere, 1966) the quartz monzonite is a high-strength rock of average modulus ratio.

Weathered and cracked samples taken from the same boring had lower strengths, and lower sonic velocities at zero axial stress. The weathered specimens also exhibited a lower modulus.

Rock Mass Quality

The presence of discontinuities in the rock mass tends to lower the in-situ modulus from the intact modulus. Initial displacements in the cavity were predicted on the basis of an in-situ modulus equal to one-half the intact modulus. This ratio was considered appropriate for a fair to good quality rock. The method by which this modulus ratio was obtained is discussed in Appendix A.

Natural State of Stress

The natural vertical stress in the vicinity of Cavity III was assumed equal to the stress due to the weight of overburden (400 psi). Horizontal stresses were initially assumed equal to one-half the vertical, but the large horizontal movements observed on the walls of the cavity indicated

that higher horizontal stresses might be present. Deformation-overcoring test results from a depth of approximately 1000 feet in the Climax stock were received at this time which verified this conclusion. The tests showed that the natural horizontal stresses were equal to or slightly greater than the vertical stresses. The vertical stresses were approximately equal to the stress due to the weight of overburden.

CHAPTER 4

OBSERVED BEHAVIOR OF THE CAVITIES IN TUFF

4.1 MEASUREMENT OF ROCK DISPLACEMENT WITH EXTENSOMETERS

Rock movement in the cavities was measured with extensometers which were installed in holes drilled radially from the freshly excavated cavity surface. During construction of the cavities movements were recorded on a daily or semi-weekly basis and compared with excavation progress. The extensometers recorded the movements which occurred subsequent to their installation. These movements occurred as a result of continued excavation of the cavities and as a result of progressive loosening of the rock mass.

Multiple anchors were placed at varying depths to determine the depth at which movements were concentrated. According to theory, movements caused by the cavity excavation decrease with distance from the cavity; therefore, the absolute movement of the deepest anchor of a set will be the smallest. For this reason displacement-depth relations have been plotted with respect to the deepest anchor. The absolute movement of this anchor is not known.

In the tuff, both single- and multiple-position extensometers were used to measure rock movement (Fig. 20). For comparison purposes, the two types of extensometers were installed within a few feet of each other on the plane face in Cavity II. Their movements were quite similar, as shown in Fig. 21. (In the granite, only single-position units were used.)

Description of Single-Position Extensometer

The single-position extensometer was designed by Dr. John Reed of the Colorado School of Mines (Fig. 20a). It consisted of a standard expansion shell anchor connected to a 1/2-inch steel rod. A depth micrometer was

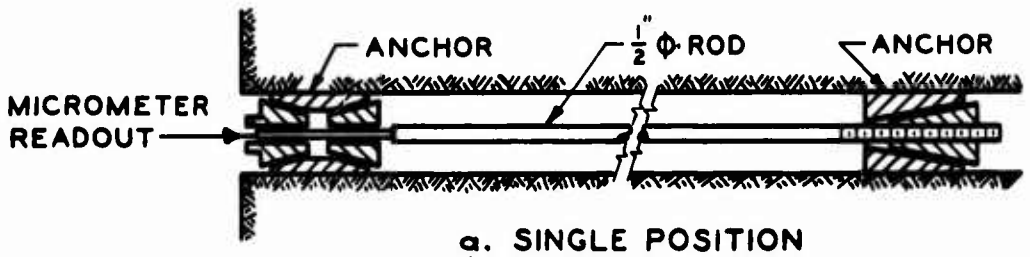

a. SINGLE POSITION

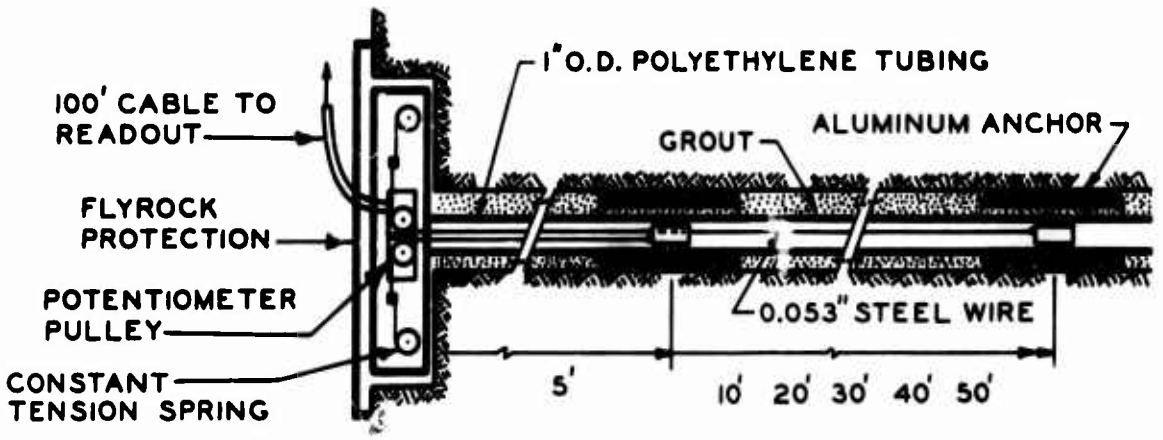

b. MULTIPLE POSITION (4 OR 6 POSITIONS)

Fig. 20. Borehole extensometers

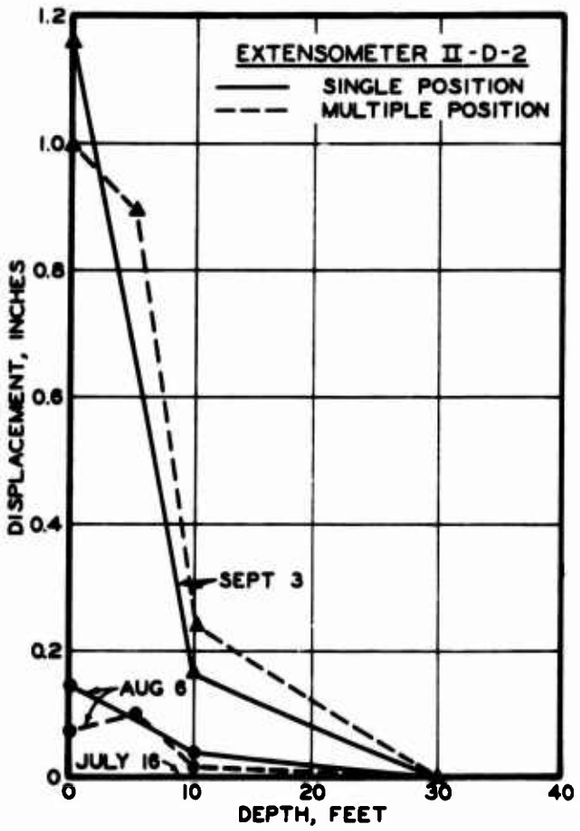

Fig. 21. Comparison of displacements of single- and multiple-position extensometers

used to measure the displacement of the anchored rod with respect to a hollow steel bolt fixed at the surface. Measurements were made to the nearest 0.001 inch.

The single-position units were commonly installed in groups of three or four, spaced 1 to 2 feet apart on the surface, with lengths varying from 5 to 50 feet.

Description of Multiple-Position Extensometer

The multiple-position extensometer (Fig. 20b) was developed during the initial stages of construction when the need arose for a remote and rapid readout of rock movements. The extensometers were designed and built by the Slope Indicator Company of Seattle, Washington. Movements were recorded to the nearest 0.002 inch. Each unit consisted of four to six anchors in a single hole, with 0.043-inch steel wire extending from the anchor to the surface, where it was connected to a flexible 0.025-inch stainless steel cable. The cable ran over a pulley which actuated a one-turn rotary potentiometer. Each cable was tensioned by two negator extension springs which provided a constant tension of 10 pounds. The extensometers were read at a central location in the cavities with a portable Wheatstone Bridge. One-hundred-foot cables led from the extensometer to the readout location.

The original anchors were placed by expanding a wedge-type mechanical anchor using an inner rod and outer pipe as a setting tool. Difficulties were encountered placing the anchors by this method: there was a tendency for wires to become tangled when installing a large number of anchors, and the installation required a large amount of time. The anchorage system was redesigned using grouted anchors. All anchor wires were placed inside a

50- to 100-foot-long, 1-inch-diameter polyethylene tube. The 1-inch tube provided protection for the anchor wires and prevented their tangling.

The anchors consisted of 2-inch-diameter aluminum cylinders, which were placed around the tubing and bolted to plugs inside the tubing. The anchor wires were tied into these plugs. When the assembly was grouted in place, the aluminum cylinders acted as anchors, while the tubing between the anchors deformed with the rock. Multiple grout and deair tubes were installed with the assembly to ensure that the hole would be filled with the pumped grout and that a positive anchorage would be obtained. The entire assembly was prefabricated with anchors placed at 10-foot intervals. The assembly could be coiled for shipment and handling, but was stiff enough to be pushed into a 2-1/8-inch-diameter hole.

4.2 ROCK DISPLACEMENTS

The observed extensometer displacements are discussed on the basis of four locations in the cavities: (A) Dome, (B) Intersection of Dome and Plane Face, (C) Curved Surfaces, and (D) Plane Face. These symbols have also been used to number the extensometers. Thus extensometer number II-D-3 is located on the plane face of Cavity II.

In Figs. 22 and 23, some typical extensometer movements are plotted with time and compared with excavation progress. For each extensometer set the movement of the surface with respect to either the 30- or 50-foot anchor has been recorded. (The displacement-depth relations for a given extensometer set are not shown in these figures.) The location of the extensometer in the cavity is shown in the insert on the upper right corner of the figure. The height of the extensometer above the cavity floor at the time of installation is shown in the upper portion of the figure.

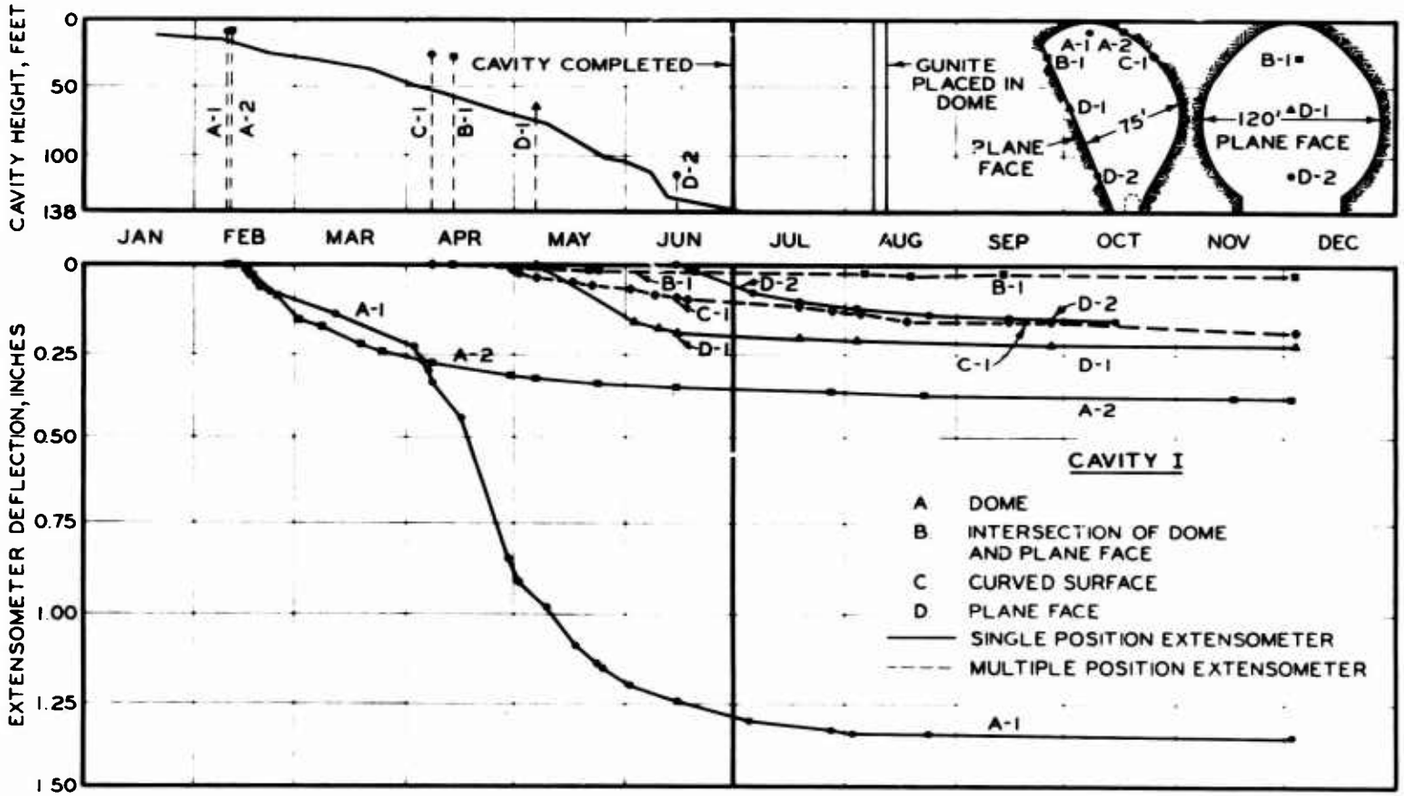

Fig. 22. Displacement of Cavity I surface with respect to deep (30- and 50-ft) extensometer anchors

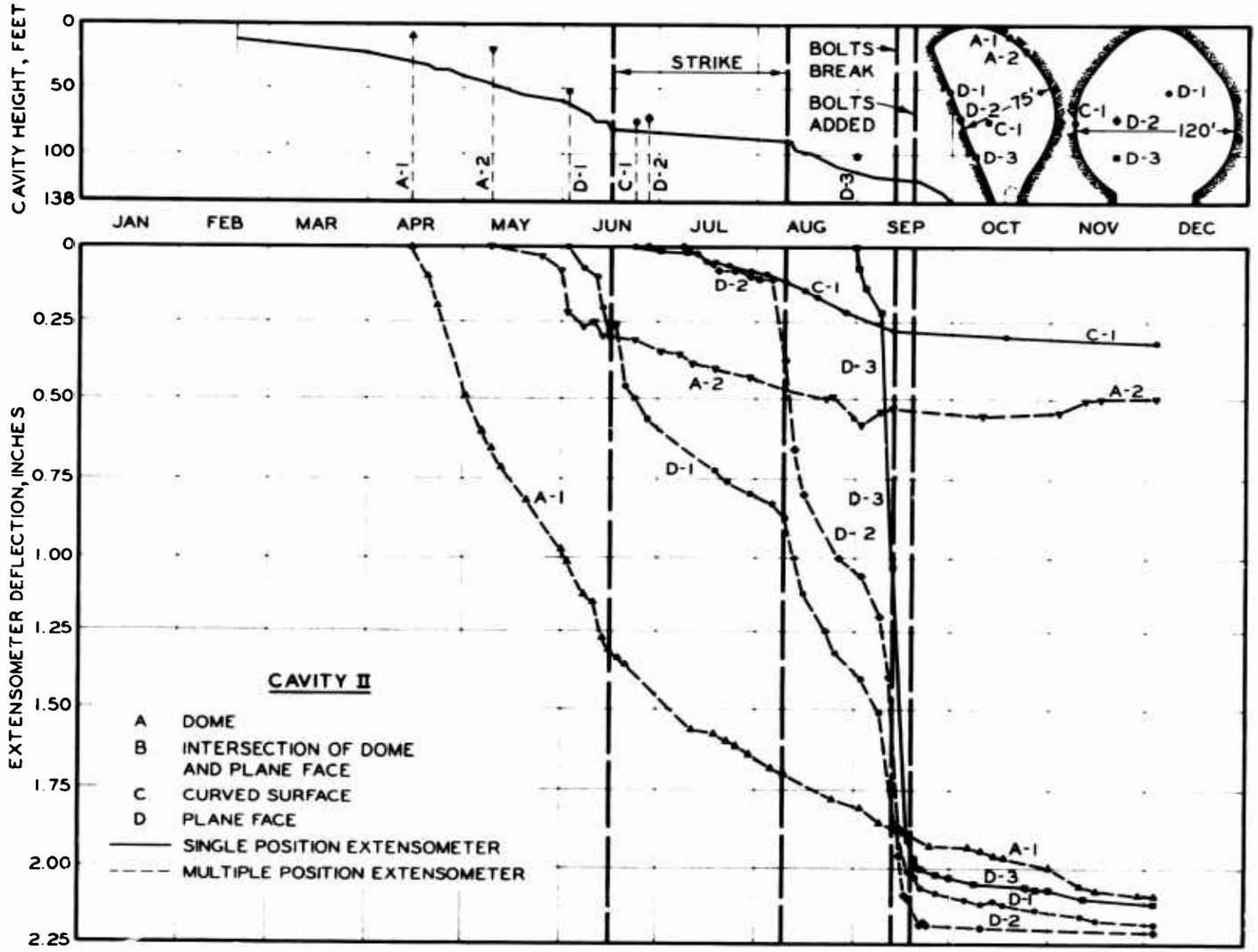

Fig. 23. Displacement of Cavity II surface with respect to deep (30- and 50-ft) extensometer anchors

Displacement-time and displacement-depth relations for all the extensometers installed in Cavities I and II are presented in Appendix B.

Dome (A)

Displacements into Cavities I and II were initially small (0.2 to 0.4 inch) and proportional to the change in span width of the cavity. Most of the initial movement was concentrated in the first 20 feet from the surface. With time, continued displacements occurred which were unrelated to the change in cavity size (Fig. 22, extensometer I-A-1; Fig. 23, extensometer II-A-1). The movements, although large, were of local extent. They were concentrated within the first 5 feet from the cavity surface and were associated with shallow slabbing and cracking of the rock surface. Rock protruding into the cavity was most susceptible to this behavior. Some of the other extensometers in the domes, not located on rock protrusions, did not exhibit these large movements (extensometer I-A-2, Fig. 22; extensometer II-A-2, Fig. 23).

Intersection of Dome and Plane Face (B)

The horizontal movements at the intersection of the dome and plane face in both cavities were very small (less than 0.04 inch), and in some instances negative (indicating movement away from the cavity). There was very little continued movement with construction or time after the initial movements had occurred (extensometer II-B-1, Fig. 22).

Curved Surfaces (C)

Movement on the curved surface of the cavities was generally small (less than 0.2 inch in Cavity I, up to 0.4 to 0.6 inch in Cavity II). Surface cracking and shallow movements were not as common as in the dome. Extensometers I-C-1 (Fig. 22) and II-C-1 (Fig. 23) illustrate this condition.

Plane Face (D)

In Cavity I, movements up to 0.2 inch were measured on the horizontal diameter of the plane face (extensometers I-D-1 and I-D-2, Fig. 22). The deflection decreased uniformly to a depth of 30 feet; there was very little concentration of movement within the first 5 feet. Rock displacement was closely related to excavation of the face. Continued displacements with time were negligible and slabbing was not prominent.

In Cavity II, large movements (1 to 2 inches) occurred in August and September over large portions of the plane face, caused by the instability of wedges of rock which were bounded by joints and bedding plane weaknesses. Some significant movements were measured at depths between 10 and 30 feet, although much of the movement occurred in the first 5 to 10 feet. Extensometers II-D-1, II-D-2, and II-D-3 (Fig. 23), located on the plane face, showed a rapid increase in the rate of movement during this period. The movement ceased in mid-September when additional rock bolts were placed through the zone of movement.

4.3 FRACTURING IN THE TUFF

Excavation in the tuff provided an excellent opportunity for observing the formation of fractures around openings. The tuff had a low strength with respect to the in-situ stresses and had an excellent rock mass quality; therefore, its behavior was similar to that of a highly stressed, brittle, homogeneous material. Excavation created a failure condition at the edge of the opening which resulted in the immediate formation of fractures parallel to the surface of the opening. There were very few discontinuities in the rock mass to mask or modify the formation of the factures.

Fracturing occurred in both large and small openings. In the drifts, fracturing occurred predominantly in the side walls. Hairline fractures were observed to depths of approximately 2 feet. Thin (2- to 6-inch) slabs formed and fell from the side walls of the drift. In the cavities the size and orientation of individual slabs were strongly controlled by the fractures which formed during initial excavation. The slabs were subparallel to the surface and created an onionskin appearance in the cavities. The average thickness of the loosened, slabby rock--approximately 3 feet--was dependent on the rock excavation and support techniques used during construction.

Drifts

Access tunnels and drifts in the tuff were commonly 10 by 10 feet and

13 by 13 feet in cross section. Support consisted of steel horseshoe sets placed on 8-foot centers, lagged, and lightly blocked in the crown of the drift. The amount of slabbing and overbreak in the drifts was observed in order to obtain information on the failure characteristics of the tuff. Fractures which formed behind the walls of the main drifts were mapped when side drifts and rooms were cut into the main drifts, exposing the rock around the drifts.

The typical fracture patterns observed in the drifts are sketched in Fig. 24. Slabbing and fracturing were most prominent on the side walls of the drift, where hairline fractures formed parallel to the opening to a depth of 2 to 3 feet from the surface. The fracturing in the roof and floor was not as deep or as prominent. In many cases, fractures did not occur in the roof. At the bottom corners of the drifts the fractures were closely spaced and parallel, and close to the edge of the opening. Surface slabs on the side walls varied in thickness from approximately 1/2 to 3 inches.

The wide, oval tunnel section illustrated in Fig. 24a is a result of progressive slabbing of the side walls. This tunnel section was driven in a relatively hard, brittle tuff. Immediately after blasting, slight popping of the rock could be heard, accompanied in some instances by thin spalls from the rock surface. Rock fracturing was observed in the walls of an alcove, in the vicinity of a tunnel (Fig. 25). Some of the fractures appeared to be concentrated along a vertical plane, possibly a fault zone.

Rock failure was also observed in smaller openings. The fracturing sketched in Fig. 26 was observed in 3- and 8-inch horizontal drill holes and in a small, unsupported, 7-foot-high side drift. As in the large drifts, the

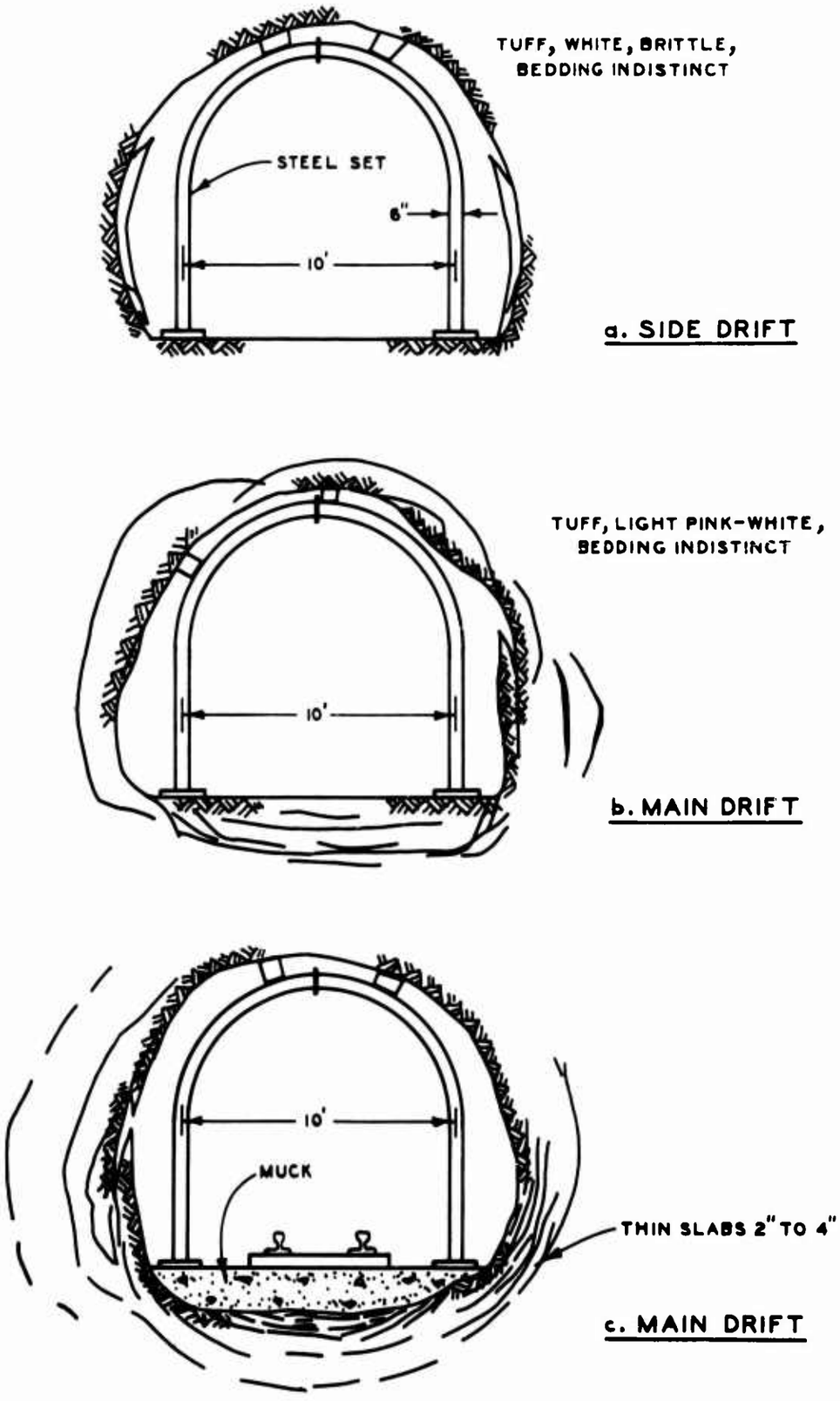

Fig. 24. Typical fracturing in Cavity II access drifts

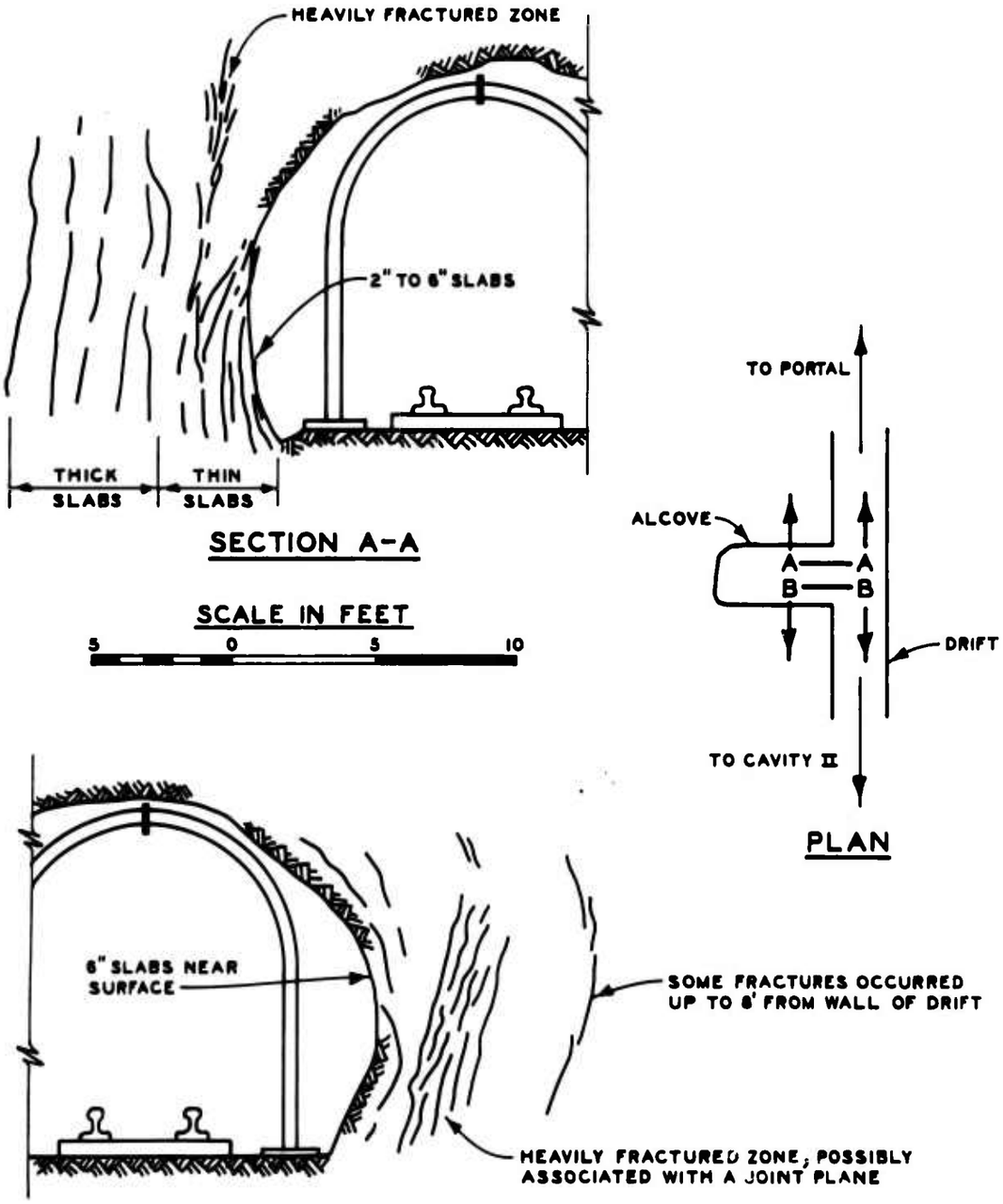

Fig. 25. Fracturing in alcove, Cavity II access drift

NOTE: 1" SLABS TYPICALLY OCCUR ON SIDE, AND FEATHER TOWARD TOP AND BOTTOM OF DRIFT; VERY FEW SPALLS OCCUR IN CROWN.

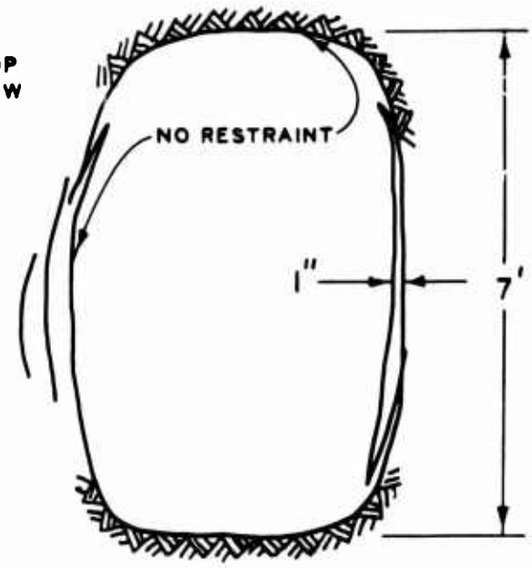

a. SMALL DRIFT, WHITE TUFF

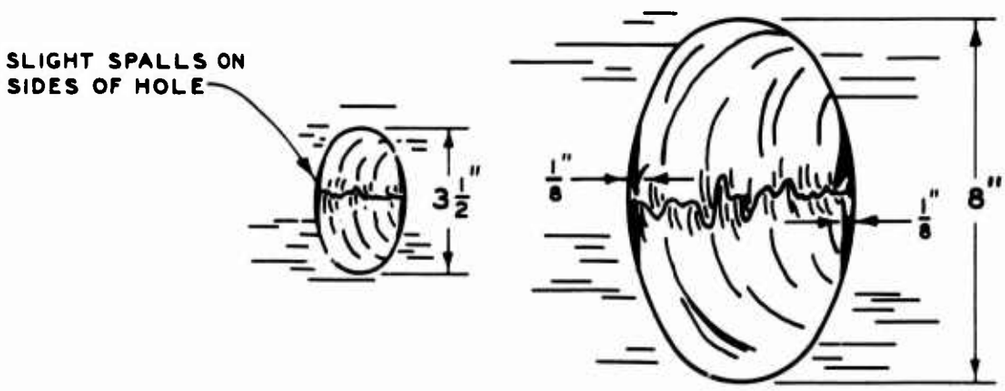

b. BORE HOLES, WHITE TUFF

Fig. 26. Fracturing in boreholes and small drift, Cavities I and II

prominent fracturing occurred on the sides of the openings. In the small drift, 1-inch slabs formed on the side wall and tapered toward the top and bottom of the wall. Only one fracture was observed in the crown; it appeared to be controlled by a bedding plane weakness.

In Fig. 27 a tunnel section is shown where fracturing in the crown, parallel to bedding planes, has occurred. The bedding planes in this portion of the drift were more prominent than in the sections illustrated in Fig. 24. It is apparent that the fractures in the crown resulted from the presence of bedding plane weaknesses.

Slabbing in the crown of the drifts was so extensive in a few instances that large amounts of overbreak occurred. In Fig. 28, two profiles are shown where the main drift intersects the lower portion of Cavity I. In the section of Fig. 28b, there was no evidence of an overbroken zone in the crown. In the section of Fig. 28a, a large overbroken zone was present, much of which had formed prior to excavation of the cavity. A photograph of this zone is shown in Fig. 29. At this location rotting timbers had allowed loosening of the rock in the crown of the drift. These timbers were being replaced when overbreak began to occur. Ten feet of rock were removed from above the crown before a condition was reached where no more large slabs formed. It is probable that bedding or joint discontinuities were present which aided the overbreak. The overbreak above the crown would not have occurred if a minimum amount of support had been maintained.

It is probable that the hairline fractures observed in the side walls of the drifts occurred immediately upon excavation, in response to the stress changes around the opening. They occurred regardless of the type of support used. However, proper support will prevent the opening of fractures

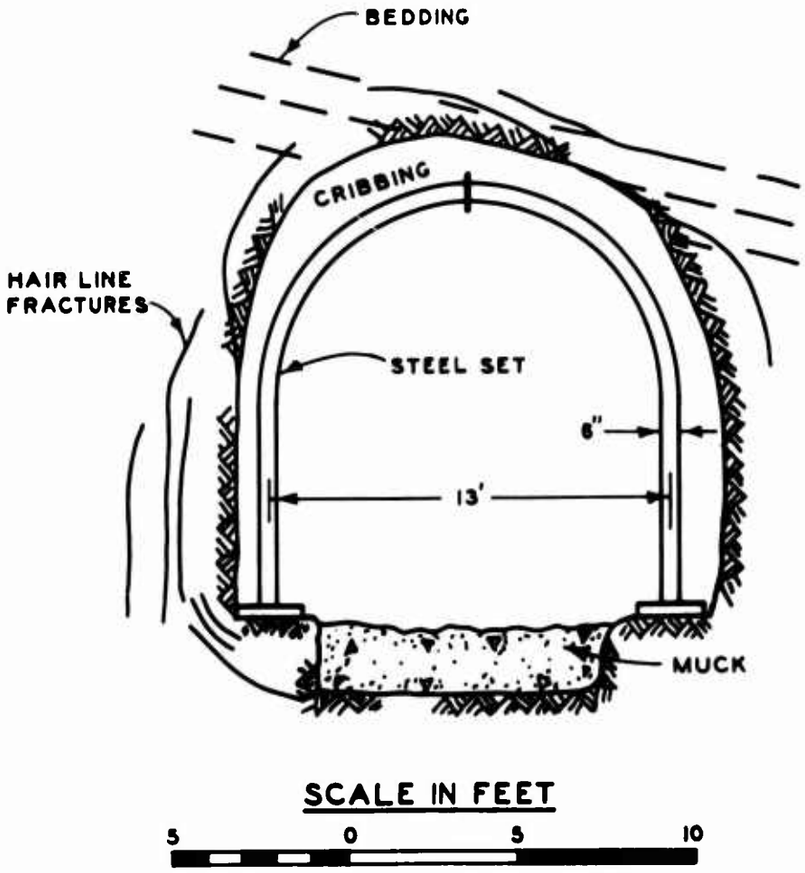

Fig. 27. Bedding plane fractures, main access drift, Cavities I and II

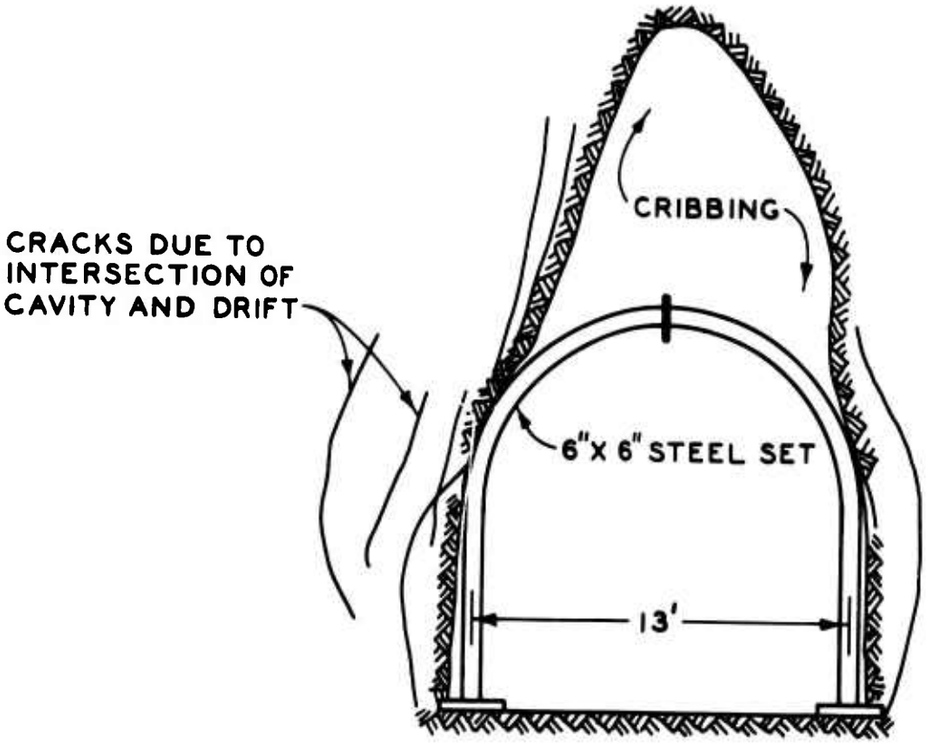

a. VIEW TOWARD PORTAL

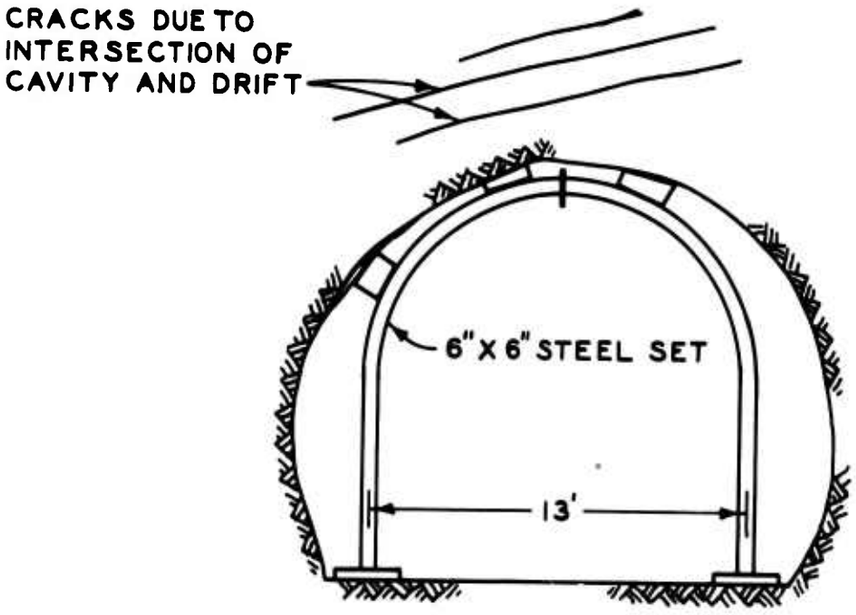

b. VIEW AWAY FROM PORTAL

Fig. 28. Overbreak in access drift at entrance to Cavity I

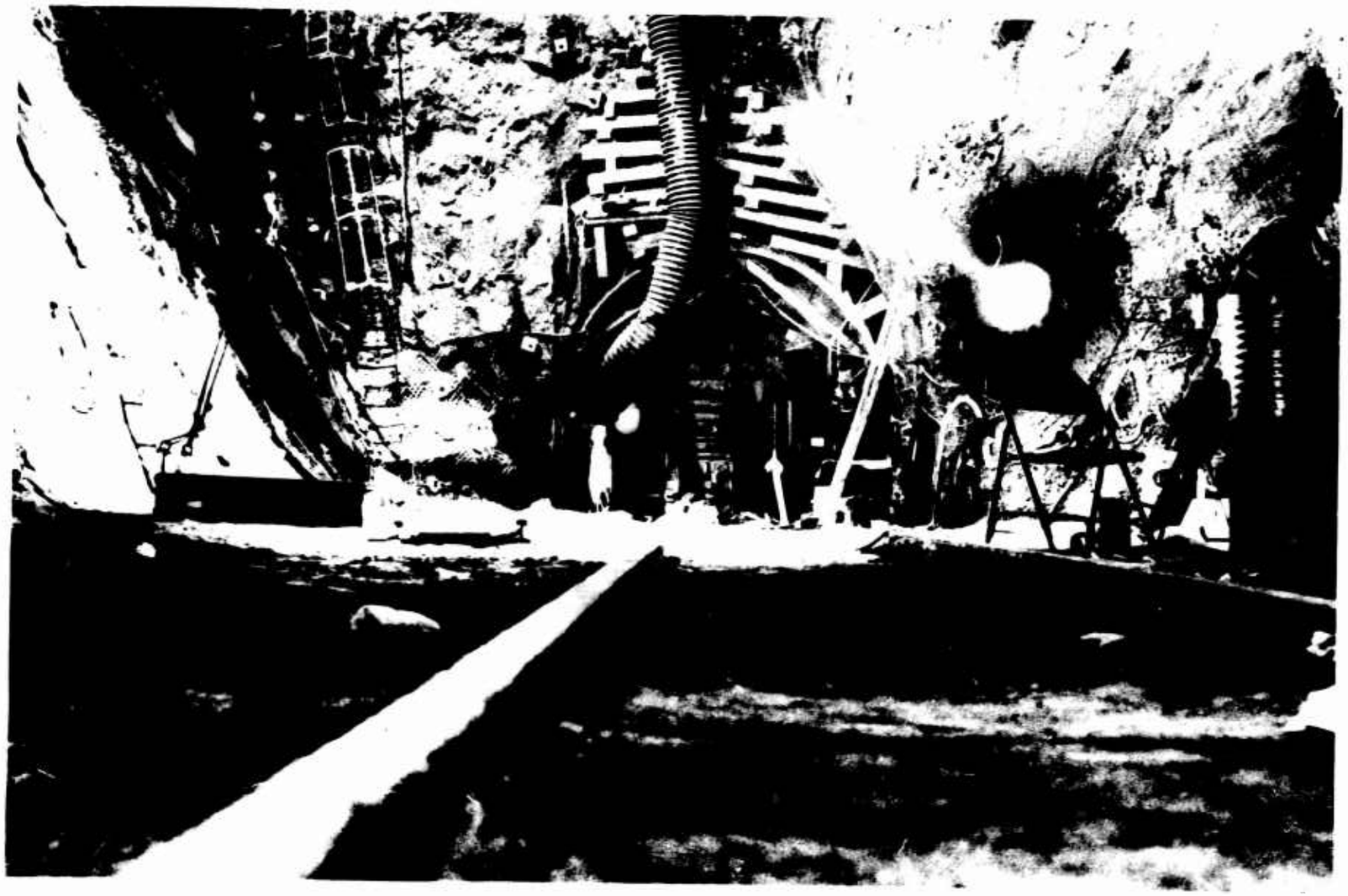

Fig. 29. Fractures and overbreak in access drifts intersecting Cavity I

and continued rock slabbing, such as occurred in the overbroken tunnel section, Fig. 29.

Cavities

Slabbing similar to that described in the drifts occurred during the initial excavation of the cavities. Slabs formed on the side walls of the cavity immediately after excavation, as illustrated in Fig. 30. The slabs varied in thickness from a few inches to approximately 1 foot and feathered out toward the top of the wall. In some cases slight popping noises were heard as thin slabs loosened after blasting in the side walls. This was most apparent when the cavity width was large with respect to the height. With this geometry, high stress concentrations tend to develop in the side walls.

In some instances fracturing in the cavity was affected by bedding plane weaknesses. Some overbreak occurred along bedding planes, particularly in zones where a change in lithology occurred, such as at the contact between a relatively hard red tuff and a soft, friable white tuff (Fig. 11).

Rock-bolting also affected the formation of slabs in the cavities. When blasting next to a bolted area it was commonly observed that slabbing did not occur beneath the tensioned bolts. Overbreak often occurred to the edge of the tensioned bolt, leaving it on a pedestal of rock, a foot or so above the overbroken zone. If bolts were not tensioned prior to shooting the adjacent rock, overbreak would often remove a foot or two of rock from beneath the bearing plate. Rapid placement of rock bolts prevented excessive opening of the extension fractures and reduced the amount of slabby rock formed. However, in some zones of highly stressed and brittle rock, overbreak and slabbing could not be prevented.

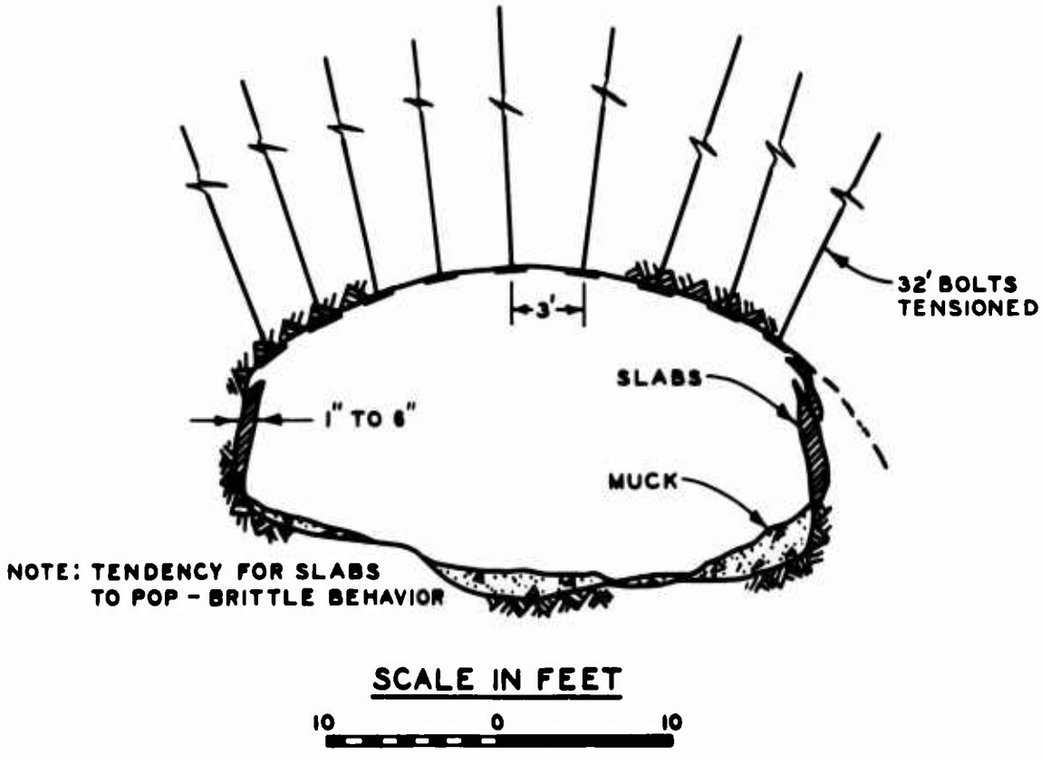

Fig. 30. Slabs formed during excavation in dome of Cavity I

Fig. 31 shows the effect of blasting in the vicinity of a tensioned rock bolt in the dome of Cavity I. Approximately 4 feet of rock had been blasted from one of the walls. As the miners barred down the loose rock in the dome, additional fractures and slabs formed parallel to the fresh surface. Barring of loose slabs was continued until a stable arch was formed. This arch was supported on one side by the wall of the cavity and on the other by a tensioned rock bolt. Loose slabs did not form beneath the rock bolt, although fractures were observed to extend beneath the bolt from the slabbed area. The tensioning of the bolt restrained the rock mass, preventing its slabbing and progressive failure.

The cavities, unlike the tunnel sections, were constructed in stages from the top down. At any stage of construction, fractures formed around the opening in response to the existing stress conditions. Because of the absence of rock bolts in the lower portion of the excavation, new slabbing and fracturing at any stage of excavation were concentrated near the intersection of the floor and wall. The fractures which formed in this part of the excavation paralleled the surface and therefore dipped downward and into the cavity. Further excavation exposed the fractures formed at earlier stages of excavation. Thus, the slabs formed from these fractures also trended downward and into the cavity. This was observed in both cavities. Fig. 32 shows the orientation of the slabs in Cavity I. Fig. 33 is a photograph of slabs formed on the curved surface of Cavity I, which dip into the cavity. (These slabs are not typical for the curved surface of the cavity; most slabs were much less prominent.)

There were a few instances of "bumping" in Cavity I during construction. The bumps were concentrated in the floor of the cavity. On April 1

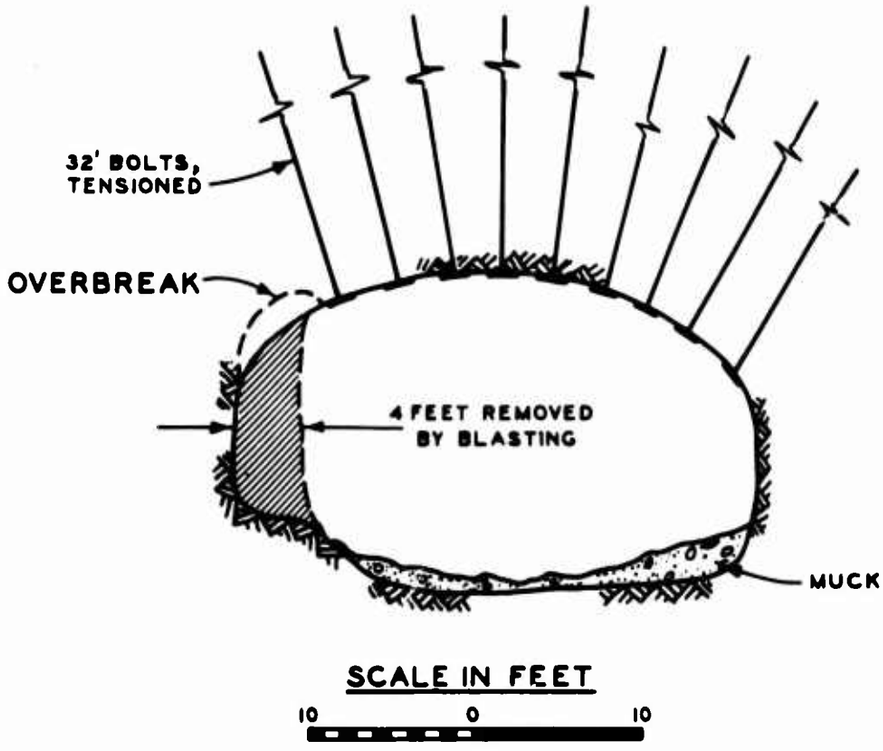

a. CAVITY SHAPE

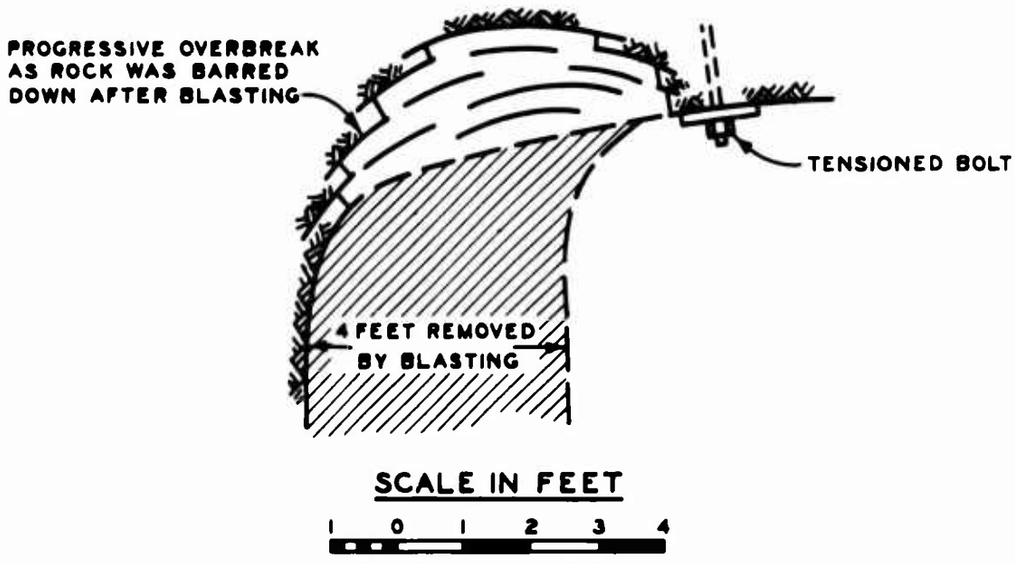

b. OVERBREAK

Fig. 31. Overbreak after blasting 4 ft from wall in dome of Cavity I

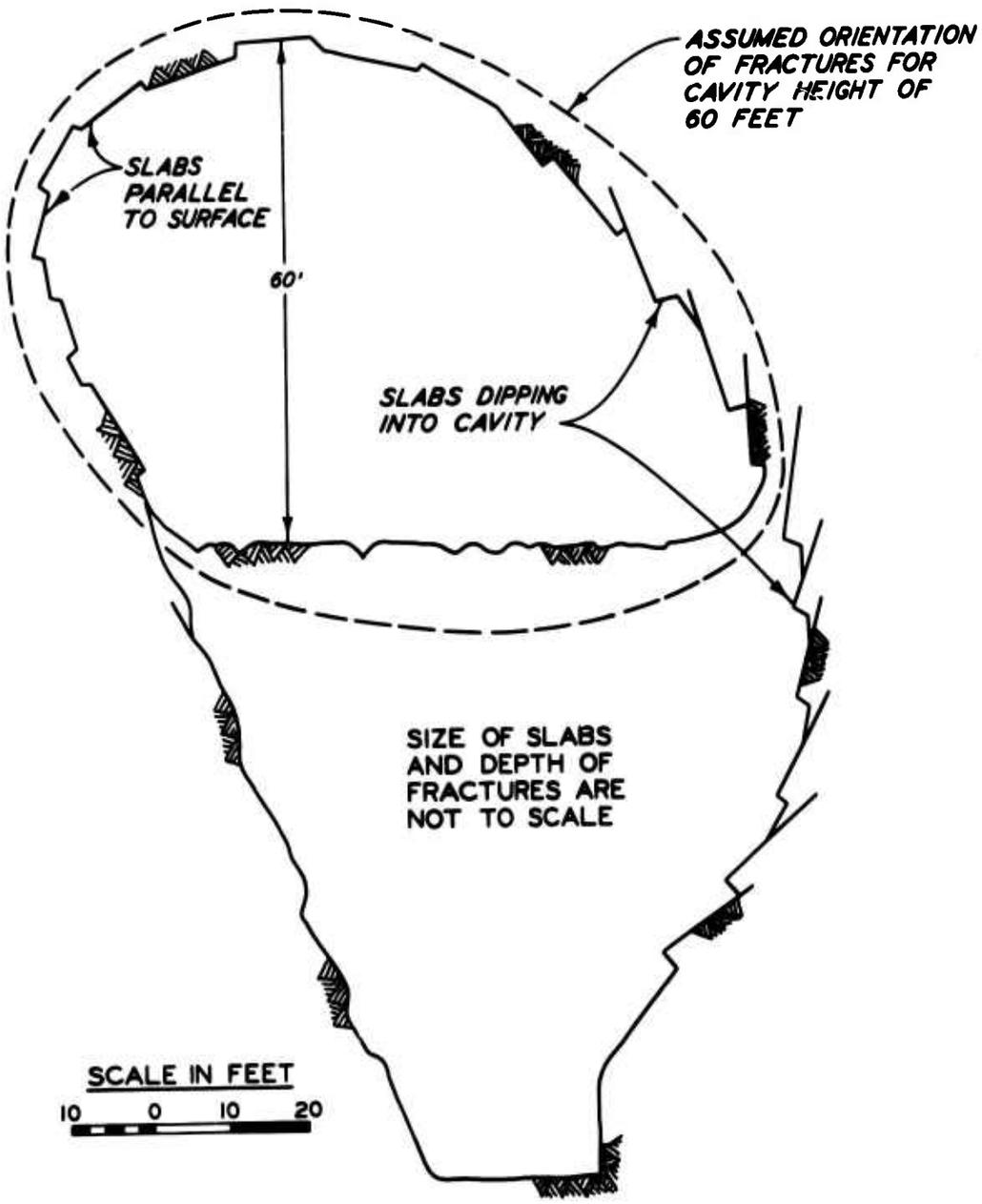

Fig. 32. Slabs and overbreak due to extension fracturing, curved surface, Cavity I

Fig. 33. Orientation of fractures in Cavity I

a small bump occurred in Cavity I approximately 6 hours after blasting, when the cavity was 44 feet high (one-third of its completed height). Miners working in the cavity at the time heard a sharp report and felt the movement which appeared to be concentrated in the floor in the vicinity of the plane face. Miners near the plane face reported that the movement made their legs ache. Men in other portions of the cavity observed some vertical movement of the miners at the plane face: "It appeared as if they went a foot in the air." A smaller bump occurred during the next shift, approximately eight hours later. Extensometers in the dome and upper portion of the plane face showed no increased movement due to the bumps. It seems probable that the bumps resulted from a rapid release of strain energy which was associated with fracturing behind the floor and plane face of the cavity, parallel to the cavity surface.

Lateral movement along fractures occurred in the cavities and was observed by examining offsets of old drill holes. One- and 2-inch offsets were found at depths up to 7 feet in the dome of both Cavities I and II and on the plane face of Cavity II. Some of the offsets on the plane face of Cavity II are shown as arrows in Fig. 12. Large rock slabs and protrusions were commonly offset along fractures at their base. The relative displacement of the shallow rock was usually in the direction of the feathered edge of the slab. These shearing displacements were related to the local geometry of the fractures rather than to a displacement pattern for a continuum.

4.4 SEISMIC REFRACTION SURVEY

Seismic refraction surveys were performed in the tuff cavities by the United States Geological Survey to determine the nature of the destressed rock surrounding the cavities (Scott and Cunningham, 1965).

High-frequency accelerometers were placed at 10-foot intervals along linear arrays on the rock surface. The total length of the refraction lines ranged from 60 to 120 feet. By shooting at both ends of the array, the thickness of the low-velocity zone at each gage location could be determined (Scott and Cunningham, 1965).

The seismic dilatational velocities and the thickness of the low-velocity zone at various locations in the cavities are summarized in Table II. Sections in the dome of Cavities I and II are presented in Figs. 34 and 35.

The in-situ dilatational (deep refraction) velocity averaged 7200 fps, 17% less than the velocity of the intact specimen. Velocities in the shallow, fractured rock surrounding the cavity averaged 3300 fps. The average thickness of the shallow, low-velocity zone was 3.3 feet. Where protrusions of rock into the cavity were present, the thickness of the low-velocity zone increased to 5 to 7 feet.

Effect of Fracturing on the Deep Refraction Velocity

The prominent fracturing and slabbing in the cavities occurred within the first 3 feet from the surface and were measured as a velocity discontinuity with the seismic refraction method. However, fracturing was not limited to this depth. The presence of fractures at greater depth was indicated by lower values for the deep refraction velocity. The deep refraction velocity is determined from a pulse which travels directly behind the low-velocity zone over the entire length of the refraction line; the velocity of the pulse is therefore affected by fractures behind the low-velocity zone.

Velocities were also determined at depth, perpendicular to the plane

TABLE II

SEISMIC REFRACTION SURVEY, CAVITIES I AND II

	Average Thickness of Low-Velocity Zone ft	Shallow Refraction Velocity fps	Ratio of Shallow Refraction Velocity to Lab Velocity	Deep Refraction Velocity V_{pf} fps	Ratio of Deep Refraction Velocity, V_{pf} to Lab Velocity, V_{pl}
			Cavity I		
Dome, line 1	1.7			5800	0.67
Dome, line 2	3.5 (7.0)*			7325	0.84
Plane face	3.7	3190	0.36	7350	0.84
Curved surface	3.0			8350	0.96
Avg	3.4			7550	0.86
			Cavity II		
Dome	3.1 (5.0)*			6760	0.77
Plane face	3.5	3360	0.37	6425	0.73
Curved surface	3.0			7450	0.85
Avg	3.2			6880	0.79

* Thickness at prominent protrusion.

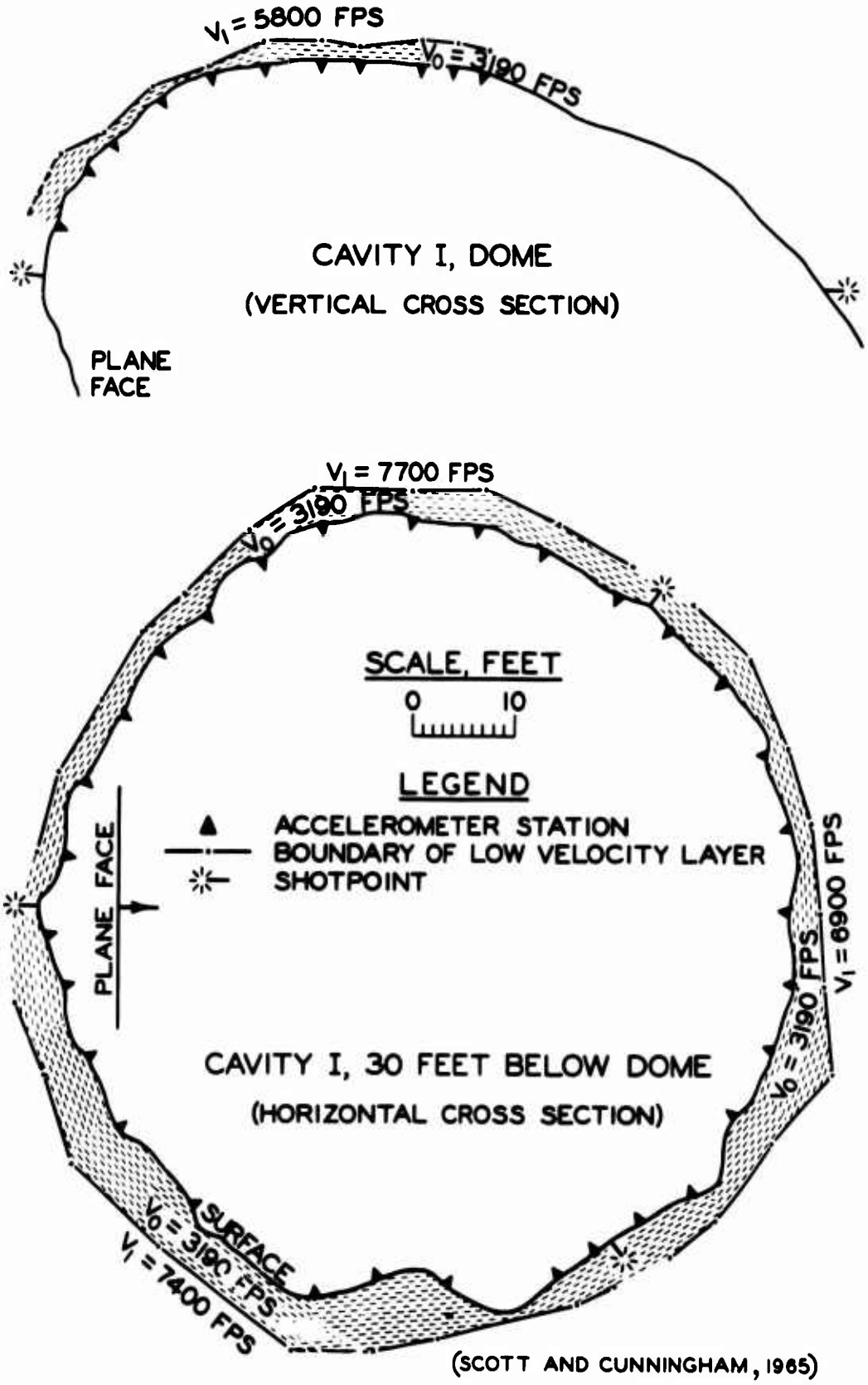

Fig. 34. Seismic refraction profiles, Cavity I

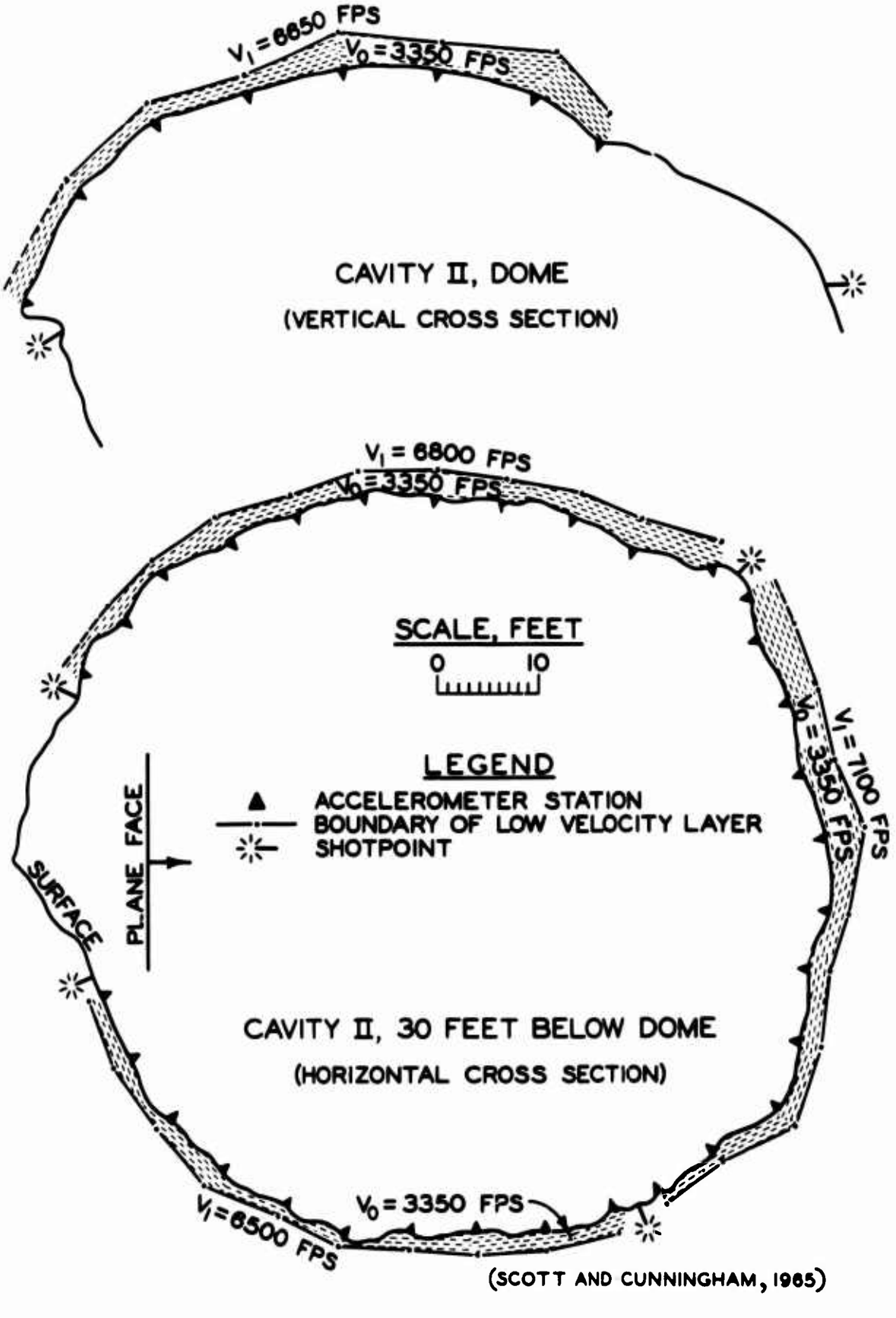

Fig. 35. Seismic refraction profiles, Cavity II.

face of the cavity, by measuring the travel time of a directly propagated wave between the plane face of the cavity and a drift located 155 feet behind the plane face. In Table III these values have been compared with the deep refraction velocities obtained from the refraction surveys on the surface of the plane face. The deep refraction velocities were generally lower than the directly propagated velocities. This seems to indicate that slight fracturing behind the low-velocity zone had decreased the deep refraction velocity. The differences between the two types of velocity cannot be attributed to the direction of propagation of the waves; there does not appear to be a significant velocity anisotropy due to bedding in the tuff.

In the refraction line run across the dome of Cavity I, the deep refraction velocity was significantly lower (5800 fps) than in other portions of the cavity (Table II). The thickness of the low-velocity zone was only 1.7 feet at this location. It is probable that this was a result of loosening of thin slabs in the dome, which created a velocity discontinuity at 1.7 feet. The low value of the deep refraction velocity indicates that fracturing behind the first velocity discontinuity had occurred. Because of the short length of the refraction line, it could not be determined if there was a second velocity discontinuity at greater depth.

Effect of Rock Movement on Depth of Low-Velocity Zone

The depth of the low-velocity zone along the horizontal diameter of the plane face of Cavity II is illustrated in Fig. 12. Refraction surveys were performed in June when that portion of the cavity had just been excavated and again in September when the cavity was completed. During this time, there was no significant change in either the shallow velocity or the

TABLE III

COMPARISON OF DEEP REFRACTION AND DIRECTLY PROPAGATED

SEISMIC VELOCITIES WITH LABORATORY SONIC VELOCITY

Location	V_{pf} fps	V_{pf}/V_{pl}	V_{sf} fps	μ_{df}	E_{df} psi x 10^6	$\left(\frac{V_{pf}}{V_{pl}}\right)^2 \approx \frac{E_{df}}{E_{dl}}$	E_{df}/E_t
Cavity I, plane face, horizontal diameter							
a. Deep refraction velocity	7000	0.80	3860	0.28	0.99	0.64	1.98
b. Directly propagated velocity	7610	0.87	3930	0.32	1.08	0.76	2.18
Cavity I, plane face, vertical diameter							
a. Deep refraction velocity	7700	0.88	3850	0.33	1.06	0.78	2.12
b. Directly propagated velocity	7790	0.89	4090	0.31	1.16	0.79	2.32
Cavity I, avg	7530	0.85	3890	0.31	1.06	0.72	2.12
Cavity II, plane face, horizontal diameter							
a. Deep refraction velocity	6600	0.75	3180	0.34	0.71	0.56	1.42
b. Directly propagated velocity	6950	0.79	3820	0.28	0.98	0.62	1.96
Cavity II, plane face, vertical diameter							
a. Deep refraction velocity	6250	0.71	3730	0.22	0.89	0.50	1.78
b. Directly propagated velocity	6530	0.74	3680	0.27	0.90	0.55	1.80
Cavity II, avg	6580	0.75	3600	0.28	0.87	0.56	1.74

Note: Deep refraction velocity is determined from pulse propagated directly behind low-velocity zone; directly propagated velocity is determined from a pulse propagated in undisturbed rock, perpendicular to rock surface.

V_{pf} = seismic compressional velocity, field.

V_{pl} = sonic compressional velocity, lab (V_{pl} = 8750 fps for tuff).

V_{sf} = seismic shear velocity, field.

E_{df} = Young's modulus determined from field seismic velocity.

E_{dl} = Young's modulus determined from lab sonic velocity.

E_t = Young's modulus, tangent at one-half unconfined compressive strength, intact specimen ($E_t = 0.5 \times 10^6$ psi for tuff).

μ_{df} = Poisson's ratio determined from field seismic velocities.

Elastic relations:

$$\left(\frac{V_p}{V_s}\right)^2 = \frac{2(1 - \mu_d)}{1 - 2\mu_d} .$$

$$E_d = \frac{\gamma}{g} (V_p)^2 \left[\frac{(1 + \mu_d)(1 - 2\mu_d)}{1 - \mu_d}\right] ; \gamma = 121 \text{ pcf for tuff.}$$

$$\left(\frac{V_{pf}}{V_{pl}}\right)^2 = \left(\frac{E_{df}}{E_{dl}}\right) ; \text{ if } \gamma_f = \gamma_l \text{ and } \mu_f = \mu_l .$$

deep velocity. The depth of the low-velocity zone did not change on the right side of the plane face, but increased slightly on the left side (by approximately 1 to 2 feet).

The increase in the thickness of the low-velocity zone appears to be related to the large movements which occurred on the left side of the cavity after the initial refraction survey had been performed. It is believed to have been caused by additional fracturing and opening of old fractures within the first 10 feet, during the period when the large movements occurred in this portion of the cavity. Large movements occurred on the right side of the cavity between 10 and 30 feet (extensometer D-4), but did not cause any significant change in either shallow or deep velocity, or in the depth of the low-velocity zone.

Comparison of Field and Laboratory-Determined Moduli and Velocities

Velocities and moduli are compared in Table III. Definitions and equations used are shown at the bottom of the table.

Both dilatational and sheer velocities in the field were obtained from the time-amplitude record of the accelerometers (Scott, 1965). Elastic moduli were computed from the field velocities.

The ratio of E_{df} to E_{dl} was approximated by the square of the velocity ratio $(V_{pf}/V_{pl})^2$. The relation is valid if the field values for density and Poisson's ratio are equal to the laboratory values.

In Table III, it can be seen that the field velocity is lower than the laboratory velocity for all the seismic lines. This is probably a result of fracturing in the rock mass which is not present in the intact sample. The directly propagated velocity in Cavity I is 11% lower than the laboratory velocity; in Cavity II, it is 21% lower. The average ratio of E_{df}

to E_{dl}, for the directly propagated velocity determination, is 0.78 for Cavity I and 0.59 for Cavity II.

The field seismic modulus, E_{df}, although lower than the laboratory seismic modulus, E_{dl}, is approximately twice as large as the laboratory static modulus, E_t. This is primarily due to strain-rate and stress-level effects, which mask the differences between laboratory and field characteristics.

Conclusions

The refraction seismic method was useful for determining the thickness of the heavily fractured, shallow rock zones in the cavities. The results also indicated that fracturing was not confined to the shallow zone. However, because the deep fractures were fairly tight and the changes in rock fracturing gradual with depth, it was difficult to obtain definitive information on fracturing in the deep zone using the refraction method. There is enough information to conclude that the fracturing behind the low-velocity zone caused the deep refraction velocities to be lower than the velocity in the undisturbed rock (measured by the directly propagated pulse).

Velocities at depth were generally lower in Cavity II than in Cavity I. This is probably a result of a difference in in-situ rather than intact rock properties: there is a greater frequency of natural fractures in Cavity II than in Cavity I; there was not a significant difference in the intact properties of samples taken from the two cavities (Table 1).

Deep refraction velocities were high and the depth of the shallow velocity zone was low along the curved surfaces of both cavities (horizontal line at cavity midheight). The curved surface of the cavity was least

affected by slabbing and cracking, and recorded movements were low in these areas.

CHAPTER 5

COMPARISON OF OBSERVED AND THEORETICAL BEHAVIOR IN THE TUFF

5.1 INTRODUCTION

Rock movement and rock fracturing observed in the cavities (Chapter 4) are compared with theoretical continuum relations for displacement and stress around openings in elastic and elastic-plastic media. The rock properties and construction procedures discussed in Chapters 2 and 3 are important factors in determining the applicability of the theoretical behavior to the observed behavior: the assumed material properties of the theoretical medium must approximate the actual rock mass characteristics (Chapter 3); the assumed boundary conditions must be appropriate to the actual boundary conditions in the cavities, which include the geometry of the opening, and the support and excavation techniques used during construction (Chapter 2).

In some instances, there are significant differences between the theoretical and observed behavior, due to limitations of the theory in describing real behavior. Often an analysis of these differences provides further insight into an understanding of the behavior of the rock mass.

5.2 SIMPLE ELASTIC SOLUTIONS FOR PREDICTION OF CAVITY BEHAVIOR

During construction of the cavities, rock movements were compared with simple elastic theory. Displacements on the curved surfaces of the cavities were estimated using the theory for a sphere in a hydrostatic stress field. Displacements on plane surfaces were determined using the theory for a uniform pressure on an elastic half space. The depth of the yielded zone surrounding the cavities was estimated from the theory for a cylinder

in an elastic-plastic (Navier-Coulomb) material subjected to hydrostatic loading.

These relations are simplified approximations of the complex geometry and stress conditions present in the cavities. The simple theories were used during excavation for rapidly comparing predicted with observed behavior. The use of a more refined analysis would have required time-consuming arithmetic manipulations, which might have resulted in a decreased appreciation for the physical situation. After the cavities had been completed, more refined analyses were made. One of these, presented in Section 5.3, solves for displacements and stresses using a finite element method.

Displacements Around a Sphere in Elastic Medium, Hydrostatic Loading

The equation for the radial deflection, d, at any radial distance, r, due to the excavation of a spherical opening of radius, a, in an infinite elastic medium subjected to a uniform, hydrostatic stress, p, is:

$$d = \frac{a^3}{2r^2}\left[p\,\frac{(1+\mu)}{E}\right] \qquad (1)$$

where E is Young's modulus and μ is Poisson's ratio. This equation may be obtained from the stress equations for an elastic thick-walled spherical shell subjected to internal pressure (Timoshenko and Goodier, 1951).

Predicted displacements in the dome of the cavities were calculated by substituting into the equation the average span width of the cavity for $2a$, and the natural vertical stress for p. For the tuff, substitution of $p = 1000$ psi, $E = 0.50 \times 10^6$ psi, and $\mu = 0.24$ into equation (1) gives:

$$d = 1.24 \times 10^{-3}\,\frac{a^3}{r^2} \qquad (2)$$

A vertical (inward) surface displacement of 0.75 inch was estimated for the dome, for the maximum span width of 100 feet. The two-dimensional finite element solution (which does not closely approximate the three-dimensional boundary conditions in the dome) predicts 1.4-inch total displacement in the dome (Section 5.3).

For the granite, substitution of $p = 400$ psi , $E = 4 \times 10^6$ psi , and $\mu = 0.2$ into equation (1) gives:

$$d = 0.6 \frac{a^3}{r^2} \times 10^{-4} \qquad (3)$$

The vertical surface displacement of the dome for the maximum span width of 50 feet was estimated to be 0.018 inch.

The finite element solution presented in Section 5.3 is strictly two-dimensional, but is applied to three-dimensional problems. It is therefore of interest to compare the two conditions. The simplest case is a circular cross section: a sphere and a tunnel. Fig. 36 is a plot of the displacement versus radial distance from the surface of an opening of radius a . The displacement at the surface of the sphere is one-half the displacement for a tunnel of the same size. The displacements also attenuate much more rapidly with depth for the sphere ($1/r^2$ for the sphere as compared to $1/r$ for the tunnel). Similar conditions exist for the more complex boundary conditions.

Displacements Due to a Uniform Pressure on an Elastic Half Space

Displacements at depth for a uniform pressure over a finite area of an elastic half space are obtained by integration of Boussinesq's equations for a point load on an elastic half space. These equations were used to estimate the displacements due to unloading of the plane surface of the

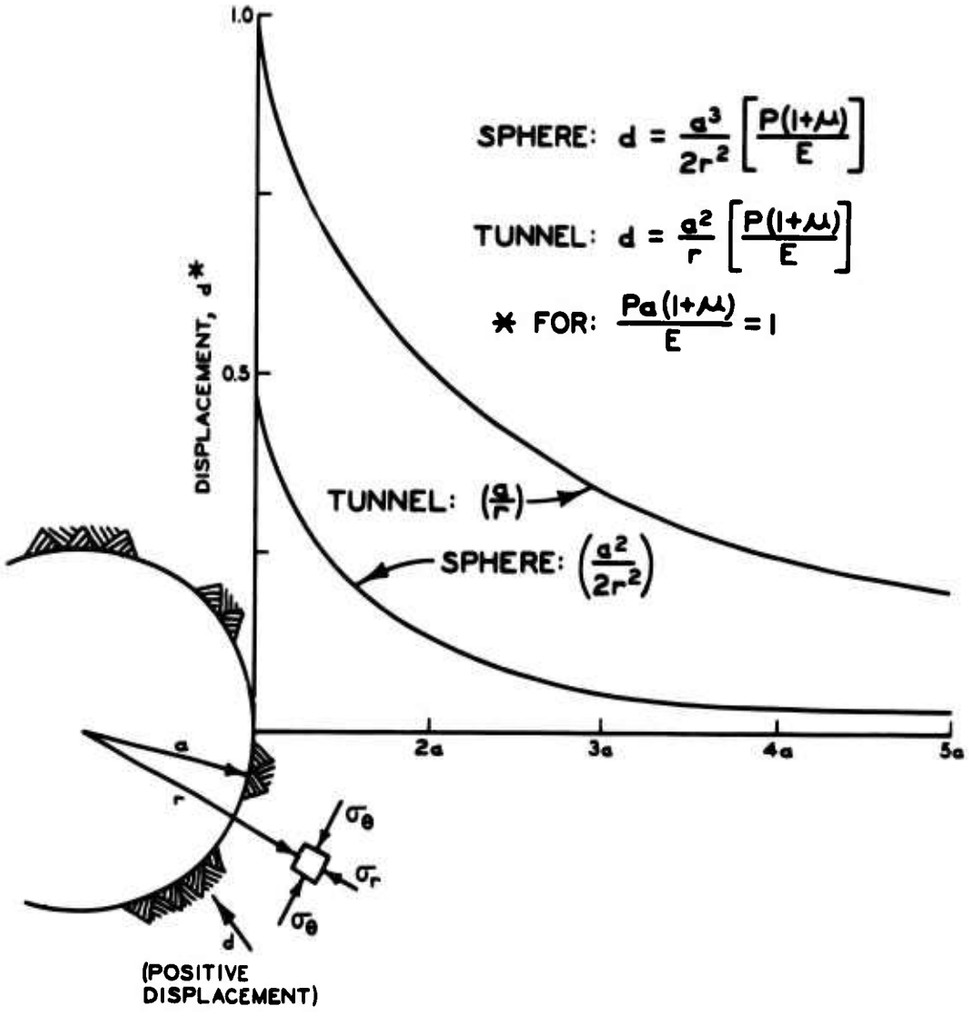

Fig. 36. Comparison of displacements for sphere and tunnel in uniform stress field

cavity by excavation. The change in the normal stress at the surface of the plane face due to excavation of the cavity was substituted for the uniform pressure; and the area of the excavated face was substituted for the loaded area of the half space.

The equation for the surface displacement, d , due to a uniform pressure, q , acting over a circular area (of radius a) on an elastic half space is (Terzaghi, 1943):

$$d = 2a\left[\frac{q(1 - \mu^2)}{E}\right] \qquad (4)$$

Using this equation, with q equal to the natural horizontal stress of 500 psi, the total surface deflection at the center of the plane face of the tuff cavities was calculated to be 1.4 inches. The total displacement of the plane face determined by the finite element method was also 1.4 inches (Section 5.3). However, the displacements dropped off more rapidly with depth for the finite element solution, which is a closer approximation to the actual boundary conditions of the plane face (refer to Fig. 37).

The total surface deflection at the center of the plane face of the granite cavity was calculated to be 0.08 inch, for $q = 400$ psi .

Yielded Zone Around a Circular Tunnel in an Elastic-Plastic Medium, Hydrostatic Loading

The zone of yielding due to excavation of a circular tunnel of radius a in an elastic-plastic medium subjected to a uniform hydrostatic pressure p may be obtained by substituting a yield (or failure) condition into the equilibrium stress equation. Jaeger (1962) determined the size of the yielded zone and solved for the stresses using a Navier-Coulomb yield criterion, where the yield stress is a function of the confining pressure.

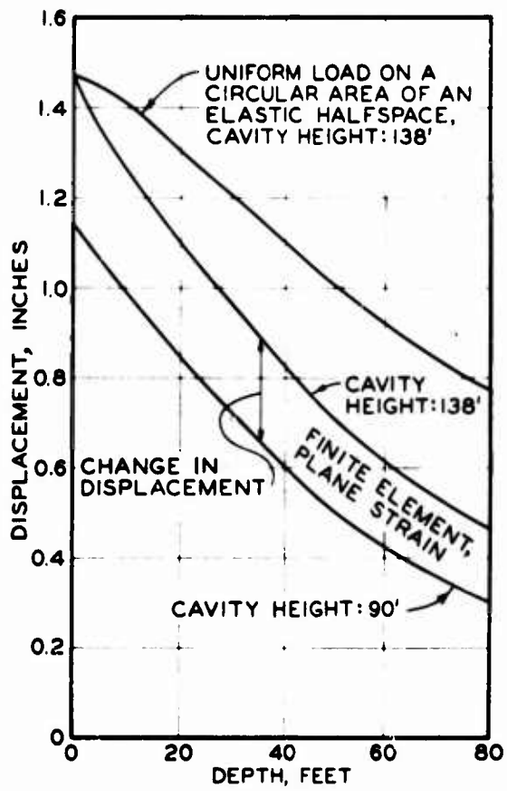

Fig. 37. Theoretical elastic displacement-depth profiles at center of plane face, Cavities I and II

(Yielding occurs when the shear stress, τ , exceeds ($c + p \tan \phi$) on any plane of a given element.) When the yield stress is reached in any part of the medium perfectly plastic behavior ensues. The plastic zone will first form in the highly stressed areas near the surface of the opening. With increasing external pressure, p , the boundary of the plastic zone will move radially away from the surface of the opening. Outside this boundary, the medium behaves elastically.

The radius, R , of the boundary between the plastic and elastic zones is (Jaeger, 1962):

$$\frac{R}{a} = \left(\frac{2[p(t^2 - 1) + 2ct]}{[p_i(t^2 - 1) + 2ct](1 + t^2)} \right)^{\left(\frac{1}{t^2-1}\right)} \qquad (5)$$

where

a = radius of tunnel

p = external hydrostatic pressure

p_i = internal hydrostatic pressure

$t = \tan (45 + \phi/2)$

ϕ = angle of friction

c = cohesion

2ct = unconfined compressive strength, σ_{ult}

The effect of internal pressure and material properties on the depth of the yielded zone can be seen in Fig. 38. It is apparent that the depth of yielding increases with decreases in strength (ϕ and c). For a material with no cohesion or internal pressure, the predicted yielded zone is infinite. It should be noted, however, that this elastic-plastic failure theory is based on stress and does not account for the deformation

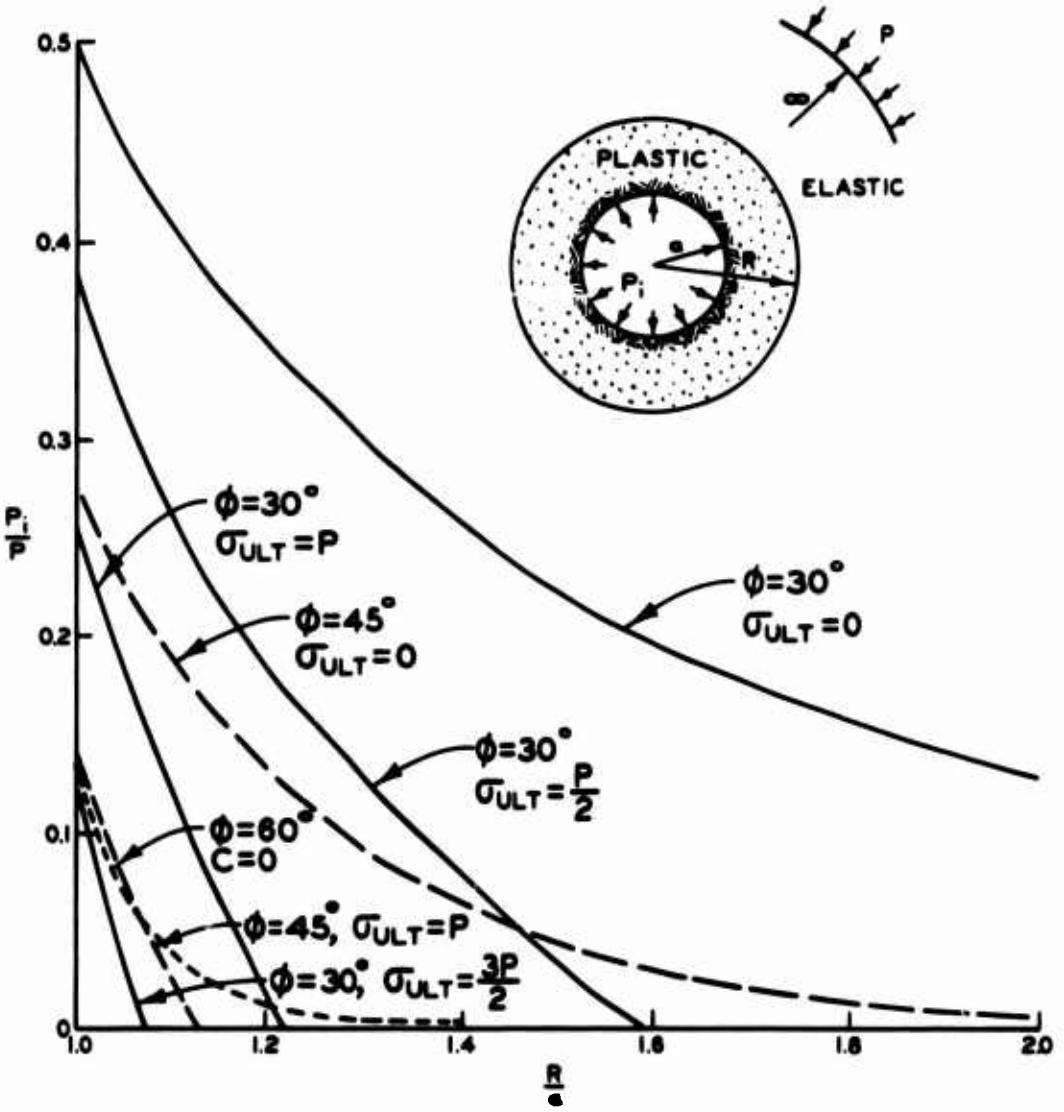

$$\frac{R}{a} = \left[\frac{2\left[P(t^2-1)+2ct\right]}{\left[P_i(t^2-1)+2ct\right]\left[1+t^2\right]}\right]^{\left(\frac{1}{t^2-1}\right)}$$

$$\sigma_{ULT} = 2ct$$

$$t = \tan\left(45+\frac{\phi}{2}\right)$$

Fig. 38. Size of yielded zone around tunnel in an elastic-plastic (Mohr-Coulomb) medium subjected to uniform stress field

characteristics of the material. It assumes that yielding of a material can occur at infinitesimal strains.

For a material having a ϕ but no cohesion, a slight change in the internal pressure changes the size of the yielded zone significantly. However, for a material with high cohesion, slight changes in the internal pressure have very little effect on the size of the yielded zone. Increasing the strength of the material (either ϕ or c) while maintaining a constant internal pressure will cause a significant decrease in the size of the yielded zone. Thus, changes in material properties have an important effect on the size of the yielded zone, while changes in the internal pressure, except in cases where the cohesion is small, have a relatively minor effect on the size of the yielded zone. The implications of this theory for the behavior of a real material are discussed in Section 5.5.

Slip lines in the plastic region are inclined at an angle of $45 - \phi/2$ to the direction of the major principal compressive stress (which is the tangential stress). The equation for the slip lines in the plastic region around the tunnel is:

$$r/a = c \pm \theta \cot (45 + \phi/2) \qquad (6)$$

Thus the slip lines are logarithmic spirals as shown in Fig. 39 for various values of ϕ .

Stresses Around a Circular Tunnel in an Elastic Medium, Biaxial Loading

Equations for the stresses around circular two-dimensional openings under uniaxial stress were developed by Kirsch in 1898. The solution for biaxial stress is obtained by superposing, at right angles, the solutions

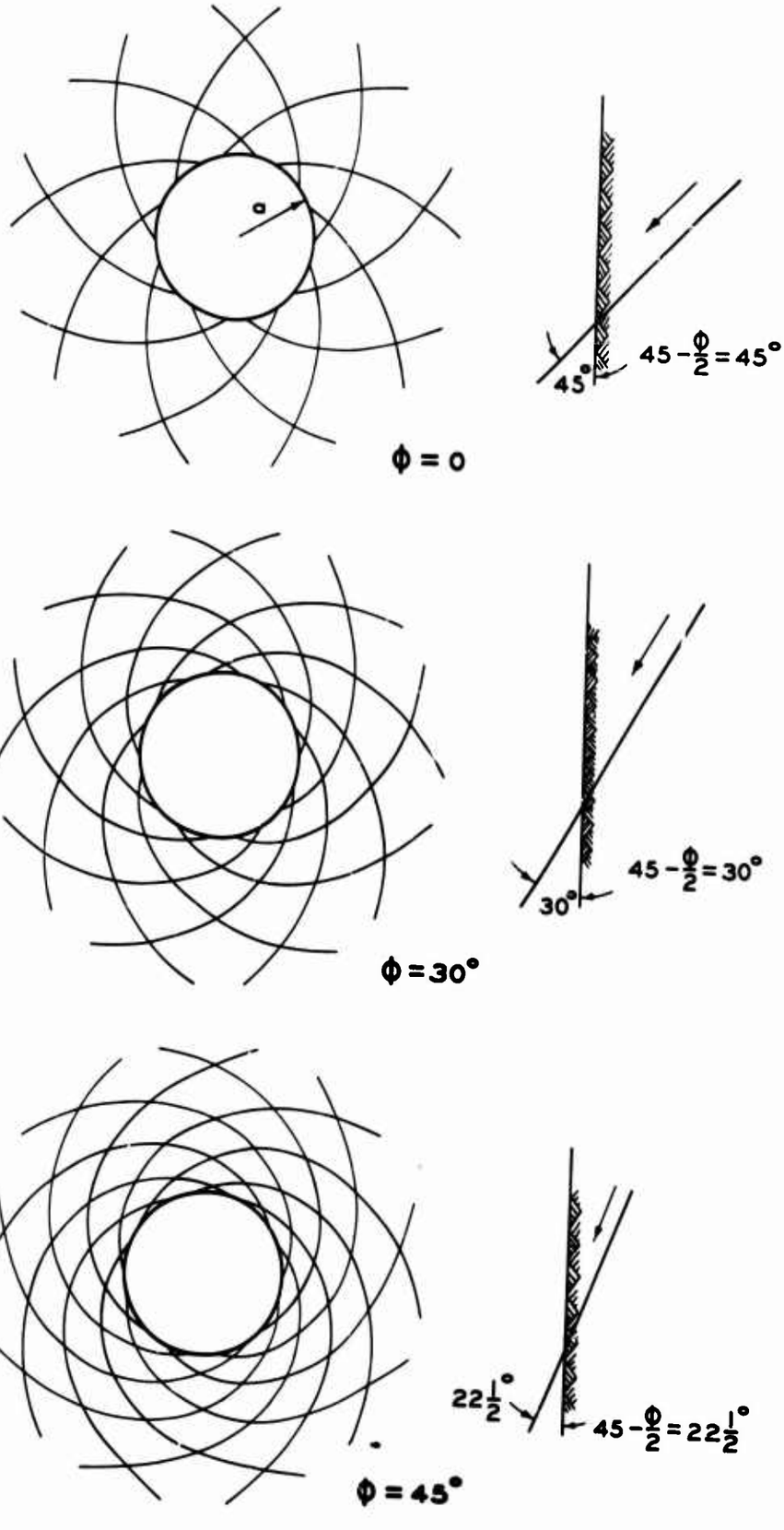

Fig. 39. Orientation of slip lines around tunnel in an elastic-plastic (Mohr-Coulomb) medium subjected to uniform stress field

for two uniaxial stress conditions. The tangential stresses around the edge of a tunnel are shown in Fig. 40 for varying ratios of vertical to horizontal stress. The variation of tangential and radial stresses with depth along the horizontal diameter is shown in Fig. 41.

From these figures a rough estimate of the portions of a tunnel which would be subjected to fracturing may be obtained by comparing the compressive strength of the tuff with the elastic stresses around the opening. Where the tangential stress exceeds the strength of the tuff, failure will occur. (This is strictly an elastic solution and does not account for stress redistribution.)

For the hydrostatic loading case, failure will occur around the entire perimeter whenever the stress concentration of 2000 psi exceeds the unconfined compressive strength of the material. The depth of the overstressed zone determined by the elastic solution, for $\phi = 45$ deg and $c = 250$ psi, is 0.08a. The elastic-plastic solution of the previous section accounts for stress redistribution and predicts a depth of approximately 0.12a for the yielded zone.

For the condition existing in the tuff ($\sigma_v = 2\sigma_h = 1000$ psi, $c = 250$ psi, and $\phi = 45$ deg) the depth of the overstressed zone is 0.10a at the horizontal diameter and extends from 54 deg above the horizontal to 54 deg below the horizontal diameter. Fig. 42 shows the approximate overstressed zones for three loading cases: $\sigma_v = \sigma_h$, $\sigma_v = 2\sigma_h$, and $\sigma_h = 0$.

5.3 ELASTIC FINITE ELEMENT SOLUTION FOR STRESSES AND DISPLACEMENTS

Description of Method

A plane strain, finite element computer solution developed by Reyes (1966) was used to determine the elastic displacements and stresses around

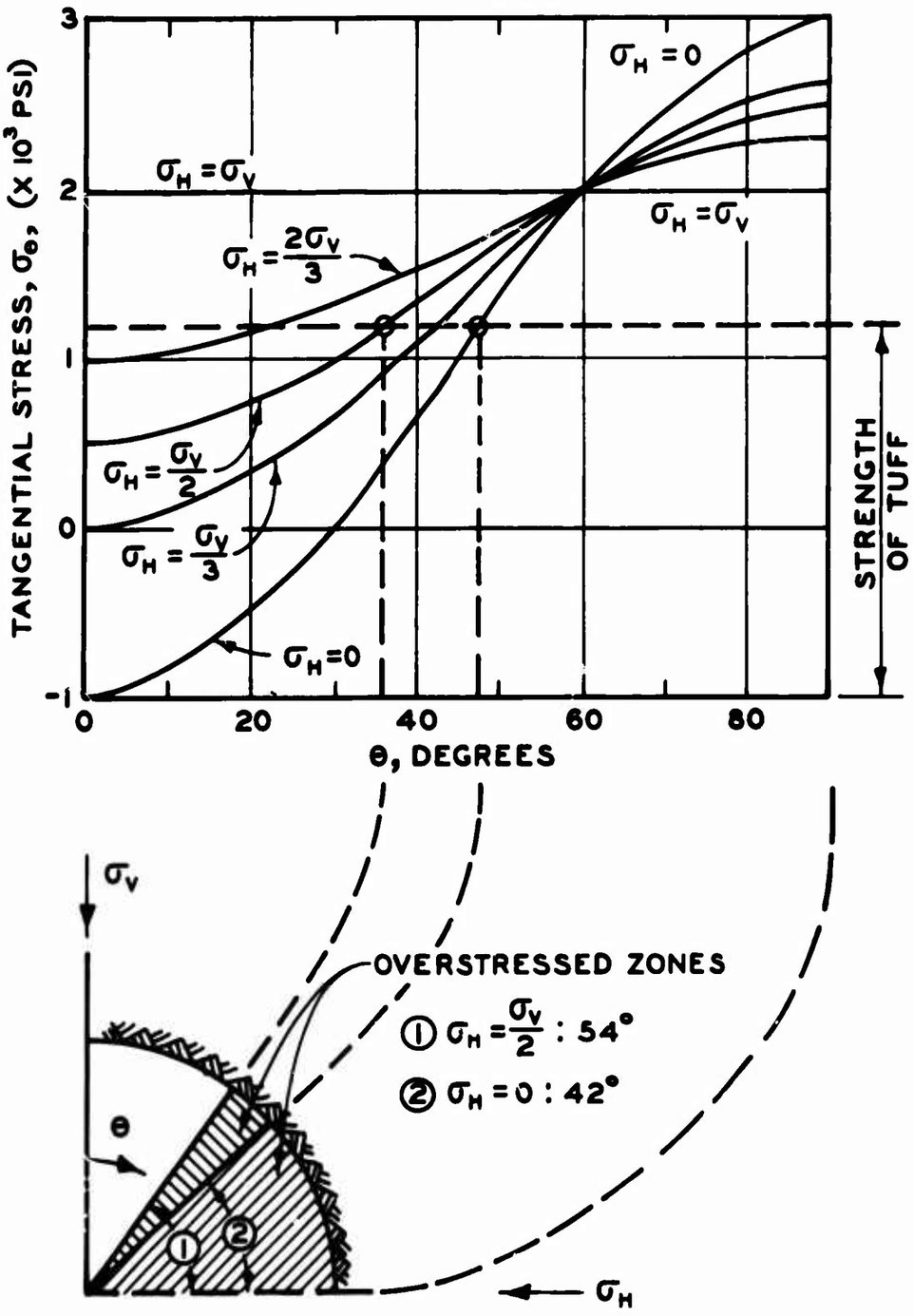

Fig. 40. Elastic stresses and overstressed zones around circumference of tunnel in medium subjected to various ratios of vertical to horizontal natural stress

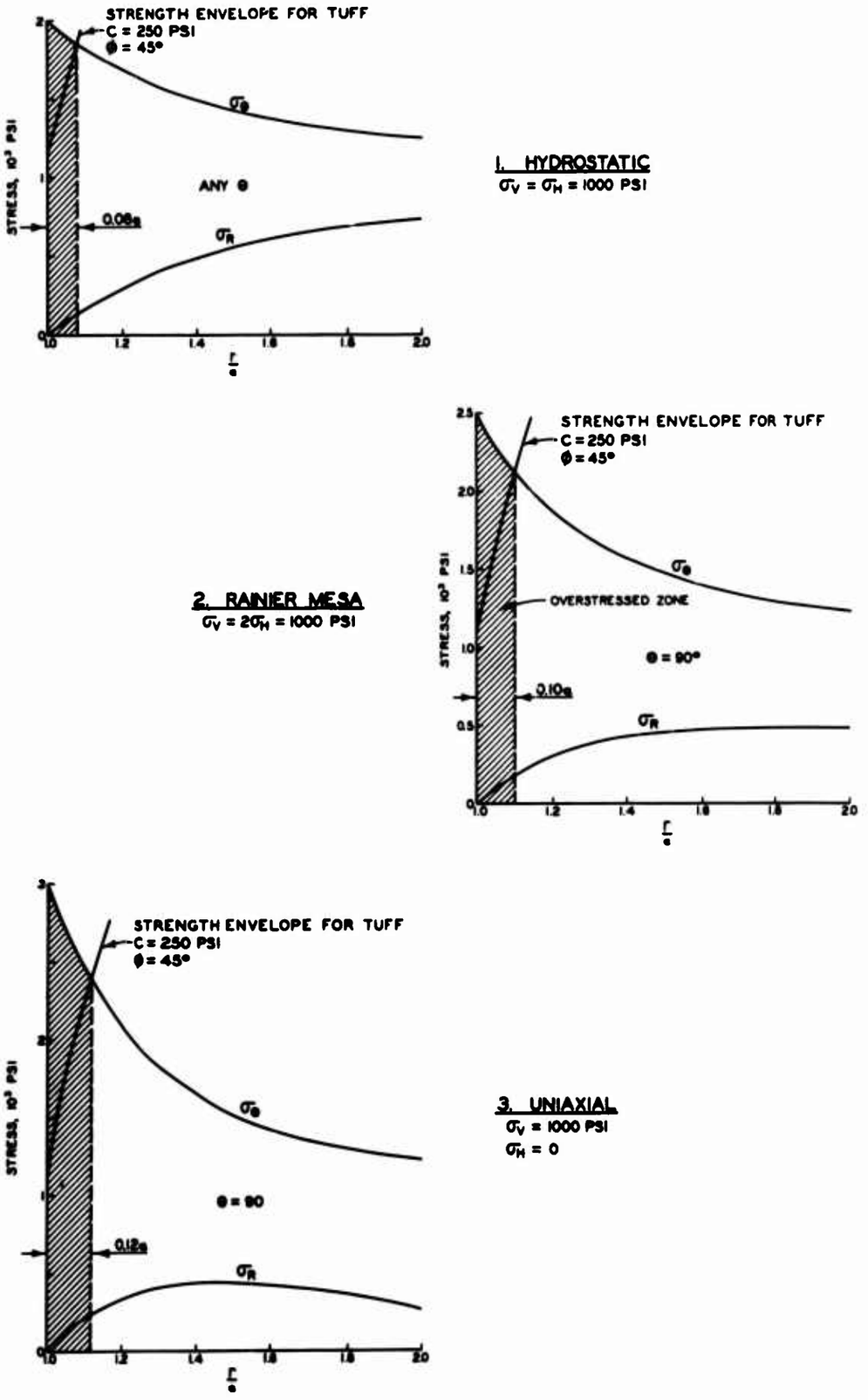

Fig. 41. Elastic stresses and overstressed zones along horizontal diameter of tunnel subjected to various ratios of vertical to horizontal natural stress

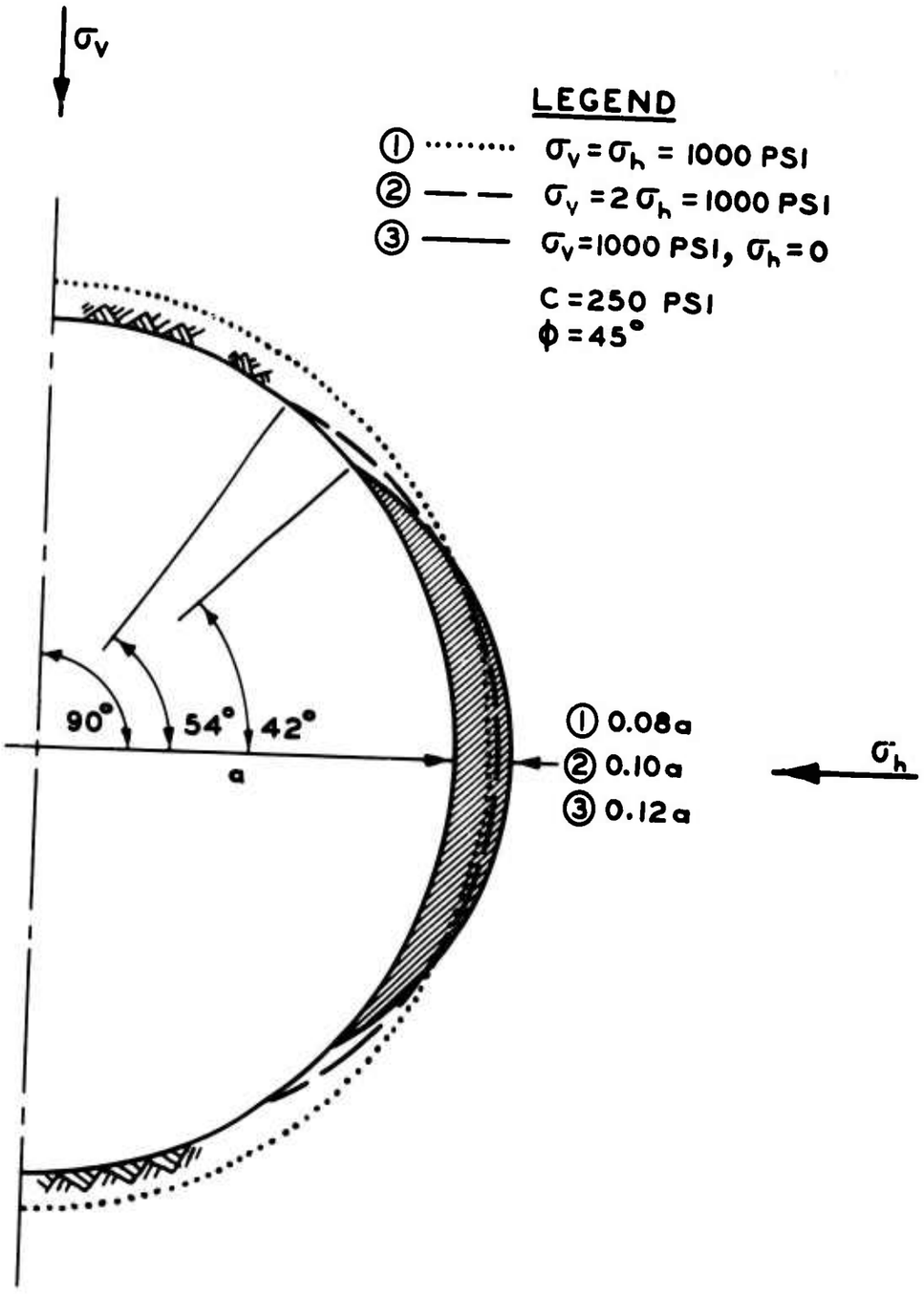

Fig. 42. Overstressed zones around a tunnel subjected to various ratios of vertical to horizontal natural stress

a vertical section of the nonsymmetrically shaped cavities in the tuff.

In the finite element method, the medium is approximated as a network of triangles. All stresses are concentrated as forces at the corners of the triangles. Continuity is maintained at the corners and along the edges of the triangles. Each triangle behaves as a continuum having elastic properties. As the mesh size is reduced, the solution for the entire network approaches a continuum solution.

The stiffness of each triangular element is determined by matrix methods. The stiffness of the entire mesh is then determined using an iteration process. At each mesh point, the computer solution gives values of stress and displacement.

Assumed Material Properties and Boundary Conditions

For the finite element approximation of the cavities in the tuff, it was assumed that the medium was elastic with a Young's modulus of 0.5×10^6 psi and a Poisson's ratio of 0.22. The natural vertical stress was 1000 psi and the horizontal stress was 500 psi. Both stresses were principal stresses. Displacements around the opening occurred as it was excavated in the previously stressed medium.

A vertical section through the plane face of the cavity was used to determine the inner boundary of the medium. Zero stress was assumed on this boundary. The medium extended 200 feet (approximately 4 radii) beyond the cavity surface and was assumed fixed at its outer boundary. The mesh consisted of approximately 300 triangular elements. The elements at the edge of the opening extended to a depth of 3.5 feet. Elements farther from the opening were larger.

The finite element solution used was for plane strain conditions; thus

the vertical section of the cavity was approximated as a long tunnel. Displacements determined by the plane strain solution are larger than those which would be obtained using a three-dimensional solution (as illustrated in Section 5.2). The depth at which displacements occur is also greater for the plane strain solution. The greatest error occurs in regions where the dimensions of the cavity in a direction perpendicular to the vertical section are small with respect to those within the section. This condition is most critical for the curved surfaces of the cavity, particularly the domed area at the top of the cavity. The plane strain solution is most appropriate when used in analyzing the conditions in the vicinity of the plane face of the cavity.

Displacements

Displacement contours are shown in Figs. 43 through 45 for three shapes which approximate the shapes of Cavities I and II during various stages of their excavation. Both the magnitude and direction of the displacements may be obtained from these figures.

To obtain the theoretical displacement of an extensometer at any given location in the cavity wall, the magnitude of the displacement in the direction of the extensometer must be determined from the displacement contour plots for the cavity shape of interest. The displacements which existed at the time of installation of the extensometer are determined in a similar manner. To determine the change in displacement, the initial displacement is subtracted from the final displacement.

The theoretical displacements in various portions of the cavity were determined by the method described in the preceding paragraph. Figs. 37, 46, and 47 show the theoretical displacement-depth relation at the center

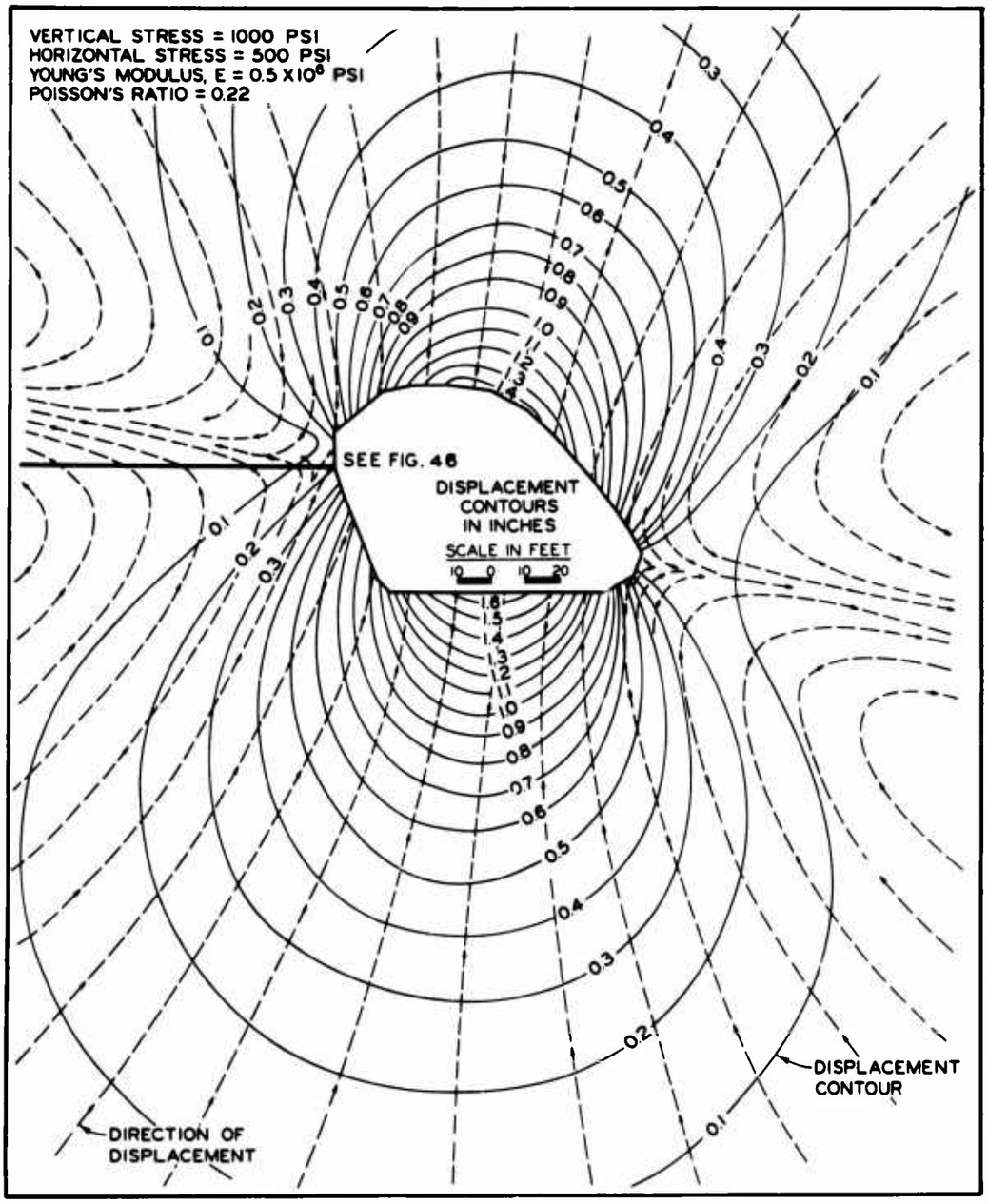

Fig. 43. Theoretical displacement contours for cavity height of 60 ft, elastic finite element solution

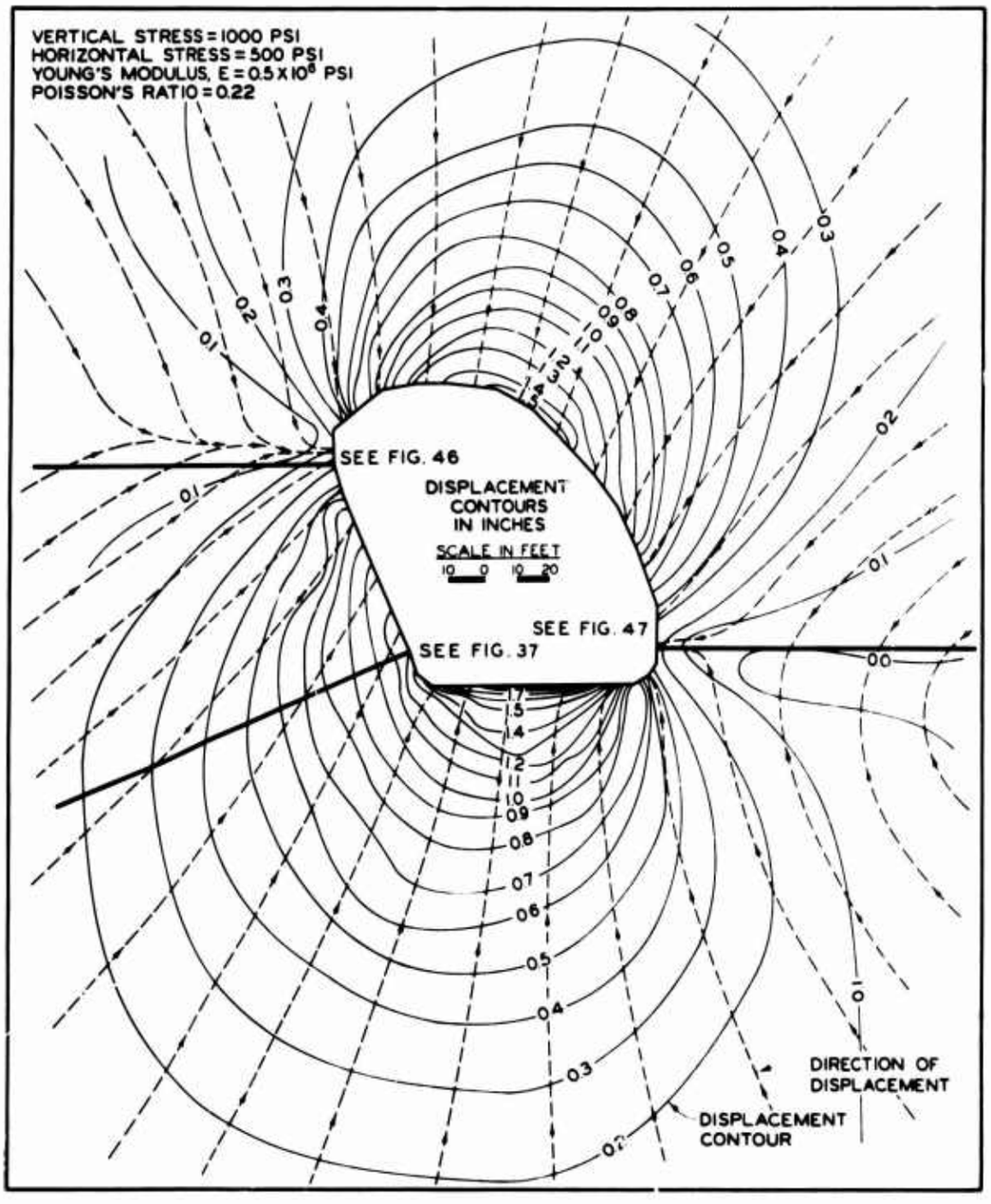

Fig. 44. Theoretical displacement contours for cavity height of 90 ft, elastic finite element solution

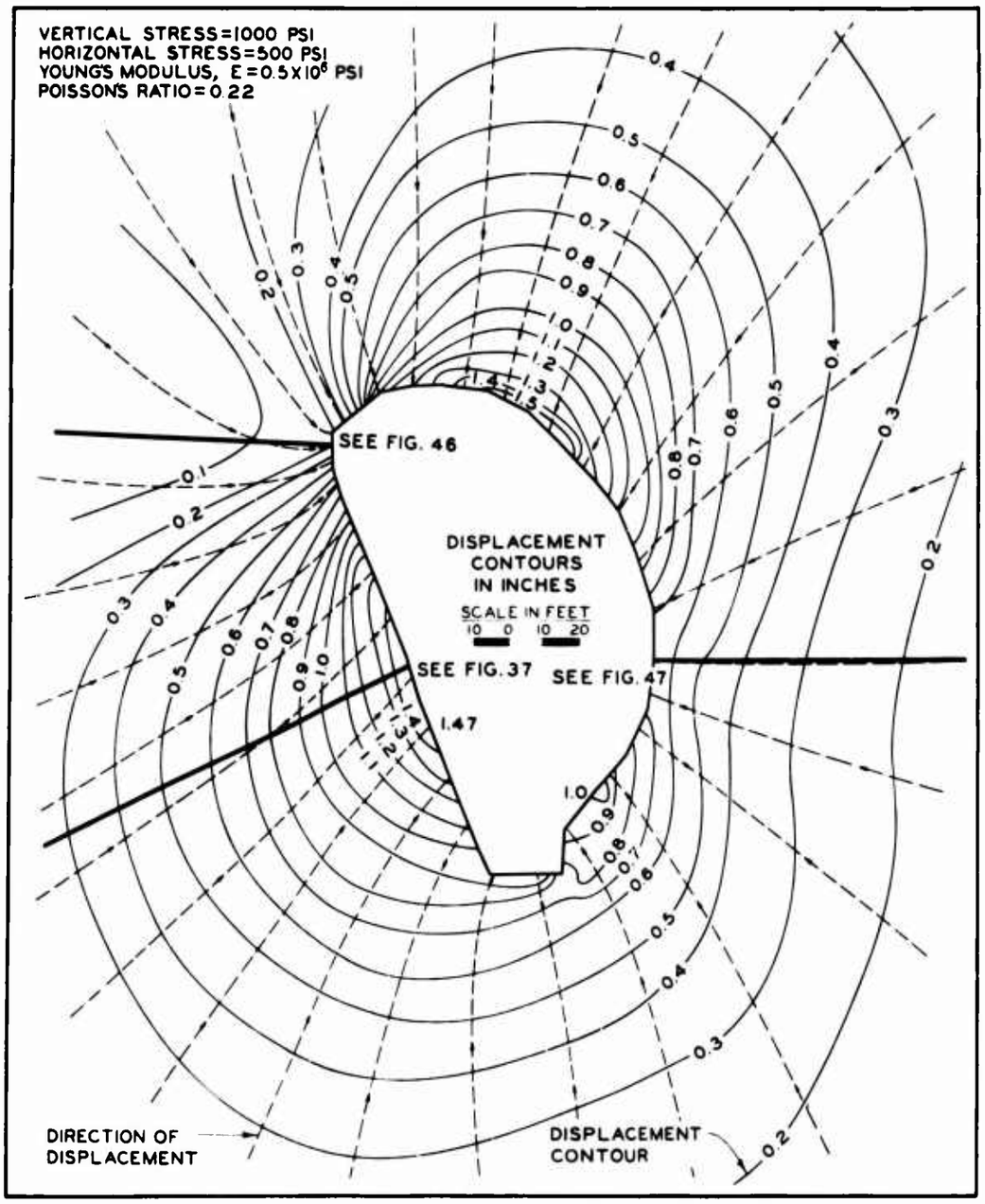

Fig. 45. Theoretical displacement contours for completed cavity (height = 148 ft), elastic finite element solution

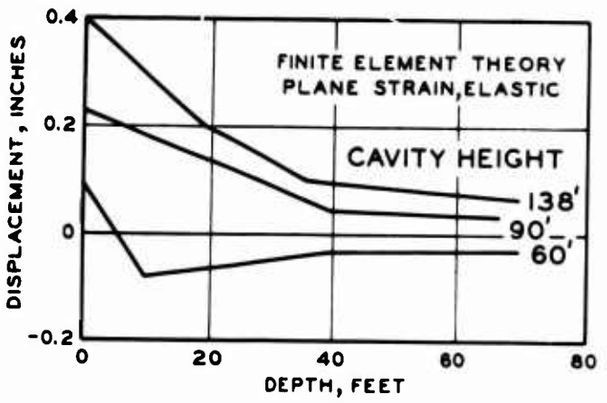

Fig. 46. Theoretical horizontal displacement-depth profiles, intersection of dome and plane face, elastic finite element solution

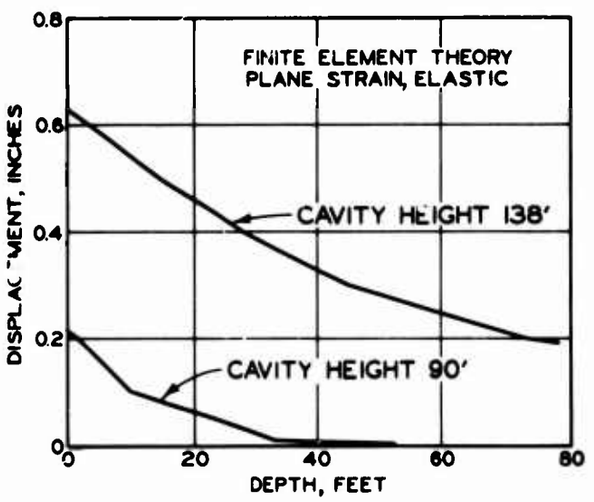

Fig. 47. Theoretical horizontal displacement-depth profiles, curved surface, elastic finite element solution

of the plane face, the intersection of the dome and plane face, and the curved surface, respectively. Displacements are termed positive if the direction of rock movement with respect to a given extensometer is toward the cavity. Recorded movements away from the cavity are termed negative.

In Figs. 43 through 45 it is apparent that the direction of displacement into the cavities tends to be parallel to the direction of the major principal compressive stress (in this case the vertical stress), and perpendicular to the longest dimension of the cavity. Thus, in Fig. 43 (cavity height: 60 feet), the direction of the displacements is predominantly vertical, while in Fig. 45 (cavity height: 138 feet) the longest dimension is vertical so that the direction of the displacements is shifted toward the horizontal.

The theoretical vertical displacements in the dome appear to be proportional to the maximum horizontal span width of the cavity. When the maximum horizontal width is reached (at a cavity height of 60 feet) the displacement in the dome is 1.4 inches. Further excavation causes no further increase in the horizontal width, and there is no further increase in the displacements in the dome: it is still 1.4 inches when the cavity is completed.

Theoretical displacements are lowest at the sharp corners of the cavities. In Fig. 43, the horizontal displacements at the intersection of the plane face and the dome are slightly negative at or near the surface. They become increasingly negative to a horizontal depth of 10 feet, where they then begin to approach zero with increasing depth (Fig. 46, cavity height: 60 feet). Further excavation causes the rock at this location to move

inward again (Fig. 46, cavity heights: 90 and 138 feet).

Positive movements would be smaller and negative movements more pronounced for a true three-dimensional solution. This fact has been used in discussing the movements observed on the curved surface and at the intersection of the dome and plane face of the cavity.

Stresses

Principal stresses are contoured in Figs. 48 and 49 for the completed cavity shape (138 feet high). Principal stress directions are shown in Fig. 48 as dashed lines. Values for the tangential stress concentration at the walls of the opening may be obtained from the major principal stress contours, Fig. 48. The maximum elastic stress concentrations occur at the intersection of the dome and plane face, where the stress concentration is 2.7 times the vertical stress. A stress concentration of 1.8 occurs on the curved surface, and 1.7 in the bottom of the cavity. A low stress concentration (0.6) occurs on the reentrant near the bottom of the cavity. The stress concentration over most of the plane face varies from 0.8 to 1.4. These concentrations exceed the strength of the tuff and would not occur in the real cavity; yielding or fracture of the shallow rock would occur with a resulting redistribution of the stress.

Although the major principal stresses are high at depth behind the sharp corners of the cavity, the minor principal stresses (Fig. 49) are also high; therefore, the rock is not overstressed at depth behind the corners. On the long, plane surfaces, however, the minor principal (essentially radial) stresses are quite low at depth, so that slight concentrations of the tangential stresses will cause overstressing to fairly large depths. The medium around the opening is subjected to a changing

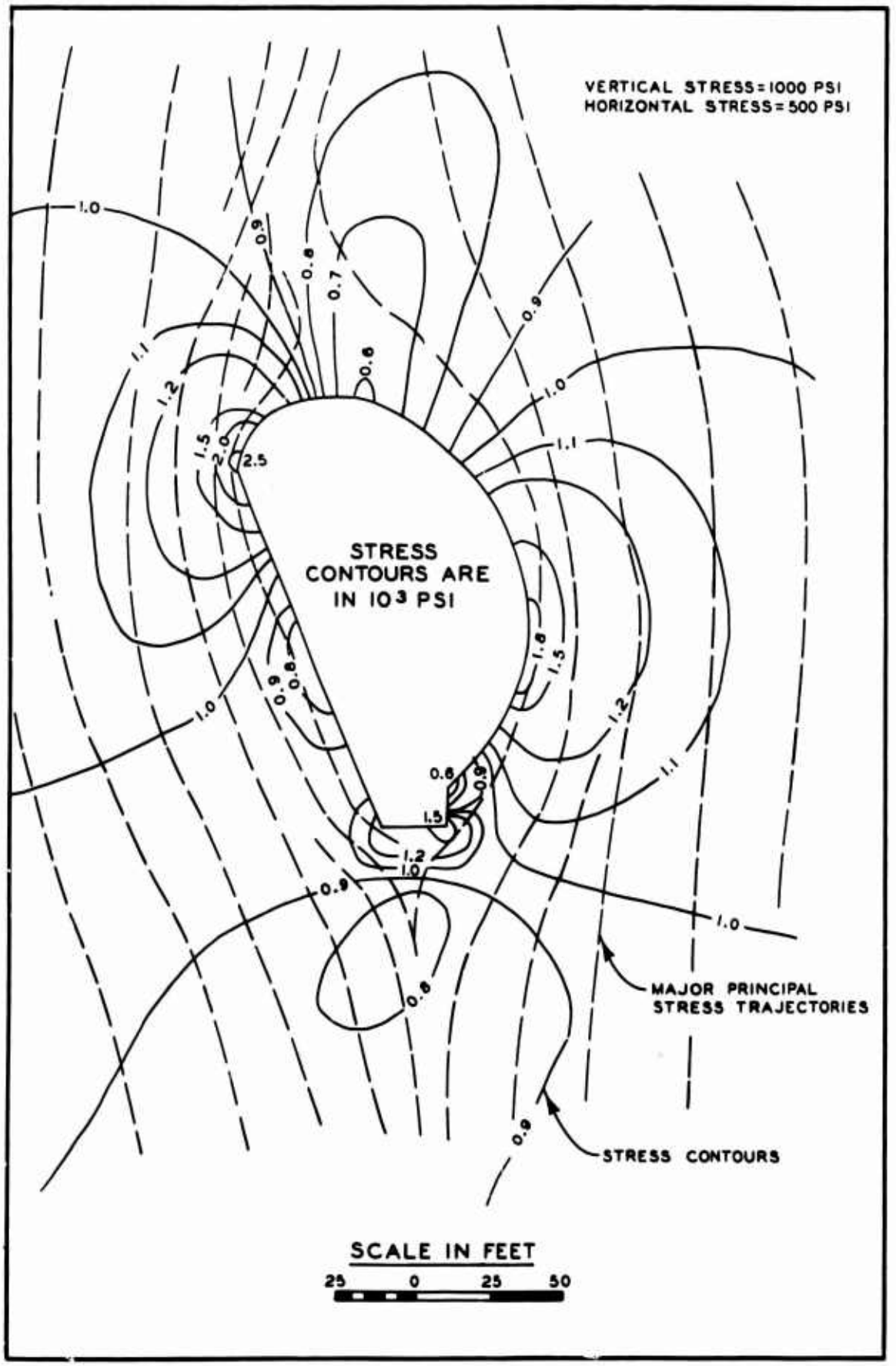

Fig. 48. Major compressive principal stress contours around completed cavity, elastic finite element solution

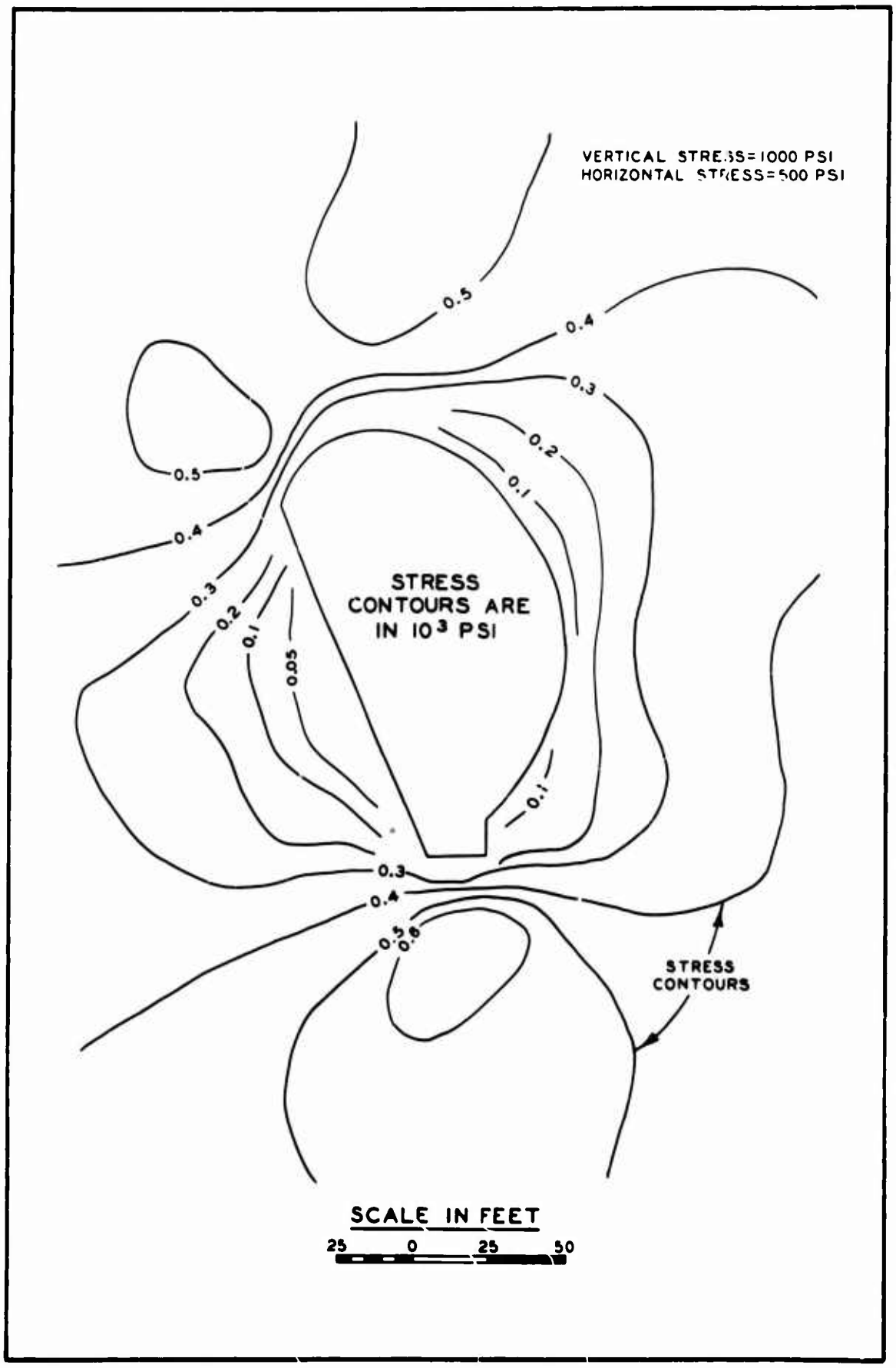

Fig. 49. Minor compressive principal stress contours around completed cavity, elastic finite element solution

stress field as construction proceeds downward, so that overstressing (or failure, for a real material) may occur at an earlier stage of excavation.

5.4 DISCUSSION OF OBSERVED DISPLACEMENTS IN THE CAVITIES IN TUFF

Three types of displacement were typically observed in the cavities (Fig. 50). The first was the elastic displacement occurring due to removal of internal support by excavation. These displacements were on the order of 0.2 to 0.5 inch and were directly related to changes in cavity size. They usually had the same magnitude as the predicted elastic displacements; however, more of the observed displacement was concentrated within the first 10 feet from the surface than would be predicted from elastic theory. The increased shallow movement can be accounted for by assuming that the shallow zone has a lower modulus as a result of slight cracking and loosening of the near-surface rock.

The second type of observed displacement was shallow and discontinuous. The displacements were not directly related to cavity excavation, but developed with time from the essentially elastic displacements described previously. Displacements of 1 to 2 inches occurred which were concentrated within the first 5 feet from the surface and were usually caused by opening of a single crack at the base of a shallow slab. The condition was most common in the vicinity of rock protrusions in the dome of the cavities. Although the rock bolts in the dome were capable of supporting the rock load, they were spaced far enough apart that loosening of slabs between the bolts and cracking of slabs beneath the bearing plates could occur. The shallow displacements were indicative of a gradually developing unstable situation which was easily corrected by placing a 2-inch layer of gunite in the slabby rock zones.

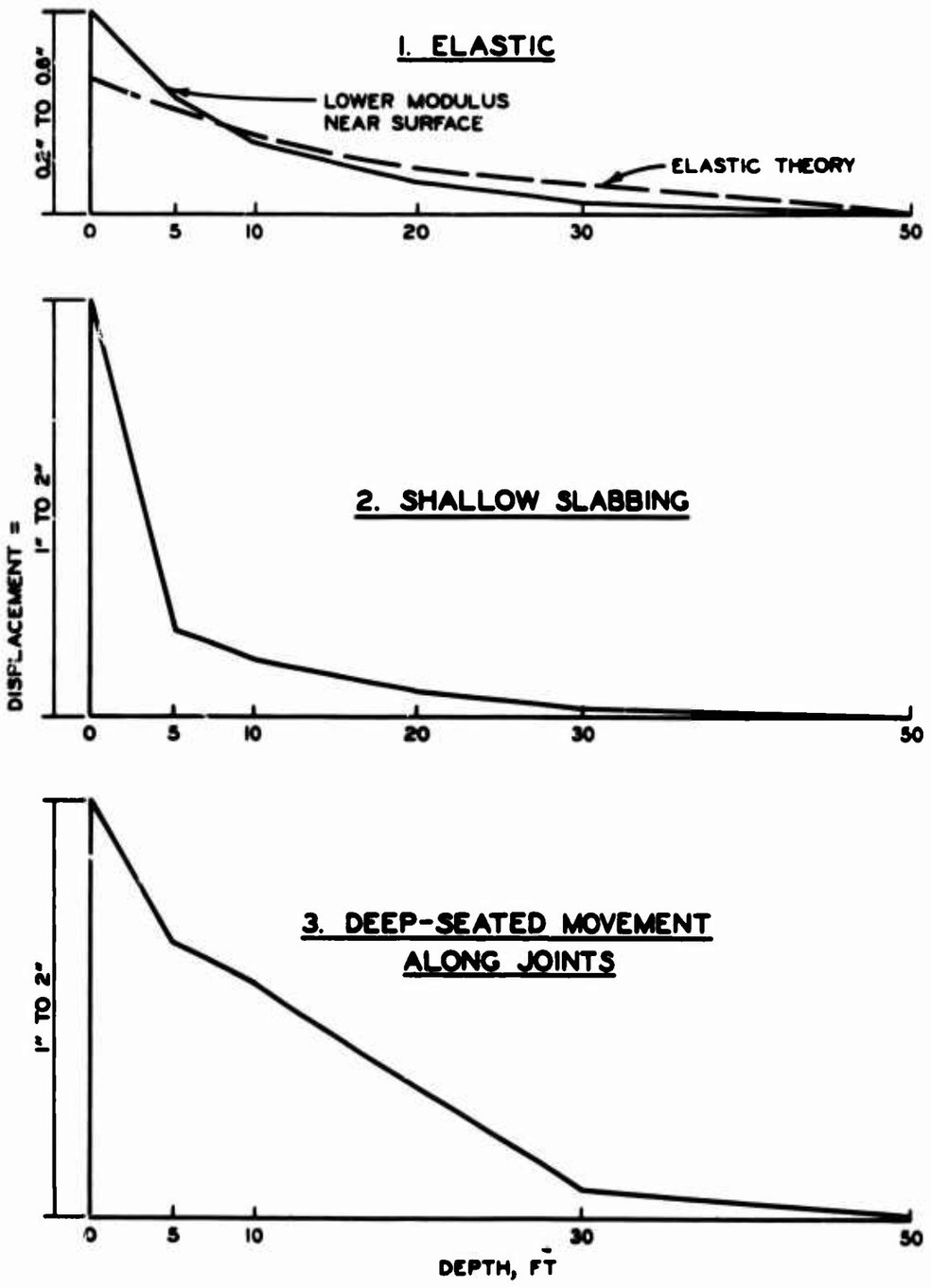

Fig. 50. Typical displacements in Cavities I and II

The third type of observed displacement was deep-seated and discontinuous. The displacements were 1 to 2 inches in magnitude and were concentrated along joint planes at depths from 10 to 30 feet over large areas on the plane face of Cavity II. The displacements were large with respect to continuum theory, and they showed an increasing rate with respect to time and stress; thus they satisfied the criteria for instability. Breaking of 11 bolts over a 2-day period also indicated that the stability of the plane face was rapidly decreasing. It was apparent that the rock-bolt support on the plane face was inadequate. A large number of long rock bolts were added and the face immediately stabilized.

The rock movements observed at different locations in the cavities are discussed in more detail in the following paragraphs.

Dome (A)

Extensometer I-A-1, located on a 3-foot-thick protrusion in the dome of Cavity I, showed the typical behavior for extensometers in the dome of the cavities. The predicted and measured displacement-time relations are compared in Fig. 51. The displacement-depth relations are shown in Fig. 52.

In the first two months after installation of the extensometer, the measured and predicted displacements were quite comparable. The change in displacement was proportional to the change in the average width of the cavity, and the measured displacement-depth distribution approximated the elastic distribution.

After this period, large displacements occurred, even though there was no further increase in the cavity diameter. (The finite element solution predicted that no further deflection in the dome would occur after the

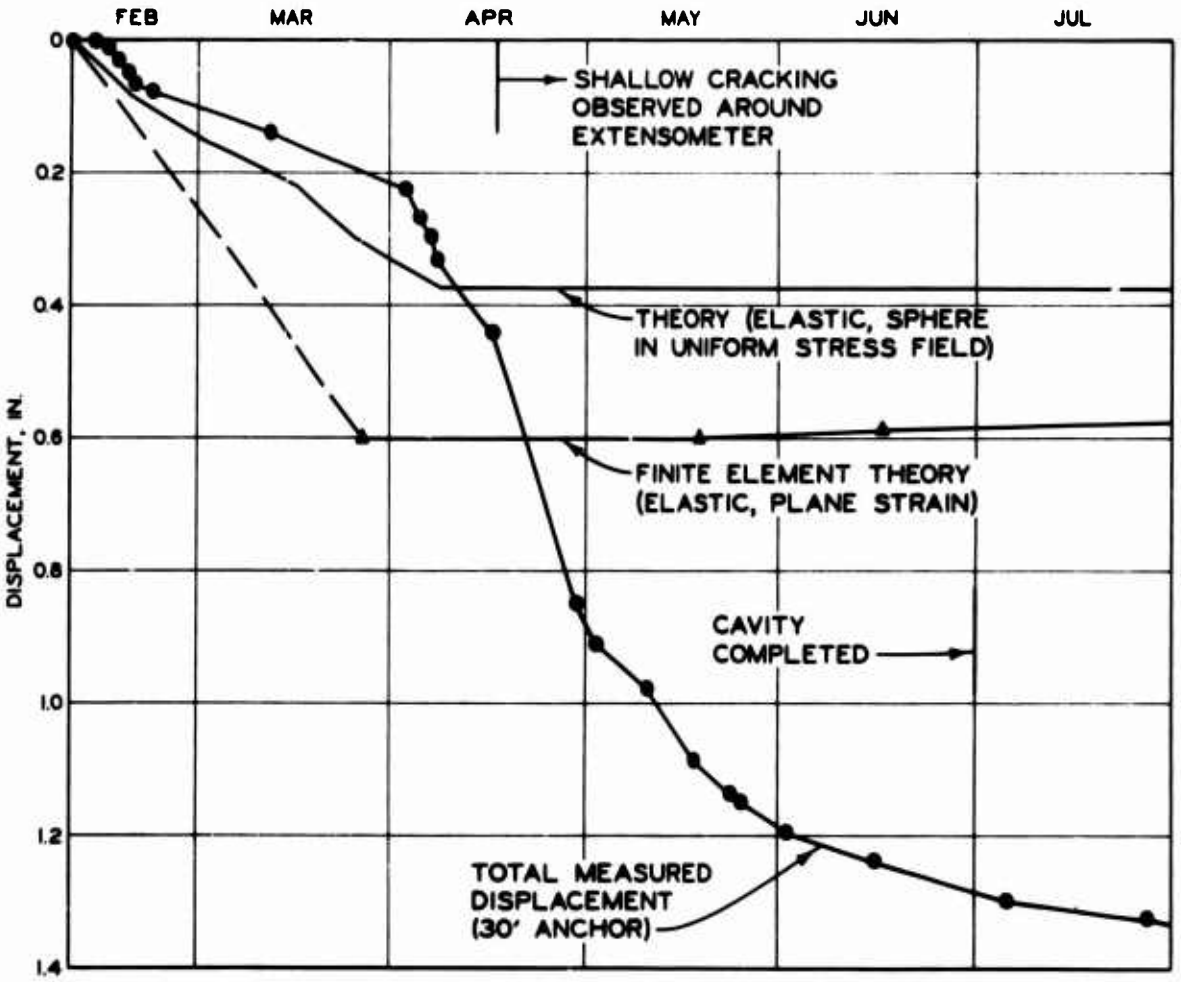

Fig. 51. Typical displacement-time relations in dome of Cavities I and II; extensometer I-A-1

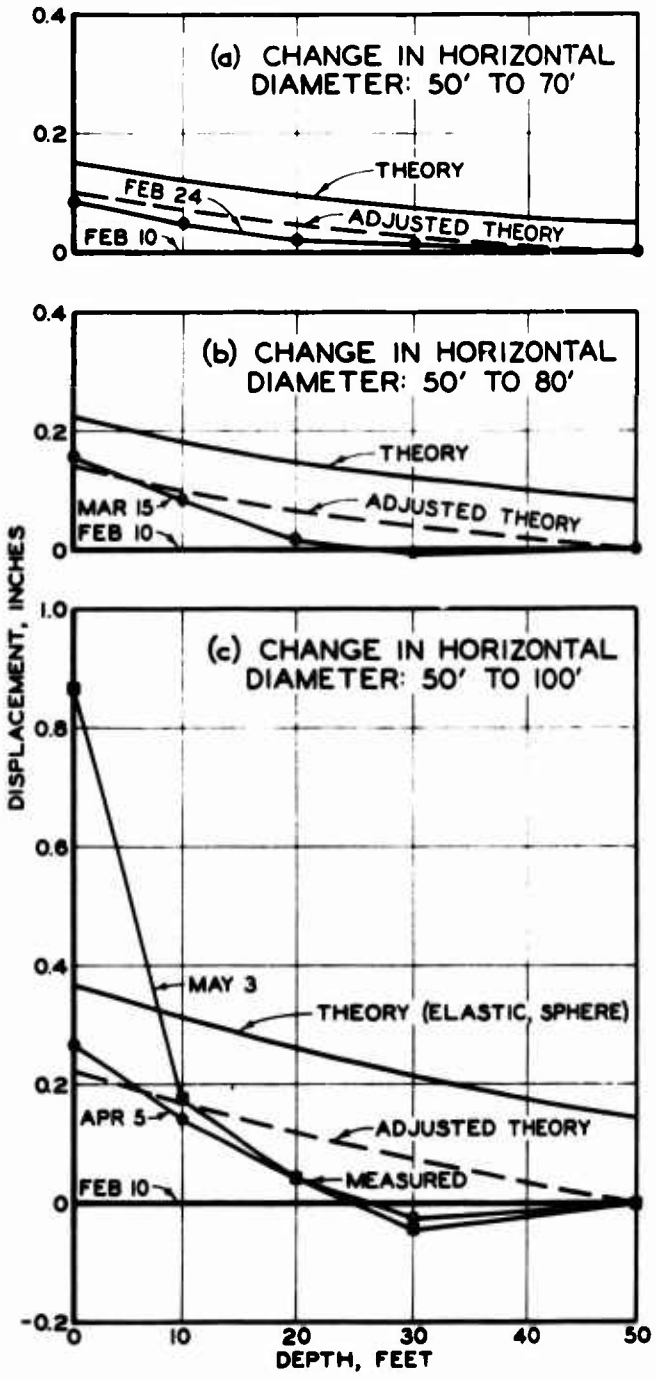

Fig. 52. Typical displacement-depth relations in dome of Cavities I and II; extensometer I-A-1

cavity height had reached 60 feet. At this height, the maximum cavity width was reached.) The continued movement (April 5 to May 3) was concentrated in the first 10 feet from the surface of the cavity.

At this time, it was discovered that hairline cracks were forming on the rock surface in the vicinity of the extensometer, and an extension fracture previously formed at the base of the protrusion was beginning to open. It was apparent that the continued rock movement was concentrated within the first 3 feet from the cavity surface and was caused by opening of the extension fracture. The continued movement was not due to creep of the intact portion of the rock mass.

The bolts which were spaced on 3-foot centers in the vicinity of the extensometer were considered adequate for continued support of the slab and no remedial measures were carried out at this time. During May, the rate of movement began to decrease. By August, however, cracking and slabbing of the near-surface rock throughout the dome of the cavity had proceeded to the point that the bearing of the rock-bolt bearing plates was endangered. Gunite was placed in the dome of the cavity at this time to prevent further drying and disintegration of the rock slabs.

In Figs. 52a and 52b, the measured displacement curve is steeper than the elastic displacement curve in the shallow zone. This indicates that the shallow rock has either (1) deformed plastically, (2) a decreased modulus at the lower confining pressures (near the surface), or (3) cracked and thereby become a new material with a lower modulus. Slight cracking of the material appears to be the most logical explanation of the decreased modulus because (1) the stress-strain curve for the tuff is reasonably linear to failure, indicating that significant plastic deformation will not occur prior to cracking;

(2) the change in modulus due to confinement does not appear to be very large, according to the results of triaxial tests performed on dried specimens (Obert, 1964); (3) extension fractures were observed to form immediately upon excavation; therefore, a decrease in the shallow rock modulus would be expected, even though extensive opening of these fractures does not occur when the rock is properly bolted. Slight cracking at depth (beyond the low-velocity zone) was also indicated by the measured deep refraction velocities which were lower than the directly propagated velocities (measured in undisturbed rock away from the cavity)(Section 4.4).

Extensometer I-A-1 also illustrates a condition observed with various extensometers located in both cavities. Movements between the 30- and 50-foot anchors were very slight. Figs. 52a and 52b show that the 30-foot anchor had displaced into the cavity a very slight amount more than the 50-foot anchor; in Fig. 52c, it can be seen that the 30-foot anchor moved away from the cavity with respect to the 50-foot anchor. The small movements between the deep anchors seem to indicate that the deepest (50-foot) anchor was at sufficient depth to be unaffected by the cavity excavation and could therefore be assumed fixed. However, the theories used in analyzing the cavity displacements predict significant elastic displacements at the depth of the 50-foot anchor. The apparent discrepancy could not be resolved, because of the difficulty involved in measuring small displacements over large distances, at large depths.

It is possible that the outward (negative) displacements of the 30-foot anchors with respect to the 50-foot anchors resulted from a local flattening or reversal of the slope of the displacement-depth curve which could not be predicted from the simple elastic theory. Figs. 46 and 47

provide some basis for this argument: at certain locations and depths around the cavity, the more complex finite element theory predicts flat and, in some instances, negative slopes for the displacement-depth relation.

To properly compare the elastic and measured displacements, the curves should be fitted at the 50-foot depth. The adjusted elastic curve is shown as a dashed line in Fig. 52.

Intersection of Dome and Plane Face (B)

A horizontal extensometer was installed in the cross drift at the top of the raise in Cavity II, prior to excavation of the dome. During the enlargement of the cross drift, when the cavity shape approximated a flat ellipsoid, a maximum negative displacement (away from the opening) of approximately 0.02 inch was recorded by the extensometer. After the dome had been opened and excavation was proceeding downward, no further movements occurred. The theoretical displacements at this location, determined from the plane strain finite element theory, are also negative during the initial stages of excavation (Figs. 43 and 46). However, with increasing excavation, positive movements are predicted. A three-dimensional solution would more closely approximate the geometry at this location and would predict more negative movement and little, if any, positive movement. The displacement-time relation for the 50-foot anchor of extensometer I-B-1, located below the dome on the plane face of Cavity I, is shown in Fig. [illegible]. The extensometer was placed after the cavity had been excavated 30 feet below the intended gage location; therefore, much of the initial elastic movement (which may have been negative) was not recorded. Small positive displacements (0.04 inch) were recorded following installation of the extensometer, as excavation of the cavity continued. Approximately

0.2- to 0.3-inch displacement is predicted from the plane strain, finite element solution for the same period. At the intersection of the dome and plane face of both Cavities I and II, the extensometer movements ceased soon after the excavation in the vicinity of the extensometers had been completed. Positive movements due to loosening of slabs did not occur in either cavity, even though predicted stress concentrations were high at this location. Some fracturing due to the high stress concentrations undoubtedly occurred near the surface; however, the minor principal stress builds up rapidly behind a sharply curved surface such as this, so that the stress difference at depth is small and fracturing is therefore confined to a very shallow depth. The sharp radius of curvature of the surface forms an arch which, in combination with the rock bolts, keys the rock blocks and permits the rock to support itself.

Curved Surfaces (C)

Displacements measured on the curved surfaces were less than 0.2 inch in Cavity I. The larger movements (0.4 to 0.6 inch) in Cavity II were at shallow depth and probably associated with shallow slabbing. The finite element theory predicts approximately 0.35-inch displacement within the first 50 feet from the surface (Fig. 47) for extensometers installed after the cavity has been excavated to 90 feet. The finite element theory also indicates that some negative movements occur on the curved surfaces (as shown in Figs. 43 and 44). Negative movement is most likely to occur when the excavated floor is near the extensometer. There is an even greater possibility of negative movement for the three-dimensional case.

Two extensometers installed on the curved surface, near midheight of Cavity I, showed erratic and slightly negative movements as excavation

proceeded. Subsequent movements were slightly positive--and still erratic. A three-dimensional, elastic theory would probably predict very small--almost zero--displacements in this portion of the cavities.

There was no extensive loosening of the near-surface rock on the curved surfaces of the cavities, and movements did not continue after construction was completed. The seismic refraction survey also showed that slabbing and fracturing on the curved surfaces of the cavities were not extensive.

Plane Face (D)

Cavity I. In Fig. 53 the measured displacement at the center of the plane face of Cavity I is compared with the elastic finite element solution. The theory predicts that approximately two-thirds of the rock movement will occur at depths greater than 30 feet (the length of most of the extensometers on the plane face). However, the theoretical and observed movements within the first 30 feet are quite comparable: the displacement of the 30-foot extensometer is 0.1 inch and the slope of the displacement-depth curve is approximately uniform to a depth of 30 feet. There is very little evidence of increased displacement near the surface which would indicate the presence of a cracked zone having a low rock modulus. There was also very little evidence of slabbing or opening of extension fractures in the vicinity of the extensometers on the plane face. However, the seismic survey did not indicate that the fracturing was less prominent on the plane face: along the seismic lines located in the vicinity of the extensometers, the average depth of the low-velocity zone was as deep as in other areas of the cavity.

Movements were measured at various points along the horizontal

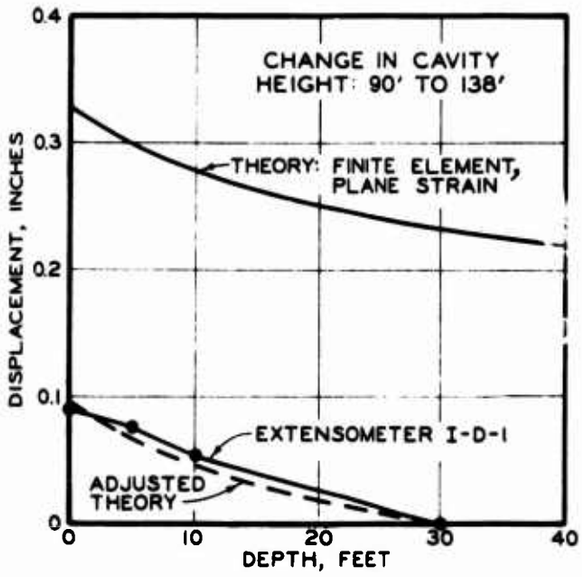

Fig. 53. Typical displacement-depth relations at center of plane face, Cavity I

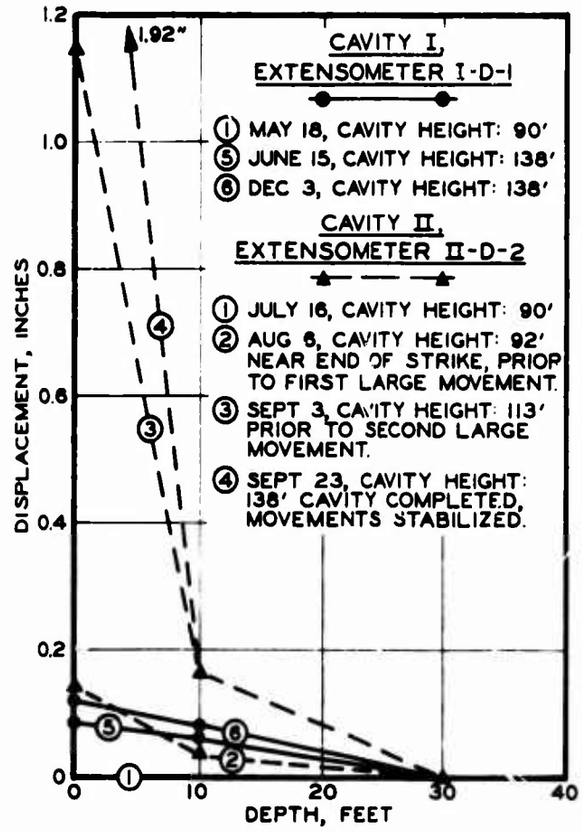

Fig. 54. Typical displacement-depth relations at center of plane face, Cavities I and II compared

diameter of the plane face of Cavity I. Most of the movements were of the same magnitude as the typical movement shown in Fig. 53. Extensometers which were placed near the edge of the plane face (approximately 20 feet from the curved surface) showed the same amount of movement as the extensometers near the center of the plane face. Decreased movement near the edge of the plane face due to restraint of the curved surface was not observed.

Movements on the plane face in Cavity I were essentially elastic and showed very little evidence of either shallow slabbing or deep-seated, discontinuous movement.

Cavity II. It is apparent from Fig. 54 that movements on the plane face of Cavity II were much larger than the movements observed in Cavity I. Large, discontinuous movements of approximately 1 to 2 inches were recorded by all the extensometers located on the plane face of Cavity II. (The displacements at three locations on the plane face of Cavity II are compared with the construction history in Fig. 23.) The first large movements occurred at the end of the strike (August 10) when the lower friable white tuff bed was exposed on the plane face (bedding plane 2, Fig. 12). Additional bolts were placed across the joints (joint set No. 1) on the upper left side of the face, and the rate of movement decreased.

A month later (September 10) the rate of movement again increased. At this time, approximately 25 feet of rock remained to be excavated from the plane face. Portions of the cavity floor had been broken through to the main tunnel. A crack opened along a friable white tuff bed in the upper left portion of the cavity (bedding plane 1). The rock above the bed displaced 1 inch along the bedding plane, into the cavity. Twelve bolts

broke and many bearing plates dished on the left side of the cavity. Vertical en echelon shear zones developed along the left edge of the plane face, at the contact with the curved surface of the cavity. The estimated depth of the unstable area is illustrated in Fig. 12. The instability encompassed a large volume of rock and was definitely deep-seated.

Large, relatively deep movements were recorded by all the extensometers on the plane face, indicating that the local instabilities on the left side of the face were affecting the stability of the entire face: some of the movement was concentrated within the first 10 feet; much of the movement was concentrated between 10 and 30 feet. Extensometer II-C-1, located just outside the shear zone on the curved surface, showed no excessive movement, indicating that the instability of the plane face had not affected the curved surface of the cavity.

To stabilize the face, excavation was halted and the left side of the plane face was heavily reinforced with approximately 200 rock bolts, 48 feet in length, placed on 3-foot centers. The movements stabilized as soon as the additional bolts were placed.

Several factors affected the stability of the plane face. The primary cause of the instability was the presence of joints and bedding planes which formed isolated wedges of rock on the plane face. The plane faces of both Cavities I and II were supported with 24-foot bolts on 6-foot centers; however, the face of Cavity I was stable while Cavity II was unstable. The only difference between the two cavities was the nature of the jointing. Cavity I had very few joints while Cavity II had joints oriented subparallel to the face of the cavity so that thin wedges of rock were isolated at the surface.

Another factor affecting stability was the large plane surface of the cavity. There was no curvature on the plane face to provide the keying support which helps prevent opening and movement along extension fractures and joints; therefore, there was a tendency for buckling of the rock on the plane face. Joints on the face accentuated this condition by isolating slabs of rock and reducing the restraint provided by the coherence of the rock mass.

The delay in construction due to the 2-month strike may also have contributed to the instability of the plane face. At the time of the strike, bolting was completed on the walls of the cavity but no bolts were supporting the floor of the opening. The long delay may have allowed loosening and gradual failure of the rock in the bottom of the cavity, so that, when the strike was over and excavation was resumed, these loosened zones were intersected by the face of the cavity and failures began to occur.

Finally, bolts on the plane face of the cavities were placed on 6-foot centers while those on the curved surfaces were placed on 3-foot centers, even though the plane face was the more critical condition. The plane face of Cavity II stabilized when the number and the length of the bolts were increased.

5.5 DISCUSSION OF FRACTURING AND FAILURE IN TUFF

Applicability of Elastic-Plastic Theory to Rock Behavior

Basic to a continuum theory, such as the elastic-plastic theory described in Section 5.2, is the assumption that the material maintains its continuity throughout its loading history. In an elastic-plastic medium an element which reaches its yield stress will behave plastically until unloaded, when it again becomes elastic. Throughout the loading and

unloading process, the material maintains its continuity. Continuum theory does not account for the possibility of the discontinuous, sometimes catastrophic, behavior which is typical for most rock masses stressed to failure. Most highly stressed rock masses do not yield plastically; rather, they fail by the formation of new fractures or by movement along preexisting fractures. During the process of fracturing and loosening, the material properties of the rock mass are changed: both the strength and the modulus are decreased. (Changes in the deformation modulus are discussed in Section 5.4.)

In most cases, an unsupported rock mass around an opening cannot yield (or fail) and still maintain its continuity. Once the failure process is initiated, discontinuous movements begin to occur, which, if allowed to continue, may result in the instability of large portions of the opening. However, if large discontinuous movements and gross failures are prevented by proper support of the opening, a continuum theory may closely approximate the behavior of a real rock mass; the formation of fractures and the movement along fractures are then considered to be part of the yielding process.

Therefore, by assuming the proper material properties for both the undisturbed rock mass and the fractured, near-surface rock, continuum solutions may be used to aid in evaluating the behavior of real rock materials. One of the difficult steps in the problem, however, is determining the properties of the near-surface, fractured rock. It is apparent that these properties will not only be determined by the characteristics of the rock mass--its intact strength and modulus, and its in-situ joint characteristics--but by the boundary conditions imposed during construction--

primarily, by the nature of the support system. However, if the effect of the support system upon the rock mass were known it would not be necessary to resort to a theoretical solution. Thus, the problem appears to be one without a simple, determinate solution. Because of the indeterminacy of the problem and the dependence of the behavior upon construction details, field observation of real rock behavior is necessary to provide an understanding of the problem. Theoretical studies, although limited, do provide further insight into the problem by defining the parameters and basic relations for certain limiting conditions of rock behavior. Simple rock models may also aid by providing a means of observing failure modes which cannot be predicted from theory.

Jointed Rock Model

The results of direct shear tests performed by Patton (1966) on saw-toothed and square-toothed Kaolin-plaster models are useful in illustrating the behavior of a jointed rock mass. Some conclusions as to the effectiveness of rock support procedures may be obtained from these tests.

The strength envelope for a jointed rock mass should fall somewhere between the strength envelope for an intact specimen and the strength envelope for a smooth joint plane. The actual position of the strength envelope between these two limits depends on a number of variables which were investigated with the simple joint models and are discussed in the following paragraphs.

Fig. 55a shows typical shear force-displacement curves for a sawtooth joint model tested at three different normal loads, N_1 , N_2 , N_3 . For the test performed with the normal load equal to N_3 , the shear force built up to a peak, and then a brittle failure occurred through the base

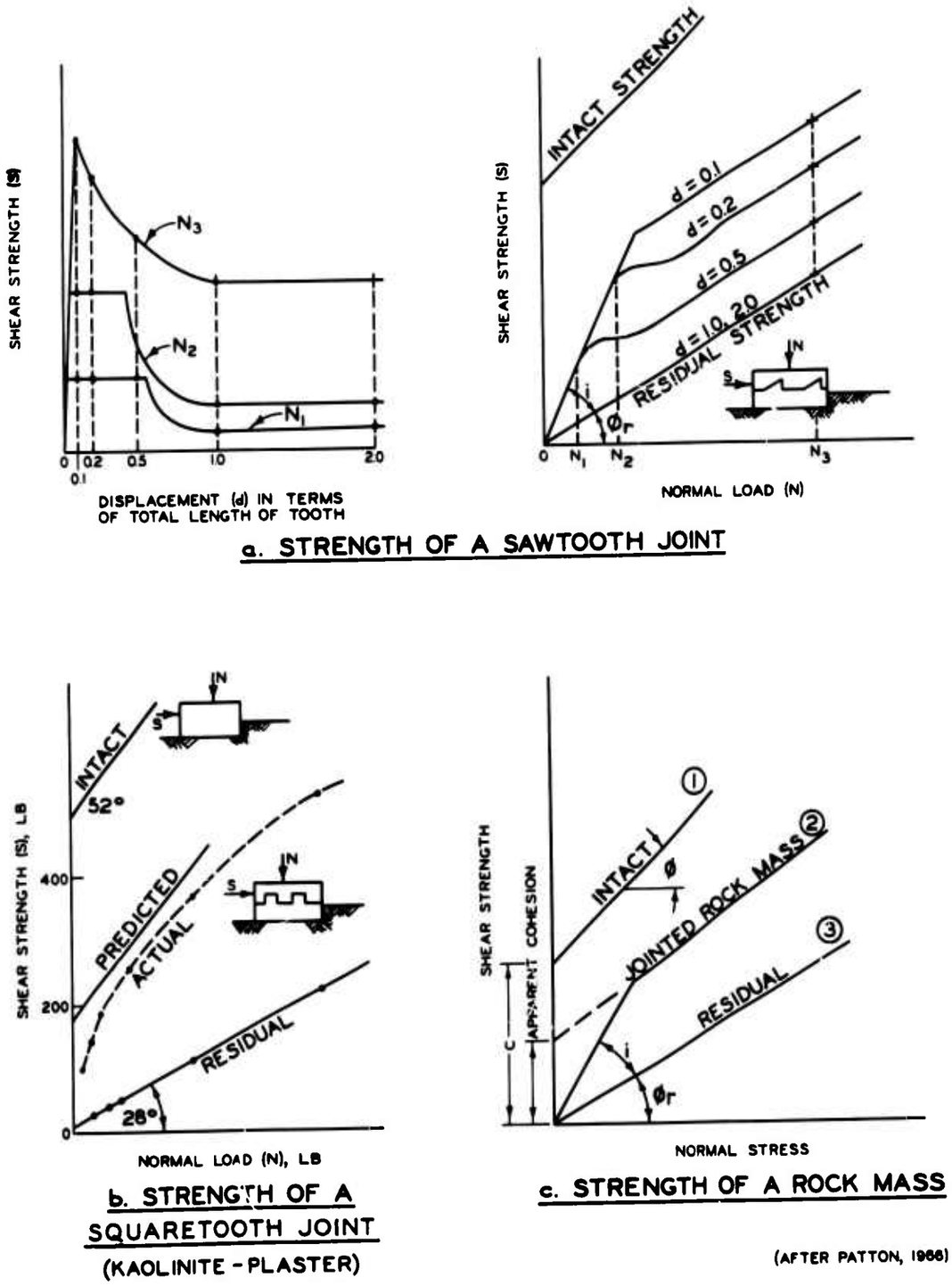

Fig. 55. Effect of joints on strength of rock mass

of the tooth. With continued displacement, irregularities along the joint plane were removed and the strength was reduced to a residual value equal to the strength along a plane surface. For the other tests, the normal forces N_1 and N_2 were low enough that sliding up the tooth occurred under a constant shearing force, before the tooth was sheared off; therefore, these shear force-displacement curves exhibited a mesa-like peak before the strength dropped to its residual value.

The corresponding strength envelopes for various displacements are shown in the shear strength-normal force diagram of Fig. 55a. The angle i is the angle of inclination of the tooth; it produces an apparent increase in the angle of friction for the jointed material when riding up the tooth occurs. When the normal forces are high enough to shear the tooth, the envelope breaks over. In this portion of the curve, the material has a lower angle of friction, but a high value for the apparent cohesion intercept. After the material has reached its ultimate strength, further displacement causes a reduction in the apparent cohesion intercept. With continued displacement, the strength envelopes are reduced until they match the envelope for a plane joint surface.

Several conclusions on the strength of a jointed rock mass can be drawn from this figure. It is apparent that as displacements become large, the interlock is sheared off and the strength is reduced. The experience in underground construction verifies this conclusion: the sooner adequate supports are placed, the less chance that failure will occur. If supports are not placed properly, large displacements often occur and interlock of the rock blocks is lost. The remedial support required to maintain the

stability of this partially failed mass is often much greater than the support required to prevent the initial failure.

In Fig. 55a, the displacements along the shear plane are not in terms of the total length of the shear plane (a shearing strain) but are in terms of the joint irregularity--in this case, the total length of the sawteeth. This is the only appropriate way of normalizing the displacements. Very large displacements may occur before a large irregularity will shear off, but a small irregularity may shear off or be overridden at such a small displacement that it may have little or no practical effect on increasing the shear strength of the rock mass. One of the problems in designing a support system is in determining that the system is rigid enough and strong enough to prevent excessive loss of interlock. This requires a knowledge of the joint characteristics.

At low normal loads, an interlocking, jointed rock mass will have a very high angle of friction but no cohesion. At higher normal loads (or confining pressures) the rock mass can be treated as having an apparent cohesion intercept, and a lower angle of friction. The value chosen for the apparent cohesion intercept is dependent on the amount of displacement which the rock mass is capable of undergoing throughout the life of the project. This depends to a large extent on the boundary conditions of the problem. Patton (1966) describes the behavior of a large number of natural rock slopes in the Western United States which have bedding planes parallel to their slope. He concluded that the stable slopes were inclined at angles only one or two degrees greater than the residual angle of friction (ϕ_r) along a bedding plane. The broad, low-angle irregularities along the

bedding planes provided some additional resistance to failure, but the short, steep irregularities were progressively sheared and overridden and therefore provided no long-term resistance to failure. Patton refers to the zone intermediate between the intact and residual envelopes as a zone of unstable equilibrium. For an underground opening, however, the geometry is such that a relatively small amount of internal support can

maintain the strength of the rock mass above its residual joint strength. Stability may therefore be achieved in this zone of unstable equilibrium.

Fig. 55b illustrates a typical strength envelope for square-toothed specimens. The envelope for the square-toothed specimen can be predicted on the basis of the area of the tooth and the intact strength of the specimen. This envelope intercepts the zero normal load axis; thus it has cohesion. The actual envelope is a line which curves up from the origin and approaches the predicted curve as the normal load increases. The envelope initially has a very high angle of friction and no cohesion. The loss in cohesion at low normal loads might easily have been the result of minor apparatus errors. But it does point up the significance of minor boundary conditions on the strength of the rock mass at low normal loads. If the proper boundary restraint were provided, the square-toothed joint would have a cohesion intercept.

Rock bolts and the curved geometry of underground openings may provide this restraint to a rock mass. Only a very small amount of normal load is required to move up the strength envelope so that a sufficient strength is developed to maintain the stability of the opening. Or the restraint provided by the support system may be such that the material can develop an actual cohesion at low normal loads. Either way of looking at the problem is correct. It should be emphasized, however, that the cohesion and angle of friction values selected for use in theoretical solutions, such as elastic-plastic continuum relations, may not necessarily be the true or "intrinsic" strength properties of the material. Rather, they are merely a slope and an intercept value which provide a straight-line approximation

of the strength envelope in the pressure range of interest.

Estimate of Fractured Zone in Tuff
on the Basis of Elastic-Plastic Theory

Some insight into the effect of rock strengthening and rock support on the depth of fracturing around the cavities can be obtained from the elastic-plastic theory developed in Section 5.2. The depth of the yielded zone around a 100-foot-diameter tunnel for various assumed values of the material properties of tuff is given in Table IV. Although the strength envelope for a fractured rock is nonlinear, the elastic-plastic equation used (equation 5) requires a single value for ϕ as well as for c. Table IV also shows the effect of the internal pressure applied by the rock bolts (approximately 20 psi for bolts on 3-foot centers) upon the size of the destressed zone.

Excavation of the cavities caused fracturing in the rock surrounding the opening. The properties of the tuff changed from an essentially intact material having high cohesion (material 1) to a fractured material of little or no cohesion (materials 2 and 3, Fig. 55c). As discussed in the preceding paragraphs, the rock support system will strongly affect the properties of the near-surface rock. With adequate support, the fractured rock mass (material 2) will have a high angle of friction at low confining pressures and, at the higher confining pressures, an apparent cohesion intercept which approaches the cohesion of the intact specimen. If the support is not adequate and large deformations occur around the opening, the material properties will be further affected: the apparent cohesion intercept will be lost and the angle of friction will be reduced so that the strength will tend to approach the residual strength (material 3).

TABLE IV

DEPTH OF YIELDED ZONE FOR VARYING MATERIAL PROPERTIES AND INTERNAL PRESSURES, 100-FOOT-DIAMETER TUNNEL IN AN ELASTIC-PLASTIC MATERIAL SUBJECTED TO A HYDROSTATIC PRESSURE OF 1000 PSI

Assumed Material	Material Properties		Depth of Yielded Zone, ft, for	
	φ	2 ct, psi*	$p_i = 0$	$p_i = 20$ psi
1. Intact tuff, and in-situ tuff away from vicinity of opening	45°	1250	3	3
	45°	1000	6.5	6.5
	30°	1500	4	4
	30°	1000	11	10
	30°	500	29	26
2. Fractured tuff near opening; supported	60°	0	∞	7.5
Fractured tuff near opening	45°	0	∞	35
3. Fractured tuff near opening; residual joint strength, unsupported	30°	0	∞	200

* 2 ct = 2 c tan $(45 + \frac{\varphi}{2})$ = unconfined compressive strength, σ_{ult}.

The size of the yielded zone for these 3 materials varies greatly. For essentially intact materials (material 1), the yielded zone ranges from 3 to 30 feet; a reasonable range is 5 to 12 feet. For these high cohesion, intact materials, the internal pressure applied by the bolts has almost no effect on the size of the yielded zone. The size of the yielded zone for the properly supported, but fractured, near-surface rock ($\phi = 60^{\circ}$, $c = 0$, $p_i = 20$ psi) is approximately the same as for the intact material, 7.5 feet. (The observed depth of fractured rock in the cavities was also approximately the same.) If both p_i and c are assumed equal to zero (an impossible condition for a stable rock mass), the size of the destressed zone is infinite. For the unsupported rock with no cohesion and little internal pressure, the size of the yielded zone is extremely large. Even if it is assumed that the full internal pressure is applied by the bolts, the yielded (fractured) zone is still excessively large (200 feet deep). If the rock mass has no effective cohesion and no restraint at the surface, slabbing and fallout will accompany the fracturing process until the failed rock fills the opening or the cavity reaches a stable dome configuration where the radius of curvature is small enough to prevent blocks from falling out. From the above discussion, it is apparent that the support in the cavities was sufficient to maintain the strength of the tuff so that it behaved as material 2.

It should be noted that the presence of a yielded or failed zone around an opening is not, in itself, indicative of an unstable condition. In the process of yielding, stresses are transferred away from the opening into the unfailed, deeper rock, thus reducing the stress concentrations in the near-surface rock. This process continues until a stable condition is reached. As long as the failed rock is properly supported, a portion of its strength will be maintained and failure of the opening will not occur.

However, much of the fractured rock in the yielded zone must be artificially supported. For this reason, it is desirable that the fractured zone be small and not require a large amount of support. If the size of the fractured zone becomes extremely large and extends to depths greater than the length of the bolts, it is very possible that unstable behavior will occur.

One of the important factors affecting the size of the fractured rock zone is the amount of unbolted surface area exposed at any given time during excavation. The cavities were excavated in 6-foot increments. Adjacent areas were not excavated until bolts were placed and tensioned on exposed rock surfaces. In this manner, excessive slabbing and loosening of the rock mass were prevented; thus the strength of the mass was preserved. The average thickness of the slabbed and fractured rock in the cavities, as determined by the seismic refraction survey, was 3 feet. The seismic survey also indicated that some deeper fracturing had occurred. Fracturing and offsets along fractures were observed up to a depth of approximately 10 feet around the opening. These depths are quite similar to the depth of yielding estimated from the two-dimensional elastic-plastic theory, using the strength properties for a stable, jointed mass (material 2, fig. 55c).

If the cavity had been excavated in larger sections and if bolting had been delayed, slabbing around the cavities would have been more pronounced, the depth of fracturing would have been larger, and rock falls might have occurred. Reduced values for ϕ and c would have to be used to estimate the depth of fracturing around the opening. The large movements on the plane face of Cavity II which occurred when construction was resumed after a two-month strike seem to illustrate the change in properties caused by a delay in bolting. The strike may have provided time for the unbolted floor of the cavity to loosen and lose a portion of its strength.

The theory discussed above suggests that rock bolts must be of sufficient length to extend through the heavily fractured zone. They must be strong enough to support the loosened rock load (which could possibly be approximated by the depth of the yielded zone). The bolts must have enough strength and stiffness to prevent extensive loosening and loss of strength of the rock mass.

Fracturing in the Drifts

Excavation of the drifts provided a good opportunity for observing the formation of fractures and slabs around a simple opening, excavated full-face. The fractures were concentrated in the side walls of the drifts, indicating that the highest tangential stresses were acting at the sides of the opening, a condition which occurs when the natural vertical stress exceeds the natural horizontal stress. The elastic solution for biaxial stresses around a circular opening (Section 5.2 and Fig. 42) illustrates this condition. Fig. 42 shows the location of the overstressed zones around a circular tunnel in tuff (having a given ϕ and c) for three different loading conditions: $\sigma_h = \sigma_v$, $\sigma_h = 1/2\sigma_v$, and $\sigma_h = 0$. For $\sigma_h = \sigma_v$ the overstressed zone extends around the entire opening to a depth of 0.08a. In the drifts and boreholes in the vicinity of Cavities I and II, the natural vertical stresses were approximately twice the horizontal so that the maximum depth of the overstressed zone, from Fig. 42, is 0.10a and extends from 54° above to 54° below the horizontal. The failures observed in the circular boreholes (Fig. 26) closely approximated this condition. Failures in the drifts were also similar to this; however, some variations in the pattern were present due to the irregular shape of the opening. Figs. 56b and c show two of the typical cross sections for

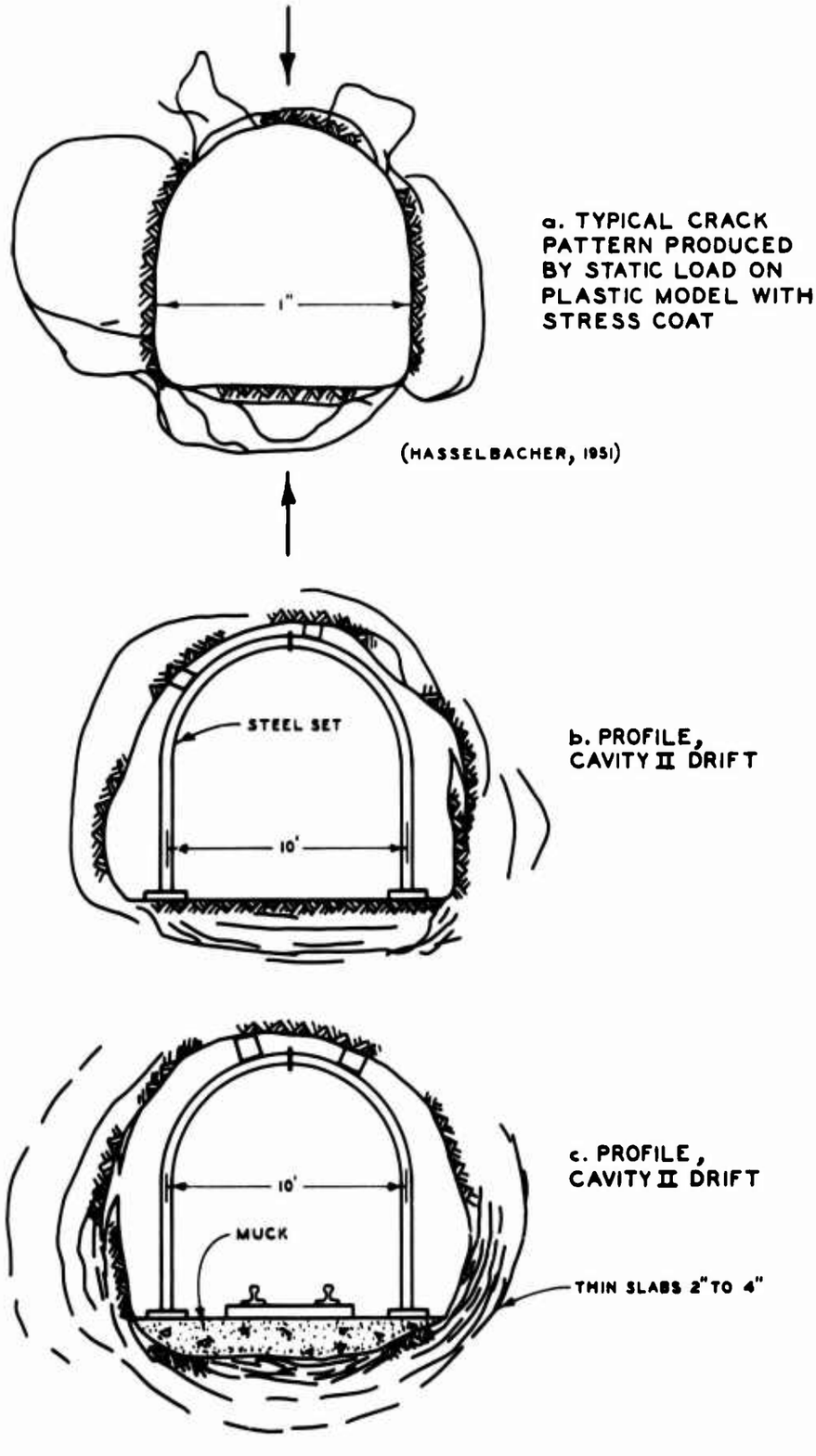

Fig. 56. Fracture patterns of drifts in tuff compared with fracture patterns of uniaxially loaded model opening

drifts in the tuff. Fig. 56a illustrates the fractures observed in a stress-coated lucite model opening, similar in shape to the tunnels, which was loaded statically in uniaxial compression (Hasselbacher, 1951). The fractures in the model are very similar to those observed in the drifts and provide further evidence that high vertical stresses and low horizontal stresses were the cause of the observed fracture patterns in the drifts.

There was a concentration of closely spaced, shallow fractures around the sharp corners at the invert of the drifts, while on the side walls the fractures were deeper and more widely spaced. It would be reasonable to assume that both the spacing and the maximum depth of fractures formed around an opening are related to the radius of curvature of the surface. In Section 5.3 it was pointed out that, around corners, tangential stress concentrations are high and the radial stress builds up rapidly with depth so that the depth of the overstressed zone is small. Conversely, on the large plane surfaces, although tangential stresses are low, the overstressed zone is deep because of the slow buildup of radial stress with depth. The portions of the cavity having a small radius of curvature were least affected by slabbing and discontinuous movement, while on the large plane surfaces, more difficulty was encountered with deep slabbing and large movement.

Orientation of Fractures and Mode of Failure

Most investigators separate the failure of brittle materials into two distinct groups: shear failures, which consist of a sliding of particles over one another, and splitting or cleavage failures, which consist of a breaking of bonds and a separation of particles. (Patton, 1966,

summarizes much of the literature concerned with the investigation of failure modes, emphasizing the work done in concrete.) Terzaghi (1945) considers a third type of failure: a pseudo-shear failure which is a combined shear and splitting failure. Many of the failures observed in simple laboratory tests are of this type. For example, Nadai (1950) describes the diagonal failure in the unconfined compression test as a series of en echelon cleavage fractures which tend to be oriented parallel to the compressive stress direction. It is commonly observed that fractures form parallel to the major principal (compressive) stress in triaxial extension tests, where the axial stress is reduced below the radial confining pressure. Terzaghi (1945) notes that, at low confining pressure, failure is primarily a pseudo-shear failure and that at higher confining pressures, failure by shear becomes more frequent.

The rate of loading is another factor affecting the mode of failure. Rocks which are normally ductile and exhibit shear-type failures under static conditions may under dynamic conditions behave in a brittle manner and exhibit cleavage-type failures. Nadai (1950) cites bursting tests performed on thin-walled steel cylinders by Davis (1948) as an example. Under dynamic rates of loading, cleavage fractures predominated, while under statically applied pressures, shear failures predominated. Nadai also describes test results which show that the velocity of propagation of cleavage fractures is more rapid than the velocity of propagation of shear fractures.

In the preceding sections it was shown that the depth of fracturing in the drifts and cavities compared closely with the depth predicted by a Mohr-Coulomb failure criterion. This theory predicts that failure will

occur when the maximum shear strength, $c + p \tan \phi$, is exceeded along a plane oriented at $45 - \phi/2$ deg to the direction of the major principal stress. According to this theory, the slip lines around a circular opening in a hydrostatic stress field intersect the surface at an angle varying from approximately 22 to 45 deg, depending on the value of ϕ (Fig. 39). However, in the cavities and drifts it was commonly observed that the fractures were formed parallel to the surface of the opening (and parallel to the major principal stress). Refer to Figs. 24, 31, and 33. Fractures which form parallel to the major principal stress have been observed in many other situations in both the field and laboratory and have been variously described as stress relief fractures, splitting fractures, extension fractures, and cleavage fractures. These fractures typically occur in the more brittle and unjointed rocks--such as the tuff--but have also been observed in jointed rock masses, such as jointed granites. Moye (1959) reported the occurrence of extension fractures around the tunnels and openings for the Tumut I powerhouse, excavated in a jointed granite. Extension fractures and popping rock were observed by Serafim (1961) during the excavation of Picote Power Station, also in a jointed granite. The mining literature contains many other examples of fractures and slabs formed parallel to the sides of drifts and pillars.

Rockbursts often result in the formation of fractures parallel to the surface of an opening. Spalding (1949) describes this as a typical mode of failure for drifts subject to rockbursts. An excellent example of the failure of drifts due to rockbursts is illustrated by Isaacson (1958), in a photograph which shows closely spaced cleavage fractures formed in a completely closed drift in quartzite, Kolar Goldfields.

Extension fractures have also been observed in natural slopes and valley walls. These fractures are usually attributed to relief of stress caused by the removal of overburden, either by erosion of a natural slope, or in some cases, excavation of a foundation. "Sheeted granites" is a term commonly used to describe massive granites which exhibit natural extension fractures. Many of the rock slopes and domes in the Sierras of California exhibit an onionskin layering with sheets approximately 3 to 10 feet thick resulting from extension failures. Terzaghi (1962) describes sheeted granites in the Sierras as typically containing, within a distance of at least 40 or 50 feet from the exposed surface, a set of joints which parallel the exposed surface. Their spacing commonly increases with increasing distance from the exposed surface. Savage (1950) reports on the formation of slabs in the valley floor at the Grand Coulee Damsite. As overburden was removed from the foundation, slabs formed in the valley floor. Removal of these slabs resulted in the formation of additional slabs in the underlying foundation. High horizontal tangential stresses, which typically exist in the floor of a valley, undoubtedly contributed to the formation of the slabs.

In the examples described above, extension fractures were formed when all principal stresses were compressive. Mohr-Coulomb theory will predict the formation of a failure plane normal to a principal stress only if the principal stress is tensile. The theory is unable to account for these failures when all principal stresses are compressive. Griffith's failure theory describes the conditions which will allow propagation of cracks around elongated ellipsoidal flaws. It also predicts that fractures will form when the stresses normal to the flaw are tensile. Fairhurst and

Cook (1966) describe the applicability of a Griffith-type crack propagation theory to situations where all stresses are compressive. From elastic theory, they show that the fracture will tend to form near the end of the flaw and then curve and propagate in the direction of the major principal stress. They attribute many of the splitting failures observed in unconfined compressive tests to this mechanism and conclude that extension fractures around underground openings are initiated by the propagation of fractures around flaws, and that the failure is aided by the tendency for buckling of the exposed surface slabs.

Another means of explaining extension fractures is by an extension strain theory. Nadai (1950) in describing an article by Taylor (1947) states that "the strongest chemical bond in the substance can be stretched a certain characteristic length in order to be broken; which might be expressed as the elastic extension of a corresponding length." Thus failure occurs when a certain limiting strain is reached.

Both the extension strain and the crack propagation theories emphasize the importance of the bond between particles. Therefore, the cohesive or tensile strength characteristics of the material appear to be of greater significance than the frictional characteristics for describing extension or cleavage fractures. It would be expected that the cleavage mode of failure would be most likely to occur in materials having a low tensile strength with respect to their unconfined or triaxial shear strength.

Failures Influenced by the Size of the Opening

The failure theories described in the previous sections are independent of the size of the opening and do not account for the effect of joint spacing and gravity loads upon stability. It was observed in the tuff

that some failures appeared to be independent of the size of the opening; fractures in the small boreholes (Fig. 26) were very similar to the fractures observed in the side walls of the drifts (Fig 24). However, certain failures were observed in the larger openings which were not present in the small openings. These failures could only be explained by the gravity load and joint spacing effects.

According to scaling relations, gravity loads are dependent on the size of the opening. As the size of the opening increases, the weight of the rock which must be supported above the opening also increases, and there is, of course, no corresponding increase in the strength of the rock surrounding the opening. This can only result in a decreased stability of the larger openings.

Another factor which affects the stability of an opening is the joint spacing. Obviously, joints spaced on 2-foot centers will have little weakening effect on a 4-foot-diameter opening, but can be of critical importance for a 20-foot-diameter opening. The higher the ratio of the joint spacing to the span of the opening, the greater will be the tendency for instability.

The support system will be determined, to a large extent, by the gravity-load condition and the spacing of joints. As the size of the opening increases, the possibility of instability due to fractures and the near-surface rock load increases, necessitating the use of artificial supports. The support system must be capable of maintaining the coherency of the rock mass and decreasing the unsupported span of the opening.
For many openings, the spacing of the support system is controlled by the fracture spacing of the rock mass. If a continuous support (such as

sand-cement gunite reinforced with wire mesh) is placed on the rock surface between the individual supports (such as rock bolts), the spacing of the supports is no longer controlled by the joint spacing, and it may be possible to use a wider support spacing.

In the tuff, failures occurred in the crown of some of the drifts which did not occur in smaller openings. There was almost no evidence of fracturing in the crown of the 5-foot by 7-foot drift (Fig. 26); however, fracturing was observed in the crown of the 10-foot and 13-foot drifts. Most of these fractures appeared to be controlled by bedding plane weaknesses (Fig. 27). In some cases, where adequate support was not maintained, loosening and fallout of roof slabs occurred. If unchecked, such fallout continues until a "natural" arch is formed which is capable of supporting the rock above the opening. The large overbreak observed in Fig. 28 is an example of such a natural arch. If the rock is properly restrained, loosening of the slabs will be limited to a small area near the surface of the opening.

The height of loosened, gravity-loaded rock which must be supported above an opening is dependent on the character of the rock mass (particularly its degree of jointing) and the nature of the support system. Terzaghi (1946) describes tunneling conditions on the basis of the loosened zone above the tunnels. For very closely jointed rock the height of the loosened zone with respect to the tunnel diameter will be large; for competent rock the height of the loosened zone is small. Terzaghi also emphasizes the importance of placing tunnel supports rapidly during the "stand-up time" of the rock, in order to prevent progressive loosening of rock blocks in the crown and an increase in the amount of

loosened rock to be supported. The support requirements outlined by Terzaghi were intended for use in relatively shallow rock tunnels with steel supports, and have been the basis for much of the Civil Works tunnel design in the past 20 years.

This type of design was not intended and cannct be used for large, underground openings. Such a design would be excessively conservative in the dome and unconservative in the side walls. Construction of large openings is possible because they are excavated in increments and supported as excavation proceeds. In this way, extensive loosening of the rock above the dome will not occur. (In the tuff cavities, the fracturing in the dome was not significantly deeper than on the side walls.) The depth of loosened rock will, to a large extent, depend on the amount of unsupported rock surface exposed during a given excavation cycle. With this method of construction, it is not possible for a "natural arch" to form above the opening. Rock bolts need not extend to the maximum depth of a natural arch, but they must extend to a sufficient depth to prevent movement along joint planes which enclose potentially unstable wedges of rock. These wedges may be located on the sides and lower portions, as well as in the dome of the opening.

CHAPTER 6

BEHAVIOR OF THE CAVITY IN GRANITE AND COMPARISON WITH THEORY

6.1 MEASUREMENT OF ROCK DISPLACEMENT

Rock movement in the granite cavity was measured using single-position extensometers placed in clusters of four, with lengths ranging from 5 to 50 feet. The single-position extensometer is described in Section 4.1 (Fig. 20a). The extensometer sets were covered at the surface with wire mesh and plywood to protect against flyrock. Before this covering was placed, a few of the units were struck by flyrock, necessitating recalibration of the units. Dashed lines in Fig. 57 indicate the period in which these erratic readings occurred for a given single-position unit. Movements compatible with those of the other units were assumed for this period.

6.2 OBSERVED DISPLACEMENTS

The displacement of the cavity surface with respect to the deepest anchor (30 or 50 feet) of each extensometer set is plotted against time and compared with excavation progress in Fig. 57. Displacement-depth relations and extensometer locations are shown in Fig. 58.

Dome (A) and Curved Surface (C)

Displacements in the dome and on the curved surfaces of the cavity ranged from 0.015 to 0.040 inch and were concentrated near the surface; very little movement was recorded beyond 25 feet from the surface. (The apparently large displacement recorded at the 30-foot depth for extensometer III-A-2 appears to be an erratic reading.) No large displacements were recorded which would indicate loosened, shallow slabs or deep-seated movement along joints. Displacements were related to excavation progress;

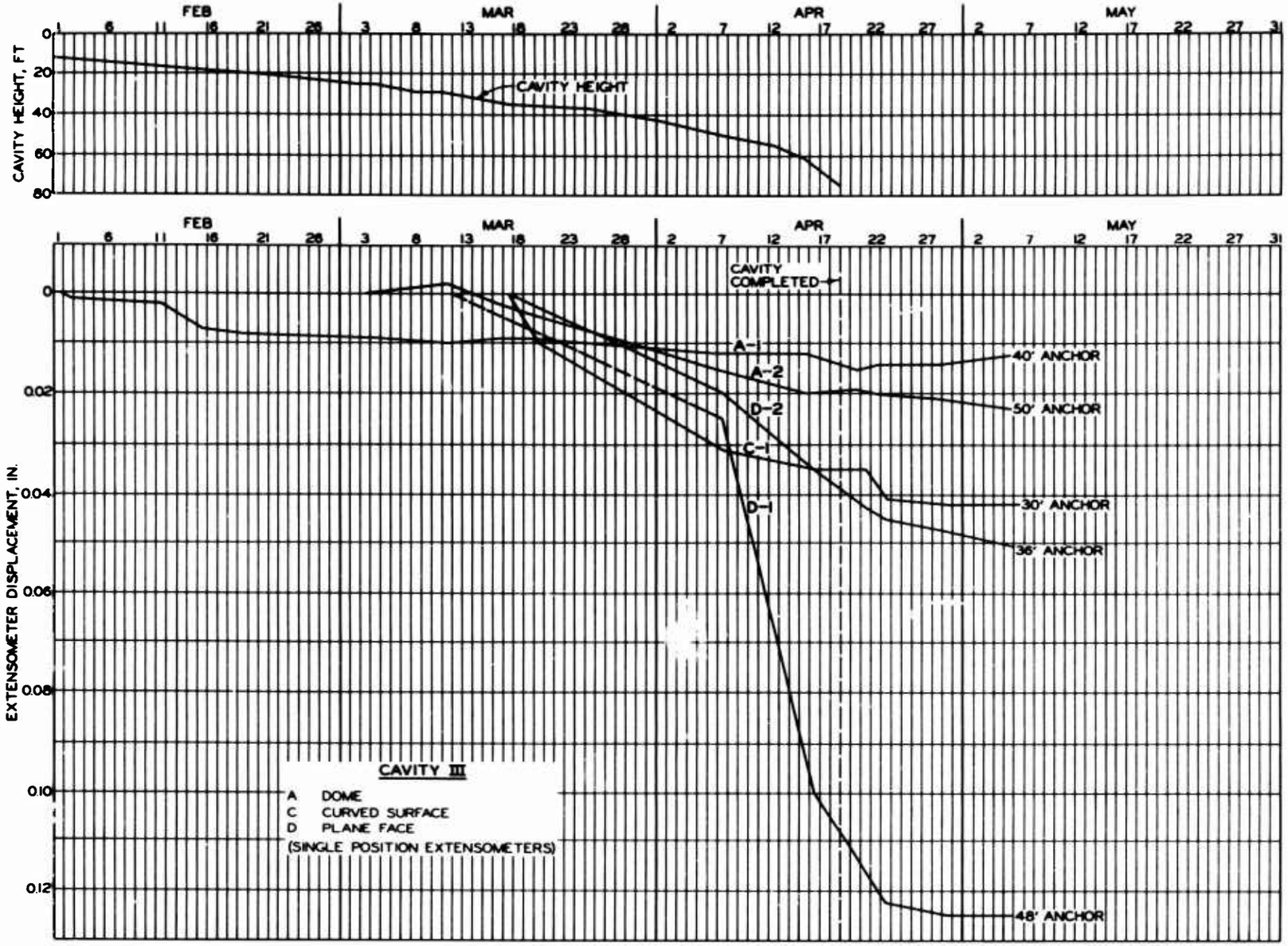

Fig. 57. Displacement of Cavity III surface with respect to deep (30- and 50-ft) extensometer anchors

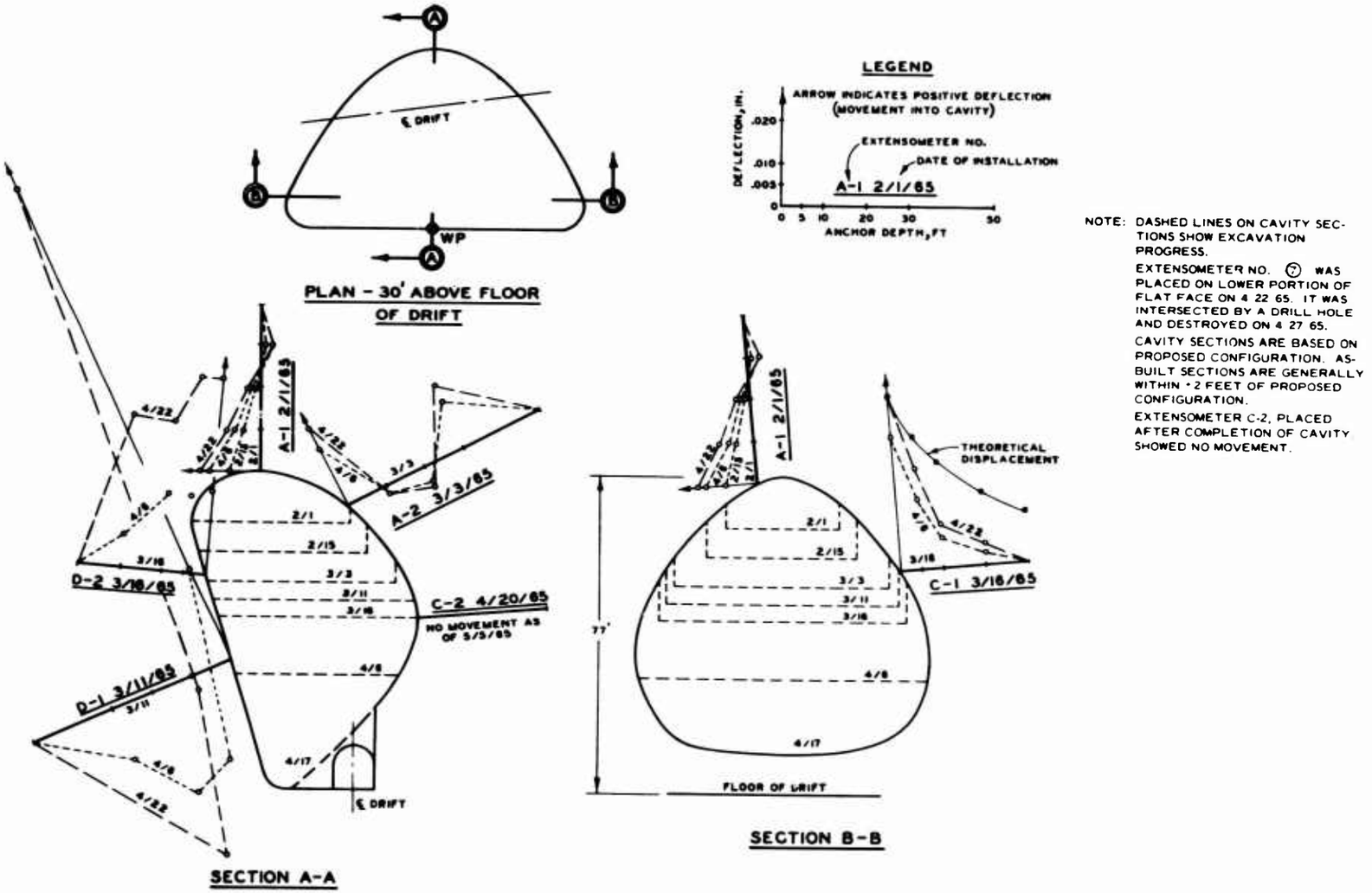

Fig. 58. Displacement-depth relations in Cavity III

upon completion of the cavity, rock movement had almost completely ceased. An extensometer (III-C-2) placed on the curved surface after completion of the cavity showed no displacement.

Plane Face (D)

Rock displacements on the plane face were much larger than on the curved surfaces. Extensometer III-D-1, at the center of the plane face, recorded a total displacement of 0.125 inch, which was concentrated in the first 10 feet from the surface. (The extensometer was installed in an alcove at the center of the plane face prior to general excavation of the cavity at that location.) Extensometer III-D-2, near the upper portion of the plane face, displaced 0.05 inch.

Much of the displacement observed on the plane face was a result of loosening of the near-surface rock, rather than an elastic response of the rock to the stresses relieved by excavation. Displacements on the plane face did not occur immediately upon excavation; at least half of the recorded displacement occurred as the cavity neared completion. After completion of the cavity, the movements stabilized.

6.3 DISCUSSION OF OBSERVED DISPLACEMENTS

The elastic displacements in the granite were much smaller than those in the tuff because of the smaller cavity size, the shallower cavity depth, and the higher deformation modulus for the granite. From elastic theory (Section 5.2) the magnitude of the displacements in the dome of the granite cavity should be approximately 1/36 times that of the displacements in the dome of the tuff cavities. Discontinuous movements in the granite should also be less than in the tuff, because of the decreased tendency for extension fracturing and shallow slabbing in the granite, and the higher

factor of safety against deep failure in the granite cavity, due to its more conservative rock-bolt support system.

Although the magnitude of displacements was much less in the granite than in the tuff, the nature of the displacements was quite similar; movements on the stable curved surfaces of all the cavities were essentially elastic, with a concentration of movement near the surface indicative of a decreased deformation modulus; shallow, discontinuous movements also occurred in all the cavities as a result of loosening of near-surface slabs.

Dome (A) and Curved Surfaces (C) of Cavity III

Displacements on the curved surfaces of the cavity correlated closely with the predicted elastic displacement, based on a spherical geometry (equation (3), Section 5.2). In equation (3) it is assumed that both the natural horizontal stress and the natural vertical stress are equal to 400 psi (a reasonable assumption, as discussed in Section 3.2, Natural State of Stress). The deformation modulus (4×10^6 psi) in equation (3) was obtained from an intact modulus (10×10^6 psi) reduced to account for the compressibility of the joints in the rock mass (refer to Appendix A). The observed extensometer displacements, from the time of installation until cavity completion, were as follows: III-A-1: 0.015 inch; III-A-2: 0.020 inch; III-C-1: 0.035 inch. During this period the approximate change in cavity radius was 15 feet at each of the three extensometer locations. For this change in cavity size, the predicted elastic displacement is 0.022 inch, a very close approximation to the actual displacements.

The change in cavity radius substituted into equation (3) was based on an average spherical cavity size and did not account for the irregular shape of the cavity. A further refinement in the displacement prediction

would be obtained by accounting for the irregular shape of the cavity--specifically, the radius of curvature of the cavity surface in the vicinity of the extensometers. According to elastic theory, the magnitude of the displacement of the surface of an opening is related to the span of the opening or the radius of curvature of the surface. For an ellipsoidal opening in a hydrostatic stress field, the largest inward displacement will occur on the surface parallel to the semimajor axis, which is the portion of the ellipse having the largest span and the largest radius of curvature. In Fig. 58, it is apparent that the largest displacements occurred on the surface having the largest radius of curvature (extensometer III-C-1), and the smallest displacements occurred in the dome, where the radius of curvature was small.

Although the magnitude of displacements at the surface was essentially elastic, the distribution of displacement with depth did not closely approximate elastic theory; displacements were more concentrated near the surface and dropped off more rapidly with depth than predicted from theory. The concentration of displacements near the surface probably resulted from slight loosening of the rock during excavation, which caused a reduction of the deformation modulus of the near-surface rock. This behavior was also observed in the tuff cavities.

Plane Face (D)

The predicted elastic displacement near the upper portion of the plane face was approximately 0.04 inch--one-half the displacement predicted for the center of the plane face, based on the theory for a uniform pressure on an elastic halfspace (Section 5.2). Extensometer III-D-2, on the upper portion of the plane face, displaced 0.05 inch. Initially, the displacement

appears to have been elastic; during the later stages of excavation some discontinuous movements probably occurred. The extensometer was installed after some of the initial rock displacement had, in all probability, already occurred. Therefore, the total displacement on the upper portion of the plane face probably exceeded 0.05 inch.

The total predicted elastic displacement at the center of the plane face was 0.08 inch. The observed displacements at the center of the plane face (extensometer III-D-1) appeared, initially, to approximate elastic theory; but during the later stages of excavation, displacements increased to 0.125 inch. Most of this movement was concentrated within the first 10 feet from the surface, and was thought to be a result of loosening of shallow rock blocks. Examination of the plane face supported this view. Cracks were found on the surface and at a depth of a few feet in boreholes on the plane face. Numerous joint planes paralleled the plane face, and some faults and natural shear zones intersected the plane face at low angles. Loosening of the blocks formed by these discontinuities was a major cause of the shallow displacements on the plane face. The 6-foot spacing of rock bolts on the plane face was adequate for the overall stability of the face, but did not prevent minor slabbing from occurring. It is almost inevitable that such a condition would exist on a large plane surface, particularly when joints are oriented parallel to the surface.

6.4 FRACTURING IN THE GRANITE

Rock failure in the granite differed considerably from the failure observed in the tuff. The tuff was relatively homogeneous, and stress levels were high enough so that extension fractures formed around the openings as they were excavated. Failure in the granite did not occur in

this manner, for two reasons: first, the granite is sufficiently jointed that failure will occur along existing weakness planes rather than through intact portions of the rock mass; second, although the stress concentrations around the openings in the granite are high enough to cause differential movement along the existing joints, they are not high enough to cause fractures to form in the high-strength, intact portions of the rock mass. The behavior subsequent to the formation of fractures was similar for both the tuff and the granite; loosening of protruding rock blocks, and loosening of wedges of rock on the plane face occurred in both tuff and granite cavities.

Most of the slabbing and discontinuous movement in Cavity III occurred on the plane face. Much of the loosening was a result of opening of joints located parallel and subparallel to the plane face, as described in Section 6.3. On the lower portion of the plane face, observations in old drill holes revealed that slight offsets had occurred along joint surfaces located a few feet behind the face. In the lower right-hand portion of the plane face, unsupported, protruding rock blocks located next to the plane face were observed to move and rotate (Fig. 59). Fractures surrounding the block opened as much as 3/4 inch. Adjacent blocks were bolted and did not exhibit movement. Large movements and rock failure were not observed on the curved surfaces of the cavity. This area was well supported and keyed so that loosening of rock blocks did not occur.

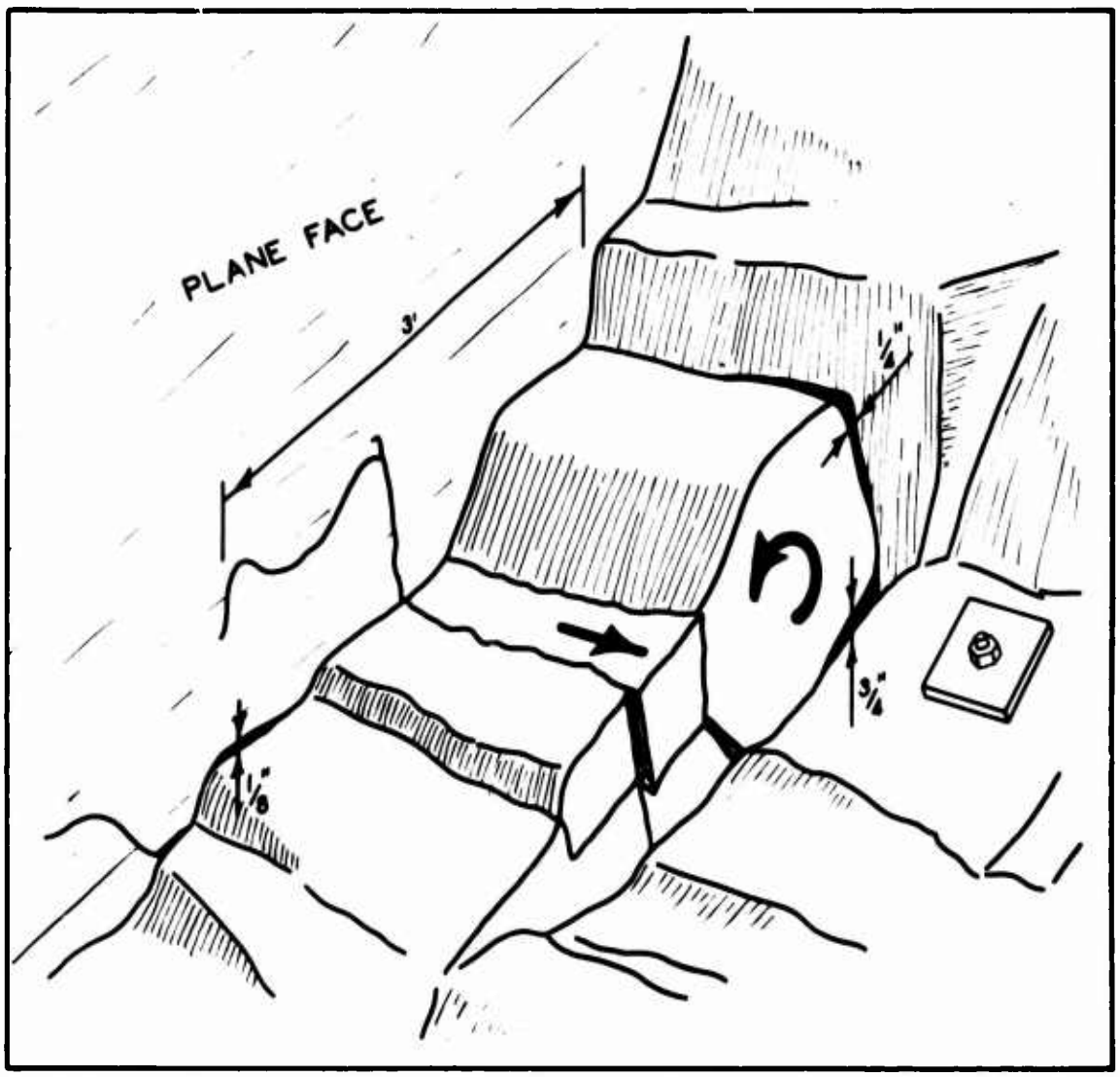

Fig. 59. Opening of joints in Cavity III

CHAPTER 7

SUMMARY AND CONCLUSIONS

7.1 PROPERTIES OF THE ROCK

Stability and deformation in the cavities were strongly dependent on the properties of the rock mass. These properties can be separated into two components: the properties of the intact portion of the rock mass, which can be determined from laboratory tests on small specimens; and the properties of the discontinuities in the rock mass, which can be inferred from a quantitative description of the discontinuities. The intact properties provide an upper limit for the strength and the deformation modulus of the rock mass. For rock containing few joints the in-situ properties may closely approach this upper limit. Discontinuities in the rock mass reduce the in-situ properties to some lower value.

Two of the rock mass quality indices used to evaluate the character of the discontinuities were the RQD and the fracture frequency (described in Appendix A). Seismic velocity and attenuation characteristics may also be used to evaluate discontinuities. A relationship between the rock mass quality indices and the in-situ deformation modulus, E_r , has been established which appears useful for obtaining a rapid estimate of the deformation characteristics of a rock mass. A rough estimate of the stability of an opening can be obtained by considering the orientation of the major discontinuities with respect to the orientation of the opening, as well as considering the rock mass quality indices.

Properties of the Tuff

The tuff in Cavities I and II was a very low-strength rock of average

modulus ratio (σ_{ult} = 1400 psi, $E_t = 0.5 \times 10^6$ psi). The unconfined stress-strain curve was linear to failure. The tuff had a natural water content of 19%. When dried, the tuff became more brittle and the strength and modulus doubled. The rock mass quality of the tuff was excellent, and jointing was not prominent. Joint frequency was slightly higher in Cavity II than in Cavity I. Some bedding plane weaknesses were present in the tuff.

The in-situ properties of the tuff were similar to the intact properties determined from laboratory tests on small specimens because of the low frequency of joints in the tuff. For this reason, the in-situ deformation modulus, E_r , was assumed equal to the intact laboratory modulus, E_t . The elastic displacements predicted using this modulus closely approximated the initial elastic displacements which occurred in the rock surrounding the tuff cavities. In-situ displacements which were significantly greater than those predicted from the laboratory deformation modulus could usually be attributed to the effect of jointing or fracturing in the tuff.

Intact properties were also used to predict the fracture characteristics of the tuff. The distribution and depth of the extension fractures which formed immediately upon excavation of the tuff could be approximated using the intact strength parameters in the Mohr-Coulomb failure equations. (Although the Mohr-Coulomb equations were used to estimate the depth of fracturing, they could not predict the orientation of the fractures parallel to the opening.)

The long-term strength of the tuff was affected by joints and other discontinuities and therefore could not be predicted from the intact

strength properties. The long-term strength is intermediate between the intact strength (as an upper limit) and the residual strength along a smooth joint (as a lower limit).

The tuff in the cavities behaved in a brittle manner; extension fractures formed immediately upon excavation, and a small bump (dynamic release of strain energy) occurred in the floor of Cavity I during excavation. The

time-dependent movements which occurred in the later stages of excavation were related to opening of discontinuities rather than creep of the intact portion of the tuff.

A correlation between the seismic velocity ratio, $\frac{V_{pf}}{V_{pl}}$, and rock mass quality (or degree of fracturing) was observed in the tuff. The shallow, highly fractured zones exhibited the lowest velocity ratios. These zones also had the lowest deformation modulus. In general, the tuff in Cavity I was of higher in-situ quality, had higher velocity ratios, and exhibited less discontinuous movements than the tuff in Cavity II.

Properties of the Granite

The granite in Cavity III was a high-strength rock of average modulus ratio (σ_{ult} = 27,000 psi, $E_t = 10 \times 10^6$ psi) and fair to good rock mass quality (RQD = 75%). Joints in the granite formed rock-blocks approximately 2 feet on a side. Joints were usually tight. Gouge and weathering products were present along many faults and some joints.

The in-situ properties of the granite differed significantly from the intact properties because of the presence of joints and faults. The in-situ deformation modulus, E_r, was reduced to a fraction of the intact modulus, E_t, in order to account for the effect of jointing in the rock mass. E_r was assumed equal to 0.4 E_t on the basis of a correlation between rock mass quality (RQD and fracture frequency) and E_r/E_t established in a granite gneiss at Dworshak Damsite (Appendix A). Displacements predicted using this modulus correlated closely with the actual displacements which occurred as the granite cavity was excavated.

Because of the great difference between the intact strength and the joint strength of the granite, failures in the granite almost invariably

occurred along preexisting joint and fault planes. The orientation of the discontinuities, as well as the rock mass quality, was an important factor affecting stability.

Sonic borehole logging was performed in 200 feet of corehole in the vicinity of the cavity. An approximate relationship was established between rock mass quality and the attenuation of the signal of the sonic logger (Appendix A). Highly fractured zones transmitted less energy and therefore showed greater attenuation than the more competent zones.

7.2 DISPLACEMENTS

Rock displacement measurements are useful as a means of evaluating and monitoring the stability of underground openings. Large displacements, or large rates of displacement with respect to time or excavation progress, are indicative of potentially unstable conditions.

Rock displacement in the three cavities at the Nevada Test Site was measured with two types of borehole extensometers: a single-position extensometer installed in clusters of three or four with anchors at varying depths up to 50 feet; and multiple-position, remote-readout extensometers with four to six anchors in a single hole, at depths ranging from 5 to 50 feet. The multiple anchors were useful for determining the depth at which movement was occurring in the rock mass. Both extensometer types performed satisfactorily; there were no significant differences in the type of measurements recorded by the two types of extensometers.

Observed displacements in the cavities were compared with displacements determined from elastic theory. Simple closed elastic solutions for displacements around spherical and cylindrical openings and for displacements due to uniform pressures on plane surfaces were used to predict

displacements in the cavities. The simple solutions were particularly useful for rapidly estimating rock displacements during construction. The boundary conditions for the cavities were much more complex than the boundary conditions of the simple solutions; however, the solutions yielded reasonable results when carefully used.

Elastic displacements around the irregular portions of the cavities were determined using a two-dimensional, finite element computer solution. Nonuniform stresses and an irregular cavity surface geometry were assumed. The displacements determined with the finite element solution correlated closely with the displacements determined from the simple, closed solutions.

Three types of displacement were typically observed in the cavities. The first type was the small displacements which occurred immediately upon removal of rock support by excavation of the cavity. The displacements were of the same magnitude as the displacements predicted from elastic theory, although slightly more displacement was concentrated in the shallow, fractured rock than would be predicted from theory. The deformation modulus used in the elastic equations was based on the in-situ characteristics of the rock mass (rock mass quality). The magnitude of the measured surface displacements was approximately 0.2 to 0.5 inch into the tuff cavities and 0.015 to 0.035 inch into the granite cavity. Most of the movement was concentrated within the first 20 feet from the surface of the cavity. The elastic displacements occurred regardless of the support and excavation methods used. They were indicative of a stable situation, requiring no corrective measures.

The second type was the large, shallow discontinuous displacements which indicated that loosening and slabbing were occurring near the surface

of the opening. These movements usually occurred in the later stages of excavation, after the elastic displacements had occurred. Irregularities in the rock surface, joints subparallel to large plane surfaces, extension fractures and drying (in the tuff), loss of rock-bolt tension, and stress concentrations beneath rock-bolt bearing plates were the factors which contributed to the shallow slabbing in the cavities. The displacements were concentrated along discontinuities within 5 feet of the surface of the cavities. The magnitude of the displacements was 1 to 2 inches in the tuff and approximately 0.1 to 0.2 inch in the granite. The shallow, discontinuous displacements occurred in the dome of both tuff cavities (Cavities I and II), on the plane face of Cavity II, and on the plane face of the granite cavity (Cavity III). Loosening of shallow slabs could lead to a generally unstable condition if it were to progress to the point that the bearing of the bolts against the rock surface were lost. The loss of support was prevented in the tuff cavities by applying 2 inches of sand-cement gunite to the rock surface. No corrective measures were required in the granite.

The third type was the deep-seated, discontinuous displacements which occurred on the plane face of Cavity II along joints and bedding planes whose boundaries formed large wedges of potentially unstable rock. The displacements were concentrated at a depth of 10 to 30 feet from the surface and had a magnitude of 1 to 2 inches. The rate of movement was high; most of the displacement occurred within a period of one week. The displacements were definitely indicative of an unstable situation. Associated with th deep-seated movement were the formation of shear cracks at the edge of the plane face, loosening of shallow slabs of rock on the plane face, and breaking of rock bolts and dishing of bearing plates over large

portions of the plane face. Movements ceased and the face was stabilized when approximately 200 additional 48-foot bolts were placed.

The elastic movements in the cavities were related to the change in size of the cavity, the natural stresses in the rock mass, and the deformation modulus of the rock mass. The discontinuous movements in the cavities were primarily controlled by the nature of the support system, the nature of the joints and fractures, and the geometry of the cavity surface.

Movements similar to those observed in the cavities typically occur in many other types of underground openings, including mines, tunnels, and underground powerhouses. In the examples presented in the introduction displacements at the surface of the openings were often 3 to 10 times the values predicted for the elastic displacement (even when using a deformation modulus which was based on the in-situ rock mass quality). These movements were discontinuous and usually associated with some definite plane of weakness. Because continuity is lost when these displacements occur, a "deformation modulus" has very little meaning. The discontinuous displacements most commonly occurred along reentrant corners, on large plane surfaces, and in places where joint and wall geometries were such that thin wedges of rock were isolated near the surface. Fault zones and other planes of weakness were often the seat of large movements. Proper support of these areas minimized the large movements.

In many cases, rock located at some distance behind the surface of the opening was not affected by the local failures around the openings. The measured displacements in this rock were usually of the same magnitude as the predicted elastic displacements, using an in-situ deformation modulus in the elastic equations. (For rocks having an excellent rock mass

quality, the deformation modulus was assumed equal to the intact modulus.)

Excavation of an opening involves a reduction of stress (decompression) normal to the surface of the opening, which usually results in an expansion of rock into the opening. The rock mass is much more likely to lose its continuity in this situation than in situations where the rock is compressed--where increasing pressure creates an increased interlocking of the rock mass. If the continuity of a decompressing rock can be maintained by proper support, the "decompressed" deformation modulus will have approximately the same magnitude as the "compressed" deformation modulus. If the support is not maintained, large discontinuous movements--an order of magnitude greater than predicted by the deformation modulus--may occur. Some of the shallow discontinuous movements can be tolerated, as long as rock falls and a general loss of support are prevented. However, deep movements which affect large portions of the underground opening are almost invariably indicative of an unstable condition and must be corrected.

7.3 ROCK FAILURE

Failure in the Tuff

Extension fracturing was the predominant type of rock failure occurring in the tuff. The fractures formed parallel to the surface of the opening, at a depth of approximately 6 inches to 3 feet, as soon as the surface was exposed. The tangential stresses surrounding the openings were higher than the intact strength of the rock; therefore, extension fractures formed regardless of the excavation and support procedures employed. However, opening of the fractures and slabbing of the shallow fractured rock were minimized by prompt placement of rock bolts.

In some instances, shearing displacements of approximately 1 inch

occurred along previously formed extension fractures on the plane face of Cavity II and in the upper portion of both cavities. Rock protrusions commonly exhibited shearing displacements which were in the direction of the feathered edge of the protrusion (the direction in which the fracture intersected the cavity surface). One-inch shearing displacements also occurred along bedding and joint planes on the plane face of Cavity II, during the period when the stability of the plane face was endangered.

Using seismic refraction techniques, the depth of the heavily fractured (low velocity) zone surrounding the cavities was found to range from 1 to 7 feet, and average 3 feet. Some extension fractures and shearing displacements were observed at depths up to 7 feet.

Extension fractures also formed parallel to the surface of the drifts. The fractures were concentrated on the side walls of the drift, providing evidence that the natural vertical stresses in the rock mass exceeded the natural horizontal stresses. Hairline fractures were located at depths up to 3 to 5 feet behind the side walls, and shallow slabs (2 to 6 inches thick) formed and fell from the sides of the drift.

The spacing of extension fractures was dependent on the radius of curvature of the surface of the drift. Around the sharp corners at the bottom of the drift, the fractures were shallow and closely spaced. On the larger plane surfaces at the side of the opening, the fractures were deeper and more widely spaced.

The fracturing and overbreak which occurred in the crown of the drift were caused by bedding plane weakness and by the gravity load of the near-surface rock.

The depth of fracturing in the tuff could be approximated using

elastic-plastic relations, and a Mohr-Coulomb failure criterion. However, the orientation of extension fractures parallel to the surface of the opening could not be explained using a Mohr-Coulomb theory. The formation of fractures parallel to the minor principal (compressive) stress suggests that an extension strain theory might apply, where the limiting strain is reached when the bond between particles is broken. This suggests that the cohesive and tensile properties of the rock are more important than its frictional properties for describing the occurrence of extension fractures.

Failure in the Granite

Failure in the granite almost always occurred along preexisting joint and fault planes. The stresses surrounding the cavity were not high enough, and the rock was too heavily jointed, to allow extension fractures to form.

The orientation of joints and faults was a major factor influencing stability. In the cavity, joints and faults which paralleled the plane face contributed to loosening and local slabbing of the near-surface rock on the face. In the 10-foot drifts, the most common condition affecting stability was the fault zones which paralleled the drift and intersected the crown of the drift. (Both low- and high-angle faults created this condition.) Light steel supports with wood lagging were used to prevent gravity failures of the loose rock in the crown. In other portions of the drift, good to excellent quality rock was encountered and the only support required was a few 6-foot bolts to pin occasional loose slabs in the crown.

Failures in Other Underground Openings

Rock failure similar to the failures observed in the cavities also

occurred in the underground openings discussed in the introduction. Many of the failures occurred along joint and fault surfaces. Some of the failures, however, were extension fractures which formed parallel to the surface of the opening through the intact portion of the rock mass. The extension fractures occurred not only in massive, unjointed rocks, but also in typically jointed rocks, such as granites. At these sites the stresses surrounding the opening were apparently high enough, and the joint strengths great enough, to force new fractures to form through the intact portion of the rock mass.

7.4 ROCK SUPPORT

Stability in the cavities was maintained using tensioned rock bolts placed in a regular pattern. Wire mesh and, in some cases, gunite were placed on the rock surface to support the loose rock between the bolts. The purpose of the support system was to provide sufficient restraint to prevent loosening and loss of strength of the rock mass, leading to local or general instability of the opening.

The strength of a rock mass is intermediate between the residual strength along a smooth joint and the intact strength of the rock. When large displacements occur along discontinuities, irregularities are overridden and interlocks are broken, so that the strength of the rock mass is reduced and tends to approach the residual strength of the joint. One of the primary functions of the rock bolts is to apply sufficient pressure to the rock surface to restrain the rock mass and prevent the occurrence of large displacements with a resulting loss of strength. By preventing discontinuous displacements, a high apparent cohesion intercept is maintained in the rock mass. Rapid placement of the bolts is important to prevent

initiation of the discontinuous displacements.

The bolts also provide a confining pressure to the near-surface rock. Because of the high friction angle of a fractured rock mass, the confining pressure can substantially increase the shearing resistance of the near-surface rock. The ability of the rock surrounding an opening to fracture, decompress, and redistribute high stresses into the stronger rock away from the opening is another important factor influencing stability. As long as the bolts are capable of holding this fractured rock in place, stability is maintained.

Rock bolts must be capable of supporting two zones: (1) the fractured (decompressed) rock surrounding the opening (the thickness of this zone can be estimated from elastic-plastic theory; in the cavities it was estimated to be less than 10 feet thick); and (2) any potentially unstable wedge of rock bounded by assumed or known discontinuities. Rock bolts must be long enough to penetrate these zones and must apply sufficient pressure to the rock surface to restrain the rock within the zones. The length of the bolts (with respect to the span of the opening) and the pressure applied by the bolts are both dependent on the stresses in the rock mass and the strength of the rock mass (of particular concern are the joint strength characteristics).

Another consideration in the design of a support system is the bearing of the rock bolts on the rock surface and the support of the surface rock located between rock bolts. Improper support at the surface can cause loosening and local fallout which could lead to a general loss of rock-bolt support. The bolts must be spaced closely enough to prevent failures between bolts; or a continuous support, such as sand-cement gunite, should

be placed to support the rock between bolts.

Rock bolts should be tensioned upon installation so that discontinuous displacements cannot be initiated in the rock mass. It is most desirable to completely grout the bolt after tensioning in order to prevent the possible loss of tension due to partial failure of the bearing surface or the anchorage of the bolt.

The rock-bolt pressures and lengths used in the cavities are summarized below:

Location	Bolt Spacing ft	Pressure psi	Span ft	Bolt Length/ Span
Tuff, dome	3	20	100	0.33
Tuff, curved surface	3	20	100	0.25
Tuff, plane face, Cavity I	6	5	140	0.17
Tuff, plane face, Cavity II				
Prior to failure	6	5	140	0.17
During failure	6	10	140	0.17
After stabilization	3	20	140	0.33
Granite, dome	3	15	60	0.40
Granite, curved surface	3	15	60	0.27
Granite, plane face	6	4	80	0.20

Because of user requirements, the bolt design on the plane faces was less conservative than the design on the curved surfaces. In general, the bolt length to span ratio should be higher on plane surfaces than on curved surfaces, because the plane surface does not have the curvature which provides additional support by "keying" the rock mass. Dynamic design requirements dictated the bolt design in the granite cavity. The design was therefore more conservative than the design in the tuff cavities.

The plane faces of Cavities I and II were originally bolted with the

same pattern and the same bolt lengths. However, additional support was required in Cavity II because of the large movements which occurred along the joints intersecting the plane face. The plane face of Cavity I did not contain as many joints and was therefore stable with less support.

It is very difficult to determine the magnitude of the pressures to be applied to the rock surface by the rock-bolt system. The pressure is strongly affected by the nature of the discontinuities and by the amount of displacement which will cause overriding of joint irregularities. The bolts provide stability to the opening by maintaining the continuity of the rock mass. However, the bolt pressures required to maintain the continuity cannot be determined solely from elastic-plastic or elastic continuum relations.

7.5 SUGGESTIONS FOR FUTURE RESEARCH

Field Observations

The most valuable information concerning rock behavior is to be found in the field, where the performance of full-scale structures (rock foundations, rock slopes and cuts, and underground openings) can be observed and evaluated. In order for these observations to be of general applicability it is extremely important that uniform, quantitative descriptions of the engineering properties of the rock mass be made. It is recommended that the description of a rock mass include an evaluation of its intact strength and modulus, an estimate of its degree of jointing using the rock mass quality indices, and a general description of the rock type and joint characteristics (to include a description of the tightness, filling, weathering, and irregularity along joints and faults).

Before the performance of the structure can be properly evaluated it

is also necessary to describe the geometry of the structure, the orientation of discontinuities with respect to the orientation of the structure, the natural stresses in the rock mass, and the excavation and support procedures used during construction.

Displacement or deflection measurements are a valuable means of determining both the deformation and the stability characteristics of a rock mass. These measurements are relatively easy to obtain and interpret, and provide a continuing estimate of the stability of the rock structure.

Seismic tests are useful for obtaining an estimate of rock mass quality and for determining the location of the fractured zones and other velocity boundaries in the rock mass. Both uphole and refraction surveys may be used to determine the depth of the fractured zones. Sonic logging is useful for determining the location of individual fracture zones and for obtaining a detailed estimate of rock mass quality in a borehole. Visual observation of boreholes is another method of locating joints and fractured zones. The borehole camera and the stratascope are used for this purpose. Much information can be obtained by observing fractures and offsets in old boreholes using nothing more than a steel tape measure.

Other useful field tests include the measurement of the loads applied to the support system, and the determination of the initial state of stress in the rock mass using the deformation-overcoring technique.

Rock Mass Quality Indices

Further correlations between rock mass quality and deformation modulus, and rock mass quality and strength, need to be made in order to establish and verify the relations between these parameters. A correlation between rock mass quality and deformation modulus was obtained which appears

to be valid for predicting the deformation modulus from site to site. Further field results are needed to establish the general validity of the relationship. However, the correlation of rock mass quality with strength and stability is more difficult and has not been established. One possible means of estimating the relationship between rock mass quality and stability is to observe failure and support of small drifts in a rock mass. It is very difficult to relate rock mass quality to the strength of the rock mass because of the dependence of strength upon individual discontinuities in the rock mass. This is most pronounced in the analysis of rock slope stability. In this case, the residual strength and the irregularities along critically oriented joints are more important for determining stability than the rock mass quality.

Seismic velocity and attenuation characteristics are also related to rock mass quality. One of the problems in using velocity as a rock mass quality index is the insensitivity of the velocity to fractures which are water-filled. Further study is needed in order to determine the effect of saturation upon velocity in a jointed rock mass. The attenuation and dispersion characteristics of seismic waves appear to have promise as a rock mass quality index. One of the major problems to be overcome is the difficulty in producing, receiving, and analyzing the signal so that variations in test procedure are minimized and will not affect the index determination.

In addition to the seismic instruments used for research purposes, there is a need for portable tools which will give reproducible results capable of analysis and which can be used in the field to determine rock mass quality characteristics.

Failure in a Rock Mass

There is a need for further study of the failure characteristics of a rock mass. This is a difficult area of study because failure is controlled to a large extent by minor boundary effects and detailed characteristics of individual joints.

Emphasis should be placed upon determining the relation of rock deformation to failure. Deformations are often a controlling factor affecting the strength of a jointed rock mass; furthermore, they are a quantity which is relatively easy to measure in the field. Of particular interest are the deformations required to reach peak and residual strength along multiple joint planes. A knowledge of the amount of deformation which a rock mass can undergo prior to failure will provide some insight into rock support requirements.

The internal support pressure required to restrain the rock mass and maintain the stability of the opening is one of the major unknowns in the design of underground openings. The pressure cannot be determined strictly from continuum theory, or from any theory which requires a complete knowledge of the rock properties, for the rock properties themselves are dependent on the nature of the support system and the deformations which occur in the rock mass. Field observations and model tests are the best sources of information on support pressures. A series of instrumented test sections in a tunnel, supported with bolts of varying length, spacing, and applied tension, would provide valuable information on support requirements. Sections lacking adequate support would be allowed to fail. Measurements of bolt load and rock deformation would be made during the failure process. A test such as this might be justified for a large project; a

less expensive alternative would be model testing.

Research should be conducted to determine the types of failure occurring around an opening (or other rock structure). The factors controlling shear and extension (or cleavage) failures need to be defined. The effect of jointing upon rock failure should also be studied. Specifically, when does failure occur along joints and when is it controlled by the intact portion of the rock mass?

Failure in a rock mass is affected by the rate of loading. Dynamic rates of loading must be considered in the design of protective structures and in the design of openings subject to rockbursts. The mode of failure and the strength of the material are both dependent on the rate of loading, particularly in a jointed rock. Information on these effects is needed for proper design of openings to resist dynamic loads.

Failure effects may be studied in a number of ways. Continuum theories are limited in their application, because when rock failure occurs, the mass is no longer a continuum. Continuum theories may provide useful information on the stresses and deformations in a rock mass prior to failure, but they can not predict the mode of failure or the discontinuous effects occurring in a rock mass. The best means of obtaining this information is field observations with supporting laboratory and model tests.

Model tests may provide a great deal of information that cannot be obtained in the field. However, it is important that model tests be interpreted in the light of observed field behavior. Two types of models are of interest: (1) a model which simulates an actual structure in a rock mass, such as an underground opening, and (2) a model which simulates a

portion of a rock mass under varying stress and deformation conditions, such as a direct-shear test along a single joint.

The first type of model can be related or scaled to the prototype so that the requirement for knowing all applicable parameters is not as great as for the second type of model. The second type of model is useful for studying basic behavior of a rock mass. However, it is difficult to relate this directly to a field situation, where the boundary conditions are not completely defined. This type of test is particularly susceptible to minor boundary effects which do not simulate the prototype.

A series of tests with model openings would be useful for studying the deformations occurring at failure, and the support pressures required to maintain stability. (This type of test would not model the gravity-load condition.) The character of the discontinuities and the intact properties of the model rock mass can be varied to determine their effect on the mode of failure and the stability of the opening. The rock mass quality of the model could be evaluated by methods similar to those used in the field. Rapid loading of the model may prove feasible for determining its stability under dynamic conditions.

A natural continuation of the study of model joints would be the study of a multiple joint system, or a rock-block model. The loading of this model would be much more complex than the loading conditions for a single joint system.

Laboratory tests on intact specimens to determine strength and deformation properties under varying confining pressures and rates of loading will also provide information on rock failure. Strain rate tests on

samples with single joints would be useful for determining dynamic failure effects in a rock mass.

Finite Element Method

The finite element method is useful because of its general applicability to a wide range of boundary conditions and material properties. The solutions are useful for comparing continuum stress and deformation behavior with the real behavior of a given rock structure. The finite element method promises to be able to handle a variety of stress-strain and failure criteria. For example, it may be possible to cause extension fractures to form by applying some limiting strain criterion to the behavior of the medium. To simulate cracking or loosening of the rock mass, the strength and deformation properties can be reduced when the initial strength of the rock mass is exceeded. Solutions of this type depend heavily on field and laboratory observations for information on the material properties to be used in the equations.

Care must be taken in attempting to make a finite element (continuum) solution approximate the discontinuous behavior of a real rock mass. Although the theory may be able to handle some of the anisotropic properties of a jointed rock mass, it is difficult to make it handle the discontinuous movements along joint surfaces, which are often a controlling factor in rock mass behavior.

REFERENCES

Alexander, L. G., G. Worotnicki, and K. Aubrey, 1964. "Stress and Deformation in Rock and Rock Support, Tumut I and II Underground Power Stations", Australia-New Zealand Conference on Soil Mechanics and Foundation Engineering.

Clough, R. W., 1965. "The Finite Element Method in Structural Mechanics", in Stress Analysis, Zienkiewicz, O. C. and G. S. Holister, Eds., Wiley, pp. 85-119.

Cochrane, T. S., O. F. Carter, and K. Barron, 1964. "Studies of Ground Behavior in a Metal Mine", 4th Intl. Conf. on Strata Control & Rock Mech., H. Krumb Sch. of Mines, Columbia University, N. Y.

Davis, E. A., 1948. "Journal of Applied Mechanics", pp 216-221.

Deere, D. U., 1964. "Personal Communication".

Deere, D. U., A. J. Hendron, F. D. Patton, and E. J. Cording, 1967, "Design of Surface and Near-Surface Construction in Rock", 8th Symposium on Rock Mechanics, Minneapolis (in print).

Dutro, H. B., 1966. "Rock Mechanics Study Determines Design", Civil Engineering, ASCE, Vol. 36, No. 2.

Ege, John R., 1965. "Written Communication", USGS.

Emerick, W. L., 1963. "Written Communication", USGS.

Endersbee, L. A., and E. O. Hofto, 1963. "Civil Engineering Design and Studies in Rock Mechanics for Poatina Underground Power Station, Tasmania", Institution of Engineers, Australia, Journal, Vol. 35, No. 9, Sept. 1963, pp 187-209.

Fairhurst, C. and N. G. W. Cook, 1966. "The Phenomenon of Rock Splitting Parallel to the Direction of Maximum Compression in the Neighborhood of a Surface", 1st International Conference on Rock Mechanics, Lisbon, Portugal.

Grosvenor, Niles E. and John F. Abel, 1966. "Measurements on the Pilot Bore for the Straight Creek Tunnel".

Hartmann, Burt E., 1966. "Rock Mechanics Instrumentation for Tunnel Construction", Terrametrics, Inc., Colorado.

Hasselbacher, George E., 1951. "A Method for Determination of Stresses Around an Opening Under Impact Loads", An Introduction to the Design of Underground Openings for Defense, Quarterly Colorado School of Mines, Vol. 46, No. 1.

Hoyt, A. D., 1958. "Some Engineering Studies of Rock Movement in the Niagara Area", Engineering Geology Case Histories Number 3, Symposium on Rock Mechanics, Geological Society of America.

Houser, F. N. and F. G. Poole, 1961. "Written Communication", USGS.

Isaacson, E. de St. Q., 1958. "Rock Pressures in Mines", Mining Publications Ltd., London.

Jaeger, Charles, 1955. "Present Trends in the Design of Pressure Tunnels and Shafts", Part 4, Water Power.

Jaeger, J. C., 1962. "Elasticity, Fracture and Flow", John Wiley & Sons, Inc., New York , pp 190-193.

Julin, D. E., 1964. "Combatting Extreme Weight Problems at Climax", Proceedings 6th Symposium on Rock Mechanics, University of Missouri, Rolla, Missouri.

Lane, R. G. T. and J. W. Roff, 1961. "Kariba Underground Works Design and Construction Methods", 7th International Congress on Large Dams, Question No. 25, Paper No. R16, Rome.

Lang, T. A., 1957. "Rock Behavior and Rock Bolt Support in Large Excavations", Symposium on Underground Power Stations. American Society of Civil Engineers, Power Division, N. Y.

Lang, T. A., 1959. "Underground Experience in the Snowy Mountains--Australia."

Lang, T. A., 1964. "Rock Mechanics Considerations in Design and Construction", Proceedings 6th Symposium on Rock Mechanics, University of Missouri, Rolla, Missouri.

Merrill, R. H., 1954. "Design of Underground Mine Openings, Oil-Shale Mine, Rifle, Colorado", U. S. Department of the Interior, Bureau of Mines Report of Investigations 5089.

Merrill, R. H., 1957. "Roof-Span Studies in Limestone", U. S. Dept. of the Interior, Bureau of Mines Report of Investigations 5348.

Merrill, R. H., 1962. "Changes in Stress Concentration Created by Undercutting in Block Caving", U. S. Dept. of Interior, Bureau of Mines Report of Investigations 5999.

Merrill, R. H. and G. H. Johnson, 1964, "Changes in Strain and Displacement Created by Undercutting in Block Caving", 4th Intl. Conf. on Strata Control & Rock Mech., H. Krumb Sch. of Mines, Columbia University, N. Y.

Merrill, R. H. and T. A. Morgan, 1958. "Method of Determining the Strength of a Mine Roof", U. S. Dept. of Interior, Bureau of Mines Report of Investigations 5406.

Miller, R. P. and D. U. Deere, 1967. "Engineering Classification and Index Properties for Intact Rock", University of Illinois Engineering Experiment Station Bulletin, in press, Urbana, Illinois.

Missouri River Division, 1964. "Laboratory Tests on Granite, Piledriver Project", No. 64/90, Corps of Engineers, U. S. Army.

Monahan, C. J., 1964. "Personal Communication."

Monahan, C. J. and E. A. Sibley, 1965. "Rock Mechanics for Dworshak Dam", Geological Society of America, Annual Meeting.

Moruzi, G. A. and A. R. Pasieka, 1964. "Evaluation of a Blasting Technique for Destressing Ground Subject to Rockbursting", Proceedings 6th Symposium on Rock Mechanics, University of Missouri, Rolla, Missouri.

Moye, D. G., 1959. "Rock Mechanics in the Investigation and Construction of Tumut I Underground Power Station", Engineering Geology Case Histories No. 3, Symposium on Rock Mechanics, Geological Society of America.

Nadai, A., 1950. "Theory of Flow and Fracture of Solids", Vol. I, McGraw-Hill Book Co., New York, pp 175-228.

Obert, L., 1964. "In Situ Stresses in Rock, Rainier Mesa, Nevada Test Site, Operations Nougat and Storax", WT-1869, U. S. Bureau of Mines, College Park, Md.

Onodera, F. T., 1962. "Dynamic Investigation of Foundation Rocks In-Situ", Proceedings 5th Symposium on Rock Mechanics, University of Minnesota, Pergamon Press, New York, pp 517-533.

Ortlepp, W. D. and N. G. W. Cook, 1964. "The Measurement and Analysis of the Deformation Around Deep Hard-rock Excavations", 4th Intl. Conf. on Strata Control & Rock Mech., H. Krumb Sch. of Mines, Columbia University, N. Y.

Patton, F. D., 1966. "Multiple Modes of Shear Failure in Rock and Related Materials", Ph. D. Thesis, University of Illinois, Urbana, Illinois.

Pinkerton, I. L. and E. J. Gibson, 1964. "Tumut 2 Underground Power Plant", Proc. Amer. Soc. of Civil Engrs., Vol. 90, No. PO 1, Paper 3855. (Closure of Discussions 1966, Vol. 92, No. PO 1.)

Potts, E. L. J., 1964. "Current Investigations in Rock Mechanics and Strata Control", 4th Intl. Conf. on Strata Control & Rock Mech., H. Krumb, Sch. of Mines, Columbia University, N. Y.

Rabcewicz, L. V., 1955. "Bolted Support for Tunnels, Parts I and II", Mine and Quarry Engineering, March and April.

Rabcewicz, L. V., 1964. "The New Austrian Tunneling Method, Part I", Water Power.

Raphael, J. M. and R. W. Carlson, 1956. "Measurement of Structural Action in Dams", James J. Gillick and Co., Berkeley, California.

Reyes, S. F., 1966. "Elastic-Plastic Analysis of Underground Openings by the Finite Element Method." Ph.D. Thesis, University of Illinois, Urbana, Illinois.

Savage, J. L. and R. Rhoades, 1950. "Applications of Geology to Engineering Practice (Berkey Volume)", Geological Society of America, pp xi to xix.

Schilling, Adolph A., 1966. "Rock Mechanics Engineering: Boundary Project", ASCE Water Resources Engineering Conference, Conference Preprint 360.

Scott, J. H. and D. R. Cunningham, 1965. "Written Communication", USGS.

Scott, James J. and Jack Parker, 1964. "Instrumentation of Room and Pillar Workings in a Copper Mine of the Copper Range Company, White Pine, Michigan", Proceedings 6th Symposium on Rock Mechanics, University of Missouri, Rolla, Missouri.

Seely, F. B. and J. O. Smith, 1952. "Adv. Mech. of Materials", J. Wiley & Sons Inc., N. Y.

Serafim, J. L., 1961. "Internal Stresses in Galleries", Paper No. R1, 7th International Congress on Large Dams, Rome.

Seery, J. D., 1966. "Construction of Morrow Point Powerplant and Dams", ASCE Water Resources Engineering Conference.

Shannon and Wilson, Inc., 1964. "Personal Communication."

Spalding J., 1949. "Deep Mining", Mining Publications Ltd., London.

Stapeldon, D. H., 1961. "Geological Studies for the Planning and Construction of Tumut II Underground Power Station", Engineering Geology Report S. G. 86, Snowy Mountains Hydroelectric Authority, Thesis presented for M. Sc. degree, University of Adelaide.

Strandberg, Herbert V., 1966. "Design and Construction Features: Boundary Project", Proceedings of the American Society of Civil Engineers, Vol. 92, No. PO 2.

Taylor, Nelson W., 1947. "Journal of Applied Physics", Vol. 18, p 943.

Terzaghi, K., 1943. "Theoretical Soil Mechanics", J. Wiley and Sons, Inc., N. Y.

Terzaghi, K., 1945. "Stress Conditions for the Failure of Saturated Concrete and Rock", Proceedings ASTM, Vol. 45, pp 777-801. (Reprinted in "From Theory to Practice in Soil Mechanics", John Wiley and Sons, Inc., 1960, pp 181-196.)

Terzaghi, K., 1946. "In Rock Tunneling with Steel Supports", R. V. Proctor and T. L. White, Commercial Shearing and Stamping Co., Youngstown, Ohio.

Terzaghi, K., 1962. "Dam Foundation on Sheeted Granite", Geotechnique, Vol XII, No. 3.

Terzaghi, K., and F. E. Richart, Jr., 1952. "Stresses in Rock About Cavities", Geotechnique, Vol III, No. 2.

Timoshenko, S. and J. N. Goodier, 1951. "Theory of Elasticity", 2nd ed. McGraw Hill, N. Y.

Tincelin, E. and Sinou, P., 1964. "Control of Weak Roof Strata in the Iron Ore Mines of Lorraine", International Journal of Rock Mechanics and Mining Sciences, Vol. I, No. 3, May.

Underwood, L. B. and Carl J. Distefano, 1964. "Development of a Rock Bolt System for Permanent Support at NORAD", Proceedings, 6th Symposium on Rock Mechanics, University of Missouri, Rolla, Missouri.

Waddell, G. G., 1964. "Application of Instrumentation in Determining Rock Behavior During Stoping at the Star Mine, Burke, Idaho", Proceedings 6th Symposium on Rock Mechanics, University of Missouri, Rolla, Missouri.

APPENDIX A

ROCK MASS PROPERTIES

A.1 INTRODUCTION

To properly evaluate the performance of a structure in a rock mass and to relate performance from one site to another, an accurate description of the in-situ properties of the rock mass must be made. These properties will be suitable as an index of rock mass behavior if they are simple, quantitative, easily obtained from exploratory information, and related to the significant engineering properties of the rock mass. These criteria are satisfied by the rock mass quality indices developed and used during the exploration and construction of the three cavities. The indices aided in finding a suitable location for Cavity III (in the granite), and aided in estimating the strength and deformation characteristics of the rock surrounding all three cavities. During construction, several methods were used to determine rock mass quality. The rock mass quality indices thus determined were compared with the observed behavior of the rock around the cavities.

Rock mass properties can be separated into two components: the properties of the intact portion of the rock mass, which can be determined from laboratory tests on small specimens; and the properties of the discontinuities in the rock mass, which can be inferred from a quantitative description of the discontinuities. The intact properties establish an upper limit for the strength and deformation characteristics of a rock mass. Discontinuities in the rock mass reduce these properties to some

lower value. For rock containing few joints, the in-situ properties may closely approach the intact properties.

Simple laboratory tests on a variety of rock types were performed at the University of Illinois (Miller and Deere, 1967) in order to establish index properties for intact rock. A classification based on the strength and modulus of specimens tested in unconfined compression was developed. Other properties, such as tensile strength, triaxial strength (ϕ and c), unit weight, hardness, sonic velocity, and water content, are useful for obtaining a more complete picture of the intact characteristics of the rock.

The properties of the discontinuities cannot be easily determined from direct tests; however, quantitative descriptions of the discontinuities can be used as index properties if relations can be established with the observed rock mass behavior. Rock mass quality indices were developed which quantitatively describe the character of the discontinuities in the rock mass (Deere, Hendron, Patton, and Cording, 1967). Two of the indices are the Rock Quality Designation (RQD) and fracture frequency, described in Section A.3. Seismic velocity and attenuation characteristics can also be used to estimate rock mass quality. An approximate relation between seismic refraction velocity and rock mass quality was obtained in the tuff cavities (described in Chapter 2). A correlation between the amplitude of the signal of a sonic logger and rock mass quality was established in the granite (Cavity III) and is described in Section A.3.

A correlation between rock mass quality and deformation modulus was

established at Dworshak Damsite, Idaho. It was found that jointing reduced the in-situ deformation modulus to some fraction of the intact modulus. This relation was used to estimate the deformation modulus in the granite cavity (Cavity III).

The correlation between rock mass quality and in-situ strength is not as easily obtained. The in-situ strength has, as an upper limit, the intact strength of a specimen, and, as a lower limit, the residual strength along a smooth joint plane. However, the actual strength is dependent on the orientation of joints and the amount of displacement occurring along the joints.

In this appendix, most of the emphasis is placed upon the cavity in granite, because its behavior was very dependent upon the properties of the jointed rock mass, which could be determined only in the field. The behavior of the cavities in the relatively unjointed tuff could be predicted to a large extent by means of its intact properties, as described in Chapter 2.

A.2 INTACT PROPERTIES OF THE GRANITE

Unconfined compression tests were performed at the University of Illinois on NX core samples taken from hole U-1, at the center of the plane face of Cavity III. (Cavity III was located at a depth of 350 feet in the Climax Stock, which is predominantly a quartz monzonite.) Four tests were performed on unweathered specimens; and two tests were performed on slightly weathered specimens taken from a zone bounded by iron-stained joints. Sonic compressional pulse velocity measurements were made while the specimens were axially loaded between 0 and 5000 psi. After the load was cycled to 5000 psi, the pulse transducers were removed

and the specimens were loaded to failure. Test results are summarized in Table A.1. Typical stress-strain behavior is shown in Figs. A.1, A.2, and A.3.

The velocity tests proved useful for determining the quality of the core samples. Two of the specimens exhibited almost no velocity change as they were loaded from 0 to 5000 psi. These samples were unweathered and uncracked and had a high strength. As the weathered samples and the cracked samples were loaded, the velocity increased from an initial low value. The increase can be attributed to the closure of microcracks under the increased axial load applied to the specimens. As a result of the cracking, the strength of these specimens was lower than the strength of the unweathered specimens.

Even though the strength varied, the modulus of all four of the unweathered specimens was quite consistent, ranging from 10.1×10^6 psi to 11.0×10^6 psi. The slight cracking which occurred in two of the specimens did not affect the modulus. However, the modulus of the weathered specimens was decreased in proportion with its strength, below the values determined for the unweathered specimens.

Samples from the Climax Stock were also tested by the Missouri River Division Laboratory of the Corps of Engineers (1964). Quartz monzonite NX core samples were taken from a depth of 1000 feet in the Stock. Young's modulus in unconfined compression was the same as the modulus determined for the Cavity III samples, but the strength was slightly higher than the strength of the Cavity III samples.

Triaxial tests were performed on intact specimens and on specimens with natural and sawed joints. (The upper limit of the rock mass strength

TABLE A.1

INTACT PROPERTIES, QUARTZ MONZONITE, CAVITY III, HOLE U-4, UNCONFINED COMPRESSION TESTS

Depth, Feet and Sample Number	Description	V_o fps	V_{5000} fps	E_t ($\times 10^6$ psi)	σ_{ult}, psi	E_t/σ_{ult}	γ pcf	Intact Classification
35(a)	Quartz monzonite, unweathered, uncracked	21,300	21,500	10.1	26,600	380	168	
42.5		20,600	21,600	10.6	26,600	400	167	
Average		21,000	21,600	10.4	26,600	390	167	High strength, average modulus ratio
35(b)	Quartz monzonite, unweathered, slightly cracked	21,200	20,800	11.0	10,700	1030	167	
50.6		16,800	22,400	10.6	18,500	570	167	
Average		19,000	21,600	10.8	14,600	800	167	Medium strength, high modulus ratio
14.5(a)	Quartz monzonite, slightly altered, bounded by joints with heavy limonite strains	16,800	20,400	4.7	7,600	618	168	
14.5(b)		14,200	21,400	8.8	13,100	677	164	
Average		15,500	20,900	6.8	10,300	647	166	Medium strength, high modulus ratio

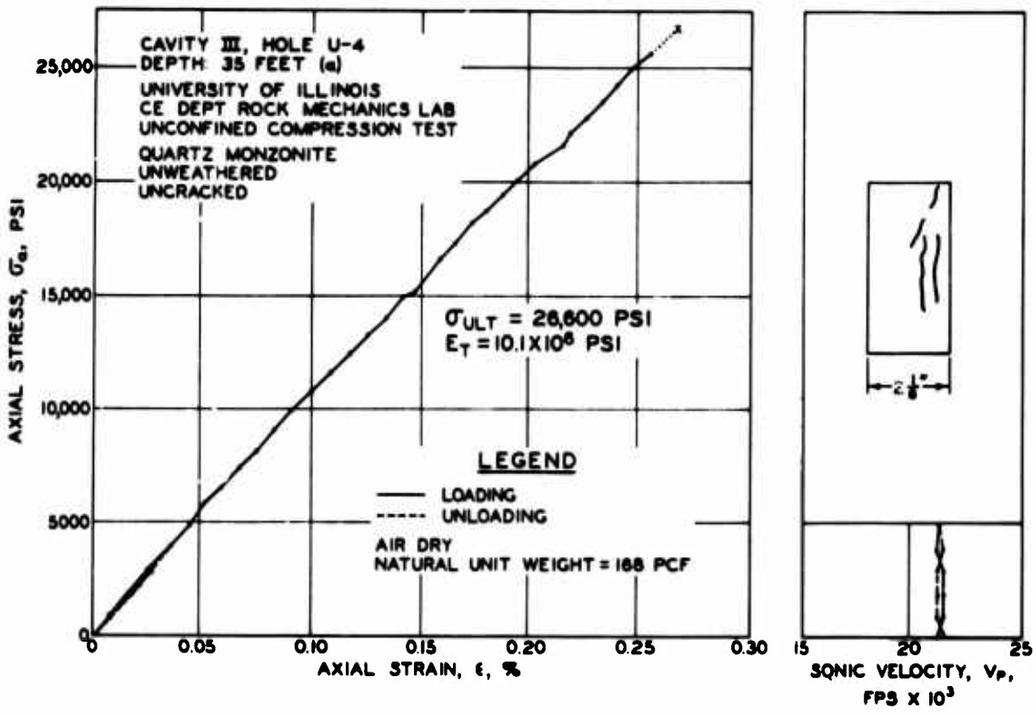

Fig. A.1. Typical unconfined stress-strain behavior; intact granite specimen

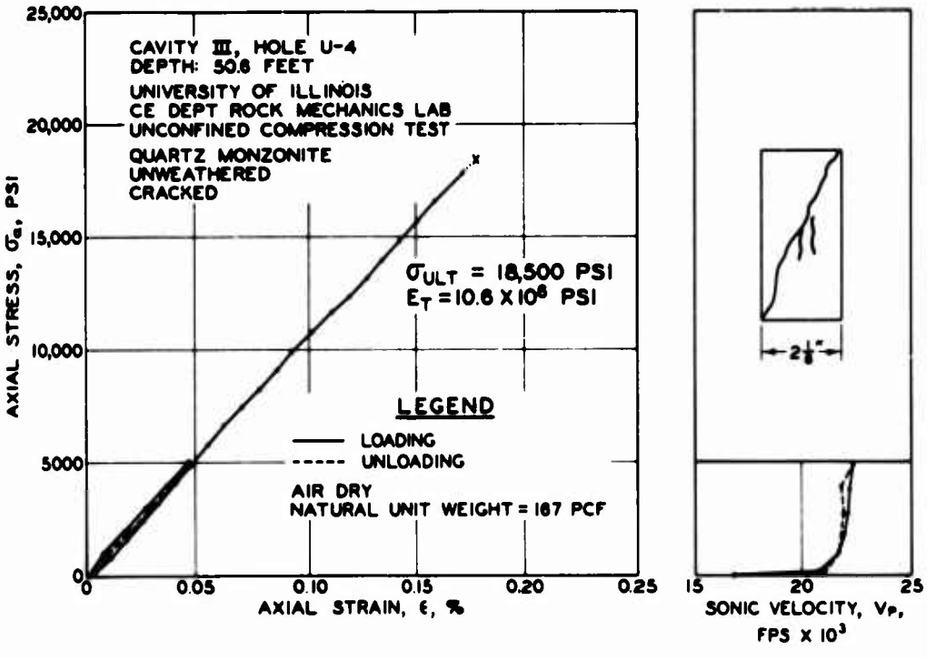

Fig. A.2. Typical unconfined stress-strain behavior; unweathered, slightly cracked granite

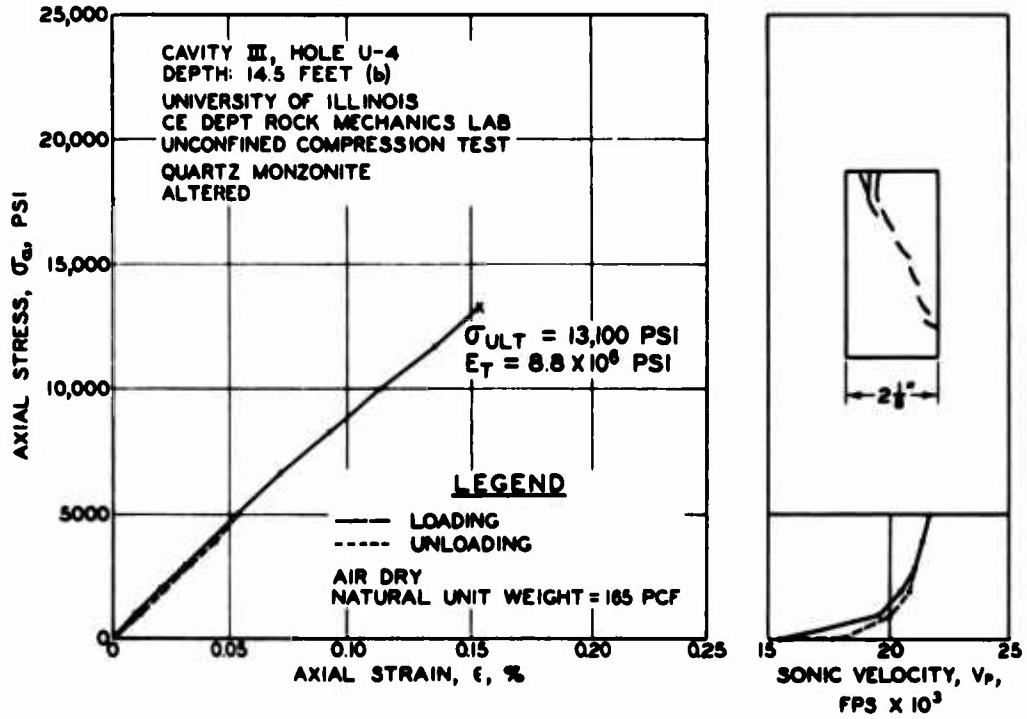

Fig. A.3. Typical unconfined stress-strain behavior; slightly cracked granite specimen

is determined by the strength of the intact specimen, the lower limit by the strength along the sawed joint.) Direct tension tests were also performed; the results are summarized in Table A.2. The strength and modulus determined from the unconfined compression tests on the Climax Stock quartz monzonite have been plotted in Fig. A.4, on the Engineering Classification for Intact Rock chart developed by Miller and Deere (1967).

With less cracking, the strength of the unweathered quartz monzonite samples is increased, but the modulus remains constant; therefore, the progression of data points is horizontal across the chart, from a high modulus ratio (for the cracked, medium-strength samples from Cavity III) to an average modulus ratio (for the uncracked, high-strength samples from the 1000-foot depth). The unweathered, uncracked samples were considered representative of the intact properties of the granite in the vicinity of Cavity III. The rock was classified as a high-strength rock of average modulus ratio.

Average values of strength and modulus for tuff samples are also plotted on the chart. The intact tuff is described as a very low-strength rock of average modulus ratio.

A.3 ROCK MASS PROPERTIES OF THE GRANITE

Development of Rock Mass Quality Indices During Exploration for Cavity III

During the initial exploration for the cavity site, a Rock Quality Designation (RQD) was proposed by Deere (1964) as a means of determining rock mass quality from the study of rock core. The RQD is a modified core recovery percentage in which only the pieces of sound core over 4 inches in length are counted as "recovery." The smaller pieces are considered

TABLE A.2

LABORATORY TESTS, QUARTZ MONZONITE,
MISSOURI RIVER DIVISION LABORATORY,
U. S. ARMY CORPS OF ENGINEERS

Porosity, 0.20% Natural Unit Weight, 166 pcf

Type of Test	E_t psi × 10^6	Poisson's Ratio μ	Ultimate Strength psi	Strain at Failure ϵ_f, %
Direct tension (8 tests)	8.5	--	1,450	0.020
Unconfined compression (7 tests)	10.4	0.27	30,500	0.30
Triaxial compression (approximately 6 tests at each confining pressure)				
150 psi	11.7	--	32,700	0.33
450 psi	11.7	--	36,300	0.37
1350 psi	11.4	--	46,050	0.58

$$\frac{\sigma_{ult(unconfined)}}{T(tensile\ strength)} = 21$$

$$E_T/\sigma_{ult} = 340 \text{ (Modulus Ratio)}$$

$$\phi(\text{sawed joint}) = 28^\circ$$

$$\phi(\text{natural joint}) = 31^\circ$$

$$\phi(\text{intact}) = 56^\circ \text{ (for range of confining pressure: 150 to 1350 psi)}$$

$$C(\text{intact}) = 4000 \text{ psi}$$

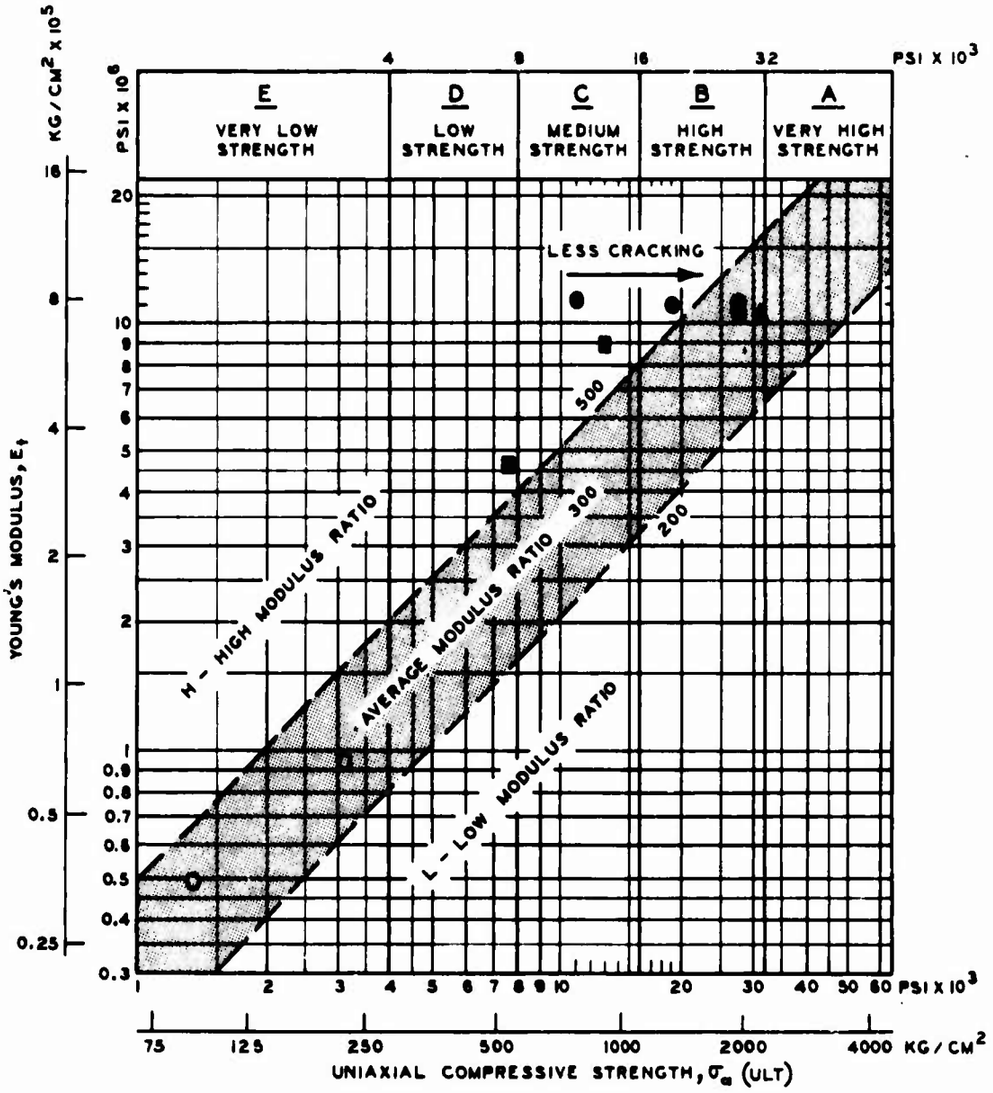

TUFF

- □ AIR DRY
- ○ NATURAL WATER CONTENT

QUARTZ MONZONITE

- ● CAVITY III, UNWEATHERED
- ■ CAVITY III, WEATHERED
- ▲ 1000' DEPTH, UNWEATHERED

NOTE: E_t = TANGENT MODULUS AT 50% ULTIMATE STRENGTH.

Fig. A.4. Engineering classification for intact rock

to be due to close shearing, jointing, faulting, or weathering in the rock mass. The RQD provided a preliminary estimate of the variation of the in-situ rock properties from the properties of a "sound" portion of the rock core. Thus, a general estimate of the engineering behavior of the rock mass could be made.

A proposed correlation of RQD with a qualitative description of rock mass quality is as follows:

	RQD	Description
I	100-90%	Excellent
II	75-90%	Good
III	50-75%	Fair
IV	25-50%	Poor
V	0-25%	Very poor

The results obtained with the RQD in the initial exploration of the cavity compared closely with a system developed at the same time by Ege (1965) which rated the core on the basis of fracture frequency, core recovery, degree of weathering, and competency based on hardness and degree of breakage.

The rock mass quality estimates described above were used to locate a zone of high-quality rock which would not create support problems during the construction of the cavity. Exploratory NX core holes were drilled from the surface, and the rock mass quality was determined. One site was rejected because the rock was heavily jointed and weathered (the rock mass quality was poor to fair).

At the second site, the NX core indicated that the proposed cavity

location was in a zone having a good rock mass quality. Fig. A.5 shows the variation of rock mass quality at this site.

Determination of Rock Mass Quality Indices During Construction of Cavity III

During excavation of Cavity III, rock mass quality was determined by logging along lines on the surface of the openings, as well as by logging of the NX core. (The rock mass quality determined in the cavity is presented in Fig. A.6.) Average RQD values obtained from the NX core compared closely with the values obtained along the surfaces of the drift and the cavity (refer to Tables A.3 and A.4). During logging along the walls of the opening, the rock mass quality was found to be affected by the orientation of the walls with respect to the orientation of the predominant joint systems. Rock mass quality was higher when measured on walls parallel to the joint system (RQD = 85%) than when measured across the joint system (RQD = 63%). The average RQD for all orientations of the walls was 73%. An average RQD of 75% was determined from the study of the NX core. The core was obtained from four 50-foot holes drilled perpendicular to the predominant joint system, on the plane face of Cavity III. (Core taken parallel to the jointing will often exhibit a low rock mass quality; when the core hole intersects a parallel fracture, excessive breakage may occur as the fracture is loosened and the rock is broken by the rotating core barrel.)

Fracture frequency and the RQD are closely related, particularly for a rock mass degraded by fracturing alone. The correlation between RQD and fracture frequency is shown in Fig. A.7. The NX core was obtained from four different sites, in four different rock types. The figure shows

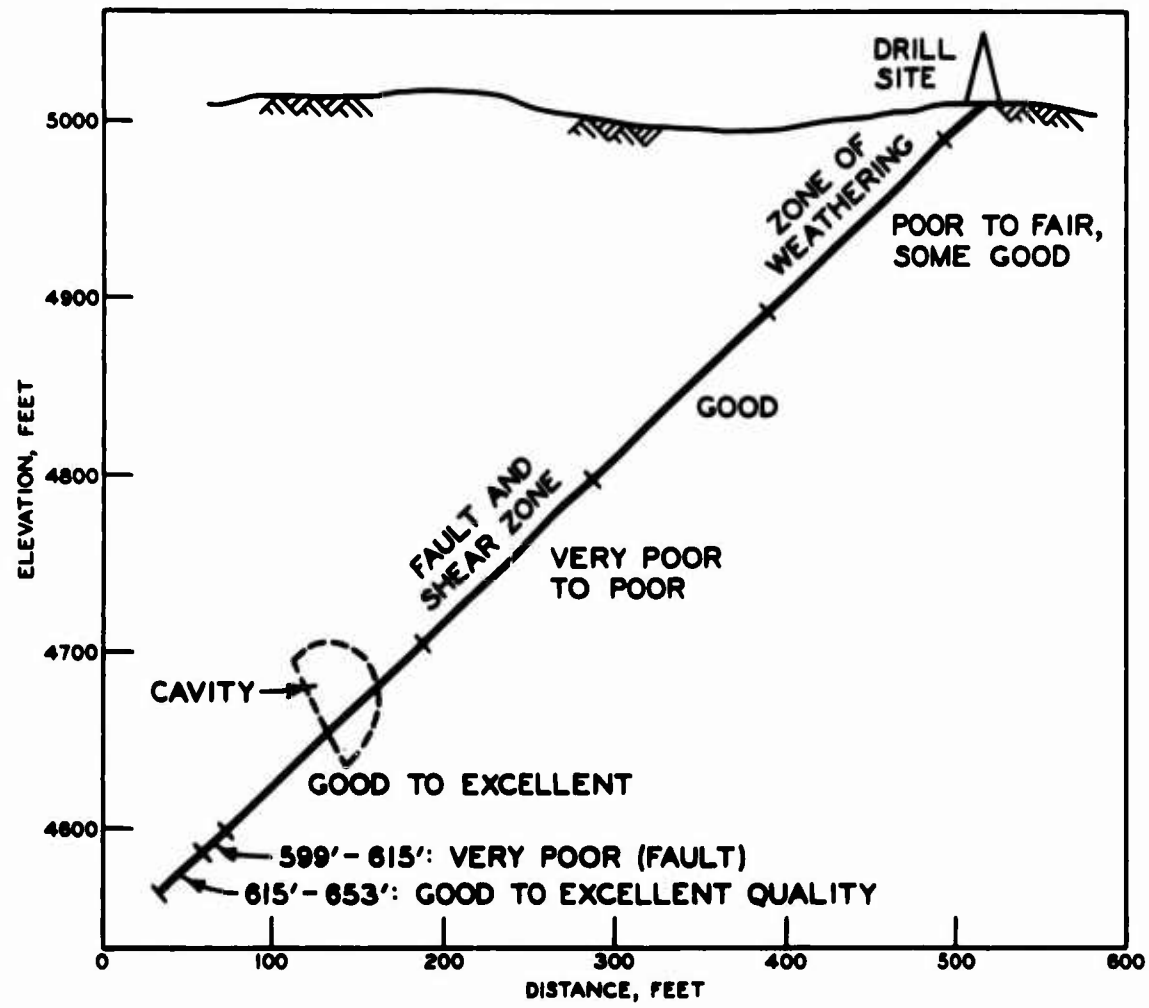

Fig. A.5. Rock mass quality determined during exploration for Cavity III site

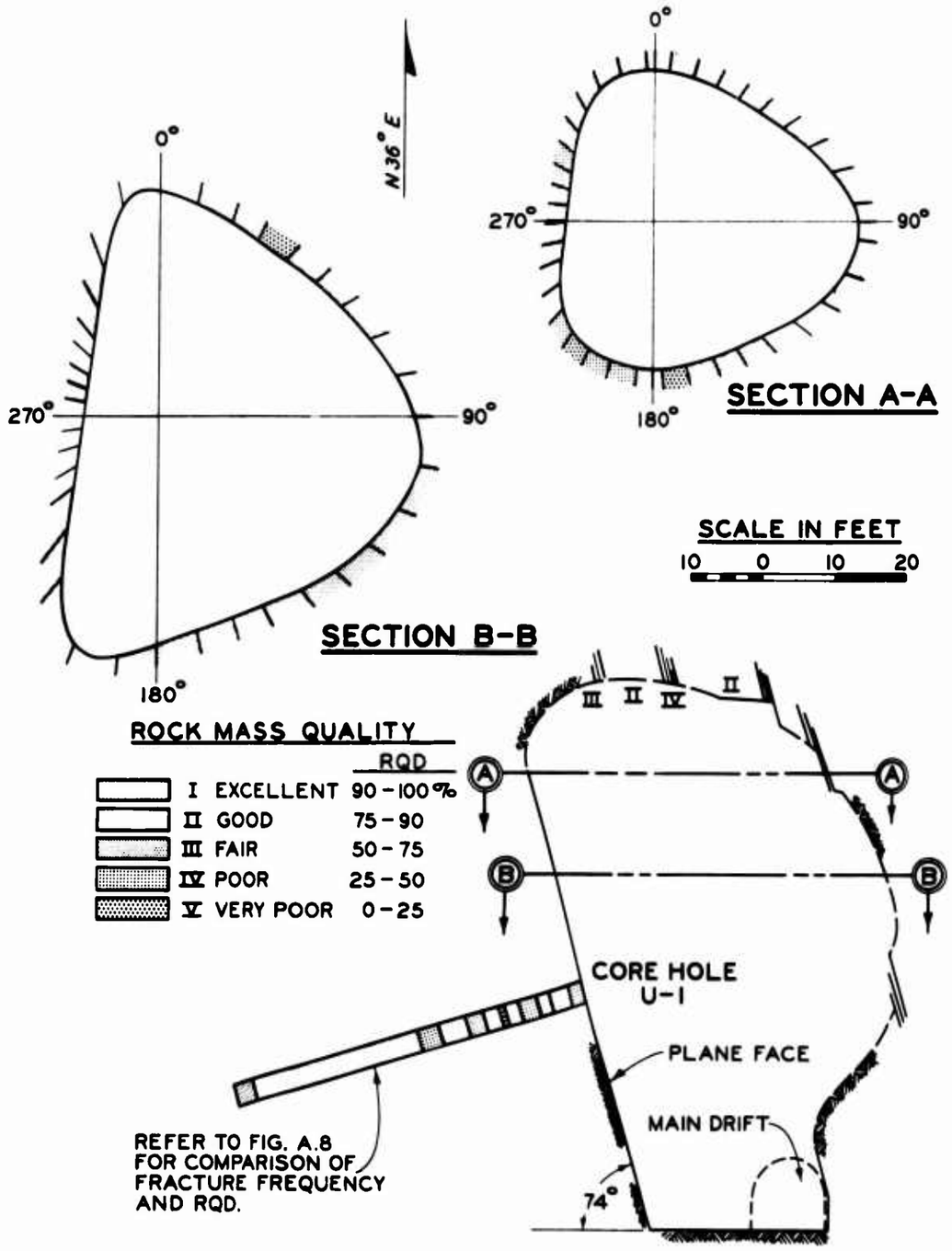

Fig. A.6. Rock mass quality in Cavity III

TABLE A.3

ROCK QUALITY IN GRANITE; DRIFT AND CAVITY SURFACES

Location	Direction with Respect to Jointing	Fracture Frequency fractures/ft	RQD %	Classification
		Drift, Station 1+50		
Line 1	Perpendicular	3.3	62	III
Line 2	Perpendicular	2.7	77	II-III
Line 3	Parallel	2.3	81	III
		Drift, Station 2+00		
Line 4	Perpendicular	2.7	69	III
Line 5	Parallel	1.0	95	I
Average for drift	Perpendicular	2.9	69	III
	Parallel	1.6	88	II-I
	Average	2.2	78	II
		Cavity, Horizontal Section I		
70°-110°	Parallel	1.4	90	I
130°-220°	Perpendicular	2.9	69	III
220°-290°	Parallel	2.3	76	II
290°-300°	Parallel	3.0	44	IV
	Average	2.3	71	III-II
		Cavity, Horizontal Section II		
70°-90°	Parallel	1.8	93	I
90°-120°	Parallel	2.4	67	III
120°-170°	Perpendicular	3.6	58	III
170°-180°	Perpendicular	1.5	96	I
190°-340°	Parallel	1.7	92	I
0°-60°	Perpendicular	3.5	56	III
20°-30°	Perpendicular	>6.0	10	V
Average for Section II	Parallel	2.0	82	II
	Perpendicular	3.7	54	III
	Average	2.8	68	III
Average; drift and cavity surface	Parallel	1.8	85	II
	Perpendicular	3.2	63	III
	Average	2.5	73	III-II

TABLE A.4

ROCK QUALITY IN GRANITE; CORE HOLES

Core Hole	Fracture Frequency Fractures/ft	RQD %	Classification
U-1, 0-24'	3.5	67	III
U-1, 24-50'	1.7	90	I-II
U-1, average	2.6	78	II-III
U-2, average		70	III
U-3, average		75	II-III
U-4, average		76	II-III
Average all core holes		75	III-II

Note: Core holes are located at center of plane face, perpendicular to predominant joint system.

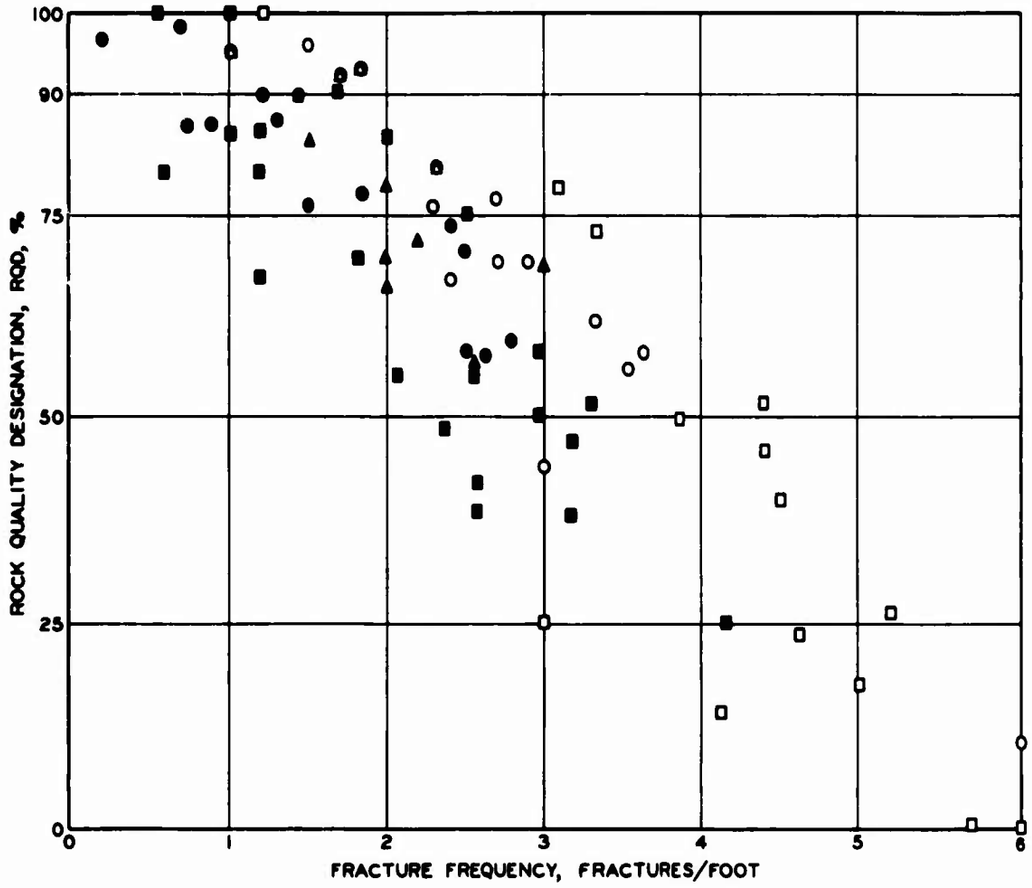

Fig. A.7. Correlation of rock quality designation and fracture frequency (see also Deere, Hendron, Patton, and Cording, 1967)

that an RQD of 100% correlates with a fracture frequency of approximately one fracture per foot, and that RQD's near zero are comparable to fracture frequencies of 5 and 6 fractures per foot. Fracture frequencies greater than 6 have very little additional significance; they are assumed equal to 6 on the plot.

The RQD is a more general estimate of core quality than the fracture frequency. In addition to fracturing, the RQD also evaluates weathered zones, very soft or unsound rock, and core loss. Thus, in rock containing these zones, the RQD is a better means of estimating the overall quality of the rock mass than the fracture frequency.

RQD and fracture frequency evaluate fractures in the core caused by the drilling process, as well as natural fractures previously existing in the rock mass. For example, when the core hole penetrates a fault zone or a joint, additional breaks may form which, although not natural fractures, are caused by the natural fractures and weaknesses existing in the rock mass. These breaks should be included in the estimate of rock quality. However, some fresh breaks occur during drilling and handling of the core which are not related to the quality of the rock mass. The ability of the driller will affect the amount of breakage and core loss which occurs. Poor drilling techniques will "penalize" the rock by lowering its apparent quality.

It is difficult to distinguish between drilling breaks and those natural and incipient fractures which reflect the quality of the rock mass. In certain instances it may be impossible to distinguish between the natural fractures and the drilling breaks. In this case, it may be necessary to include all fractures when estimating the RQD and fracture

frequency. Obviously, some judgment is involved in the core logging.

Similarly. during logging along the surface of an opening, both natural fractures and the fractures induced by excavation should be counted in the determination of RQD or fracture frequency.

It should be noted that fracture frequency is not equivalent to the average frequency of joints in a given joint system. For instance, in the granite, the joint spacing was approximately 1 to 2 feet, while the fracture frequency was approximately 2.5 fractures per foot.

Another difficulty in the use of the RQD and fracture frequency is that they are not very sensitive to the degree of openness of individual joints, whereas in some instances, the in-situ deformation modulus may be strongly affected by the openness of the joints. In certain instances, it may be advisable to account for the openness of joints by decreasing the RQD.

Correlation of Rock Mass Quality and Sonic Logging Test Results

Rock mass quality can also be determined from seismic tests. The correlation of velocity with the rock mass quality in the tuff is described in Chapter 3. The attenuation and dispersion of a seismic signal have also been suggested as an index for evaluating rock mass quality. A simple attenuation method was used during sonic logging of 8-inch-diameter, water-filled boreholes in the granite cavity. The logging was performed in order to determine the location of fault and fracture zones behind the plane face of the cavity.

The tests were performed by Welex using an Otis Model 303 Sonic Logging Instrument consisting of a transmitter and receiver spaced

50.5 inches apart. Centering of the tool in the 8-inch-diameter holes was accomplished with spring-steel centralizers attached to each end of the tool. Prior to testing, the holes were plugged at their lower end and filled with water; this provided acoustic coupling of the logging tool to the rock surface. The tests were performed by pushing the tool to the bottom of the water-filled hole, then pulling it to the surface, stopping every foot to pulse the sonic tool and obtain a response-time record.

The amplitudes of the signal recorded on each response-time record were determined. The amplitudes obtained at the different depths were then compared. (A constant energy input was maintained during the testing in the boreholes, permitting a comparison of amplitudes from different depths.) The amplitude of the signal correlated well with the quality of the NX core taken from the same location (Fig. A.8). The regions of low energy return are indicative of fault or fracture zones in the rock.

Correlation of Rock Mass Quality with Stability of an Opening

During the exploration for Cavity III, the rock mass quality indices were used to locate zones where the rock mass properties would be favorable for underground construction. The primary concern was that the cavity would be stable without causing excessive support problems. Thus, in a general way, the quality indices were used to estimate the strength properties of the rock mass.

During excavation of the 10-foot drifts, support was required when fault sets paralleled the drift and intersected the crown of the cavity. Light steel sets with wood logging were used to support the loose,

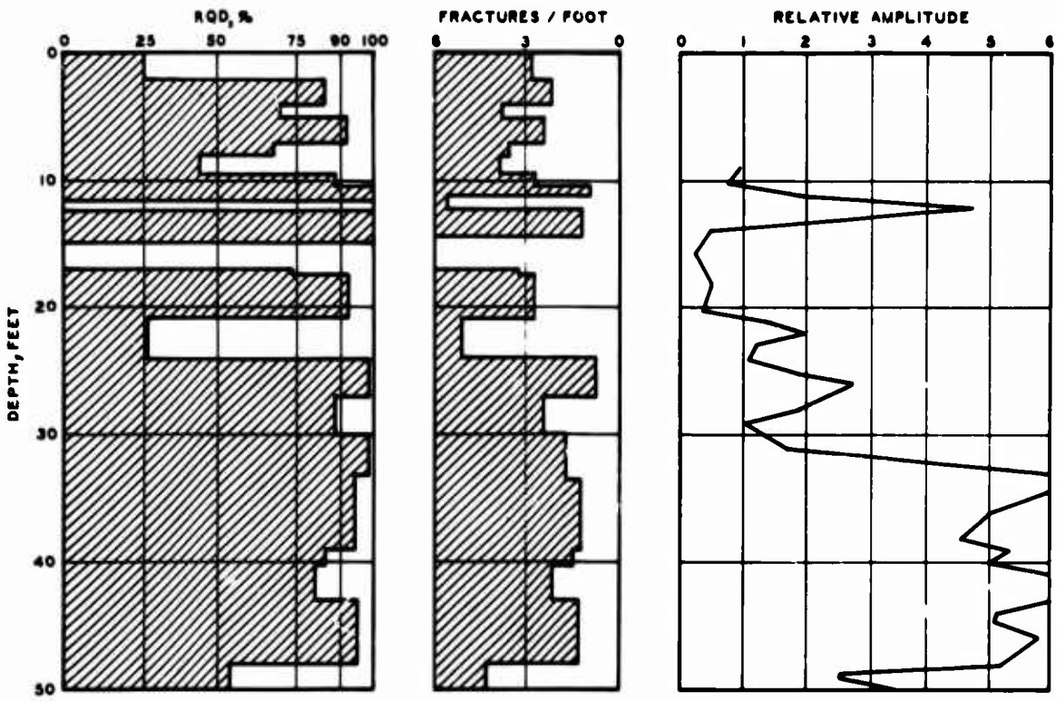

Fig. A.8. Correlation of sonic log amplitude and rock mass quality indices (see also Deere, Hendron, Patton, and Cording, 1967)

gravity-loaded rock in the crown. In the immediate vicinity of the faults, rock mass quality was poor to very poor. In zones of good to excellent rock, the only supports required were a few 6-foot bolts to pin occasional loose slabs. Thus, it can be seen that an approximate correlation exists between rock mass quality and stability of an opening. However, the orientation of the discontinuities with respect to the orientation of the opening is also an important factor affecting stability.

In attempting to relate rock mass quality to the stability of an opening it must be realized that stability is not a rock mass property, but a combination of the boundary conditions around the opening (the state of stress, and the geometry of the opening and the supports) and the strength-deformation properties of the rock mass.

Correlation of Rock Mass Quality with Deformation Modulus

Rock mass quality indices can be used to obtain a preliminary estimate of the deformation modulus of a rock mass. The deformation modulus of the granite was some fraction of its intact modulus; this fraction was related to the degree of jointing in the rock mass--the rock mass quality.

The magnitude of the deformation modulus in the granite was determined using a correlation between deformation modulus and rock mass quality established at Dworshak Damsite, Idaho. For the average RQD of 75%, the deformation modulus, E_r, in the granite was estimated to be 0.4 times the intact modulus, E_t. (Therefore, $E_r = 4 \times 10^6$ psi.)

The correlation between rock mass quality and deformation modulus at Dworshak Damsite is described in Section A.4.

A.4 CORRELATION OF ROCK MASS QUALITY AND DEFORMATION MODULUS AT DWORSHAK DAMSITE

A comparison of rock mass quality indices and deformation modulus was made at Dworshak Damsite, Orofino, Idaho, located in a high-strength granite gneiss of excellent rock mass quality. The quality indices provided a means of explaining the variations in deformation modulus obtained from plate jack tests performed at the site. A correlation between rock mass quality and deformation modulus was obtained and was used to predict the in-situ deformation modulus in the granite of Cavity III, at the Nevada Test Site.

A total of 24 vertical and horizontal plate jack tests were performed in unlined adits in the rock abutments of the dam by Shannon and Wilson, Inc., for the U. S. Army Corps of Engineers, Walla Walla District (Monahan and Sibley, 1965). The tests were performed using 34-inch-diameter Freyssinet pressure pads to provide a uniform pressure on the rock surface. Both surface deflections and the deflections of buried extensometers (Carlson jointmeters) were recorded. The buried extensometers extended from approximately 1 or 2 feet to 18 feet beneath the surface. Elastic theory was used to determine the deformation modulus from the pressure-deflection relations for both surface and buried gages. Twenty feet of NX core was obtained from beneath each jack test location. Unconfined compression tests were performed on the intact core specimens (Monahan, 1964; Shannon and Wilson, Inc., 1964).

Fracture frequency and RQD have been determined from the NX core and compared with the plate jack deformation modulus. For each jack test, the secant deformation modulus for the complete loading cycle to

1000 psi has been used. Separate moduli were determined for the surface and the buried deflection gages.

The near-surface fractures were more highly stressed and had a much greater effect on the deflection of the plate than the deeper fractures. Therefore, in order to compare the rock mass quality indices with the corresponding plate jack deformation modulus, it was necessary to weight the quality indices by the Boussinesq stress distribution beneath the plate. Fig. A.9 shows the variation in the quality indices with depth beneath one of the plate jacks, and illustrates the weighting technique used. The weighted RQD for the buried gage was 85%, corresponding to a deformation modulus of 6.0×10^6 psi. For the surface gage determination, the effect of fracturing around the opening reduced the RQD to 60%, and the deformation modulus to 1.4×10^6 psi.

In Fig. A.10 the deformation moduli have been plotted against the RQD's determined at all jack test locations. The deformation modulus (E_r) was normalized by the intact modulus (E_t). E_t was determined from the core specimens obtained at each jack test location. Variations in E_r/E_t were therefore a function of the rock mass properties and not dependent on intact properties. (The intact modulus was approximately 9×10^6 psi and did not vary greatly across the site.)

From Fig. A.10 it is apparent that the deformation modulus determined from the buried gages was consistently higher than the modulus obtained with the surface gages. Most of the buried gages had an RQD greater than 80% and E_r/E_t greater than 0.50. Most of the surface gages had an RQD less than 80% and E_r/E_t less than 0.60.

Even though the undisturbed granite gneiss at Dworshak was an

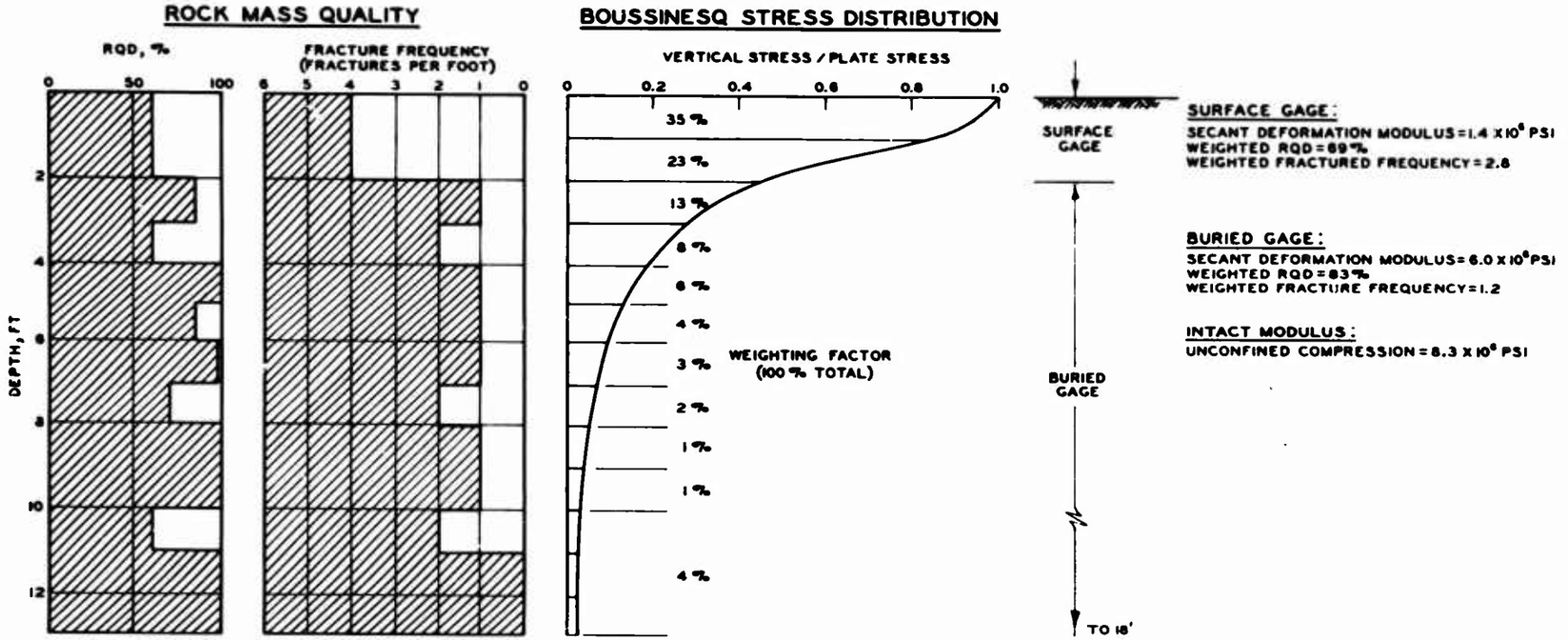

Fig. A.9. Variation of rock mass quality and elastic stress distribution with depth beneath typical plate jack test location, Dworshak Damsite (see also Deere, Hendron, Patton, and Cording, 1967)

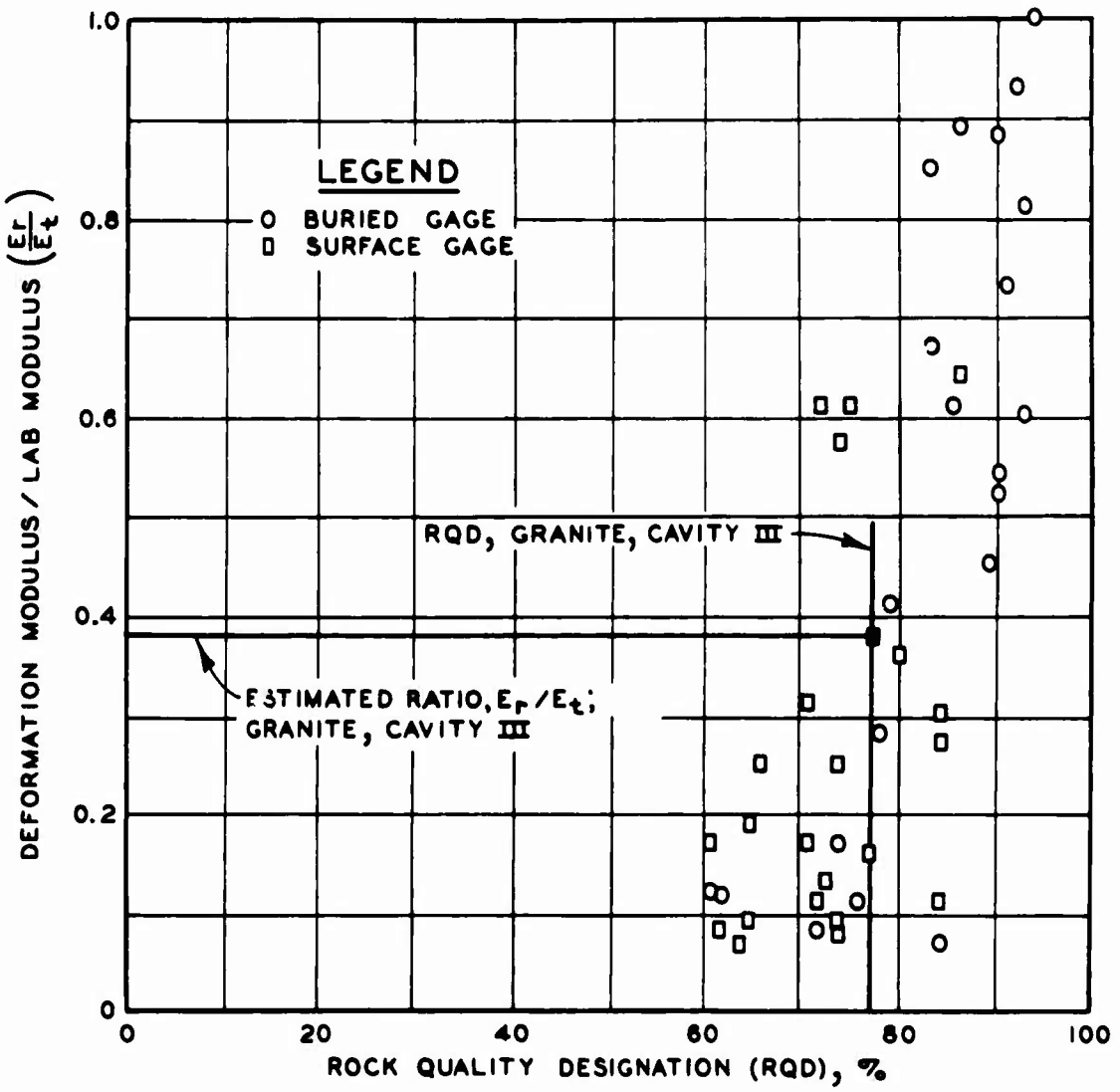

Fig. A.10. Correlation of plate jack deformation modulus with rock mass quality, Dworshak Damsite

excellent-quality rock, it is apparent that wide variations occurred in the deformation modulus determined from the plate jack tests. The purpose of the in-situ tests was to determine the deformation modulus of the dam foundation. However, it would be quite difficult to estimate a deformation modulus for the foundation strictly on the basis of the jack test results, without accounting for the character of the rock and the local geometry in the vicinity of the jack test site. The surface gages were strongly affected by near-surface fractures caused by excavation of the adits. The modulus determined from the surface gage information was therefore unsatisfactory for application to a dam foundation having a much higher overall rock mass quality. The best estimate of the dam foundation modulus appears to be the modulus determined from the buried gages. The RQD for these gages corresponds most closely to the overall quality of the foundation. By entering the graph in Fig. A.10 with the average RQD determined from exploratory drilling across the dam foundation, an estimate of the foundation deformation modulus can be obtained. In a similar manner, the deformation modulus at other sites can be determined, if the relationship shown in Fig. A.10 can be assumed to have general applicability. The average RQD of 75% for the granite cavity was substituted into this relation, and E_r/E_t was determined to be 0.4.

It is apparent from Fig. A.9 that a few fractures near the surface have a strong effect on the calculated RQD. The plate jack stresses such a small volume of rock that a small error in estimating the number of near-surface joints can cause considerable scatter in the data plotted in Fig. A.10.

Another inaccuracy in the rock mass quality indices is that they do

not account for the thickness of the joints. Most of the fractures observed in the Dworshak core were hairline, but some were slightly open. The slightly open joints would cause a reduction in the deformation modulus, even though the RQD remains high. Slightly open joints were observed with a borehole camera in the core holes beneath the plate jacks (Monahan, 1964). In the graph of Fig. A.10, most of these points were concentrated on the right side, indicating a high RQD for a low modulus. Accounting for the open joints would reduce the RQD and result in a better fit of the data.

APPENDIX B

EXTENSOMETER DISPLACEMENT-DEPTH RELATIONS, CAVITIES I AND II

The displacement-depth relations for the extensometers installed in Cavities I and II are presented in this appendix. The extensometers are designated according to their location in the cavities and according to the number assigned upon installation of the unit. For example, extensometer No. II-D-1 (7SI) is located in Cavity II, on the plane face (D), and is referred to in the main text as extensometer II-D-1. It was the seventh extensometer unit installed in Cavity II and is a multiple-position unit (SI). Extensometer No. I-D (14R) is located in Cavity I on the plane face (D) and is not included in the main text. It was the fourteenth unit installed in Cavity I and is a single-position extensometer (R).

The anchor depths marked with an asterisk in Figs. B.1-B.32 indicate that the anchor at that depth was not functioning properly; therefore, the readings were not recorded.

Extensometer units were installed normal to the cavity surface, unless otherwise indicated in the figure.

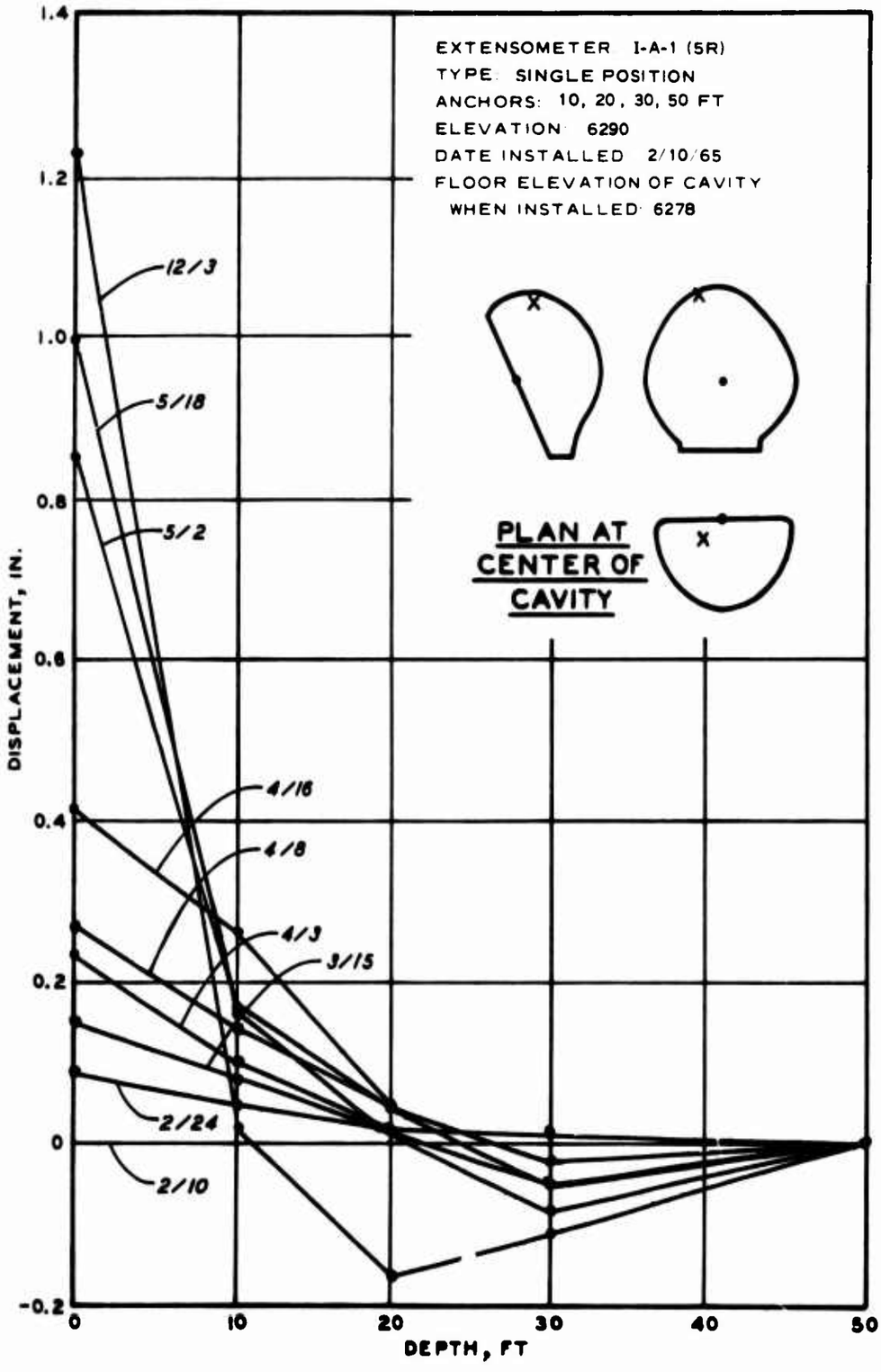
EXTENSOMETER I-A-1 (5R)
TYPE SINGLE POSITION
ANCHORS: 10, 20, 30, 50 FT
ELEVATION 6290
DATE INSTALLED 2/10/65
FLOOR ELEVATION OF CAVITY
WHEN INSTALLED 6278
PLAN AT CENTER OF CAVITY
12/3
5/18
5/2
4/16
4/8
4/3
3/15
2/24
2/10
DISPLACEMENT, IN.
DEPTH, FT
1.4
1.2
1.0
0.8
0.6
0.4
0.2
0
-0.2
0
10
20
30
40
50

Fig. B.1

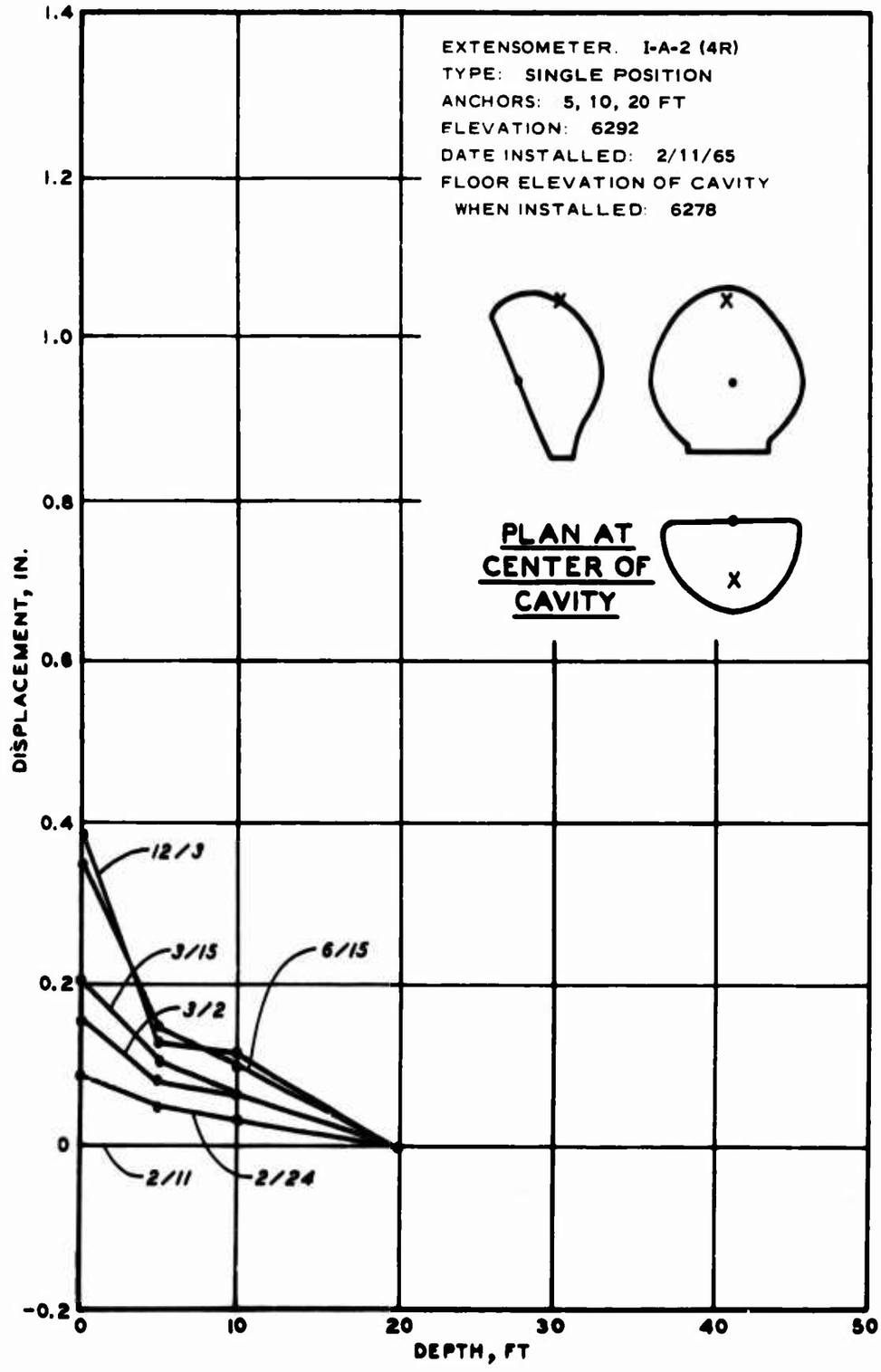
EXTENSOMETER. I-A-2 (4R)
TYPE: SINGLE POSITION
ANCHORS: 5, 10, 20 FT
ELEVATION: 6292
DATE INSTALLED: 2/11/65
FLOOR ELEVATION OF CAVITY
WHEN INSTALLED: 6278
PLAN AT CENTER OF CAVITY
DISPLACEMENT, IN.
1.4
1.2
1.0
0.8
0.6
0.4
0.2
0
-0.2
0
10
20
30
40
50
DEPTH, FT
12/3
3/15
6/15
3/2
2/11
2/24

Fig. B.2

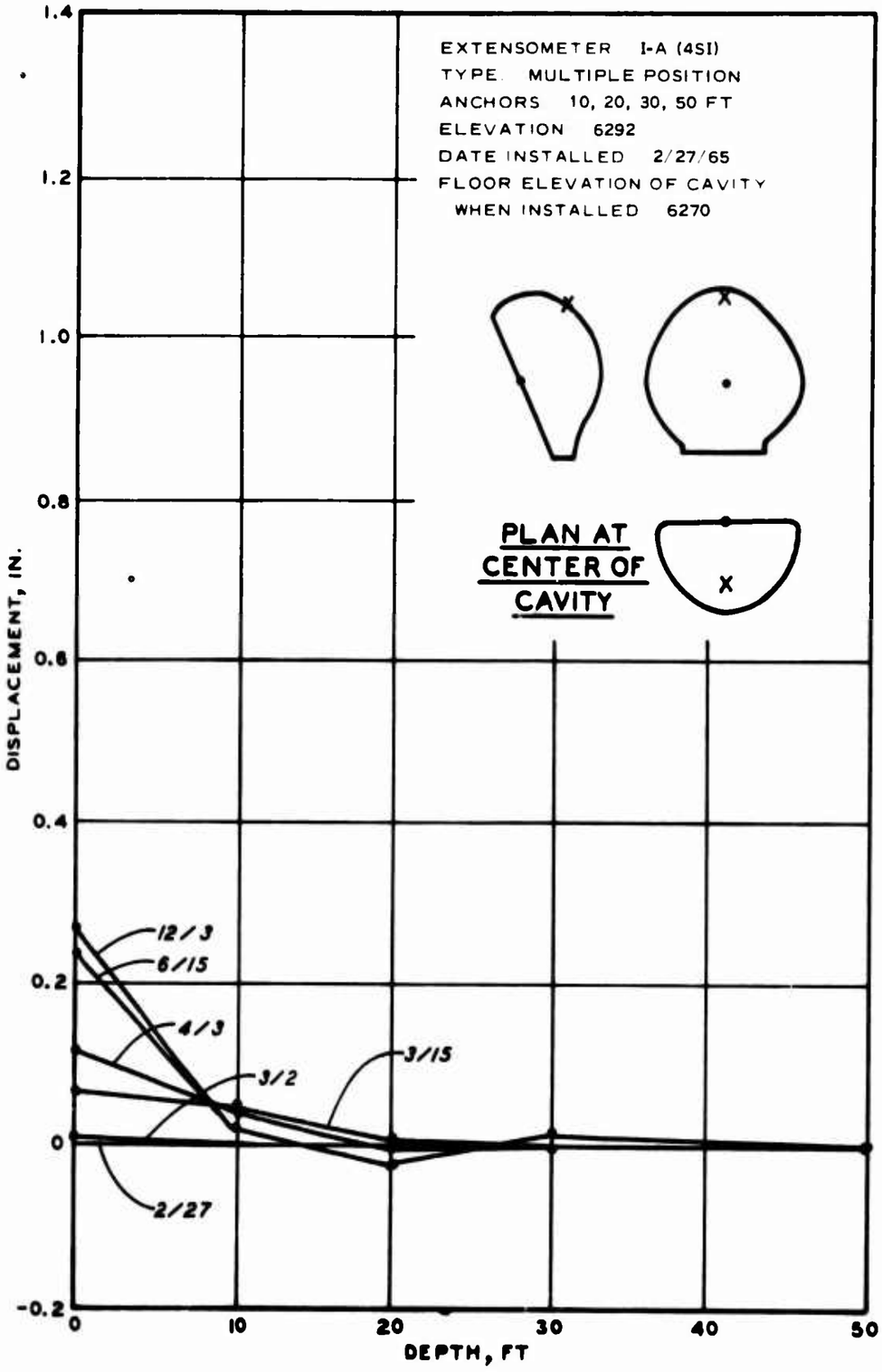
EXTENSOMETER I-A (4SI)
TYPE MULTIPLE POSITION
ANCHORS 10, 20, 30, 50 FT
ELEVATION 6292
DATE INSTALLED 2/27/65
FLOOR ELEVATION OF CAVITY
WHEN INSTALLED 6270
PLAN AT CENTER OF CAVITY
DISPLACEMENT, IN.
DEPTH, FT
1.4
1.2
1.0
0.8
0.6
0.4
0.2
0
-0.2
0
10
20
30
40
50
12/3
6/15
4/3
3/2
3/15
2/27

Fig. B.3

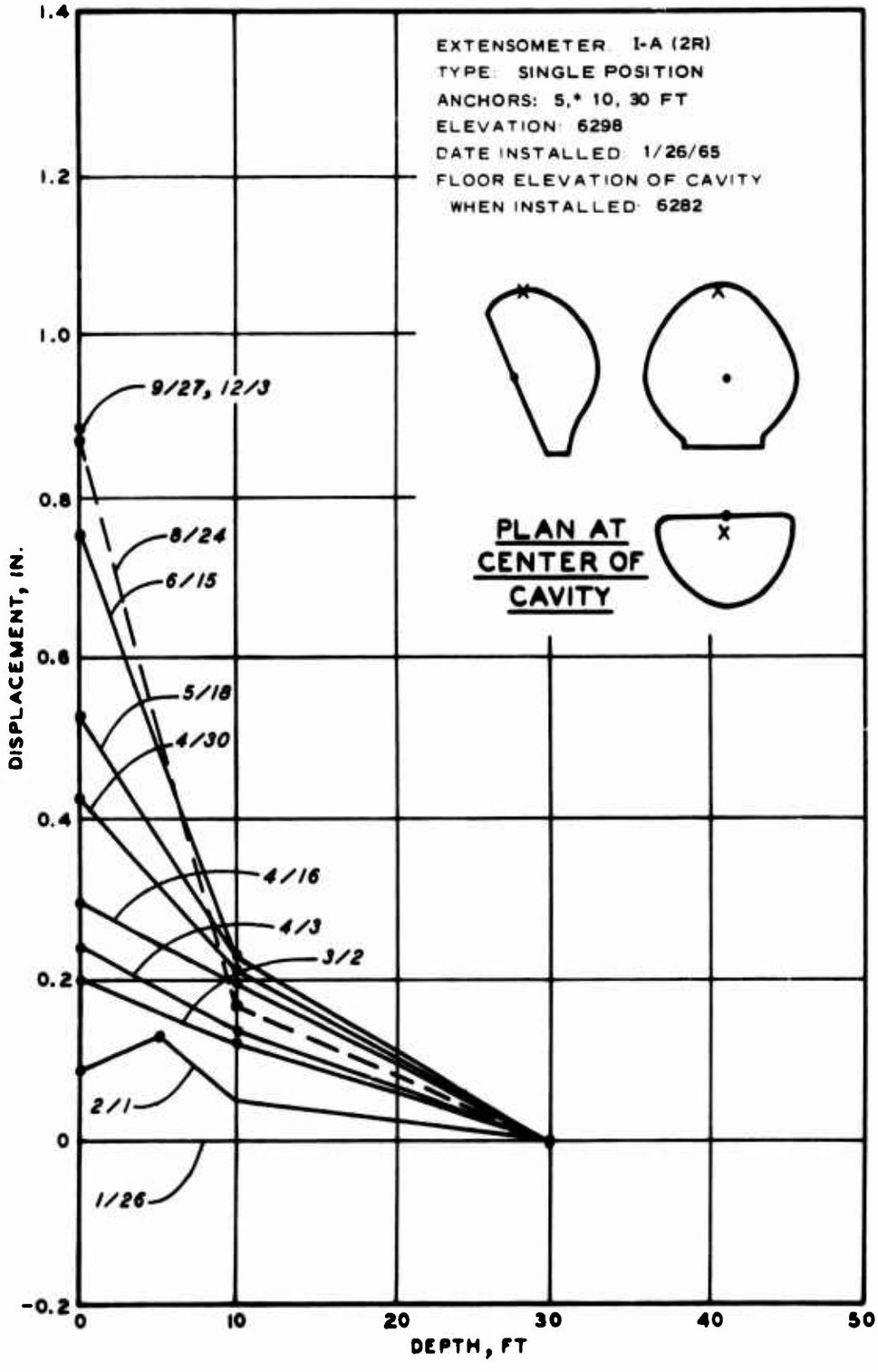
EXTENSOMETER I-A (2R)
TYPE: SINGLE POSITION
ANCHORS: 5,* 10, 30 FT
ELEVATION: 6298
DATE INSTALLED: 1/26/65
FLOOR ELEVATION OF CAVITY WHEN INSTALLED: 6282
PLAN AT CENTER OF CAVITY
9/27, 12/3
8/24
6/15
5/18
4/30
4/16
4/3
3/2
2/1
1/26
DISPLACEMENT, IN.
DEPTH, FT
1.4
1.2
1.0
0.8
0.6
0.4
0.2
0
-0.2
0
10
20
30
40
50

Fig. B.4

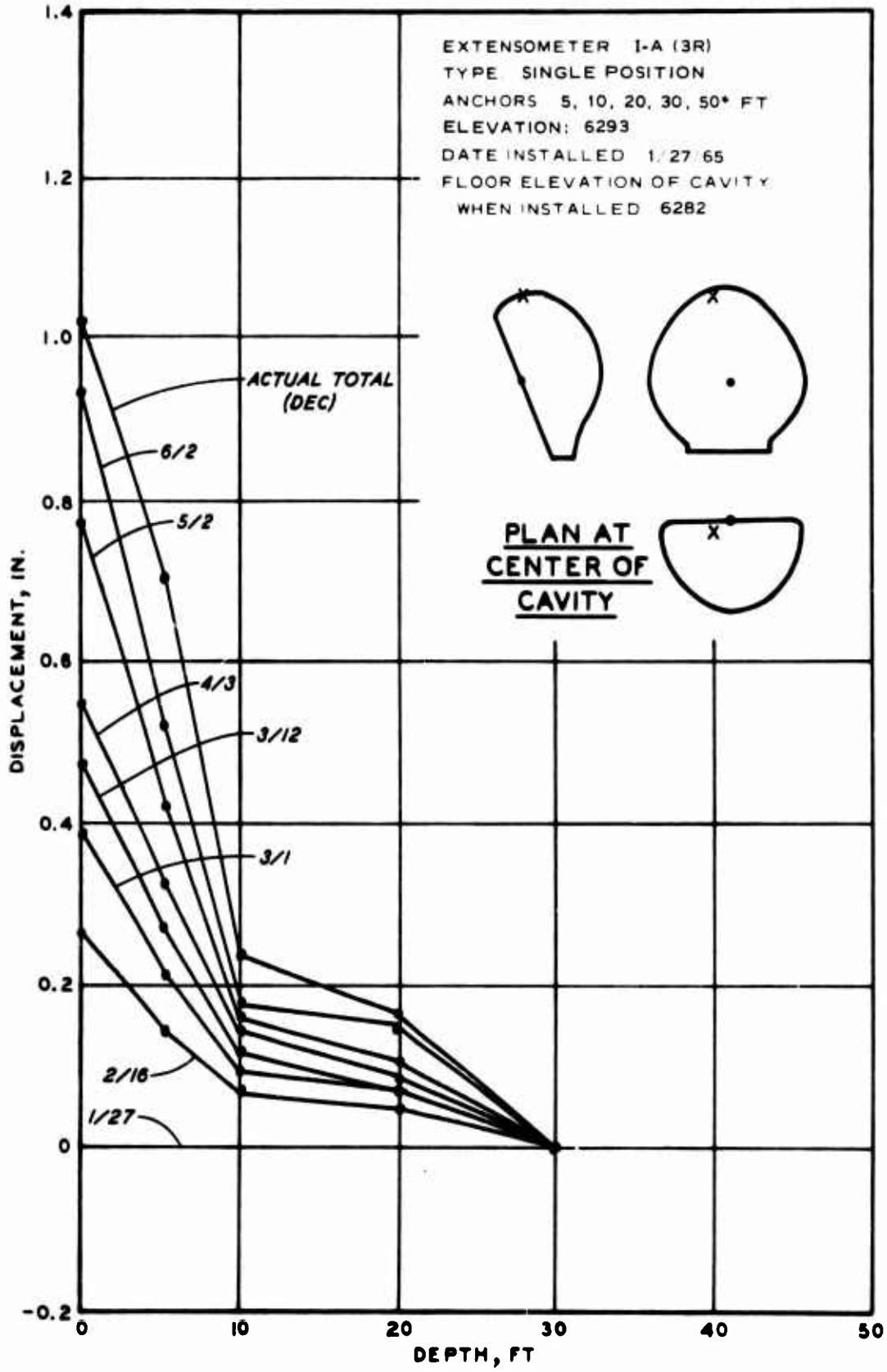
EXTENSOMETER I-A (3R)
TYPE SINGLE POSITION
ANCHORS 5, 10, 20, 30, 50* FT
ELEVATION: 6293
DATE INSTALLED 1/27/65
FLOOR ELEVATION OF CAVITY WHEN INSTALLED 6282
PLAN AT CENTER OF CAVITY
ACTUAL TOTAL (DEC)
6/2
5/2
4/3
3/12
3/1
2/16
1/27
DISPLACEMENT, IN.
DEPTH, FT
1.4
1.2
1.0
0.8
0.6
0.4
0.2
0
-0.2
0
10
20
30
40
50

Fig. B.5

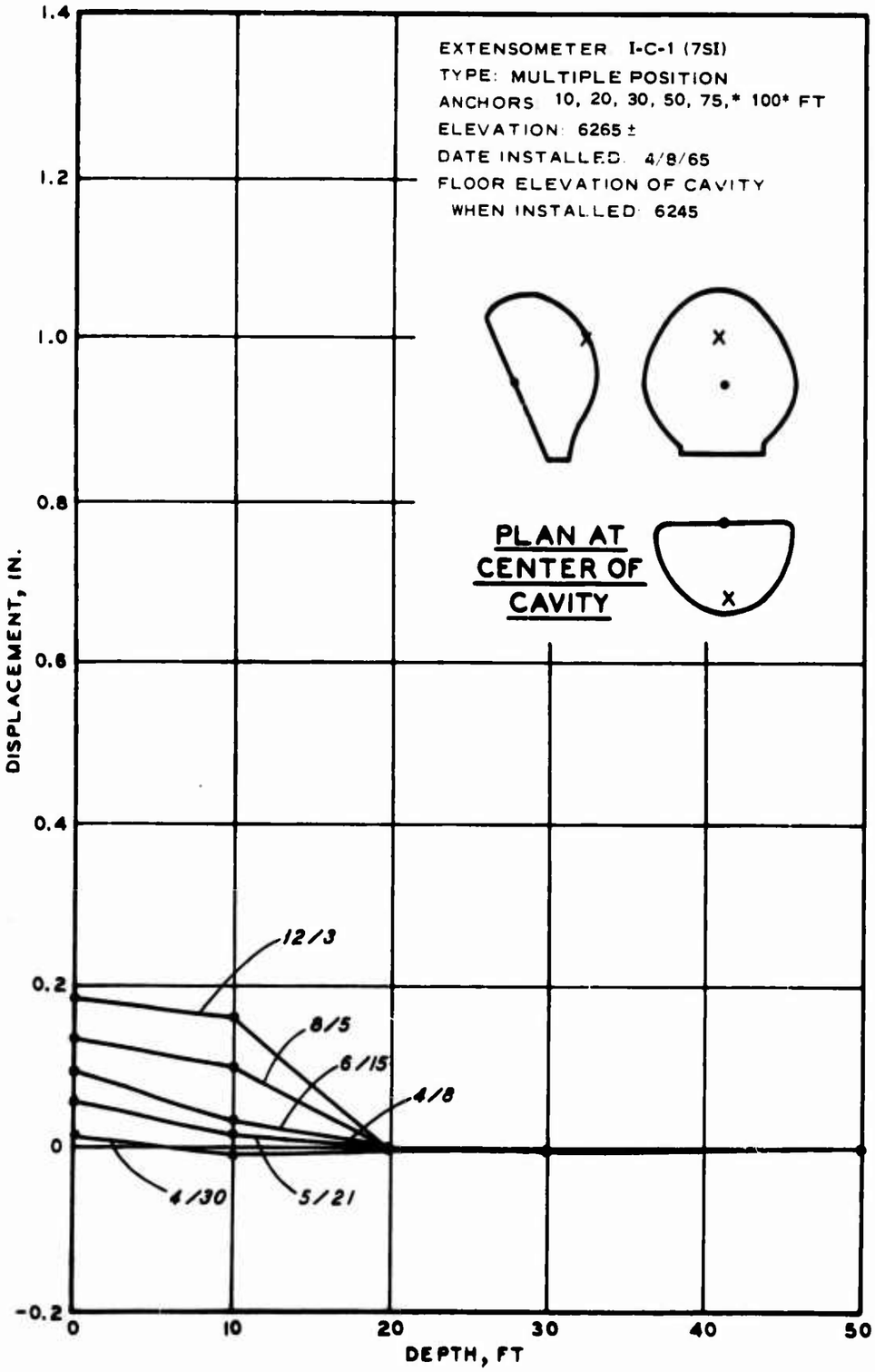
EXTENSOMETER I-C-1 (7SI)
TYPE: MULTIPLE POSITION
ANCHORS 10, 20, 30, 50, 75,* 100* FT
ELEVATION: 6265 ±
DATE INSTALLED: 4/8/65
FLOOR ELEVATION OF CAVITY
WHEN INSTALLED: 6245
PLAN AT CENTER OF CAVITY
DISPLACEMENT, IN.
1.4
1.2
1.0
0.8
0.6
0.4
0.2
0
-0.2
0
10
20
30
40
50
DEPTH, FT
12/3
8/5
6/15
4/8
4/30
5/21

Fig. B.6

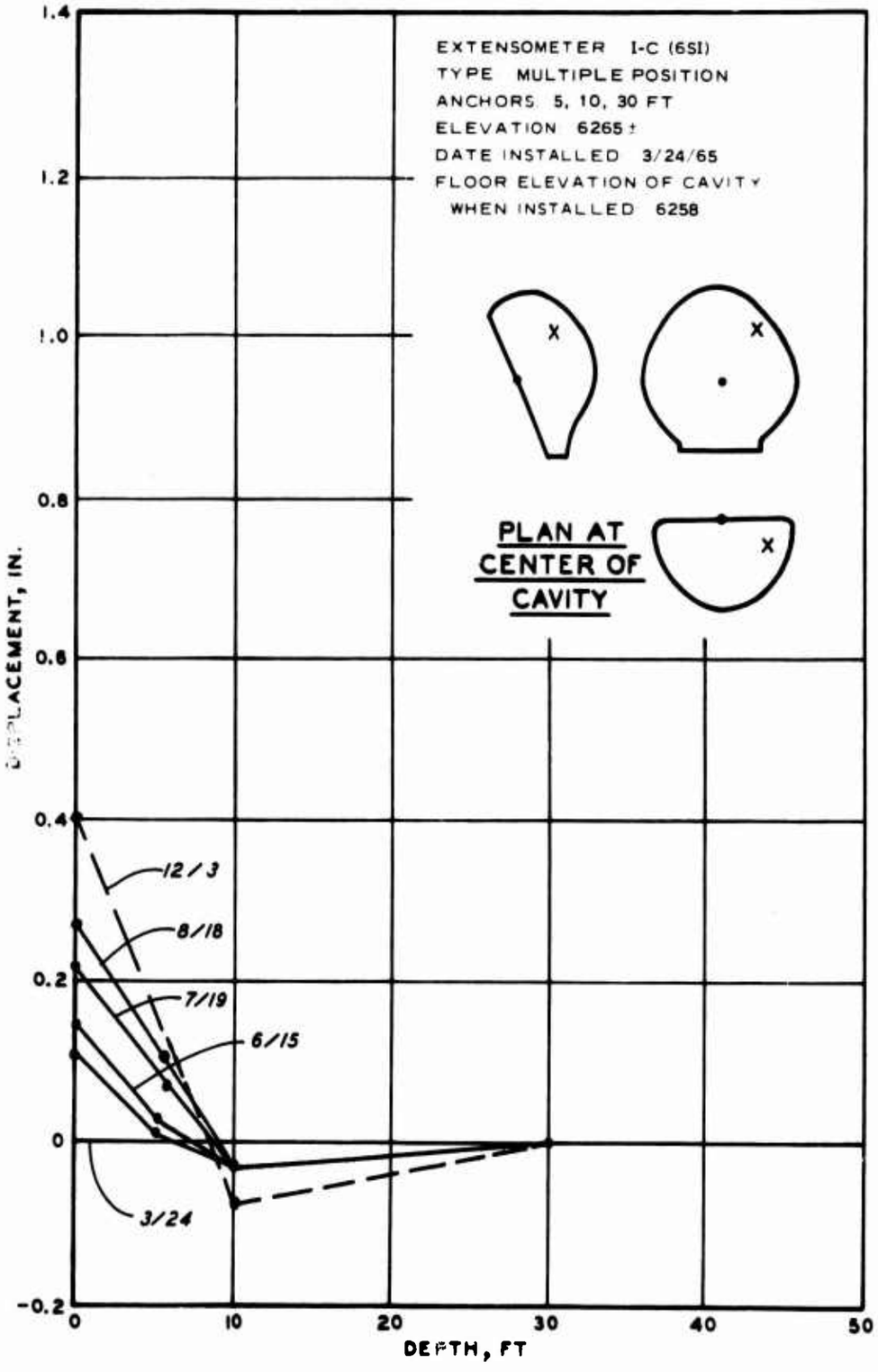
EXTENSOMETER I-C (6SI)
TYPE MULTIPLE POSITION
ANCHORS 5, 10, 30 FT
ELEVATION 6265±
DATE INSTALLED 3/24/65
FLOOR ELEVATION OF CAVITY WHEN INSTALLED 6258
PLAN AT CENTER OF CAVITY
DISPLACEMENT, IN.
DEPTH, FT
1.4
1.2
1.0
0.8
0.6
0.4
0.2
0
-0.2
0
10
20
30
40
50
12/3
8/18
7/19
6/15
3/24

Fig. B.7

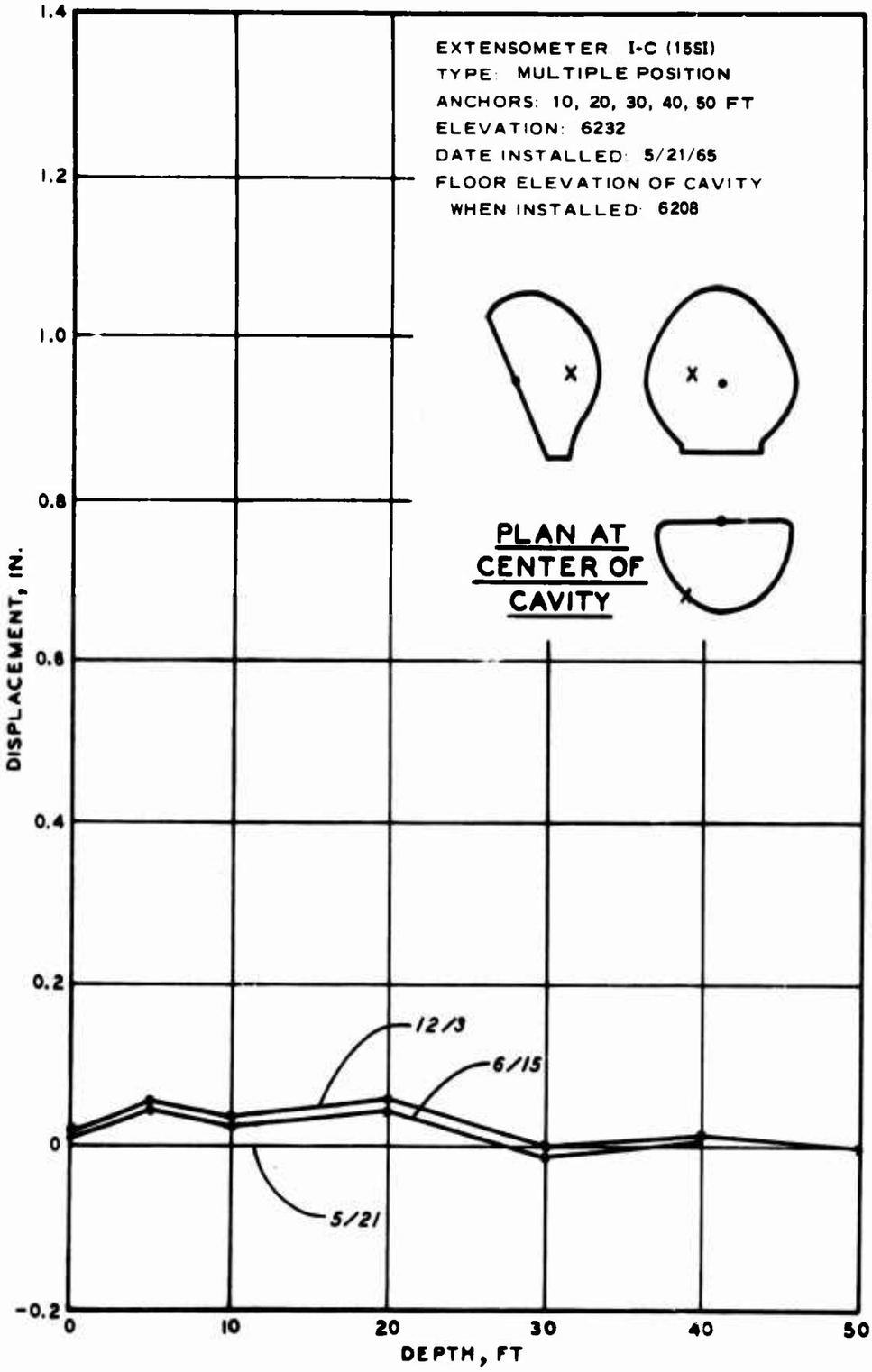
EXTENSOMETER I-C (15SI)
TYPE: MULTIPLE POSITION
ANCHORS: 10, 20, 30, 40, 50 FT
ELEVATION: 6232
DATE INSTALLED: 5/21/65
FLOOR ELEVATION OF CAVITY
WHEN INSTALLED: 6208
PLAN AT CENTER OF CAVITY
DISPLACEMENT, IN.
DEPTH, FT
1.4
1.2
1.0
0.8
0.6
0.4
0.2
0
-0.2
0
10
20
30
40
50
12/13
6/15
5/21

Fig. B.8

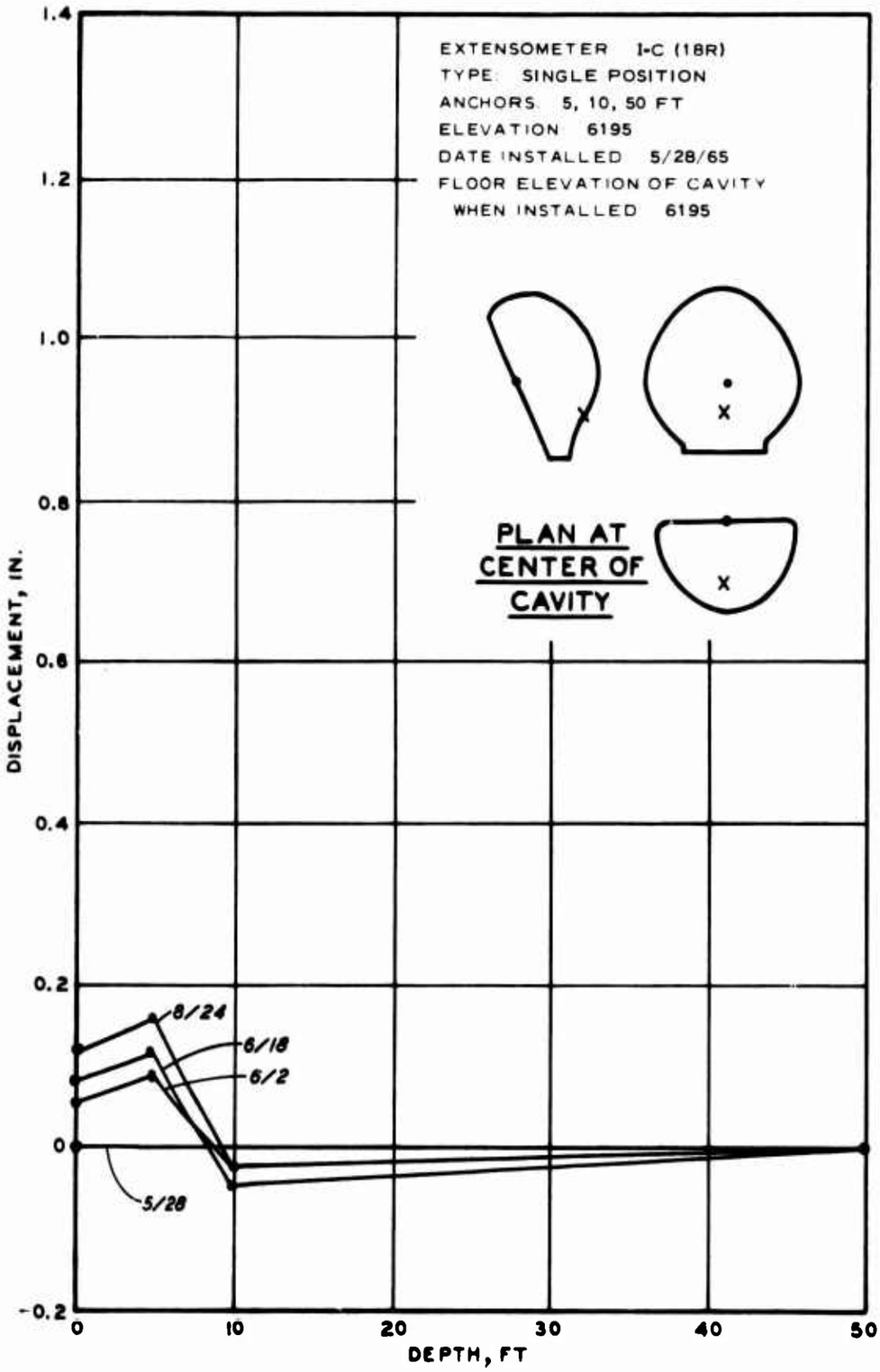
EXTENSOMETER I-C (18R)
TYPE SINGLE POSITION
ANCHORS 5, 10, 50 FT
ELEVATION 6195
DATE INSTALLED 5/28/65
FLOOR ELEVATION OF CAVITY
WHEN INSTALLED 6195
PLAN AT CENTER OF CAVITY
DISPLACEMENT, IN.
DEPTH, FT
1.4
1.2
1.0
0.8
0.6
0.4
0.2
0
-0.2
0
10
20
30
40
50
8/24
6/18
6/2
5/28

Fig. B.9

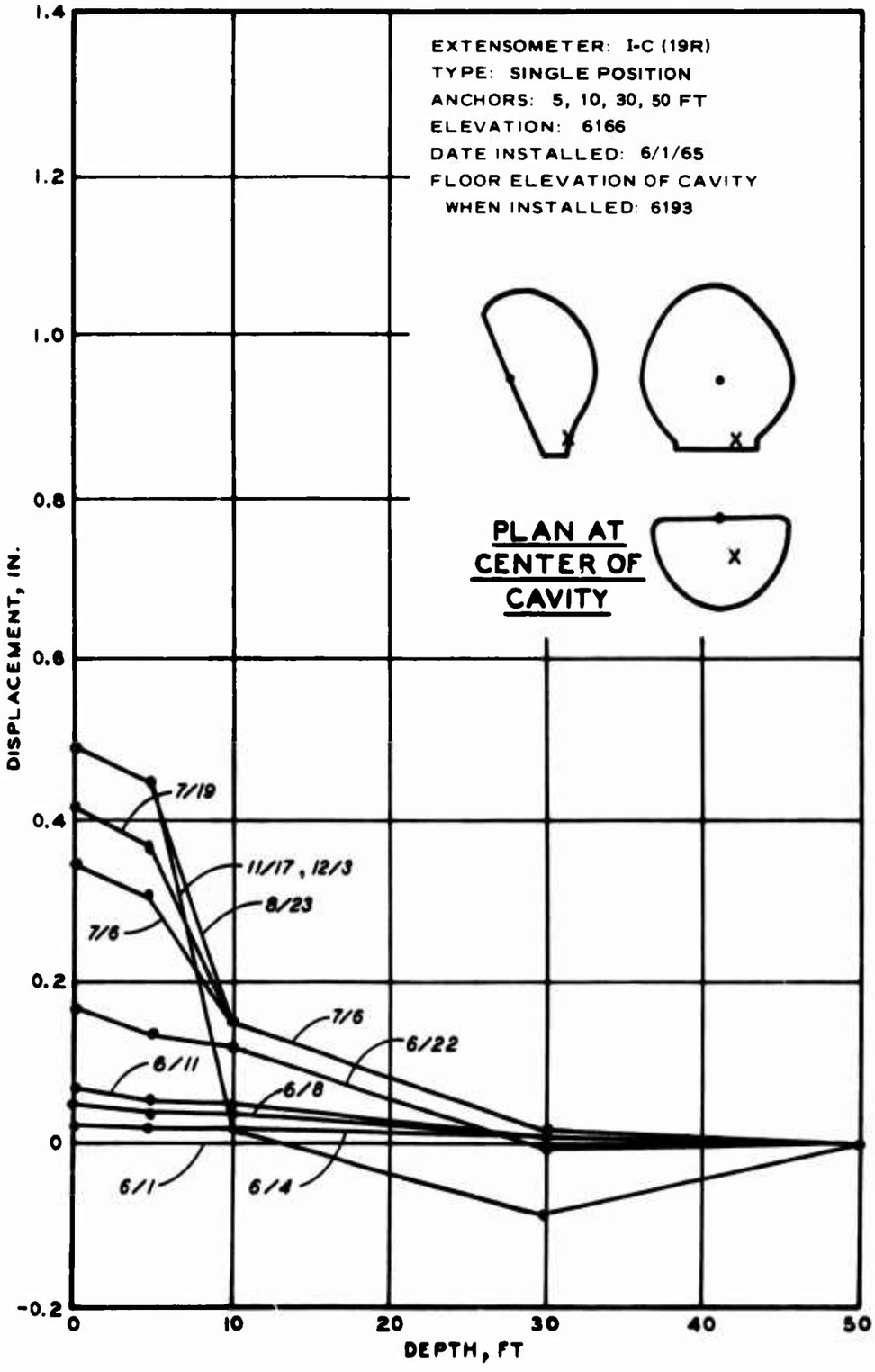
EXTENSOMETER: I-C (19R)
TYPE: SINGLE POSITION
ANCHORS: 5, 10, 30, 50 FT
ELEVATION: 6166
DATE INSTALLED: 6/1/65
FLOOR ELEVATION OF CAVITY WHEN INSTALLED: 6193
PLAN AT CENTER OF CAVITY
DISPLACEMENT, IN.
DEPTH, FT
1.4
1.2
1.0
0.8
0.6
0.4
0.2
0
-0.2
0
10
20
30
40
50
7/19
11/17, 12/3
8/23
7/6
7/6
6/22
6/11
6/8
6/1
6/4

Fig. B.10

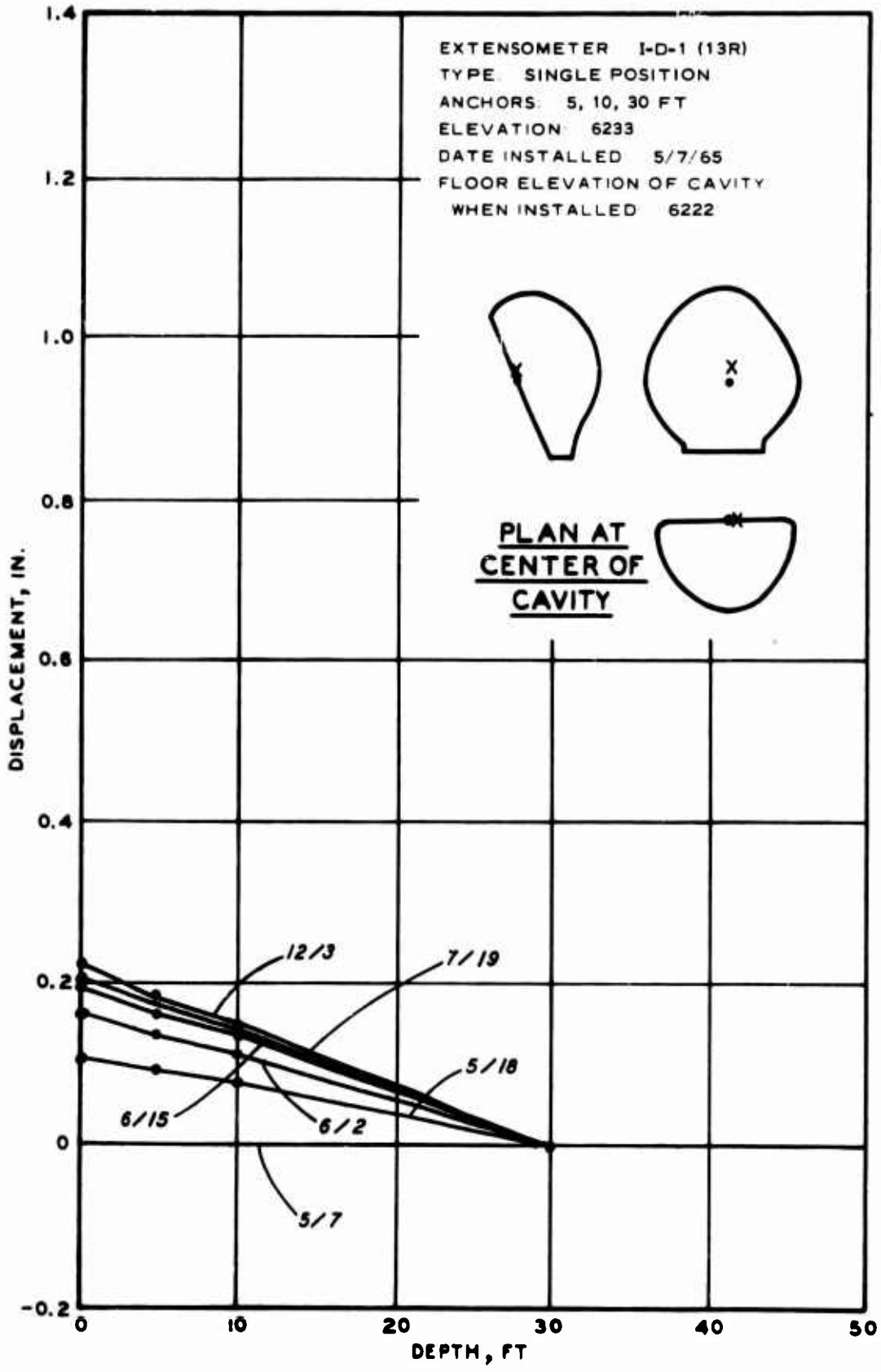
EXTENSOMETER I-D-1 (13R)
TYPE SINGLE POSITION
ANCHORS 5, 10, 30 FT
ELEVATION 6233
DATE INSTALLED 5/7/65
FLOOR ELEVATION OF CAVITY
WHEN INSTALLED 6222
PLAN AT CENTER OF CAVITY
DISPLACEMENT, IN.
DEPTH, FT
1.4
1.2
1.0
0.8
0.6
0.4
0.2
0
-0.2
0
10
20
30
40
50
12/3
7/19
5/18
6/15
6/2
5/7

Fig. B.11

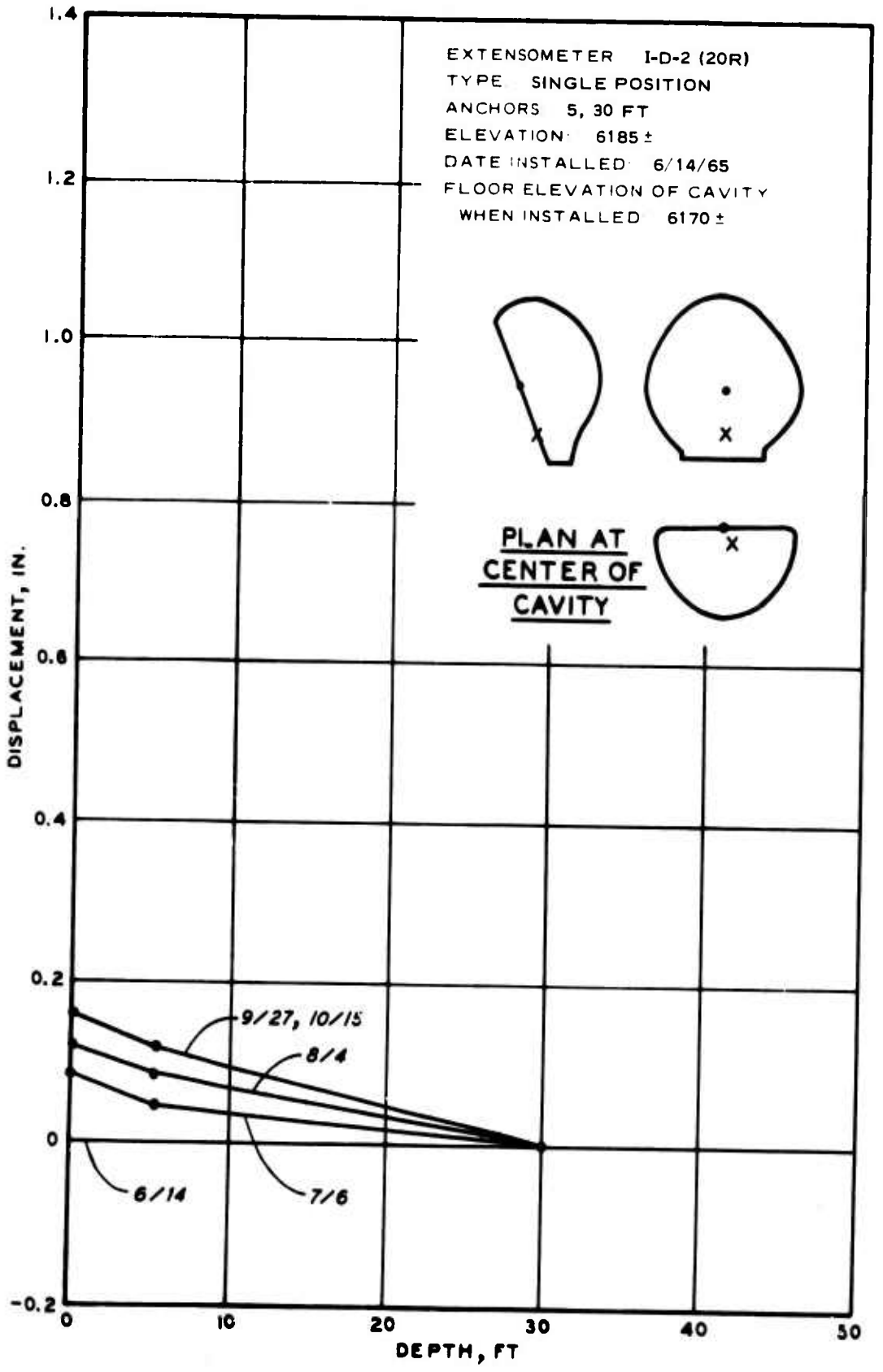
EXTENSOMETER I-D-2 (20R)
TYPE SINGLE POSITION
ANCHORS 5, 30 FT
ELEVATION 6185 ±
DATE INSTALLED 6/14/65
FLOOR ELEVATION OF CAVITY WHEN INSTALLED 6170 ±
PLAN AT CENTER OF CAVITY
DISPLACEMENT, IN.
DEPTH, FT
1.4
1.2
1.0
0.8
0.6
0.4
0.2
0
-0.2
0
10
20
30
40
50
9/27, 10/15
8/4
7/6
6/14

Fig. B.12

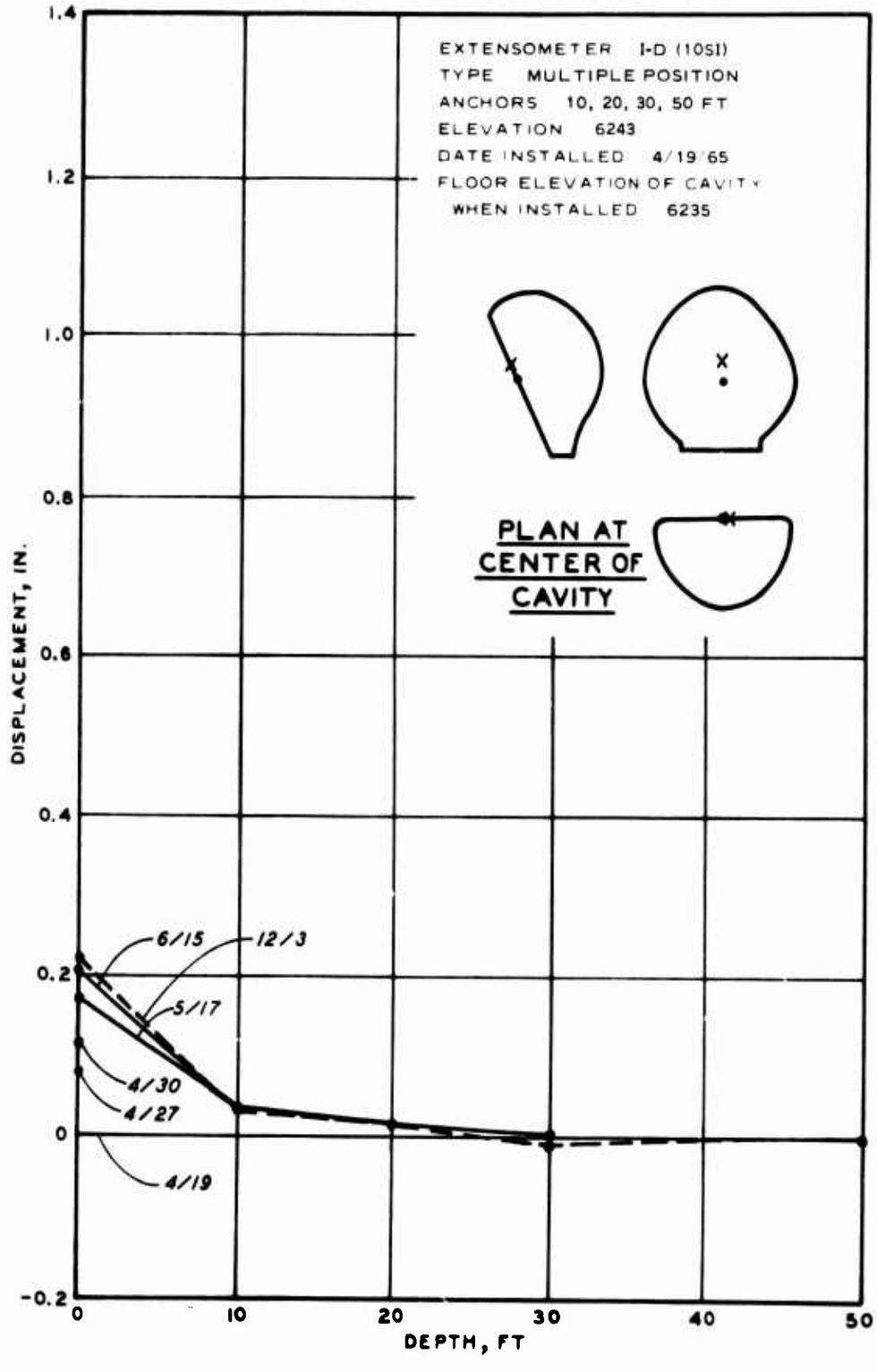
EXTENSOMETER I-D (1051)
TYPE MULTIPLE POSITION
ANCHORS 10, 20, 30, 50 FT
ELEVATION 6243
DATE INSTALLED 4/19/65
FLOOR ELEVATION OF CAVITY WHEN INSTALLED 6235
PLAN AT CENTER OF CAVITY
DISPLACEMENT, IN.
DEPTH, FT
1.4
1.2
1.0
0.8
0.6
0.4
0.2
0
-0.2
0
10
20
30
40
50
6/15
12/3
5/17
4/30
4/27
4/19

Fig. B.13

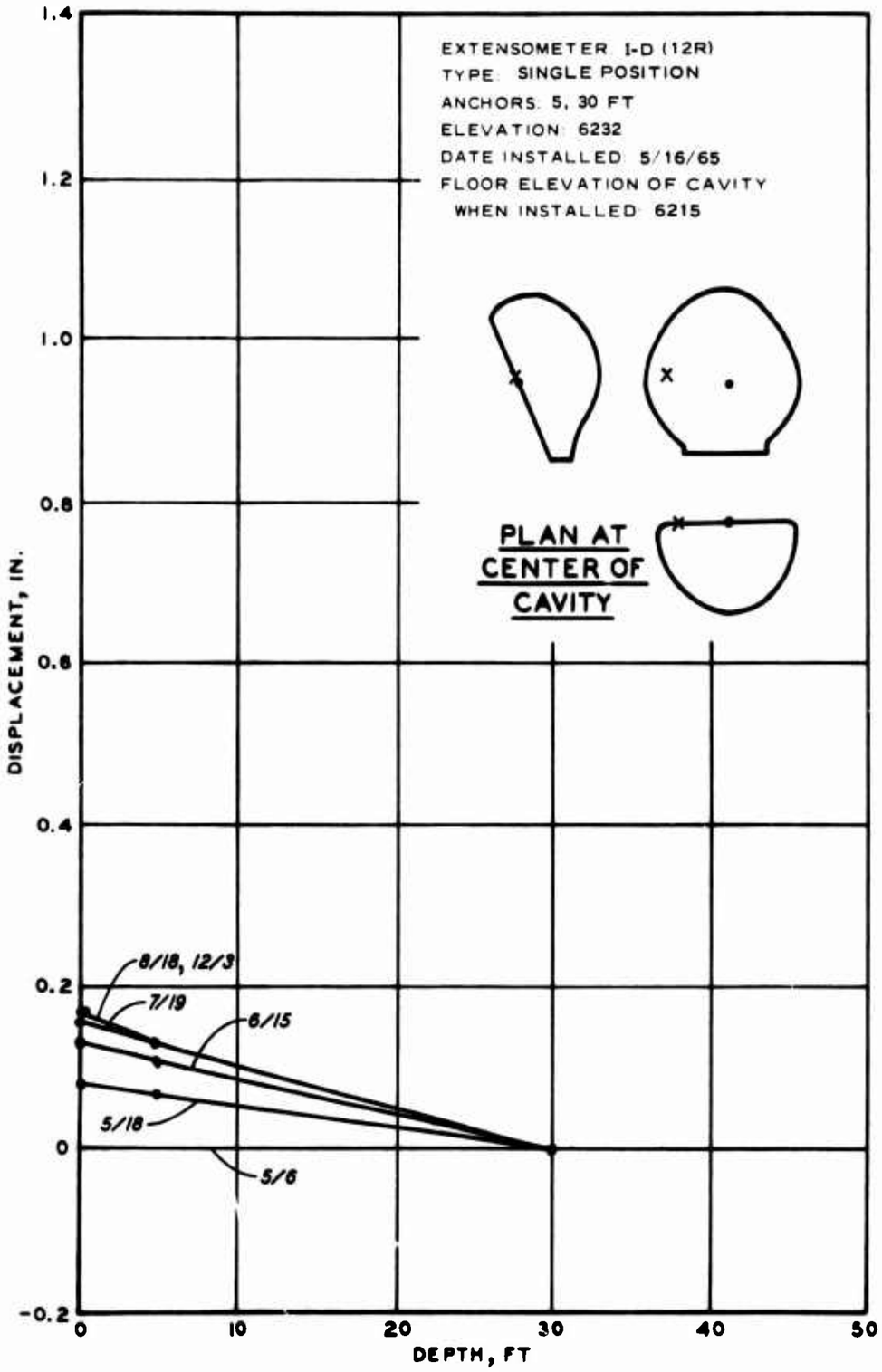
EXTENSOMETER I-D (12R)
TYPE: SINGLE POSITION
ANCHORS: 5, 30 FT
ELEVATION: 6232
DATE INSTALLED: 5/16/65
FLOOR ELEVATION OF CAVITY
WHEN INSTALLED: 6215
PLAN AT CENTER OF CAVITY
8/18, 12/3
7/19
6/15
5/18
5/6
DISPLACEMENT, IN.
DEPTH, FT
1.4
1.2
1.0
0.8
0.6
0.4
0.2
0
-0.2
0
10
20
30
40
50

Fig. B.14

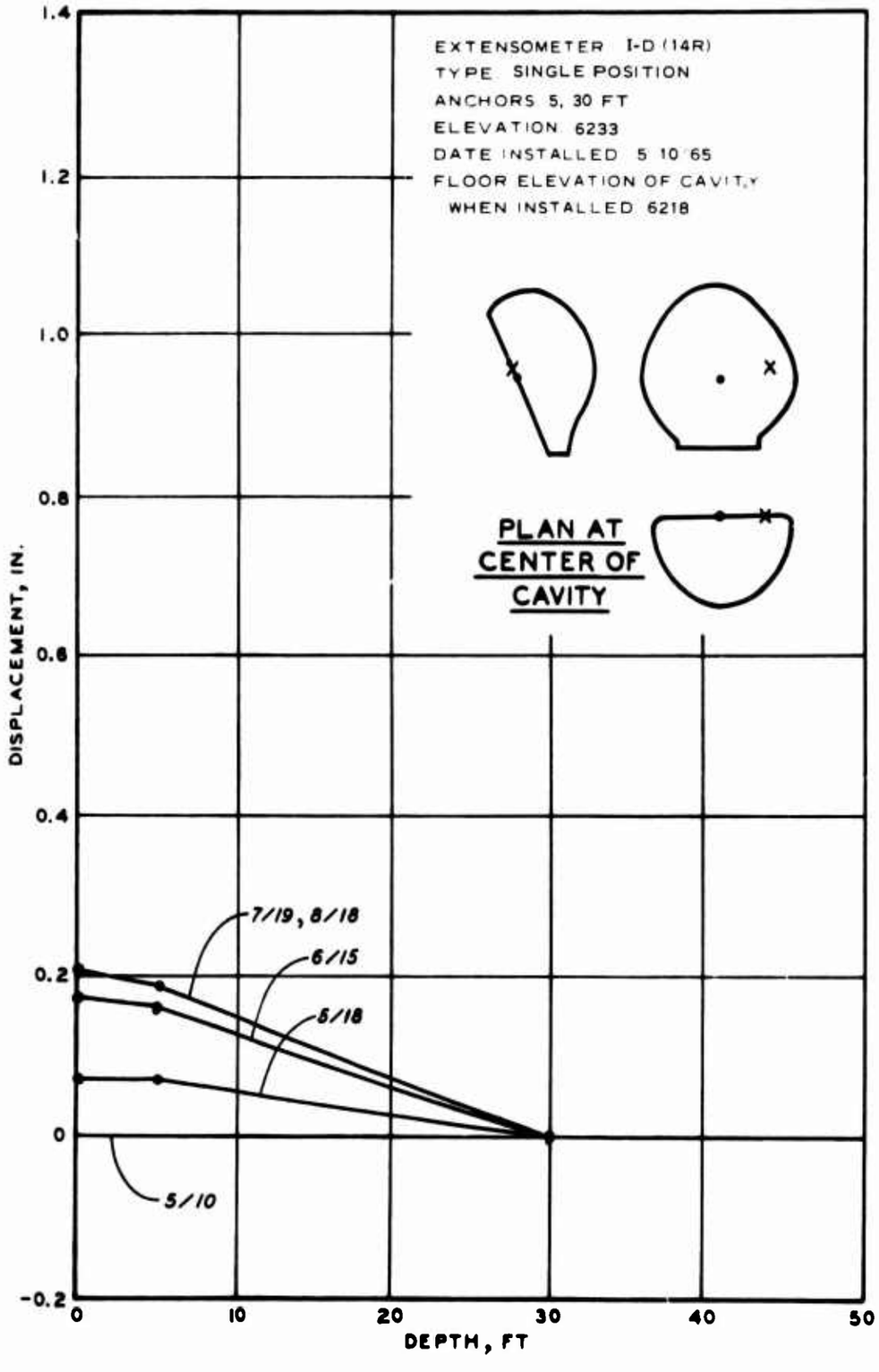
EXTENSOMETER I-D (14R)
TYPE SINGLE POSITION
ANCHORS 5, 30 FT
ELEVATION 6233
DATE INSTALLED 5 10 65
FLOOR ELEVATION OF CAVITY
WHEN INSTALLED 6218
PLAN AT CENTER OF CAVITY
DISPLACEMENT, IN.
DEPTH, FT
1.4
1.2
1.0
0.8
0.6
0.4
0.2
0
-0.2
0
10
20
30
40
50
7/19, 8/18
6/15
5/18
5/10

Fig. B.15

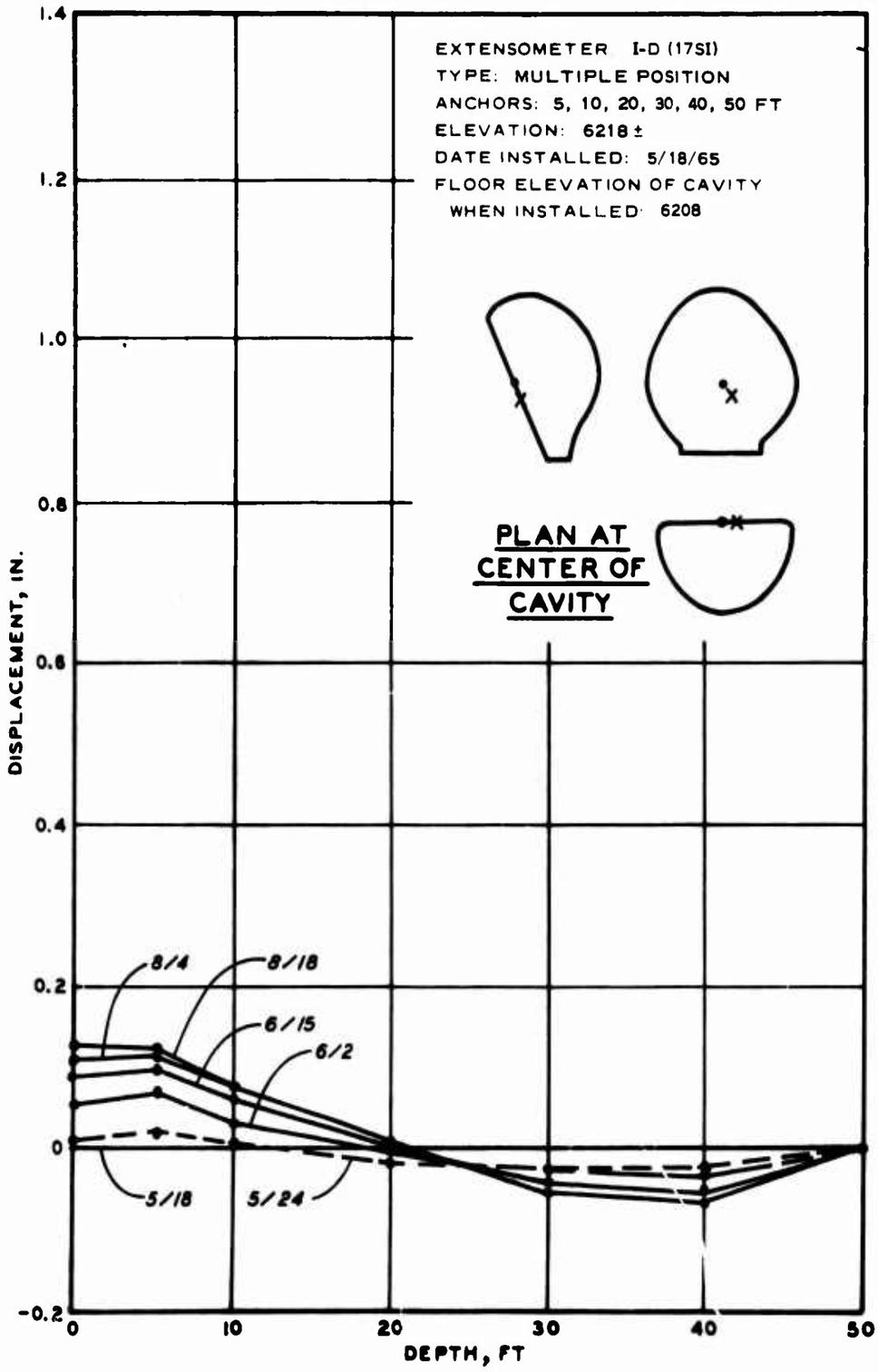
EXTENSOMETER I-D (17S1)
TYPE: MULTIPLE POSITION
ANCHORS: 5, 10, 20, 30, 40, 50 FT
ELEVATION: 6218 ±
DATE INSTALLED: 5/18/65
FLOOR ELEVATION OF CAVITY WHEN INSTALLED: 6208
PLAN AT CENTER OF CAVITY
DISPLACEMENT, IN.
1.4
1.2
1.0
0.8
0.6
0.4
0.2
0
-0.2
0
10
20
30
40
50
DEPTH, FT
8/4
8/18
6/15
6/2
5/18
5/24

Fig. B.16

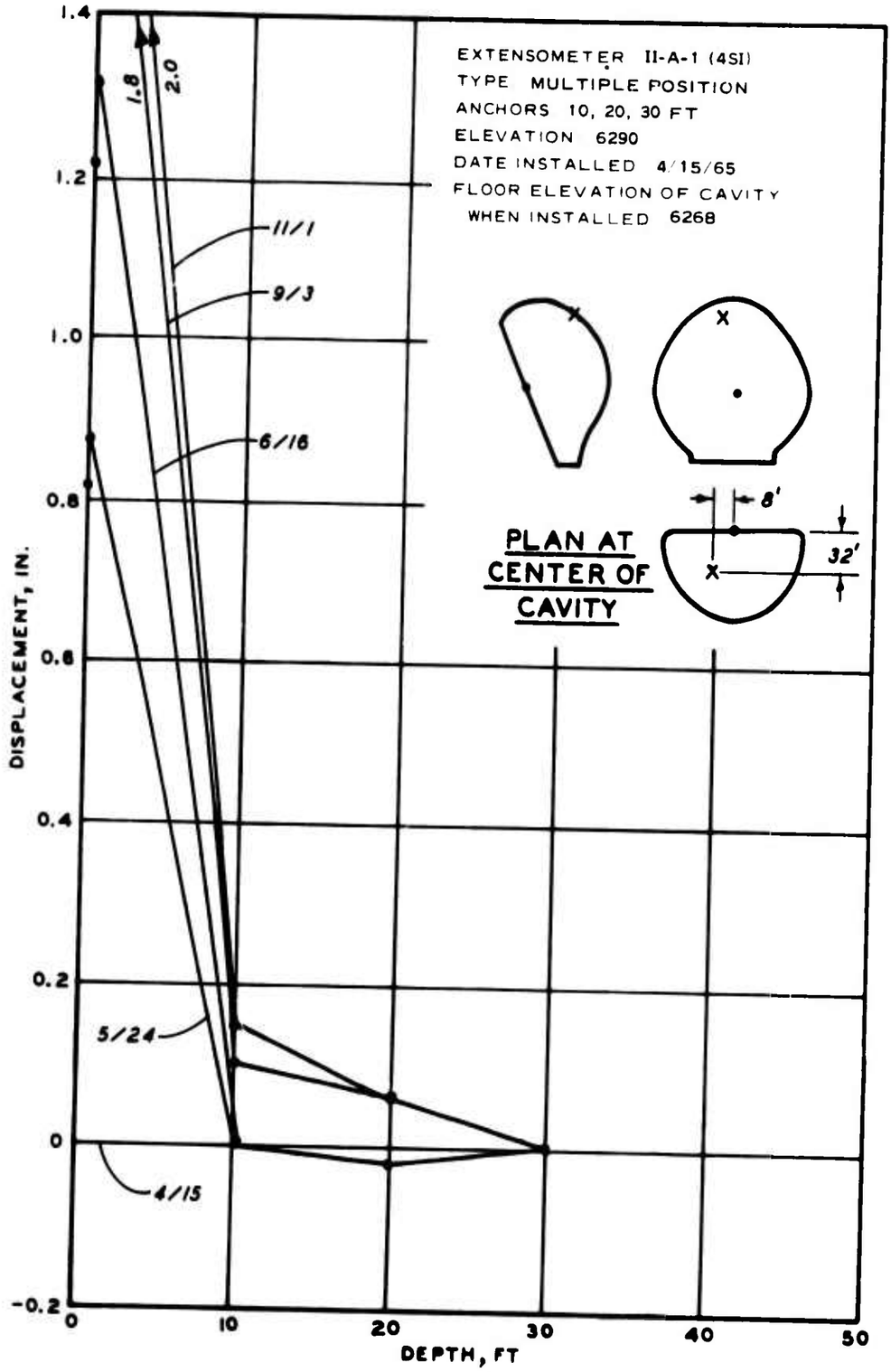
EXTENSOMETER II-A-1 (4SI)
TYPE MULTIPLE POSITION
ANCHORS 10, 20, 30 FT
ELEVATION 6290
DATE INSTALLED 4/15/65
FLOOR ELEVATION OF CAVITY
WHEN INSTALLED 6268
PLAN AT CENTER OF CAVITY
8'
32'
X
X
1.8
2.0
11/1
9/3
6/16
5/24
4/15
DISPLACEMENT, IN.
DEPTH, FT
1.4
1.2
1.0
0.8
0.6
0.4
0.2
0
-0.2
0
10
20
30
40
50

Fig. B.17

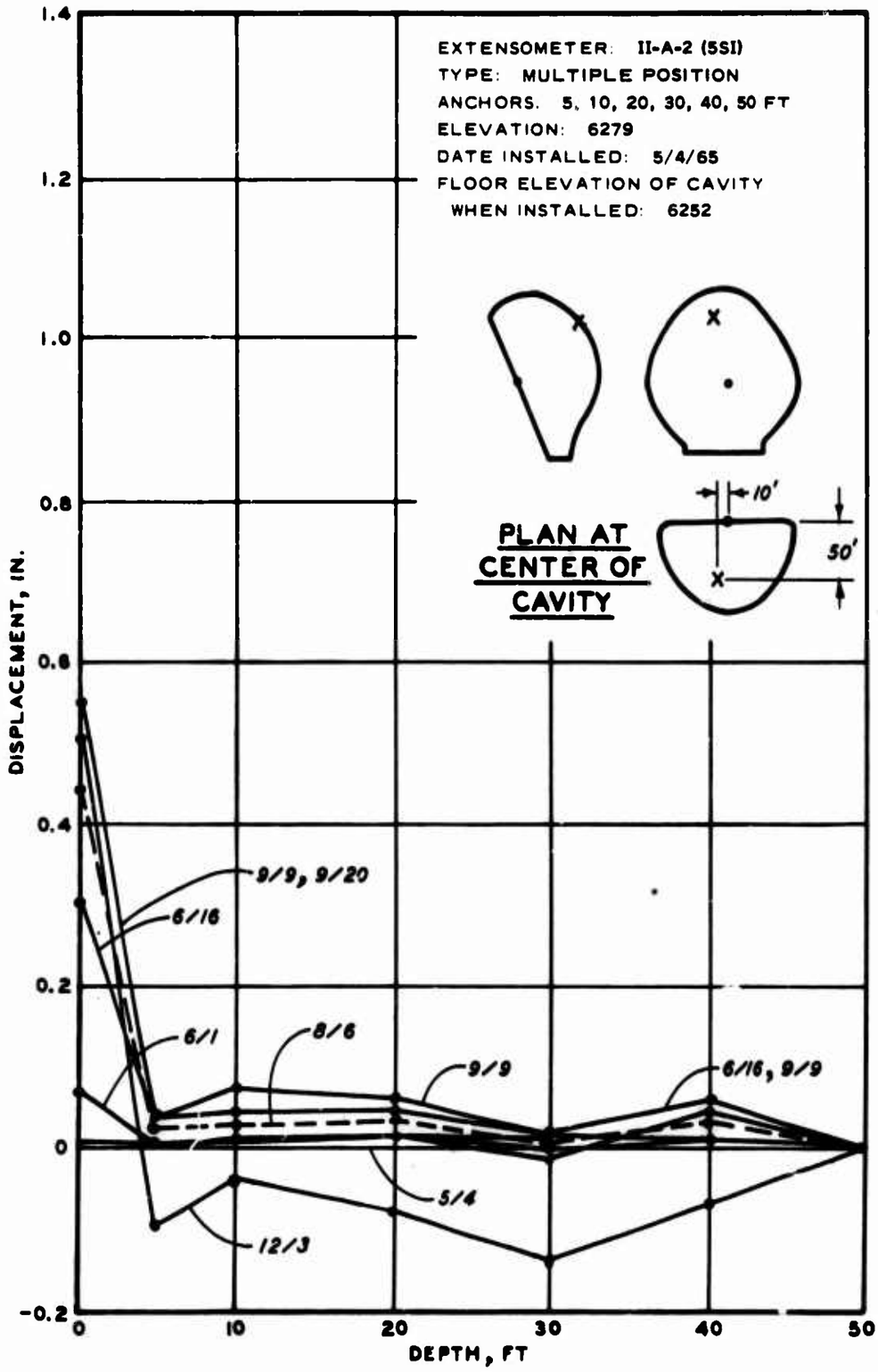
EXTENSOMETER: II-A-2 (SSI)
TYPE: MULTIPLE POSITION
ANCHORS. 5, 10, 20, 30, 40, 50 FT
ELEVATION: 6279
DATE INSTALLED: 5/4/65
FLOOR ELEVATION OF CAVITY
WHEN INSTALLED: 6252
PLAN AT CENTER OF CAVITY
10'
50'
DISPLACEMENT, IN.
DEPTH, FT
1.4
1.2
1.0
0.8
0.6
0.4
0.2
0
-0.2
0
10
20
30
40
50
9/9, 9/20
6/16
6/1
8/6
9/9
6/16, 9/9
5/4
12/3

Fig. B.18

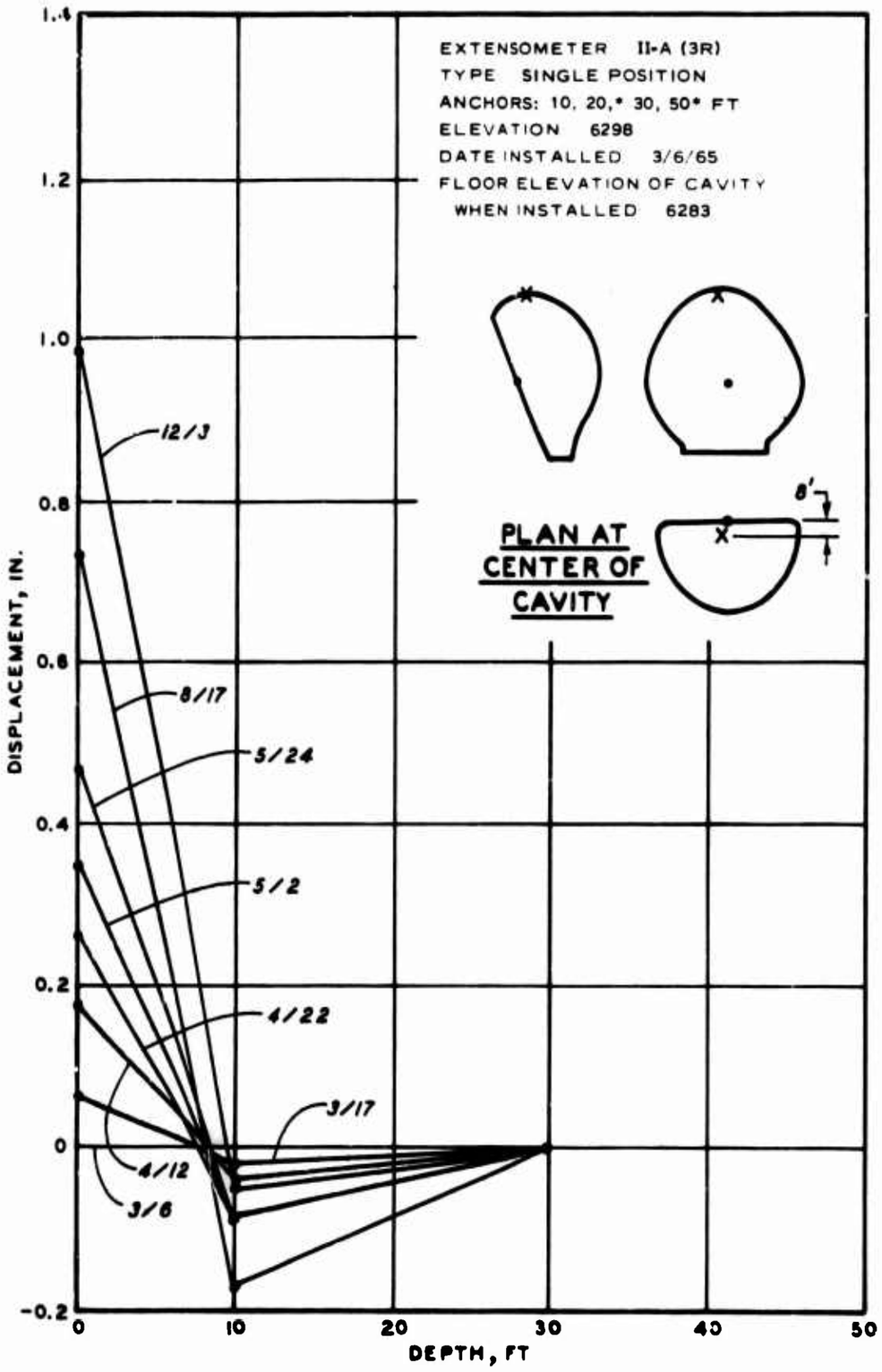
EXTENSOMETER II-A (3R)
TYPE SINGLE POSITION
ANCHORS: 10, 20,* 30, 50* FT
ELEVATION 6298
DATE INSTALLED 3/6/65
FLOOR ELEVATION OF CAVITY WHEN INSTALLED 6283
PLAN AT CENTER OF CAVITY
8'
12/3
8/17
5/24
5/2
4/22
3/17
4/12
3/6
DISPLACEMENT, IN.
DEPTH, FT
1.4
1.2
1.0
0.8
0.6
0.4
0.2
0
-0.2
0
10
20
30
40
50

Fig. B.19

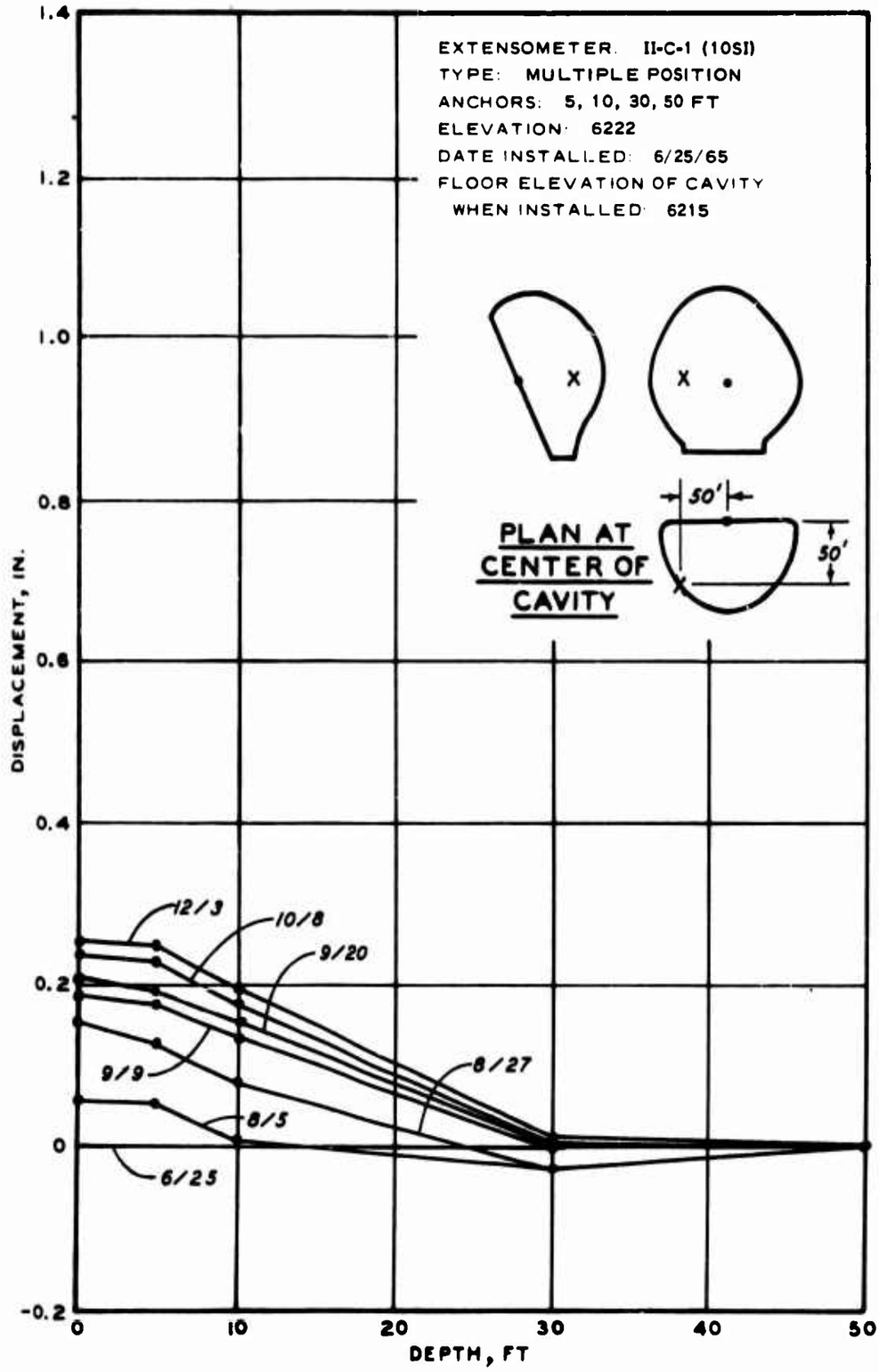
EXTENSOMETER II-C-1 (10SI)
TYPE: MULTIPLE POSITION
ANCHORS: 5, 10, 30, 50 FT
ELEVATION: 6222
DATE INSTALLED: 6/25/65
FLOOR ELEVATION OF CAVITY
WHEN INSTALLED: 6215
PLAN AT CENTER OF CAVITY
50'
50'
DISPLACEMENT, IN.
DEPTH, FT
1.4
1.2
1.0
0.8
0.6
0.4
0.2
0
-0.2
0
10
20
30
40
50
12/3
10/8
9/20
9/9
8/27
8/5
6/25

Fig. B.20

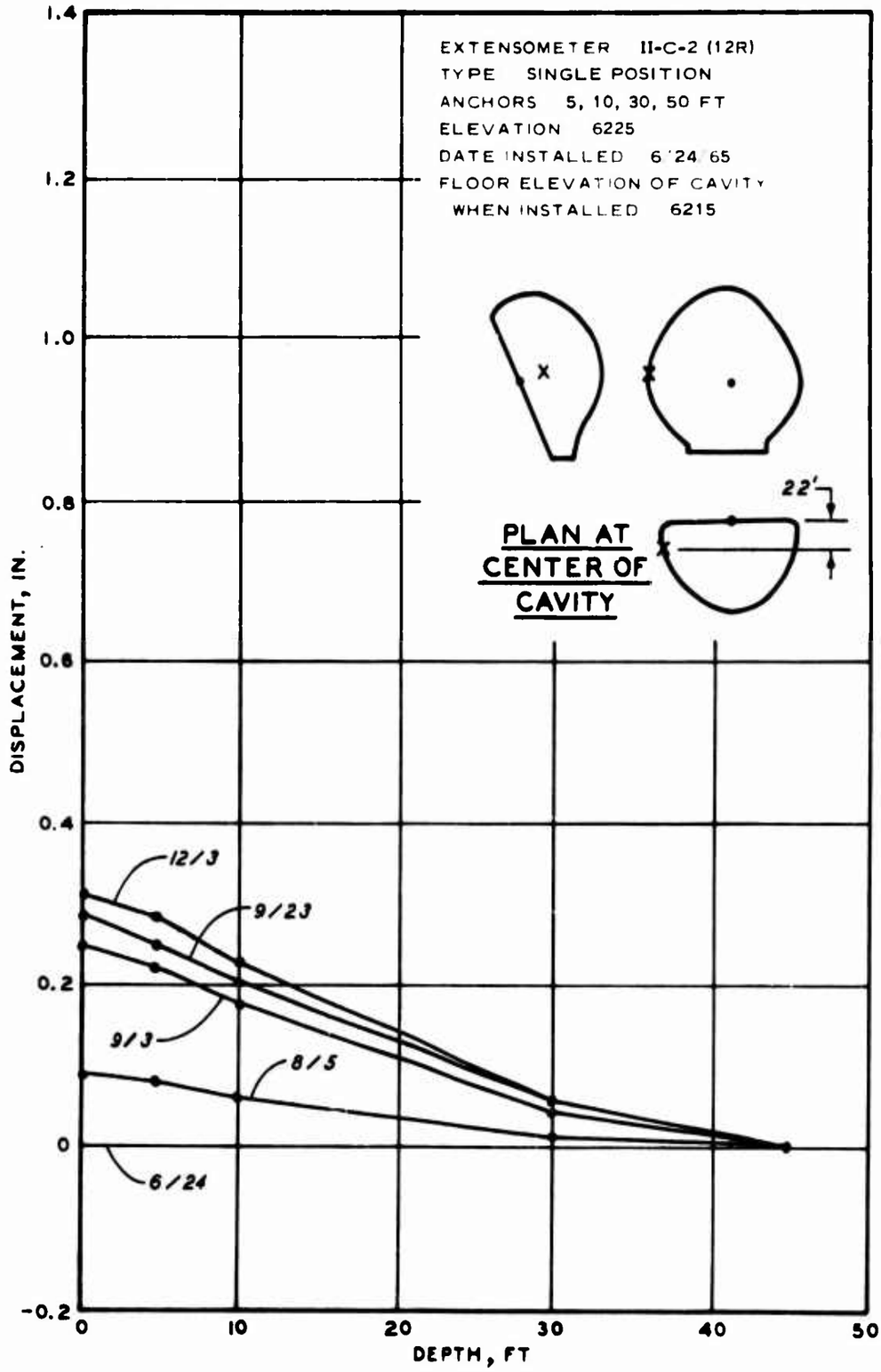
EXTENSOMETER II-C-2 (12R)
TYPE SINGLE POSITION
ANCHORS 5, 10, 30, 50 FT
ELEVATION 6225
DATE INSTALLED 6 24 65
FLOOR ELEVATION OF CAVITY
WHEN INSTALLED 6215
X
22'
PLAN AT CENTER OF CAVITY
DISPLACEMENT, IN.
1.4
1.2
1.0
0.8
0.6
0.4
0.2
0
-0.2
12/3
9/23
9/3
8/5
6/24
0
10
20
30
40
50
DEPTH, FT

Fig. B.21

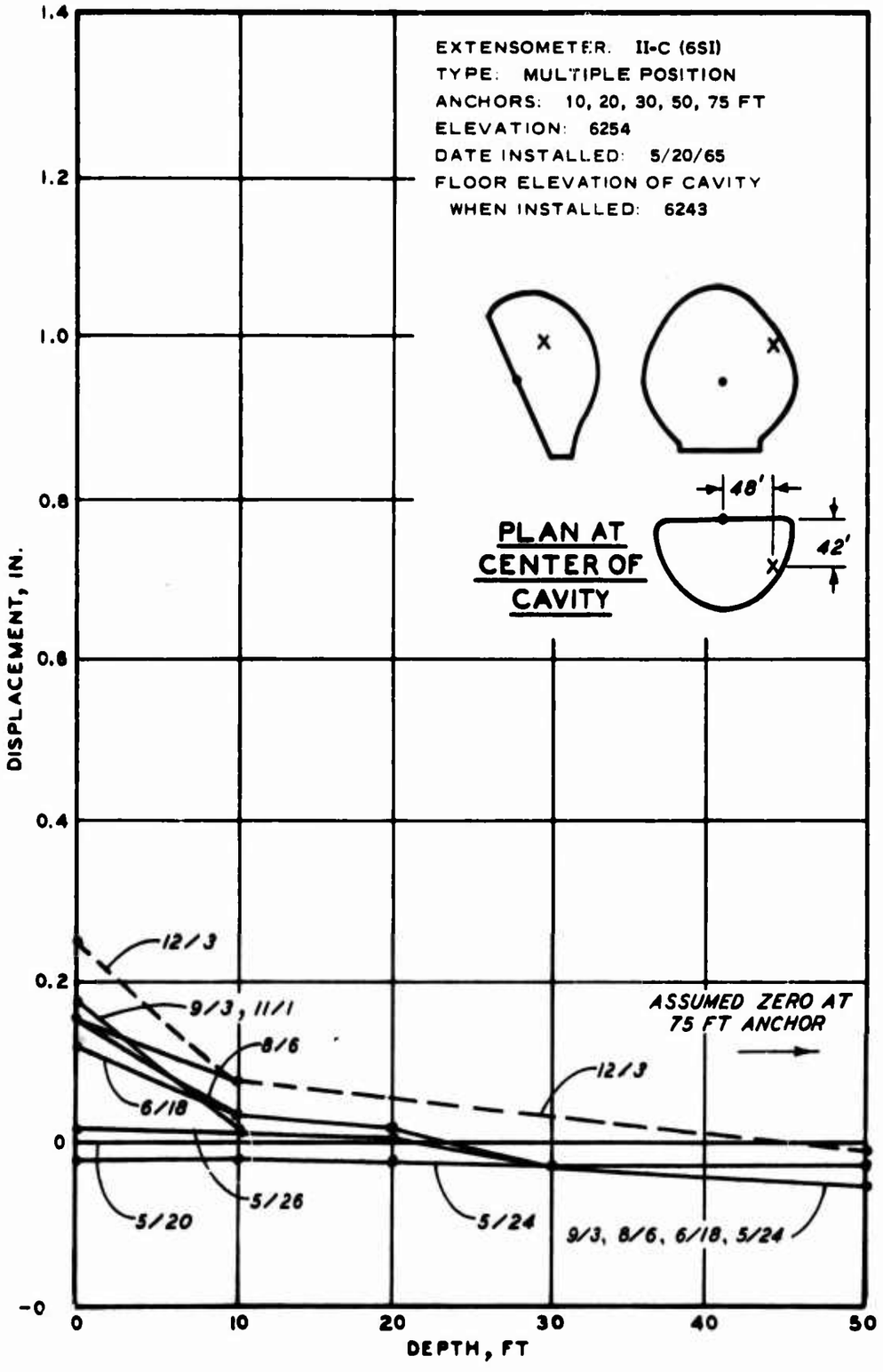
EXTENSOMETER: II-C (6SI)
TYPE: MULTIPLE POSITION
ANCHORS: 10, 20, 30, 50, 75 FT
ELEVATION: 6254
DATE INSTALLED: 5/20/65
FLOOR ELEVATION OF CAVITY WHEN INSTALLED: 6243
PLAN AT CENTER OF CAVITY
48'
42'
DISPLACEMENT, IN.
DEPTH, FT
1.4
1.2
1.0
0.8
0.6
0.4
0.2
0
-0
0
10
20
30
40
50
12/3
9/3, 11/1
8/6
6/18
5/20
5/26
5/24
12/3
9/3, 8/6, 6/18, 5/24
ASSUMED ZERO AT 75 FT ANCHOR

Fig. B.22

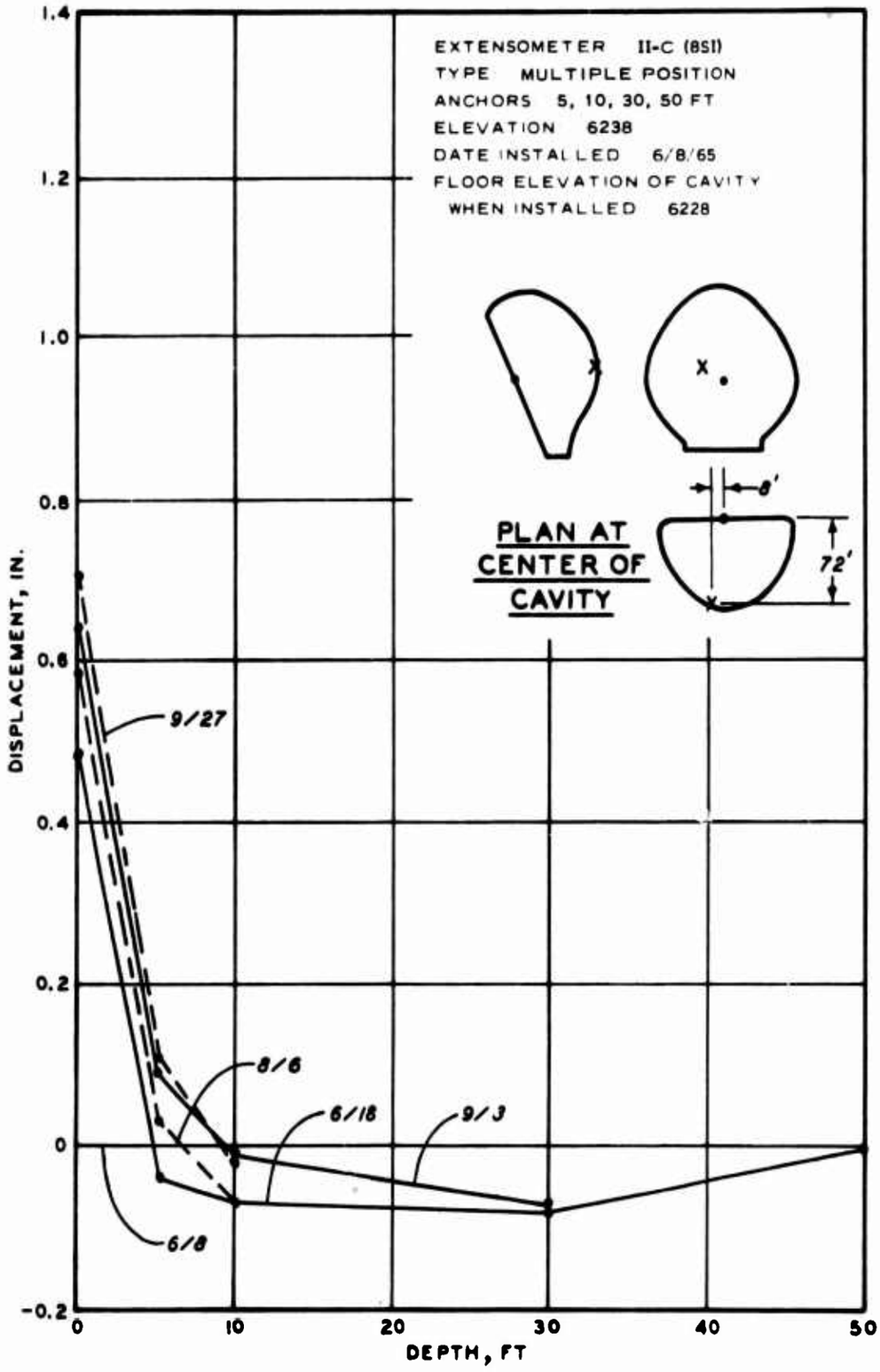
EXTENSOMETER II-C (8SI)
TYPE MULTIPLE POSITION
ANCHORS 5, 10, 30, 50 FT
ELEVATION 6238
DATE INSTALLED 6/8/65
FLOOR ELEVATION OF CAVITY WHEN INSTALLED 6228
PLAN AT CENTER OF CAVITY
8'
72'
DISPLACEMENT, IN.
DEPTH, FT
9/27
8/6
6/18
9/3
6/8
1.4
1.2
1.0
0.8
0.6
0.4
0.2
0
-0.2
0
10
20
30
40
50

Fig. B.23

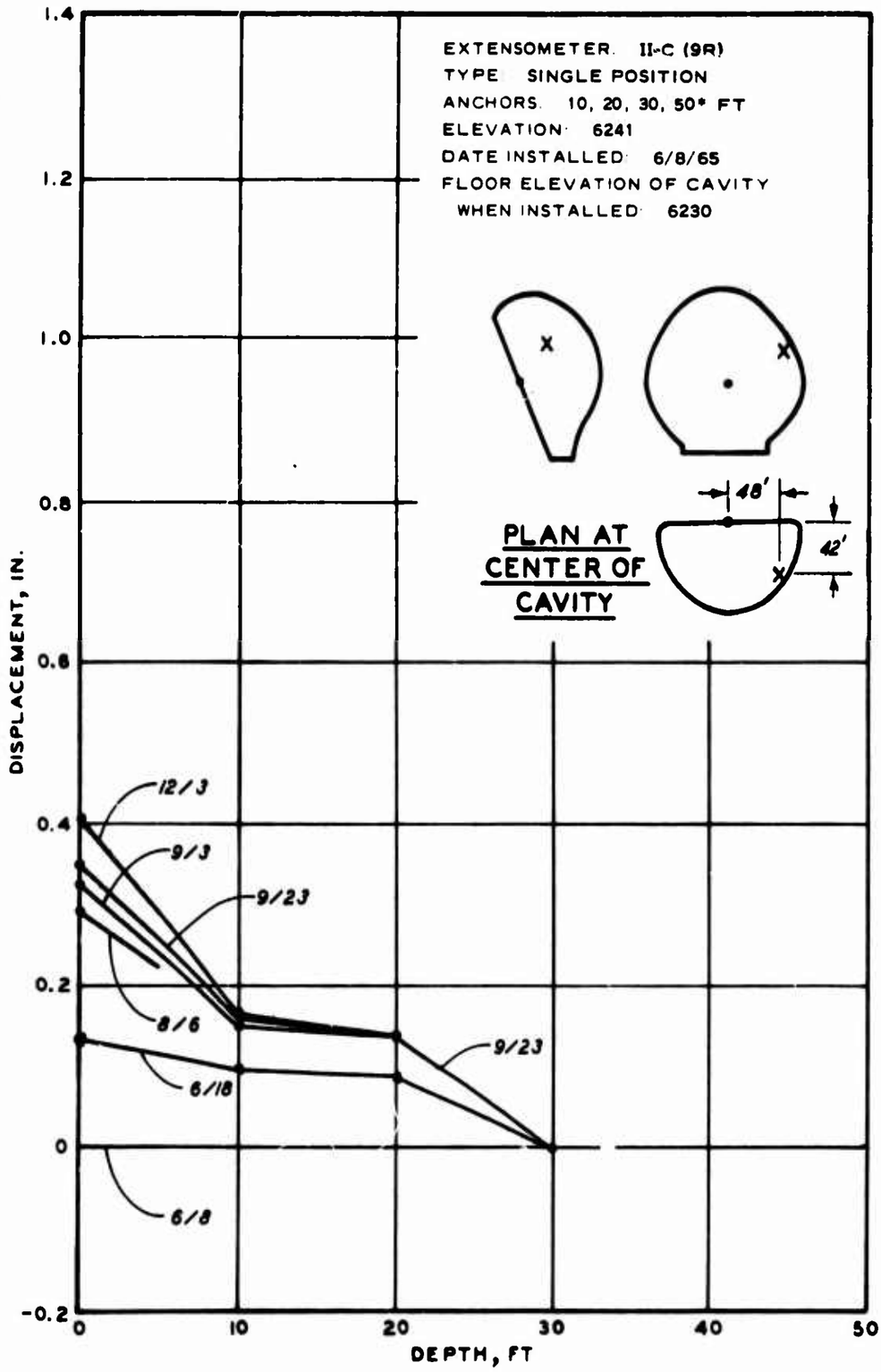
EXTENSOMETER II-C (9R)
TYPE SINGLE POSITION
ANCHORS 10, 20, 30, 50* FT
ELEVATION 6241
DATE INSTALLED 6/8/65
FLOOR ELEVATION OF CAVITY WHEN INSTALLED 6230
PLAN AT CENTER OF CAVITY
48'
42'
DISPLACEMENT, IN.
DEPTH, FT
1.4
1.2
1.0
0.8
0.6
0.4
0.2
0
-0.2
0
10
20
30
40
50
12/3
9/3
9/23
8/6
6/18
6/8
9/23

Fig. B.24

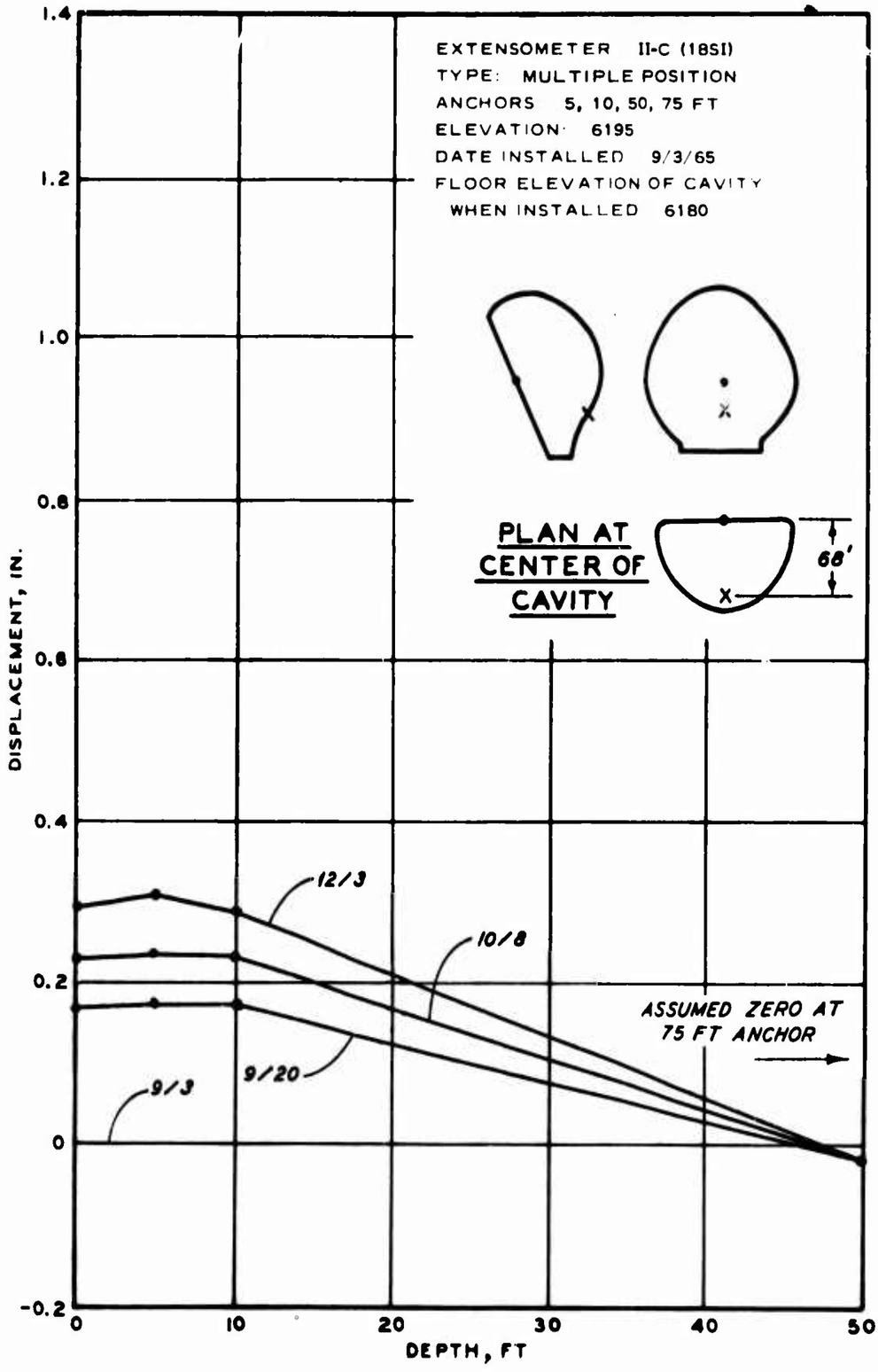
EXTENSOMETER II-C (18SI)
TYPE: MULTIPLE POSITION
ANCHORS 5, 10, 50, 75 FT
ELEVATION 6195
DATE INSTALLED 9/3/65
FLOOR ELEVATION OF CAVITY
WHEN INSTALLED 6180
PLAN AT CENTER OF CAVITY
68'
DISPLACEMENT, IN.
1.4
1.2
1.0
0.8
0.6
0.4
0.2
0
-0.2
0
10
20
30
40
50
DEPTH, FT
12/3
10/8
9/20
9/3
ASSUMED ZERO AT 75 FT ANCHOR

Fig. B.25

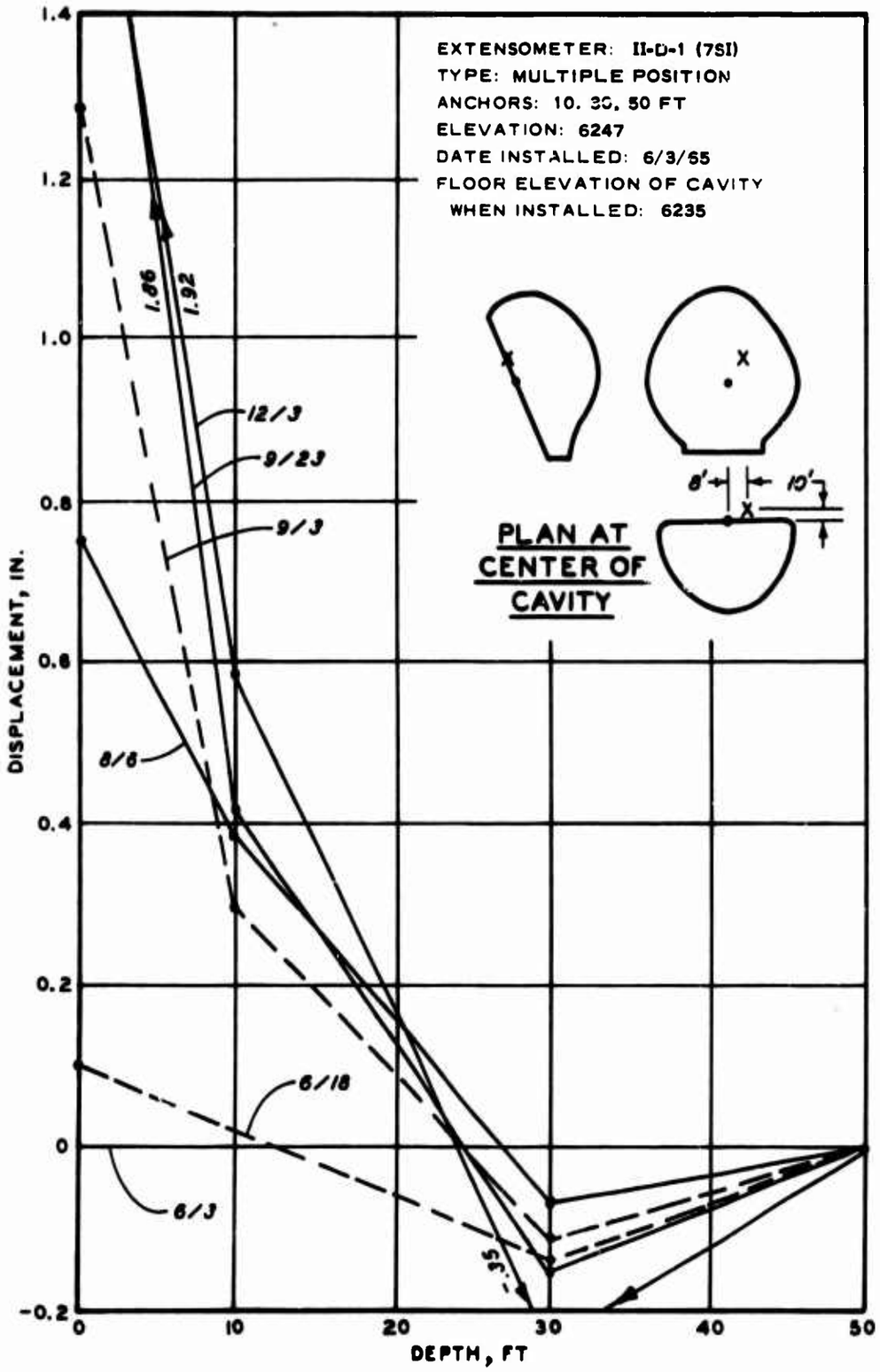
EXTENSOMETER: II-D-1 (7SI)
TYPE: MULTIPLE POSITION
ANCHORS: 10, 30, 50 FT
ELEVATION: 6247
DATE INSTALLED: 6/3/55
FLOOR ELEVATION OF CAVITY
WHEN INSTALLED: 6235
PLAN AT CENTER OF CAVITY
8'
10'
1.86
1.92
12/3
9/23
9/3
8/8
6/18
6/3
-.35
DISPLACEMENT, IN.
DEPTH, FT
1.4
1.2
1.0
0.8
0.6
0.4
0.2
0
-0.2
0
10
20
30
40
50

Fig. B.26

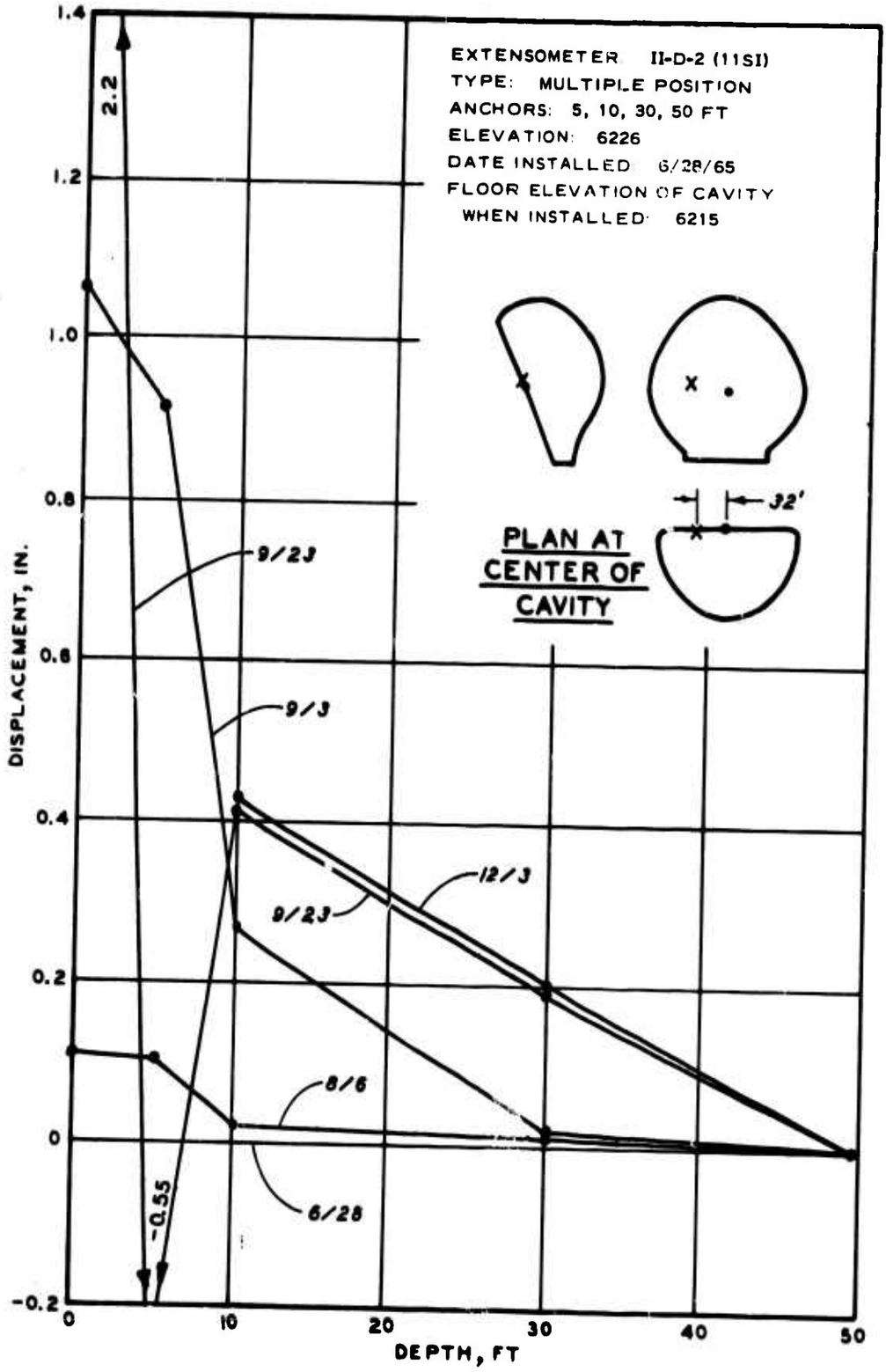
EXTENSOMETER II-D-2 (11SI)
TYPE: MULTIPLE POSITION
ANCHORS: 5, 10, 30, 50 FT
ELEVATION: 6226
DATE INSTALLED 6/28/65
FLOOR ELEVATION OF CAVITY WHEN INSTALLED: 6215
PLAN AT CENTER OF CAVITY
32'
2.2
-0.55
9/23
9/3
12/3
9/23
8/6
6/28
DISPLACEMENT, IN.
DEPTH, FT
1.4
1.2
1.0
0.8
0.6
0.4
0.2
0
-0.2
0
10
20
30
40
50

Fig. B.27

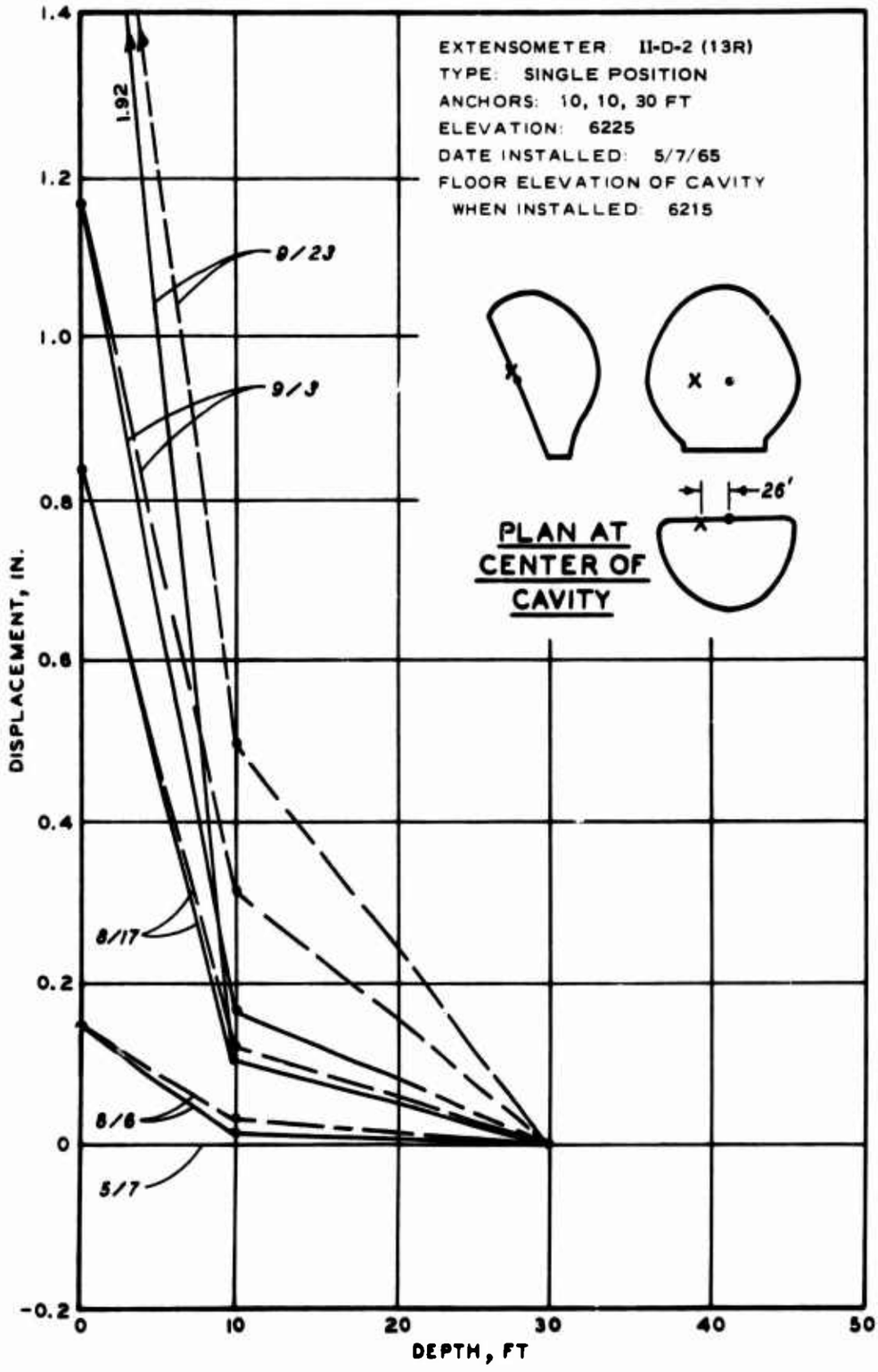
EXTENSOMETER II-D-2 (13R)
TYPE: SINGLE POSITION
ANCHORS: 10, 10, 30 FT
ELEVATION: 6225
DATE INSTALLED: 5/7/65
FLOOR ELEVATION OF CAVITY WHEN INSTALLED: 6215
PLAN AT CENTER OF CAVITY
26'
1.92
8/23
9/3
8/17
8/8
5/7
DISPLACEMENT, IN.
DEPTH, FT
1.4
1.2
1.0
0.8
0.6
0.4
0.2
0
-0.2
0
10
20
30
40
50

Fig. B.28

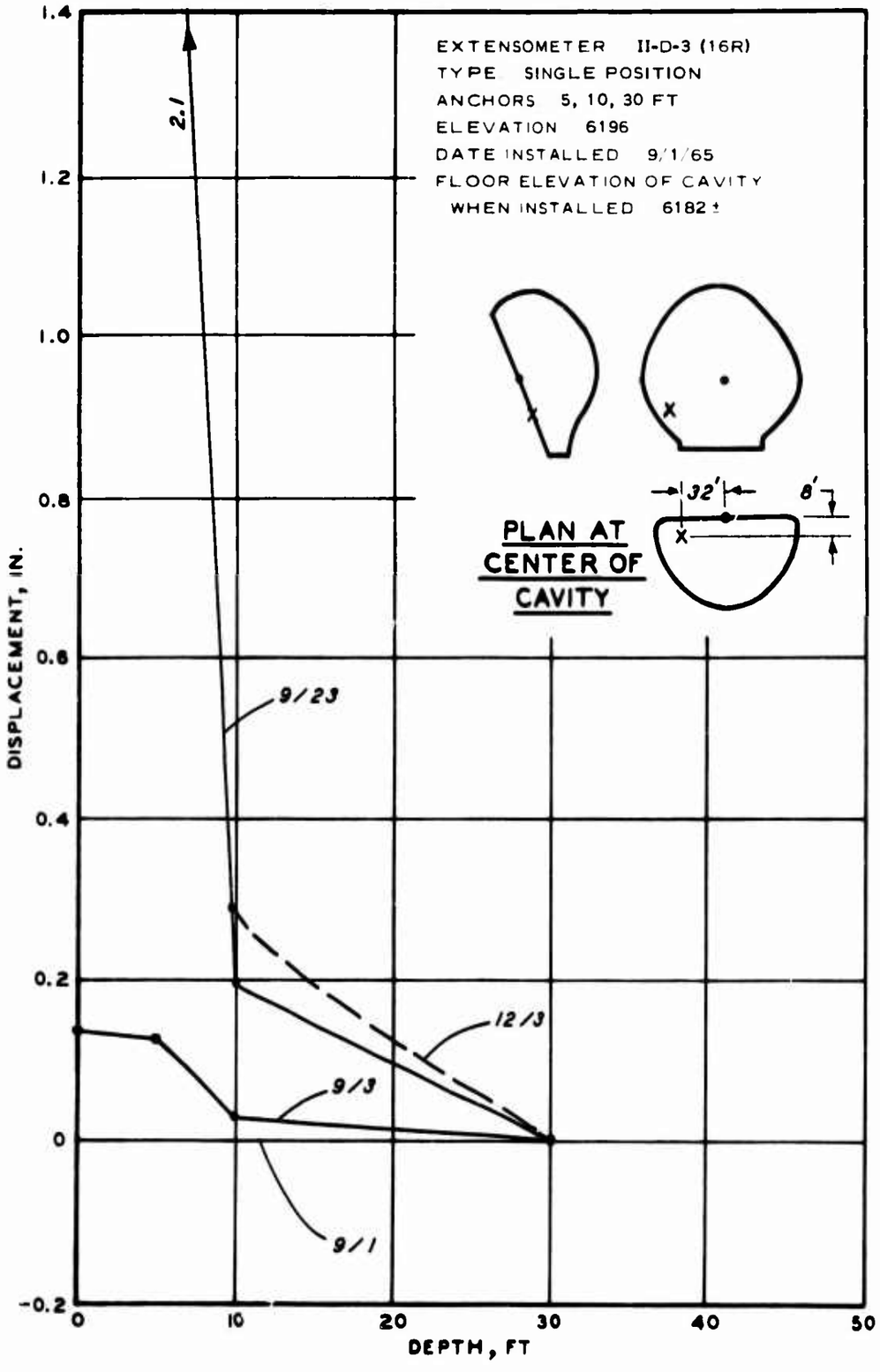
EXTENSOMETER II-D-3 (16R)
TYPE SINGLE POSITION
ANCHORS 5, 10, 30 FT
ELEVATION 6196
DATE INSTALLED 9/1/65
FLOOR ELEVATION OF CAVITY
WHEN INSTALLED 6182±
PLAN AT CENTER OF CAVITY
32'
8'
2/1
9/23
12/3
9/3
9/1
DISPLACEMENT, IN.
DEPTH, FT
1.4
1.2
1.0
0.8
0.6
0.4
0.2
0
-0.2
0
10
20
30
40
50

Fig. B.29

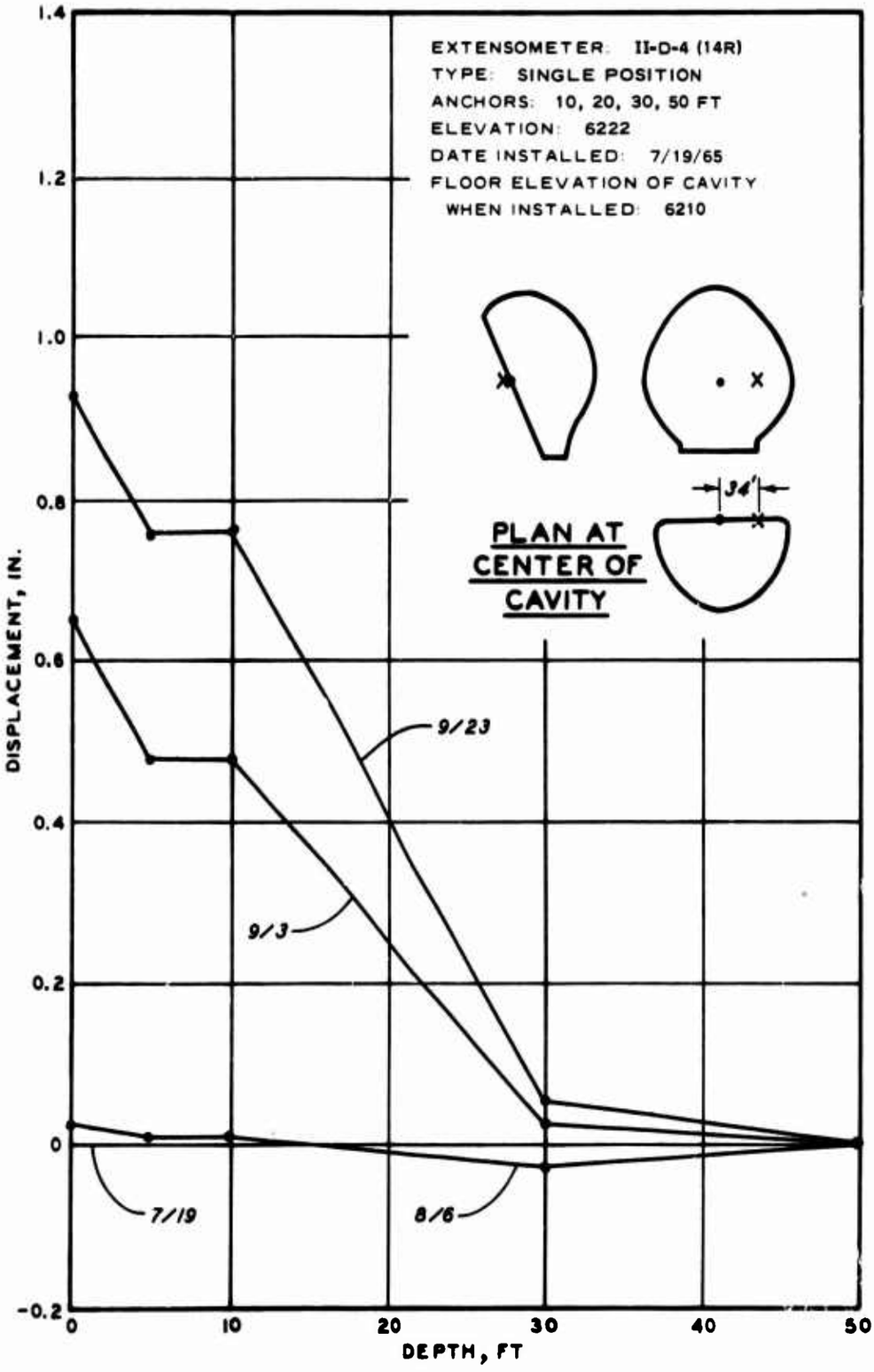
EXTENSOMETER: II-D-4 (14R)
TYPE: SINGLE POSITION
ANCHORS: 10, 20, 30, 50 FT
ELEVATION: 6222
DATE INSTALLED: 7/19/65
FLOOR ELEVATION OF CAVITY WHEN INSTALLED: 6210
34'
PLAN AT CENTER OF CAVITY
9/23
9/3
7/19
8/6
DISPLACEMENT, IN.
DEPTH, FT
1.4
1.2
1.0
0.8
0.6
0.4
0.2
0
-0.2
0
10
20
30
40
50

Fig. B.30

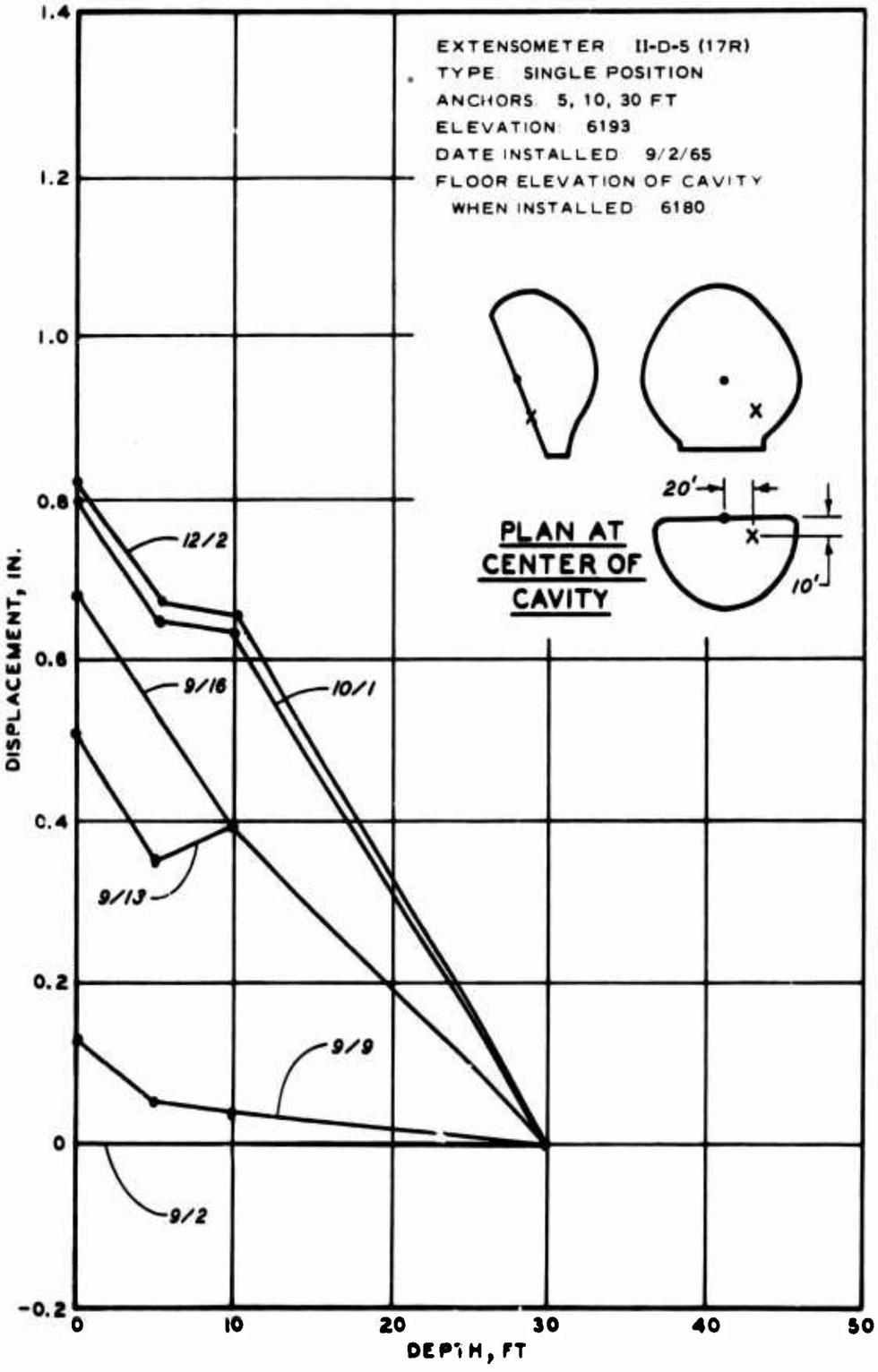
EXTENSOMETER II-D-5 (17R)
TYPE SINGLE POSITION
ANCHORS 5, 10, 30 FT
ELEVATION 6193
DATE INSTALLED 9/2/65
FLOOR ELEVATION OF CAVITY WHEN INSTALLED 6180
PLAN AT CENTER OF CAVITY
20'
10'
12/2
9/16
10/1
9/13
9/9
9/2
DISPLACEMENT, IN.
DEPTH, FT
1.4
1.2
1.0
0.8
0.6
0.4
0.2
0
-0.2
0
10
20
30
40
50

Fig. B.31

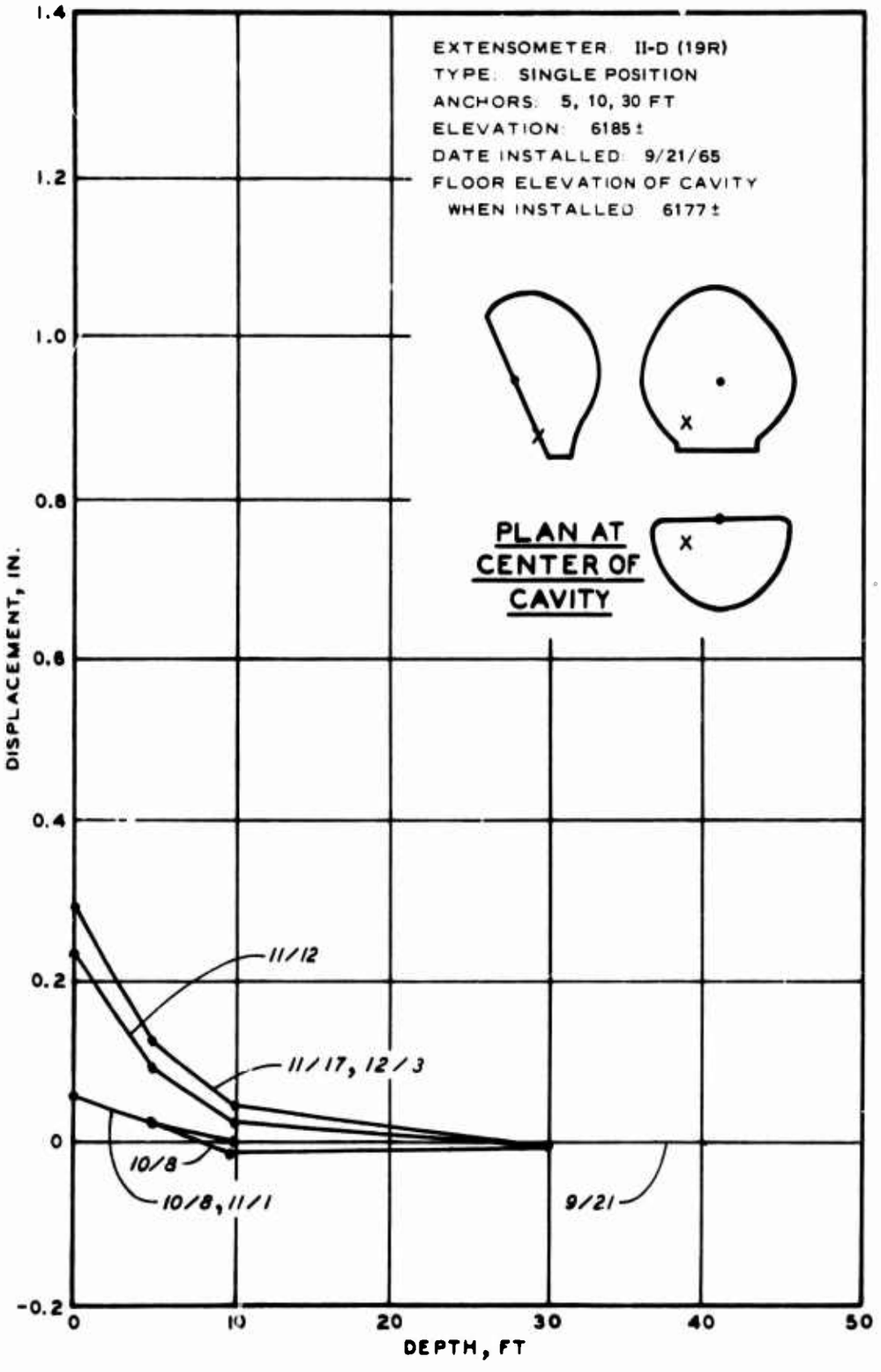
EXTENSOMETER II-D (19R)
TYPE: SINGLE POSITION
ANCHORS: 5, 10, 30 FT
ELEVATION: 6185±
DATE INSTALLED: 9/21/65
FLOOR ELEVATION OF CAVITY WHEN INSTALLED: 6177±
PLAN AT CENTER OF CAVITY
DISPLACEMENT, IN.
DEPTH, FT
1.4
1.2
1.0
0.8
0.6
0.4
0.2
0
-0.2
0
10
20
30
40
50
11/12
11/17, 12/3
10/8
10/8, 11/1
9/21

Fig. B.32

VITA

Edward James Cording [redacted]. He attended secondary schools in Wheaton, Illinois, and graduated from Wheaton College, Illinois, with a BS (geology major) in 1960. He entered the University of Illinois in the fall of 1960 and received his MS in Civil Engineering in February 1963. During the fall and spring semesters from 1961 to 1965, he was a research and teaching assistant in the Department of Civil Engineering.

He was employed as a foundation engineer by the soils consulting firm of Shannon and Wilson, Inc., of Seattle, Washington, in the summers of 1962, 1963, and 1964. In 1965 he served for seven months as a mining engineer and rock mechanics consultant for the engineering firm of Fenix and Scisson, Inc., Mercury, Nevada, during the construction of underground openings at the Nevada Test Site.

He entered on active duty in 1965 as an officer in the U. S. Army Corps of Engineers, and was stationed at Waterways Experiment Station, Vicksburg, Mississippi, where he conducted rock mechanics research for military and civil works projects. He is presently soils engineer for the U. S. Army Engineer Command, Vietnam.

He is a member of various geological and engineering professional societies.

Unclassified

Security Classification

DOCUMENT CONTROL DATA - R & D

(Security classification of title, body of abstract and indexing annotation must be entered when the overall report is classified)

1. ORIGINATING ACTIVITY (Corporate author)	2a. REPORT SECURITY CLASSIFICATION
U. S. Army Engineer Waterways Experiment Station Vicksburg, Miss.	Unclassified
	2b. GROUP

3. REPORT TITLE

THE STABILITY DURING CONSTRUCTION OF THREE LARGE UNDERGROUND OPENINGS IN ROCK

4. DESCRIPTIVE NOTES (Type of report and inclusive dates)

Final report

5. AUTHOR(S) (First name, middle initial, last name)

Edward J. Cording

6. REPORT DATE	7a. TOTAL NO. OF PAGES	7b. NO. OF REFS
January 1968	295	67

8a. CONTRACT OR GRANT NO.	9a. ORIGINATOR'S REPORT NUMBER(S)
b. PROJECT NO.	Technical Report No. 1-813
c. Nuclear Weapons Effects Research Subtask 13.191 d.	9b. OTHER REPORT NO(S) (Any other numbers that may be assigned this report)

10. DISTRIBUTION STATEMENT

This document has been approved for public release and sale; its distribution is unlimited.

11. SUPPLEMENTARY NOTES	12. SPONSORING MILITARY ACTIVITY
Report was also submitted to University of Illinois, Urbana, Illinois, as thesis for degree of Doctor of Philosophy in Civil Engineering	Defense Atomic Support Agency Washington, D. C.

13. ABSTRACT

Three large rock-bolted underground cavities were constructed at the Nevada Test Site. Two of the cavities, approximately 100 feet in diameter and 140 feet high, were constructed at a depth of 1300 feet in a very weak tuff of excellent rock mass quality. The third cavity, approximately 60 feet in diameter and 80 feet high, was constructed at a depth of 350 feet in a jointed granite of high intact strength and fair to good rock mass quality. The stability of the cavities was monitored throughout construction by measuring rock displacements, observing fractures in near-surface rock, and observing the behavior of the rock-bolt support system. Supporting field and laboratory tests were performed in order to evaluate intact and in-situ properties of the rock mass. Radial movement of the cavities was measured using extensometers anchored at various depths in holes drilled from the cavity surface. Displacement versus depth profiles were used to determine the depth at which rock movement was concentrated. By comparing rock movement with excavation and support progress, a continual estimate of the cavity stability was obtained. Large displacements, or large rates of displacement, were indicative of potentially unstable behavior. Displacements were compared with displacements predicted from elastic theory, using a finite element solution and simple closed solutions.

DD FORM 1 NOV 65 1473 REPLACES DD FORM 1473, 1 JAN 64, WHICH IS OBSOLETE FOR ARMY USE.

Unclassified

Security Classification

Unclassified

Security Classification

14 KEY WORDS	LINK A		LINK B		LINK C	
	ROLE	WT	ROLE	WT	ROLE	WT
Nevada Test Site						
Rock bolts						
Rock mechanics						
Underground structures						

Unclassified

Security Classification